

# **SOME STUDIES ON EVALUATION OF COMBUSTION, PERFORMANCE AND EMISSION CHARACTERISTICS OF QUATERNARY BLENDS IN COMPRESSION IGNITION ENGINE**

**A Thesis submitted to the Delhi Technological University, Delhi in fulfillment of  
the requirements for the award of the degree of**

**DOCTOR OF PHILOSOPHY**

**In**

**Mechanical Engineering**

**By**

**DUSHYANT MISHRA**

**(2K18/PHD/ME/507)**

**Under the supervision of**

**Dr. NAVEEN KUMAR**

**Professor**

**&**

**Dr. RAJIV CHAUDHARY**

**Professor**



**Department of Mechanical Engineering**

**Delhi Technological University**

**Shahabad Daulatpur, Main Bawana Road,**

**Delhi-110042, India**

**January 31<sup>ST</sup>,2024**

**© DELHI TECHNOLOGICAL UNIVERSITY**

**2024**

**ALL RIGHTS RESERVE**

# **DECLARATION**

I hereby undertake that the thesis entitled “**Some studies on evaluation of combustion, performance and emission characteristics of quaternary blends in compression ignition engine**” is an original work carried out by me under the supervision of Prof. Naveen Kumar, & Prof. Rajiv Chaudhary, Mechanical Engineering Department, Delhi Technological University, Delhi. This thesis has been prepared in conformity with the rules and regulations of the Delhi Technological University, Delhi. The research work reported and results presented in the thesis have not been submitted either in part or full to any other university or institute for the award of any other certificate, diploma, or degree.



**(Dushyant Mishra)**

(2K18/PhD/ME/507)

Research Scholar

Mechanical Engineering Department

Delhi Technological University, Delhi

## **CERTIFICATE**

This is to certify that the work embodied in the thesis “**Some studies on evaluation of combustion, performance and emission characteristics of quaternary blends in compression ignition engine**” by **Dushyant Mishra**, (2K18/Ph.D./ME/507) in partial fulfillment of requirements for the award of Degree of ‘**DOCTOR OF PHILOSOPHY**’ in Mechanical Engineering Department, is an authentic record of student’s work carried by him under our supervision. This is also certified that this work has not been submitted to any other Institute or University for the award of any other diploma or degree.



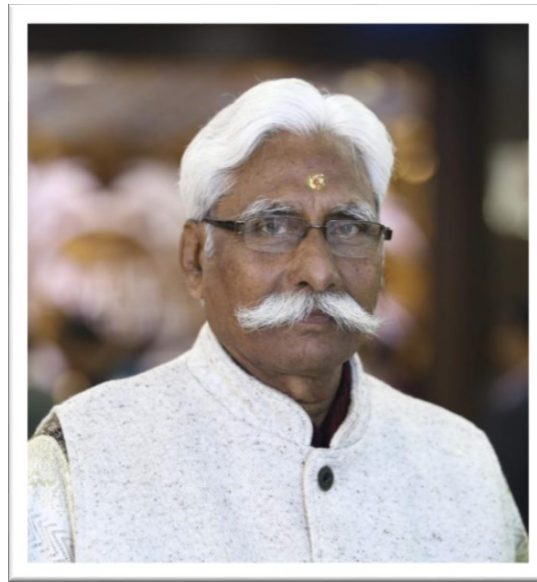
**(Prof. Rajiv Chaudhary)**  
**Mechanical Engineering Department**  
**Delhi Technological University**  
**Delhi- 110042**



**(Prof. Naveen Kumar)**  
**Mechanical Engineering Department**  
**Delhi Technological University**  
**Delhi- 110042**



***Dedicated to***  
***My beloved Late Pitajee***  
***Dr. Suresh Chandra Mishra***



# **ACKNOWLEDGMENT**

I would like to thank all the people who contributed in some way to the work described in this thesis. First and foremost, I thank my academic advisors, Professor Naveen Kumar and Professor Rajiv Chaudhary, for providing excellent supervision for the current research project. During my tenure, they contributed by providing an unwavering willingness to assist, insightful criticism, and unceasing inspiration with their panegyric efforts.

I also take this opportunity to thank Prof. S. K. Garg, the HOD and DRC Chairman (Mechanical Engineering), Prof. R. C. Singh, the librarian and other staff of DTU Library, and the entire faculty and staff members of the Mechanical Engineering Department for their support and insightful advice. I am thankful to Mr. Kamal Nain for providing all laboratory assistance. I am also thankful to Mr. Surendra Singh, Smt. Neetu Mishra (the supporting staff of CASRAE, DTU, Delhi) for their cooperation.

I am extremely thankful to Dr. Rakesh Yadav, Dr. Khushbu Yadav, Dr. Mukul Tomar, Dr. Harveer Singh Pali, Dr. Parvesh Kumar, Mr. Hansham Deval, and Mr. Shiv Prakash Singh, for their extreme support during my research work on **“Some studies on evaluation of combustion, performance and emission characteristics of quaternary blends in compression ignition engine”**

Lastly, I can never forget to thank my mother Smt. Kusum Lata Sharma and wife Dr. Shivani Kaul Mishra, for her love, encouragement, and moral support throughout the entire research project.

I want to thank God for providing me with the strength and endurance to do this program completely and for leading me to success in this program.

**(Dushyant Mishra)**

Delhi Technological University, New Delhi

## **ABSTRACT**

Energy is an important factor in the growth of the world economy. Liquid fuel is the key resource for supplying current energy demand. The present study envisages biodiesel as a promising substitute for conventional petroleum-derived fuels. The need for biodiesel production from waste cooking oil in India is mandated by the vulnerability of crude oil prices, climate change concerns, and the need for the growing economy to use its resources suitably. It can readily meet India's goal of producing biodiesel because of its enormous abundance.

In the present research work the waste cooking oil was converted to bio-diesel like fuel by using the trans-esterification process and prepared its test fuel blends with orange peel oil, n-butanol and diesel and the experiments were carried out on a CI engine to study the test fuel on its combustion, performance and emission characteristics. The aimed research work carried out in three phases.

In the first phase the biodiesel was obtained by the trans-esterification process. Due to the selection of process parameters such as reaction temperature, reaction time agitation speed, catalyst concentration, and molar ratio; it was difficult to use the value to increase its yield as well as physico-chemical properties. So that, to optimize these Response Surface Methodology tool. The alcohol-oil MR, CC, RT, R Temp, and agitation speed as input variables, while yield, CV, FP, KV, and PP are the necessary responses. The central composite design (CCRD), was used to evaluate the RSM analysis for the optimization process. The axial and factorial points in the design of the experimental runs are involved in the five-level CCRD experimental model. As observed in Table 3.3, these variables ranged at five different levels (-2, -1, 0, +1, +2). It gave favorable results of bio-diesel

production (98.95%), viscosity (5.48 cSt), calorific value (45.68 MJ/kg), flash point (169.250C), and pour point (-2.120C). The RSM optimization tool provided the error percentage range from 1% to 7%. The response showed a confidence level of 95%.

The four blends were prepared with waste cooking oil biodiesel with kept the fraction of 5% fixed, orange peel oil (3%-21%), n-butanol (2%-14%), and the remaining fraction of pure diesel and evaluate the physico chemical properties in second phase. The four blends are named O3B2, O9B6, O15B10 and O21B14. The physico-chemical properties e.g. calorific value, viscosity, density, flash point, cloud point, pour point, micro-carbon residue, sulphur content was tested on equipment according to the ASTM standards. The test fuel characterization was conducted to identify the sauter mean diameter and sauter mean surface area. The characterization study help to study about the combustion characteristic of fuel. All the tests were conducted in CASARE Lab, Delhi Technological University, Delhi. All the evaluated properties were found accepted for use in the CI engine.

These blends were subsequently used in an air-cooled, single-cylinder, four-stroke diesel engine to evaluate performance, emission, and combustion characteristics. The engine tests were carried out in third phase of research work as per IS:10000. The performance study of these blends on a single-cylinder, air-cooled compression ignition engine was found satisfactory. The brake thermal efficiency in comparison to baseline diesel, the BTE for O3B2, O9B6, O15B10, and O21B14 are 21.99%, 22.09%, 22.31%, and 22.49%, respectively,. It was also found that BSEC were 4.10%, 8.16%, 12.27%, and 18.44%, for O3B2, O9B6, O15B10, and O21B14, respectively

The emission characteristics depicted that HC, CO, smoke opacity, and NO<sub>x</sub> were lower for all the test blends than neat diesel. The combustion characteristics have shown that the cylinder peak pressure was 68.48 bar O21B14, and the peak heat release rate (HRR) was 60.12 J/°CA for O21B14. The peak HRR was lower when the engine was operated at neat diesel.

The present study concluded that prepared quaternary fuel blends of waste cooking oil biodiesel, orange peel oil, n-butanol, and diesel seemed alternative fuels for unmodified single-cylinder air-cooled CI engines. The usage of the used blends minimizes the pollution ground as well as the environment. The 40% usage of diesel was observed to reduce.

# Table of Content

<b>DECLARATION</b>	<b>I</b>
<b>CERTIFICATE</b>	<b>II</b>
<b>ACKNOWLEDGMENT</b>	<b>IV</b>
<b>ABSTRACT</b>	<b>V-VII</b>
<b>Table of Contents</b>	<b>VIII-XIII</b>
<b>List of Figures</b>	<b>XIV-XV</b>
<b>List of Plates</b>	<b>XVI</b>
<b>List of Tables</b>	<b>XVII-XVIII</b>
<b>Nomenclature</b>	<b>XIX-XXI</b>
<b>CHAPTER-1</b>	<b>1-9</b>
1.1. Human and his energy consumption	1
1.2. Climate change	5
1.3. Social and economic crises	6
1.4. Biofuels as an Alternative	8
<b>CHAPTER-2</b>	<b>10-86</b>
2.1. General Information about Biodiesel or FAME	10
2.2. Biodiesel's Historical Development	11
2.3. An objective look at biodiesel	12
2.4. Advantages	13
2.4.1. Reduction in Polluting Emissions	13
2.4.2. Lubricity	14
2.4.3. Biodegradability and Toxicity	14
2.5. Disadvantages	15
2.5.1. Higher Viscosity	15
2.5.2. Mechanical Performance	15
2.5.3. NO Emissions	15
2.5.4. Behavior at Low Temperatures	16

2.5.5.	Lubricant Dilution-----	16
2.5.6.	Corrosion Problems-----	16
2.5.7.	Oxidation stability-----	17
2.5.8.	Price-----	17
2.6.	Current panorama of biodiesel in the world (2021)-----	17
2.7.	Raw materials and reagents-----	18
2.7.1.	Traditional vegetable oils-----	18
2.8.	Rapeseed oil (Brassica napus)-Agronomic and pedological requirement-	19
2.8.1.	Seed Composition-----	20
2.9.	Anola (Brassica Rapa)-----	21
2.10.	Sunflower Oil (Helianthus Annuus)-----	21
2.10.1.	Agronomic and pedological requirements-----	21
2.10.2.	Seed Composition (Table 2.4)-----	22
2.11.	Soy Oil (Glycine Max)-----	23
2.11.1.	Agronomic and Pedological Requirements-----	23
2.11.2.	Seed Composition-----	25
2.12.	Used Frying Oils-----	26
2.13.	Alternative Vegetable Oils-----	28
2.13.1.	The Transesterification Reaction-----	29
2.13.2.	Catalysis of the Transesterification Reaction-----	31
2.13.3.	Basic Homogeneous Catalysis-----	32
2.13.4.	Homogeneous Acid Catalysis-----	34
2.13.5.	Heterogeneous Catalysis-----	34
2.13.6.	Enzymatic Catalysis-----	35
2.13.7.	Alternatives to Improve The Transesterification Reaction-----	36
2.13.8.	Industrial Processes-----	44
2.14.	Hydrogen Production-----	45
2.14.1.	Thermochemical Processes-----	46

2.14.2. Combustion-----	47
2.14.3. Pyrolysis-----	47
2.14.4. Gasification-----	48
2.14.5. Steam reforming-----	50
2.15. Factors that influence the steam reforming process-----	52
2.16. Literature review-----	53
2.17. Problem statement-----	85
2.18. Objectives-----	86
<b>CHAPTER 3-----</b>	<b>87-133</b>
3.1. Engine selection-----	87
3.2. Selection of blending elements-----	89
3.2.1. Orange Peel Oil (Straight vegetable oil) -----	89
3.2.2. Selection of Pilot Fuel (Orange Peel Oil) -----	90
3.2.3. Taxonomy-----	91
3.2.4. Proximal characteristics of orange peel-----	91
3.2.5. Natural extract-----	92
3.2.6. Natural degreaser-----	92
3.3. Waste Cooking Oil Methyl Ester (WCOME) -----	93
3.3.1. Methodology-----	93
3.3.2. Free Fatty Acid (FFA)-----	93
3.3.3. Esterification-----	94
3.3.4. Transesterification-----	95
3.4. Production and Physico-Chemical Properties optimization-----	96
3.5. Selection of Alcohol-----	99
3.5.1. Preparation of Quaternary Blends-----	100
3.6. Sample preparation from WCO-----	102
3.6.1. Kinematic Viscosity (KV) -----	104
3.6.2. Calorific Value (CV) -----	105



3.6.3.	Density-----	106
3.6.4.	Flash point (FP) -----	107
3.6.5.	Distillation-----	108
3.6.6.	Saponification value-----	109
3.6.7.	Cetane Index-----	109
3.6.8.	Cloud Point and pour point-----	110
3.6.9.	Iodine Value-----	112
3.6.10.	Fatty Acid Composition-----	113
3.6.11.	Test for calculating the average particle size of the test fuel spray-- -----	114
3.7.	Engine Test Rig-----	117
3.8.	Selection of engine test Parameters-----	121
3.9.	Measured Parameters-----	122
3.9.1.	Measurement of engine speed-----	122
3.9.2.	Engine load-----	123
3.9.3.	Measurement of flow rate of fuel-----	123
3.9.4.	Measurement of airflow rate-----	124
3.9.5.	Inside cylinder pressure-----	125
3.9.6.	Measurement of exhaust temperature-----	125
3.9.7.	Measurement of exhaust emissions-----	126
3.10.	Engine Calculated Parameters-----	127
3.10.1.	Brake Power-----	128
3.10.2.	Brake mean effective pressure-----	128
3.10.3.	Brake specific fuel consumption-----	129
3.10.4.	Brake specific energy consumption-----	129
3.10.5.	Brake thermal efficiency-----	130
3.10.6.	Heat release rate and ignition delay-----	130
3.11.	Engine trial procedure-----	131
3.12.	Accuracy and uncertainty of measuring instrument-----	132

<b>CHAPTER-4</b>	<b>133-171</b>
4.1. Introduction	133
4.2. Characterization methods	134
4.3. Results and discussion	135
4.3.1. Regression analysis (ANOVA)	135
4.3.2. RSM Optimization	138
4.3.3. Control of process variable on biodiesel yield	140
4.3.4. Control of process variable on kinematic viscosity	142
4.3.5. Control of process variable on calorific value	143
4.3.6. Control of process variable on Flash point	146
4.3.7. Control of process variable on pour point	148
4.4. Validation of experimental results	149
4.5. Preparation of Quaternary Blends	150
4.6. Physico-Chemical Properties of Fuel Blends	151
4.6.1. Kinematic viscosity	151
4.6.2. Density	152
4.6.3. Calorific Value (Heating Value)	153
4.6.4. Flash Point	154
4.6.5. Cloud point and pour point	154
4.6.6. Cetane number	155
4.6.7. Sulphur content	156
4.6.8. Micro carbon residue	157
4.7. Sauter mean diameter	158
4.8. Experimental setup	159
4.9. Performance characteristic	161
4.9.1. Brake Thermal Efficiency (BTE)	161
4.9.2. Exhaust Gas Temperature (EGT)	162
4.9.3. Brake Specific Energy Consumption (BSEC)	163

4.10.	Emission characteristic-----	164
4.10.1.	Hydrocarbon emission-----	164
4.10.2.	Oxides of nitrogen emission (NO <sub>x</sub> ) -----	165
4.10.3.	Carbon mono oxide (CO) Emissions-----	166
4.10.4.	Emissions of smoke opacity-----	167
4.11.	Combustion Characteristics-----	167
4.11.1.	Inside Cylinder Pressure-----	169
4.11.2.	Heat release rate (HRR) -----	170
<b>CHAPTER 5</b>	<b>-----</b>	<b>171-173</b>
5.1.	Conclusions: -----	171
5.2.	Future scope-----	173
<b>REFERENCES</b>	<b>-----</b>	<b>174-210</b>
<b>APPENDIX-I</b>	<b>-----</b>	<b>211</b>
<b>APPENDIX-II</b>	<b>-----</b>	<b>215</b>
<b>List of Publication</b>	<b>-----</b>	<b>216</b>
<b>Bio-data</b>	<b>-----</b>	<b>217</b>

## List of Figures

S.NO.	Title	Pg. No.
Figure 1.1	Average life-cycle CO <sub>2</sub> equivalent emissions -----	3
Figure 2.1	Estimation of global biodiesel production-----	18
Figure 2.2	Rapeseed cultivation-----	19
Figure 2.3	Rapeseed Seeds-----	20
Figure 2.4	Sunflower cultivation -----	22
Figure 2.5	Sunflower seeds. -----	22
Figure 2.6	Soyabean Cultivation. -----	24
Figure 2.7	Soybean fruit. -----	24
Figure 2.8	Frying oil-----	27
Figure 2.9	Scheme of conventional (above) and microwave (below) heating systems-- -----	38
Figure 2.10	Central composite design for two factors (a) and three factors (b)-----	43
Figure 2.11	Block diagram of biodiesel production process-----	44
Figure 3.1	Cycle to obtain natural extract-----	92
Figure 3.2	Optimization methodology-----	97
Figure 3.3	Process of transesterification-----	103
Figure 3.4	Flow diagram of Waste cooking oil biodiesel production-----	103
Figure 3.5	Waste cooking oil biodiesel production-----	104
Figure 3.6	Schematic of Spraytec machine-----	116
Figure 3.7	Test Engine schematic diagram-----	121
Figure 3.8	Engine calculated parameter-----	128
Figure 4.1	Gas chromatography of waste cooking oil biodiesel-----	134
Figure 4.2	Optimization plot: Effect of process parameters on responses-----	138
Figure 4.3	Control of process variable on yield-----	140
Figure 4.4	Control of process variable on kinematic viscosity-----	144

Figure 4.5	Control of process variable on calorific value-----	145
Figure 4.6	Control of process variable on flash point-----	147
Figure 4.7	Effect of process variable on pour point-----	149
Figure 4.8	Kinematic Viscosity-----	152
Figure 4.9	Density of Fuel Blends-----	153
Figure 4.10	Calorific Value of Fuel Blends-----	153
Figure 4.11	Flash Point of Fuel Blends-----	154
Figure 4.12	Cloud Point and Pour Point of Fuel Blends-----	155
Figure 4.13	Cetane Number of Fuel Blends-----	156
Figure 4.14	Sulphur Content of Fuel Blends-----	157
Figure 4.15	Micro-Carbon Residue of Fuel Blends-----	158
Figure 4.16	Sauter mean diameter for test fuel blends-----	159
Figure 4.17	Sauter surface area for the test fuel blends-----	159
Figure 4.18	Effect of orange peel oil addition on (a) BTE and (b) BSEC on different engine loads at 1500 rpm. -----	163
Figure 4.19	Variation of EGT with BMEP-----	164
Figure 4.20	Variation of emission parameter with BMEP-----	166
Figure 4.21	Variation of P- $\Theta$ -----	168
Figure 4.22	Heat release rate (HRR) with crank angle-----	169

## List of Plates

S.NO.	Title	Pg. No.
Plate No.3.1	Viscobath Apparatus-----	104
Plate No. 3.2	Isothermal Bomb Calorimeter-----	106
Plate No. 3.3	Anton Parr, DMA 4500 (Desitymeter) -----	106
Plate No.3.4	Pensky Martens Automatic Flash Point apparatus-----	107
Plate No.3.5	Distillation Unit-----	108
Plate No. 3.6	Cloud Point and Pour Point Apparatus-----	111
Plate No. 3.7	Sulphur Analyzer Apparatus-----	112
Plate No. 3.8	Gas Chromatograph (GC Machine) -----	114
Plate No. 3.9	Set-up of Malvern Spraytec-----	115
Plate No. 3.10	Three holes injector-----	115
Plate No. 3.11	Test fuel storage tank-----	115
Plate No. 3.12	Fuel Pump and motor assembly-----	116
Plate No. 3.13	AVL 4000 Light Di-Gas analyzer-----	119
Plate No. 3.14	AVL 437 smoke meter-----	119
Plate No. 3.15	Test CI Engine-----	120
Plate No. 3.16	Eddy current dynamometer-----	120
Plate No. 3.17	Engine speed sensor-----	123
Plate No. 3.18	Temperature measuring thermo couple-----	126
Plate No. 4.1	Prepared test fuel blends-----	151

## List of Tables

S.NO.	Title	Pg. No.
Table 2.1	Evaluation of physicochemical Characteristics of Palm Oil and Biodiesel and Petroleum diesel-----	10
Table 2.2	Variation in emissions of Soy Biodiesel (B100) and its mixture with Diesel-----	14
Table 2.3	Composition of Rapeseed-----	20
Table 2.4	Composition of sunflower seed-----	22
Table 2.5	Composition of soybean-----	25
Table 2.6	Literature review of Waste cooking Oil-----	80
Table 3.1	Engine's Specification-----	88
Table 3.2	Taxonomy of the orange-----	91
Table 3.3	Coded stages for waste cooking oil production and characterization-----	98
Table 3.4	Experimental data as per L33 RSM array-----	98
Table 3.5	Physiochemical properties of higher alcohol-----	99
Table 3.6	Nomenclature of fuel blends-----	101
Table 3.7	Equipment used for properties test-----	101
Table 3.8	ASTM D6751 and EN 14214 standards for BD fuels and ASTM D 975 for petroleum diesel fuel-----	102
Table 3.9	Technical description of the engine and alternator-----	122
Table 3.10	Emission Test rig specification-----	127
Table 3.11	Accuracy and uncertainty of measuring instrument-----	132
Table 4.1	Fatty acid composition of waste cooking oil biodiesel-----	135
Table 4.2	Physico-chemical properties of Waste cooking oil biodiesel-----	135
Table 4.3	ANOVA results for Yield and Calorific value-----	136
Table 4.4	ANOVA result for Kinematic viscosity and Flash Point-----	136
Table 4.5	ANOVA results for Pour Point-----	136
Table 4.6	Model summary-----	137

Table 4.7	Output responses equations-----	139
Table 4.8	Verification of output responses-----	150
Table 4.9	Nomenclature of fuel blends-----	151
Table 4.10	Technical specification of the engine and alternator-----	160
Table 4.11	Equipment used for properties evaluation-----	161
Table 4.12	Physical and chemical properties of fuel blends-----	161



## Nomenclature

°	Degree
°C	Degree Centigrade
ANOVA	Analysis of variance
AQI	Air quality index
ASTM	American society for testing and materials
AV	Acid value
B100	Neat biodiesel
bBDC	Before bottom dead center
BMEP	Brake mean effective pressure
bp	Brake Power
BSEC	Brake specific energy consumption
BSFC	Brake specific fuel consumption
bTDC	Before top dead center
BTE	Brake thermal efficiency
C <sub>18</sub> H <sub>34</sub> O <sub>3</sub>	Ricinoleic acid
CA	Crank angle
CC	CC Concentration for catalyst
CCD	Central composite design
CCI	Calculated cetane index
C <sub>d</sub>	Co-efficient of discharge
CH <sub>3</sub> C+6H+4SO <sub>3</sub> H	Para toluene sulfonic acid (PTSA)
CI	Compressed ignition
CN	Cetane number
CO	CO
CO <sub>2</sub>	Carbon di-oxide
C <sub>p</sub>	Specific heat at constant pressure
CV	Calorific value
C <sub>v</sub>	Specific heat at constant volume
D100	Neat petroleum diesel
DP	Differential pressure
dP/dθ	Inside pressure rate
dQ/dθ	net HRR of the inside combustion chamber
dQ <sub>w</sub> /dθ	rate of heat loss
EGT	Exhaust Gas Temperature
EPA	Environmental protection agency
Fe <sub>2</sub> O <sub>12</sub> S <sub>3</sub>	Ferric sulphate acid
FAME	Fatty acid methyl ester
FFA	Free fatty acid
g	Acceleration due to gravity
GC	Gas Chromatography
GDP	Gross Domestic Product
gr.	Gram

H <sub>2</sub> SO <sub>4</sub>	Sulphuric acid
H <sub>3</sub> PO <sub>4</sub>	Phosphoric acid
HC	Hydrocarbons
HCl	Hydrochloric acid
HR	Heat release
HRR	Heat release rate
HT	Heat transfer
HV	Heating value
IC	Internal Combustion
IDP	Ignition delay period
IV	Iodine value
IPCC	Intergovernmental panel on climate change
KB	Karanja biodiesel
Kg	Kilogram
kg/s	Kilogram/second
KO	Karanja oil
KOB	Kusum oil biodiesel
KOCH <sub>3</sub>	Potassium methoxides
KOH	Potassium hydroxides
KW	Kilowatt
LCA	Life cycle analysis
LHV	Latent heat of vaporization
m	Meter
m	mass of fuel
MJ	Mega Joule
ml	Milliliter
MOB	Mahua oil biodiesel
MR	Molar ratio
Mtoe	Million tonnes of oil equivalent
NaOCH <sub>3</sub>	Sodium methoxides
NaOH	Sodium hydroxides
NBSS&LUP	National Bureau of Soil and Land Use Planning
NOB	Neem oil biodiesel
NO <sub>x</sub>	Oxides of nitrogen
OECD	Organisation for Economic Co-operation and Development
OPO	Orange peel oil
PM	Particulate matters
PP	Pour point
ppm	Parts per million
PRR	Pressure rise rate
PTSA	Para toluene sulphuric acid
Q	heat release
Q <sub>w</sub>	heat loss through the wall
RSM	Response Surface Methodology
RT	Reaction time
RTemp	Reaction temperature

SV	Saponification value
SVO	Straight vegetable oil
T	Torque
TDC	Top dead center
UNFCCC	United nations framework convention on climate change
WHO	World Health Organization
WCO	Waste cooking oil
WCOBD	Waste cooking oil biodiesel
ZnCl <sub>2</sub>	Lewis acids
$\Delta p_{cj}$	Change in pressure rise
$\Delta p_j$	Change in Pressure

# CHAPTER-1

## INTRODUCTION

---

### 1.1. Human and His Energy Consumption

For millennia the only source of energy that man used was from his muscles, which were used to hunt, fish, grind food grains, transport loads, and other vital tasks. It would be in the Upper Paleolithic when he began to consciously use fire as a source of energy[1]. Humans captured it from natural fires caused by lightning or volcanic eruptions, and kept it in his caves, constantly adding pieces of wood. Fire not only served to protect them from the cold, scare away wild animals, and provide light at night but also to cook some foods to make them more digestible[2]. When prehistoric man managed to light the fire, he mastered one of the elements that would serve the most in the advancement of civilization. Ancient civilizations learned to use firewood to produce it, invented ovens in which the heat generated could be concentrated, and discovered charcoal. These advances made it possible to make pottery (to better preserve food) and to work iron and copper (for the production of weapons and tools)[2].

From an energy point of view, the great technical revolution was agriculture, which allowed man to store solar energy by transferring it to vegetables usable as food. It also gave the human group the possibility of settling permanently in fixed places where they lived in huts and cabins. This eliminated the nomadic-gatherer phase and brought with it important sociological changes: man became sedentary, building large or small towns built with adobe, wood, or stone. The groups become more numerous and are organized into clans or tribes[3].

By advancing agriculture, the value of the land and the ability to work it, transform it, and make it produce increased exponentially. Energy is defined as “the ability to do

work”, which explains the desperate search for energy sources throughout history. For this purpose, man also domesticated some animals or subjugated other similar ones, to assist in agricultural work and transportation. As the centuries passed, means of transportation over lakes, rivers, and seas were developed, and the wind was widely used, acting on mills and sails to drive boats that combined the use of wind energy with assisted human muscle energy [4].

The muscular energy of man (voluntary or forced), domesticated animals, as well as direct energy from the sun, wind, or hydraulic energy. They were widely used in ancient times. All of these energies can be considered renewable, however, they caused serious environmental and social impacts, such as the excessive felling of forests, pollution in urban centers, and the death of thousands of men subjected to slavery[4], [5].

It was with the Industrial Revolution when the use of mineral coal became widespread and greater energy efficiencies were achieved with the development of the steam engine, whose effects on the destiny of man and the environment have been decisive in achieving great advances in the mining industry, the steel and textile industries, as well as in transportation. Mass generation of electricity began in the late 19th century, and the growing succession of applications that this availability produced made electricity one of the main driving forces of the Industrial Revolution. For this reason, Due to its simplicity of production and distribution, it has emerged as one of the most crucial energy sources for technological advancement, in addition to its large number of applications in all fields such as lighting, transportation, telecommunications, and computing[6].

The consumer society that was created in industrialized countries depended (and depends) to a large extent on the domestic use of electricity. Artificial lighting

modified the duration and time distribution of individual and social activities, industrial processes, transportation, and telecommunications. To satisfy these requirements, different energy sources are used such as coal and oil, but also gas, nuclear energy, hydraulic energy, wind, sea, sun, and biomass. However, electricity, being a derived product, begins its boom when coal, oil, and gas serve as raw materials [7].

Although it is used less today, coal was the fuel par excellence in the most developed countries until it gave way to oil, well into the 20th century. Both constitute non-renewable energy sources, meaning that there will come a time when they will be exhausted.

Oil has a higher energy density than coal, is easier to transport, and produces less combustion waste. Until now it had been easier to extract. For this reason, its consumption was imposed after the Second World War, giving rise to the so-called oil era[8]. However, the use of coal and oil not only means the consumption of unsustainable resources and rising prices but also increases the emissions of gases, especially CO<sub>2</sub> responsible for global warming.

This increase can be confirmed by looking at the increase after World War II (1945) as can be seen in Figure [9].

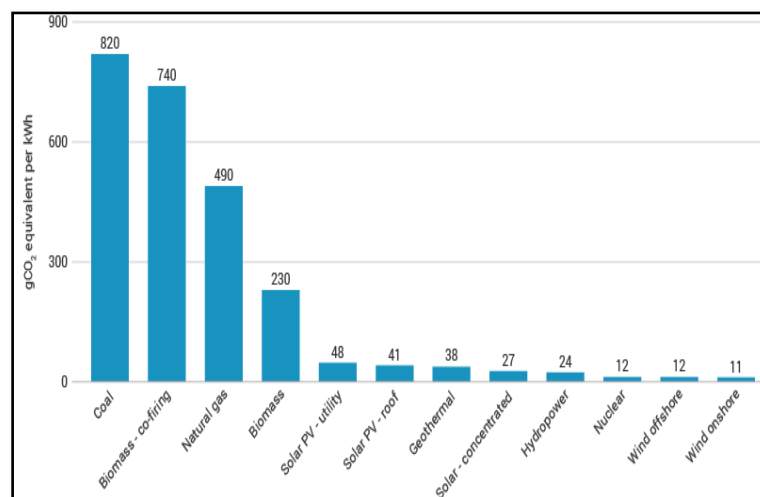


**Figure 1.1 Average life-cycle CO<sub>2</sub> equivalent emissions (source: IPCC) [8]**

The most significant energy source is oil in today's society, and almost everyone needs it. In one way or another, we depend on it for transportation, electricity, and light every day of our lives. It also lubricates machinery and creates tar to build roads.; and a wide variety of chemical products are manufactured from it that make daily life more comfortable[9].

Despite how indispensable it is in our lives; oil is seriously questioned today. In addition to the pollution it generates, it has a major associated problem: Western and Asian countries do not have enough of it and depend on countries in conflict with unstable regimes that do not guarantee their supply, a circumstance that has become a permanent source of conflict. The desired resources are largely controlled by Islamic countries with little affinity with Western society.

Other signs associated with excessive use of oil are the following [10]:

- Excessive occupation of spaces.
- Overexploitation of aquifers and water pollution.
- Large-scale migrations.
- A tendency towards an urban way of life and loss of contact with nature, with excessive growth of the suburbs of large cities.
- Wars, invasions, and repression in poor countries.
- Inequality between rich and poor.
- Globalization: power in the hands of large corporations.
- Health problems.

Presently, the depletion of oil reserves is a grave trouble, since at the existing rate of utilization, in less than 40 years, the world's reserves would be depleted. The high dependence that the world has on oil, the unpredictability of the global market, and the erratic nature of this product's pricing, have led to the search for new, more

economical, and renewable forms of energy such as solar, wind, hydroelectric, and the use of biofuels, among others [11].

An obvious fact is the exponential growth of per capita energy consumption with the development of modern society, a fact that is even more evident from the beginning of the Industrial Revolution in the mid-19th century. This is an unsustainable trend, promoted only by the development of current consumer societies, and which must be taken to acceptable limits for the benefit of the future of humanity[12].

## **1.2. Climate Change**

Climate change represents one of the gravest threats facing humankind in the 21st century. No longer is global warming a hypothetical threat, but a reality. The United Nations Framework Convention on Climate Change (UNFCCC) [13], sought to strengthen global public awareness about Climate change, and defined it as “the shift in climate that is caused by human activity and modifies the composition of the Earth's atmosphere, either directly or indirectly.” In the current energy model, which is an open system, man adds high amounts of carbon dioxide (CO<sub>2</sub>) to the atmosphere at a rate such that nature is unable to recycle said compound. This CO<sub>2</sub> of anthropogenic origin is basically due to changes in land use (mainly due to deforestation) and emissions from the use of fossil fuels. As a consequence of this increase in the atmosphere, thermal radiation reaches the Earth passing through the atmosphere more easily than thermal radiation from the Earth is transferred to space, producing warming throughout the planet. This phenomenon is known as “the greenhouse effect.” As a result of this warming, climate impacts will occur with the following consequences [14]:



- Sea level rise.
- Increase in extreme meteorological phenomena such as torrential rains, droughts, thaws,
- Tropical storms (hurricanes and tsunamis), heat, and cold waves.
- Extinction of species and destruction of ecosystems.
- Ocean acidification.

### **1.3. Social and economic crises**

Climate warming is the order of the day; The Stern report and the sixth report of the IPCC (Intergovernmental Panel on Climate Change) have confirmed this serious problem, as well as its costs, and social and economic consequences. Global warming could mean costs reaching up to 40% of the global economy's GDP. Even at the best conventional economic growth rates, the damage caused to societies by significant and more violent climate variation will outweigh them [15].

This sixth IPCC report has made it clear that the fundamental basis of climate is human; the consumption of fossil fuels and deforestation occupy the first places in his explanation. Considering industrialized countries, the members of the OECD (Organization for Economic Cooperation and Development), the Middle East, the rest of Europe, and Russia, concerning energy consumption there is great inequity, taking into account that they inhabit 36.5% of the world population.

However, approximately 64% of primary energy is consumed [16]. This is also reflected in per capita energy consumption: for example, an inhabitant of the United States emits 5,416 million tons of CO<sub>2</sub>, China 10,065 million tons of CO<sub>2</sub>, and India 2,654 million tons of CO<sub>2</sub>. Countries must take measures for an adequate and fair distribution of energy, as well as curbing the increase in demand for fossil fuels,

increasing the diversity of energy supply, and reducing greenhouse gas emissions[17].

The main issues under the summit were -

- Increase in greenhouse gas emissions due to possible deforestation of forest ecosystems.
- Increase in water consumption and pollution.
- Increase in the use of fertilizers and pesticides.
- Greater soil degradation and erosion.
- Increase in the generation of stillage in the production of ethanol, and methanol and glycerin in the production of biodiesel.
- Atmospheric emissions of local impact that require further evaluation both in their impact on human health and the environment.
- Introduction and propagation of genetically modified organisms as well as exotic species.

Following the above, strategies must be aimed at effectively incorporating environmental considerations in public and private decision-making, to potentiate the positive impacts and counteract the negative ones of the production and use of biofuels in India. Biofuels can be presented as an alternative for development and growth, as long as there is responsible management, focused on the progress of the country and the well-being of its people.

Some developing countries are blessed with lands of great agricultural wealth, suitable for production and marketing. However, if they are only satisfied with the simple extraction of the raw material without adding value to the oil if priority is not given to internal demand if crops are not diversified, and if they are not managed ethically and responsibly, this renewable wealth. They can become a double-edged sword and this great opportunity will become another vein through which a valuable

natural resource is drained that will end up feeding the voracious appetite for cars in some industrialized country. Then biofuels will be nothing more than the subsidy of the poor for the well-being of the most favored[18].

Above all perspectives, we should always keep in mind “that the most environmental and purest energy is the one used in our particular and collective commitment to saving the energy of our planet.”

#### **1.4. Biofuels as an Alternative**

One of the proposals to contribute to the solution of the energy problem that is advancing more rapidly is that of liquid biofuels. These are defined as those fuels obtained from biomass that are in a liquid state at standard temperature and pressure conditions. They are utilized in internal combustion engines or boilers that produce both heat and electricity, in which case they are called biofuels[19].

The first branch of biofuels is bio-ethanol obtained from sugary raw materials (cane, beets), starchy raw materials (corn, cassava), or cellulose. The process from starch and cellulose is more complex than from sucrose, as it involves additional pretreatment processes of the raw material (sometimes plant residues from other processes), which may consist of a combination of crushing, pyrolysis, and attack with acids and other substances, so that the biomass can then be attacked by hydrolyzing enzymes in fermentation reactors[19], [20].

The second branch of biofuels on which this thesis focuses its research is biodiesel, initially obtained from conventional oilseed plants, such as African palm, soybeans, and rapeseed; or from alternative oilseeds (Jatropha, Cynaracardunculus, castor beans, etc.) or used frying oils[21].

One of the biggest problems facing humanity is the consistent availability of clean and renewable energy. Fuels that both safeguard the environment and meet the

population's energy needs are sought, although biofuels are not a solution to the energy problem on their own. The underlying issue is not only to find a replacement for oil but also to try to reduce energy consumption and improve efficiency, which requires a change in habits and technology.

Biodiesel and bioethanol may be only a partial, and perhaps temporary, solution. Furthermore, its production and use still have social, and environmental, techniques, and policies to overcome or at least clarify [20], if production systems are not adequate and planning is not ethical and intelligent, the large-scale cultivation of oilseeds to produce biodiesel can have serious social and environmental impacts [22].

## CHAPTER-2

# LITERATURE REVIEW

---

### 2.1 General Information about Biodiesel or FAME

FAME is a renewable fuel from straight vegetable oils or fats of animal origin, which can be used totally or partially to replace diesel fuel in self-ignition engines without requiring substantial modification thereof (Agarwal, 2007; Skaib and Zedan, 2023). The Environmental Protection Agency (EPA) in the US has authorized the use of biodiesel as a fuel and additive. It has been classified as a clean fuel, as long as its physical-chemical characteristics are within the specifications of European standards. The standard norm is UNE EN 14214 (in the case of North America the standard norm is ASTM D6751) (Singh *et al.*, 2019).

**Table 2.1 Evaluation of physicochemical Characteristics of Palm Oil and Biodiesel and Petroleum diesel**(Benjumea, Agudelo and Agudelo, 2009; Ahmad *et al.*, 2012)

Property	Palm Oil	Palm Biodiesel	Diesel
Density at 15 <sup>0</sup> c (Kg/M <sup>3</sup> )	918	871.6	859.3
Viscosity at 40 <sup>0</sup> C (mm <sup>2</sup> /S)	39.6	4.73	4.33
Cloud Point ( <sup>0</sup> C)	-	16	-3
Cetane Number	42	62	46
% Carbon Residue	-	0.02-0.22	0.15
% Sulfur	0.02	0.04	0.29
Flash Point ( <sup>0</sup> C)	267	155-174	60

The most common biodiesel-diesel mixture is the one with 20% biodiesel and 80% diesel, better known as B20. But in some industrialized countries it has been used effectively in higher proportions (B30), and even in its pure form (B100). Biodiesel is also used as heating fuel(Drabik and Venus, 2019).

Vegetable oils (and also animal fats) are made up of molecules (esters) of fatty acids and glycerol. Oils and fats owe their high viscosity to the latter. Through Trans-esterification, glycerol (trivalent alcohol) is replaced by a monovalent (“lighter”) alcohol, usually methanol or ethanol, forming smaller molecules (monoalkyl esters or

FAME) with a viscosity similar to that of diesel fuel derived from oil (Table 2.1). Glycerin is also produced as a byproduct, a substance that has numerous uses in various industries. As a particular case, Table 2.1 compares the properties of palm oil with its respective biodiesel and a particular diesel (Benjumea, Agudelo and Agudelo, 2009; Ahmad *et al.*, 2012).

## **2.2 Biodiesel's Historical Development**

When Rudolf Diesel was constructing his engine in 1895, It was he who proposed the use of vegetable oils as fuel. Consequently, he used peanut oil as fuel when the diesel engine was first introduced in 1900 at the World Exhibition in Paris. (Fernández-Tirado, Parra-López and Romero-Gámez, 2021).

The high viscosity of the oils, which is roughly 10 times greater than that of diesel, was a drawback to their use because it meant that the fuel was not properly atomized, leading to incomplete combustion. Vegetable oils' high flash point and propensity to thermally oxidize hindered their use by causing deposits to build up on injector nozzles and a reduction in lubricity. With various techniques such as dilution or microemulsion, pyrolysis, or Trans-esterification, it has been attempted to alter its properties to resemble those of diesel (No, 2020). However the low price of oil at that time meant that diesel immediately took the preferential place and oil was abandoned as an alternative (Casanave, Duplan and Freund, 2007)

Paradoxically, the resurgence of Diesel's idea of using vegetable oils in its engines began to gain strength again towards the end of the 20th century, this time around, primarily due to linked environmental concerns, in the form of biodiesel (which is nothing more than modified vegetable oil), due to the necessity to discover alternatives to fossil fuels in light of climate change. Until a few years ago it was possible to identify other inspirations, in accumulation to environmental ones, to

promote its use in different regions; for example, the surpluses of soybean cultivation in the USA, or the surpluses of agricultural cultivation in Europe that promoted the policy of putting lands into rest so as not to affect the prices of agricultural products. However, since the price of vegetable oils was significantly greater than the price of diesel, it still needed hefty subsidies or tax breaks to ensure its profitability (Agrawal, Belkhode and Rokhum, 2022).

With the sharp increase in oil prices that began in 1983, and on October 2, 2023 (\$92.87) per barrel of Brent (Carlson, 2023) vegetable oils and animal fats started to cost the same as diesel and generated this recent boom of liquid biofuels worldwide, which also includes bioethanol (which is ethanol or ethyl alcohol), which can be used as a complement or substitute for gasoline.

### **2.3 An objective look at biodiesel**

Biodiesel is an alternative that has gained special attention in the global market, although it has often been questioned and is still subject to overcoming several problems and many prejudices. A tool to measure the energy cost of a product is life cycle analysis, which takes into account all the operations and treatments that are carried out from the cultivation of the raw material used (oilseeds) to the finished product. However, it works with parameters and variables with a wide margin of error that yields different results depending on the source and that can be manipulated (Pinto, 2019). For these reasons, the balance of greenhouse emissions offers many possibilities or causes many groups (some of them environmentalists) to tear their clothes.

There is a Life Cycle Analysis (LCA) study applied to biofuels, which was carried out by ISO 14040-43 standards on behalf of the Ministry of Environment and Forests,

according to which biofuels produced in India reduce greenhouse gas emissions. effect compared to diesel and petrol (Sobrino, Monroy and Pérez, 2011).

It is very important and necessary to know the advantages of biodiesel and its deficiencies to try to correct them. This challenge should motivate us to work more intensely, looking for spaces, inputs and procedures that make this alternative more technically, socially and economically viable.

## **2.4 Advantages**

Currently, the countries of the European Union, the United States and India, among many others, have supported the use of biofuels to reduce greenhouse gas emissions, promote the de-carbonization of transportation fuels, diversifying the sources of its supply, develop long-term alternatives to oil, use idle lands and reforest the vegetation layer (Singh and Singh, 2010). In rural or low-income areas, increased biofuel production is also anticipated to present fresh prospects for income and job diversification (Demirbas, 2008).

### **2.4.1 Reduction in Polluting Emissions**

A study carried out by the EPA (Environmental Protection Agency) in 2022 shows that the use of this biofuel has environmental advantages, since using it pure a reduction of 90% of hydrocarbons (HC) and a reduction of 75-90% is achieved in polycyclic aromatic hydrocarbons (PAHs). Likewise, it reduces emissions of carbon dioxide (78% less) and sulfur dioxide (SO<sub>2</sub>), particulate matter (PM), heavy metals, carbon monoxide (CO), and volatile organic compounds [40]. On the other hand, biodiesel can increase or decrease nitrogen oxides (NO<sub>x</sub>) depending on the measurement method and the type of engine (Kumar, Kumar and Singh, 2010). According to (Melikoglu *et al.*, 2016) what favors this increase are oils that have a



large composition of unsaturated acids (Majer *et al.*, 2009). Table 2.2 compares emissions between diesel and biodiesel.

**Table 2.2 Variation in emissions of Soy Biodiesel (B100) and its mixture with Diesel (B20) with compared to petroleum diesel** (Majer *et al.*, 2009; Luque and Clark, 2010)

ISSUE TYPE	B100 (%)	B20 (%)
<b><i>Regulated</i></b>		
NOx	+13	+2
Particulate matter (PM)	-30	-22
Hydrocarbons (HC)	-93	-30
Carbon monoxide (CO)	-50	-20
<b><i>Not Regulated</i></b>		
Sulfates	-100	-20
Hydroc. Arom. Police (PAH)	-80	-13
Ozone potential of spiced HCs	-50	-10

#### 2.4.2 Lubricity

Biodiesel's high oxygen content improves combustion and lowers the risk of oxidation. The combustion efficiency is higher than diesel because the oxygen mixture with the fuel is more evenly distributed during combustion. Biodiesel doesn't include sulphur and has a weighted oxygen content of 11%. Due to its superior lubricating properties over petroleum diesel fuel and the fact that its consumption, ignition, performance, and engine torque fluctuate very little from their typical values, the use of biodiesel can thereby increase the useful life of engines (Eiadtrong *et al.*, 2019).

#### 2.4.3 Biodegradability and Toxicity

Biodiesel is non-toxic and breaks down four times more quickly than conventional fuel. Because it contains oxygen, the degrading process is enhanced. The studies of biodegradability of various types of biodiesels in aquatic environments reported easy degradability for all of them. Only 18% of diesel fuel had degraded after 28 days, compared to 77%–89% of biodiesels. (DeMello *et al.*, 2007).

The mixture of biodiesel with diesel or gasoline increases the biodegradability of the fuel, due to synergistic effects of co-metabolism. As a result, for B5 (a mixture of 5%

biodiesel and 95% diesel), the time required to reach 50% biodegradation is shortened from 28 to 22 days, and for B20, it is shortened from 28 to 16 days(Pasqualino, Montane and Salvado, 2006).

## **2.5 Disadvantages**

The technical problems of biodiesel are related to its high viscosity, lower calorific value, poor behavior at low temperatures, slight increase in no emissions., injector cooking, engine wear and greater dilution of the engine lubricant. Furthermore, its biggest problem is the high cost and availability of raw materials. Some sectors have raised social questions and blame this biofuel for the increase in food prices and the deforestation of jungle areas(Pinzi *et al.*, 2009; Shereena and Thangaraj, 2009).

### **2.5.1 Higher Viscosity**

Due to its high viscosity, biodiesel may cause flow losses through the injectors and filters, potentially leading to dilution of the lubricant and coking of the injector if spray modification occurs(Ali *et al.*, 2008).

### **2.5.2 Mechanical Performance**

The engine power decreases because the lower calorific value (GV) of the biodiesel is lower. The heat of combustion is reduced by approximately 12% due to the presence of oxygen within the molecule, this decreases torque and power by about 10%, mainly due to the reduction in heat of combustion. Likewise, this decrease results in greater fuel consumption to achieve the same performance using diesel fuel (Mishra, Chauhan and Mishra, 2020a).

### **2.5.3 NO<sub>x</sub> Emissions**

Biodiesel can increase or decrease nitrogen oxides (NO<sub>x</sub>) depending on the biodiesel raw material. It was found that the higher the degree of unsaturation of the biodiesel

feed stocks (e.g., rapeseed and soybeans) produced higher NO<sub>x</sub> emissions(Pham *et al.*, no date).

#### **2.5.4 Behavior at Low Temperatures**

Biodiesel has problems operating at low temperatures. Generally, the Freezing Points, Cloud Points (CP), as well as the Cold Filter Plugging Point (CFPP) are from slightly higher to much higher depending on the origin of the ester (soybean, sunflower or palm). Saturated glycerides produce crystallizations at relatively low temperatures and increase cloud point and CFPP. For example, biodiesel produced from palm oil has a cold filter plugging point of +11<sup>0</sup>C and cloud point of +13<sup>0</sup>C (Musthafa *et al.*, 2018). These values prevent its use in winter seasons but in summer or in tropical countries (Benjumea, Agudelo and Agudelo, 2009; Ullah, Bustam and Man, 2014).

#### **2.5.5 Lubricant Dilution**

Motor oil (lubricant) can degrade much faster if the fuel used is biodiesel instead of diesel. Biodiesel tends to dissolve more easily in lubricant than diesel. The dilution produced by biodiesel in the oil causes the viscosity to decrease in the early stages (fuel dilution). In later stages, it increases over time (lubricant oxidation) due to the formation of deposits and lacquers, caused by the tendency of biodiesel to oxidize and polymerize the lubricant, due to the presence of double bonds in its structure(Knothe and Razon, 2017). For these reasons it is recommended to use a lubricant that has a higher dispersant capacity than that used with diesel, otherwise it is recommended to change the lubricating oil in shorter periods than using normal diesel.

#### **2.5.6 Corrosion Problems**

Some problems may appear due to corrosion and wear particles in the tank, which must be taken into account not only as it affects the engine, but also with respect to the installation, especially when pure biodiesel (B100) is used. Some materials

deteriorate with biodiesel: paints, plastics, rubber, etc. That is why nitrile gaskets in contact with biodiesel dissolve, so they must be replaced with Viton, Teflon or other gaskets that are more resistant. Likewise, if B100 is used, it is recommended that the paints on the fuel tank and other parts in contact with the fuel be replaced with other acrylic paints(Pradelle *et al.*, 2019).

#### **2.5.7 Oxidation stability**

If biodiesel comes from an oil with a high concentration of linolenic acid (C18:3) or unsaturated acids in general (soybean, rapeseed or sunflower), it will present oxidation stability problems because it has double bonds and oxygen in its molecule. This is important when storing biodiesel for a long time. The use of containers that contain copper, zinc, lead or some combination of these three has a very negative effect on stability since it forms a large amount of sediment, deposits in the injectors, and clogging in the filters. For this reason, it is recommended to preferably use zinc or steel materials (Amran, Bello and Ruslan, 2022).

#### **2.5.8 Price**

Although biodiesel is a viable technological substitute for diesel, it is now 1.5–3 times more expensive in wealthy countries than diesel. Government policies determine the competitiveness of biodiesel, such as subsidies and tax exemptions, because without these subsidies it is not economically feasible (Brown *et al.*, 2020).

### **2.6 Current panorama of biodiesel in the world (2021)**

Global biodiesel production has increased exponentially since its first industrial production about 20 years ago. This behavior can be observed in Figure 2.1 according to a report made by(Mizik and Gyarmati, 2021).

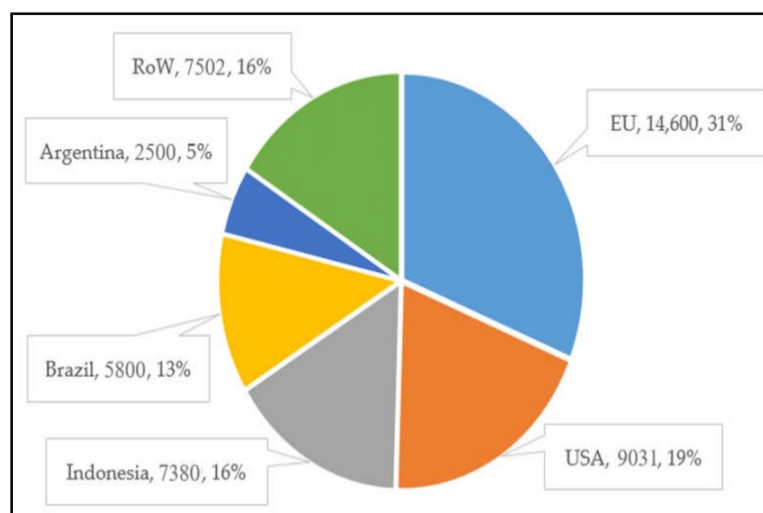


**Figure 2.1 Estimation of global biodiesel production** (Mizik and Gyarmati, 2021)

## 2.7 Raw materials and reagents

Oil seeds and the oils they produce are the primary raw materials used to make biodiesel. It may be claimed that conventional oilseeds, particularly sunflower, palm, rapeseed, and soybean are the primary sources of oil used to make biodiesel. To make biodiesel, any substance containing tri-glycerides can be used, including leftover frying oils, cow tallow, chicken and fish fat, etc. More than 300 different species can be used to produce vegetable oils. However, only a few species of economically viable oilseed plants can currently be produced due to environmental and geographical factors, crop yield, oil content, and the necessity for mechanization. Any nation or region faces difficulty in implementing procedures based on locally available raw resources, which must be optimized to produce biodiesel that is both competitively priced and meets worldwide quality standards for manufacturing. Use in diesel engines as fuel. The primary raw ingredients required to produce biodiesel are listed below, with a focus on vegetable recycled oils, which were the raw materials utilised in this study's experimental phase.

### 2.7.1 Traditional vegetable oils

Ethanol and biodiesel obtained from traditional energy crops are called first-generation biofuels, and second generation to those obtained from plant species that

do not enter into direct competition with the food market, or plant or animal waste. The products used for the production of biodiesel called “first generation” are obtained mainly from world-known oilseeds, such as soybean, sunflower and palm (No, 2020; Alhammad *et al.*, 2023; Mathur *et al.*, 2023).

## **2.8 Rapeseed oil (*Brassica napus*)-Agronomic and pedological requirements**

It is an annual or biennial plant with yellow flowers, adapted to cold climates. It requires fertile, well-drained soils, and responds favorably to nitrogen (N) and phosphorus (P) fertilization. Sunny days and cool nights favor its growth; Dry weather during harvest is essential. It tolerates annual rainfall between 300 and 2800 mm and average temperatures between 5 and 27°C. It can be planted after crops of some grains, potatoes, beets or after fallow, but not after rape, mustard or sunflower. Rapeseed in India is sown in Rabi Season (September-October), (N. Khumdemo Ezung *et al.*, 2008a; Jamil, 2023).



**Figure 2.2 Rapeseed cultivation**

Rapeseed (*Brassica napus*) Figure 2.2 is a cruciferous plant with a taproot and deepening root. When this main root encounters obstacles to go deeper, it is easy to develop secondary roots. The stem is roughly 1.5 meters in length. While the upper leaves are whole and lanceolate, the lower ones are petiolate. The tiny yellow flowers are arranged in terminal clusters. Depending on the cultivar, there are 20–25 grains

per pod of silique fruits (N. Khumdemo Ezung *et al.*, 2008b; Atabani *et al.*, 2012). When fully grown, the spherical seeds have a diameter of 2 to 2.5 mm and a colour that ranges from reddish brown to black (Figure 2.3).



**Figure 2.3 Rapeseed Seeds**

Rapeseed has a proportion of 40 to 45% oil. The production of this crop can vary depending on the time of year from 700 to 1600 kg/Ha/year (McDowell, Elliott and Koidis, 2017).

**Table 2.3 Composition of Rapeseed**

<b>COMPOSITION</b>	<b>% w/w</b>
Proteins	21.08
Non-nitrogenous extracts	19.41
Fiber	6.42
Fat	48.55
Ashes	4.54

### **2.8.1 Seed Composition**

The composition of rapeseed is represented in Table 2.3. Rapeseed is characterized by its high level of erucic acid (approx. 50%) which causes serious heart and liver problems in animal experiments. Furthermore, the presence of glucosinolates in the edible part significantly reduces its value as animal food.

## **2.9 Anola (Brassica Rapa)**

It is a variety of rapeseed with low erucic acid content ( $< 2\%$ ) and glucosinolate levels below  $30 \mu\text{mol/g}$ , making it suitable for human consumption. It has improved agronomic characteristics and has been developed through genetic engineering in Canada.

## **2.10 Sunflower Oil (Helianthus Annuus)**

### **2.10.1 Agronomic and pedological requirements**

Annual herbaceous plants best adapted to warm or temperate climates. It can grow from the equator to  $55^\circ$  latitude. In the tropics, it grows best at medium and high elevations. Intolerant of shade, but tolerant of dryness and drought, except when flowering. It can grow in poor soils, as long as they are deep and well-drained. It does not resist acidic or flooded soils. It tolerates annual rainfall between 200 and 4000 mm and temperatures between 6 and  $28^\circ\text{C}$ . In warm areas, dwarf varieties mature 2.5-3 months after planting. It should not occur in rotation more than once every 4 years, and should not be in rotation with potatoes (Supriya *et al.*, 2017; Das *et al.*, 2018; Sakthivel *et al.*, 2018).

Its root system is very powerful, it can have up to 8 cm in cotyledon state and 5 to 10 secondary roots. In the 4 to 5 leaf stage, it can reach 50 to 60 cm deep. Secondary roots tend to first grow horizontally and eventually grow perpendicular to the ground for better use of water (Figure 2.4).





**Figure 2.4 Sunflower cultivation [63]**



**Figure 2.5 Sunflower seeds.**

The stem reaches a variable height and can reach from 60 cm to 2 m. The “de boca” (sunflower for pipe consumption) can be even higher. The stem is very rough and coarse to the touch, and often has large villi (Dueso *et al.*, 2018). The fruit is called “achene” (pipe) and is a dry fruit (Figure 2.5). This almond or grain has an oil content of 45 to 55% by weight (of which 65% is unsaturated) and the shell that covers it has approximately 26.61% fiber.

#### **2.10.2 Seed Composition (Table 2.4)**

The production of this crop can vary depending on the time of year from 600 to 950 kg/ Ha/year (Dueso *et al.*, 2018).

**Table 2.4 Composition of sunflower seed (Dueso *et al.*, 2018)**

Composition	% W/W
-------------	-------

Saturated Fats	14
Monounsaturated Fats	23
Polyunsaturated Fats	65
Oleic Acid (Omega-9)	29
Linoleic Acid (Omega-6)	58
Palmitic Acid	6
Stearic Acid	5

## 2.11 Soy Oil (Glycine Max)

### 2.11.1 Agronomic and pedological requirements

Annual herbaceous plant, spring-summer, whose vegetative cycle ranges from three to seven months and from 40 to 100 cm in wingspan. It also adapts to humid tropical or subtropical climates. It does not resist excessive heat or severe winters, its temperature optimum is 24-25<sup>0</sup>C, but it resists average annual temperatures between 5.9 and 27<sup>0</sup>C. Temperatures above 40<sup>0</sup>C cause an undesirable effect on growth speed, causing damage to flowering (Gautam and Kumar, 2015; Amol and Bhati, 2021). Soybean is a short-day plant that is sensitive to day length. That is, specific light hours are necessary for a particular type to flower. It grows best in fertile, well-drained soil. This legume can fix nitrogen to the soil and does not require fertilization with this element. It has been reported to tolerate rainfall between 310 and 4100 mm. The growth period is 4 to 5 months. It is used in rotation with corn, smallgrains, otherlegumes, cotton, and rice.It may be sown following winter grain or following early potatoes and veggies.



**Figure 2.6 Soyabean Cultivation.**

The main root can reach up to a meter in depth, although it is normal for it to not exceed 40-50 cm. Nodules are found on the main root or the secondary roots, in variable numbers. Its stem is rigid and erect, it acquires variable heights, from 0.4 to 1.5 meters, depending on varieties and growing conditions. It is usually branched. It has a tendency to lodge, although there are varieties resistant to lodging.



**Figure 2.7 Soybean fruit.**

The leaves, stems and pods are pubescent, the color of the hairs varying from blonde to more or less grayish brown (Engineering, 2012; Yerrenagoudaru *et al.*, 2018). It has axillary racemose inflorescences in variable numbers. They are butterfly-shaped and whitish or purple, depending on the variety. Its fruit is a pod dehiscent at both sutures. The length of the pod is two to seven centimeters. Each fruit contains three to

four seeds. The seed is generally spherical, pea-sized, and yellow (Figure 2.6, Figure 2.7). Some varieties have a black spot that corresponds to the seed thread. Its size is medium (100 seeds weigh 5 to 40 grams, although in commercial varieties it ranges from 10 to 20 grams). The seed is rich in proteins and oils. In some improved varieties it has around 40-42% protein and 20-22% oil, compared to its dry weight. In soy protein there is a good balance of essential amino acids, highlighting lysine and leucine (Hira and Das, 2016).

### 2.11.2 Seed Composition

Soybeans have a proportion of 18 to 21% oil. The production of this crop can vary depending on the location from 280 to 580 kg/Ha/year (Ahmad *et al.*, 2012; Mshelmbula *et al.*, 2023).

**Table 2.5 Composition of soybean** (Mshelmbula *et al.*, 2023)

Composition	% w/w
Proteins	40
Fat	21
Carbohydrates	34
Ashes	4.9

Excellent sources of protein and energy for both human and animal nutrition are soybeans. In addition, it contains significant percentages of essential nutrients such as linoleic acid and lysine. Despite the apparently excellent nutritional value it has based on its chemical composition, the presence of anti-nutritional factors (antitryptic factors, lectins, oligosaccharides, etc.) Table 2.5 make it necessary to process the seed before using it as raw material in food. Said processing is also necessary when by-products derived from the industrial process of obtaining soybean oil are going to be used. Due to their importance in animal feed, soybean hulls and meal stand out (Sumangala and Kulkarni, 2019). Due to the fact that soybean meal is used as both animal feed and a source of protein for human consumption, soybean oil is the most

widely used raw material for biodiesel. Like its oil, the biodiesel produced has high levels of Iodine ( $121 - 143 \text{ g I}^2/100\text{g}$ ) that do not allow it to comply with the EN 14214 standard without the help of oxidizing additives. The main uses of this oilseed are very varied, such as salad oil, margarine, food products, soaps, paints, insecticides, disinfectants, and biodiesel. Lecithin extracted from the oil is used as an emulsifier in the food and pharmaceutical industries. Cake is an important source of protein for animal and human food (Guzeler and Yildirim, 2016).

## **2.12 Used Frying Oils**

One of the primary contributors to water pollution is leftover cooking oil (Foo *et al.*, 2021). It is challenging to remove the film from that edible oils made from raw materials like sunflower, soybean, olive, maize, or palm develop on the water's surface, affecting its oxygen exchange capacity and altering the ecosystem.

Used cooking oils are referred to as "dark or brown fats" if the percentage of free fatty acids is more than 15% w/w and as "yellow oil" if it is less than 15% (Ferdous *et al.*, 2013; Hajjari *et al.*, 2017). The need to refine some vegetable oils does not make them economically feasible for the production of biodiesel, due to the high cost of raw materials and production (Moyo *et al.*, 2021; Palüzar, 2023). The cost of refined oil represents 75 to 80% of the total price of biodiesel (Tamalampudi and Fukuda, 2011; Abdi, 2019). Waste cooking oils are mainly obtained from the restaurant industry or recycled at special sites (Rahman *et al.*, 2020) Figure 2.8. Depending on the source and availability, it could be 60% less expensive than refined oils. (Vela *et al.*, 2020). Used oils have a high level of reuse, and show good suitability for use as biofuel. However, these oils have properties of both crude and refined oil.



**Figure 2.8 Frying oil**

Heat and water cause tri-glycerides to hydrolyze more quickly, increasing the amount of free fatty acids in the oil. The un-saponifiable material, viscosity, and density increase considerably due to the formation of dimers and polymers, but the iodine value and molecular mass decrease.

For these reasons, the use of used oils presents logistical and technical difficulties, not only due to its collection but also its control and traceability due to its waste nature. Other problems encountered when using recycled oils to produce biodiesel have to do with the high content of un-saponifiable material, the amount of water, and the high content of free fatty acids, which require several processes to condition the oil for Trans-esterification. The product also usually has low oxidation stability, so it does not meet the UNE 14214 standard (Tsoutsos *et al.*, 2019) and requires the addition of antioxidants.

Finally, the quality of the biodiesel produced normally does not meet the required purity specifications, so it must be subjected to distillation. All these problems and additional processes increase production costs (Banja *et al.*, 2019). Despite these problems, recycled oils are considered one of the most promising options for producing biodiesel is using it as the least expensive raw material, which would prevent the need for waste treatment costs. For these reasons, a wide variety of

researchers have worked with different recycled frying oils for more than 26 years (Kumar and Sidharth, 2018; Mishra, Chauhan and Mishra, 2020b). India is a large consumer of vegetable oils, mainly Mustard and sunflower. Because these oils are rarely reused, they do not undergo significant changes and are well suited for use as biofuel. (Yadav *et al.*, 2022). India produced 116.5 lakh tons of edible oil domestically in 2021–2022 while importing 141.93 lakh tons. The figures indicated a total of 258.43 lakh tons of consumption and demand. Thailand, Indonesia, Malaysia, Brazil, Argentina, and Brazil are India's top suppliers of edible oils. The household sector accounts for around 70% of the total consumption structure, with the remaining portions going to the hotel and industrial sectors (Conservation, Code and <http://mospi.nic.in>, 2007).

### **2.13 Alternative Vegetable Oils**

The problem with conventional oils has led to the promotion of alternative oils. Like the ones of *Ricinus communis* (castor), *Jatropha curcas* L. (*Jatropha*) and *Millettia pinnata* (Karanja), which have been highly promoted in countries such as India and Brazil (Gusamo and Jimbudo, 2015). These oils are non-food oils used in food and are usually characterized because their crops reach high oil yields per hectare. *Jatropha* is one of the plants with the highest yield since it shows an average value of 1590 kg ha<sup>-1</sup> of oil, closely followed by castor oil with yields of 1188 kg ha<sup>-1</sup> (Gusamo and Jimbudo, 2015).

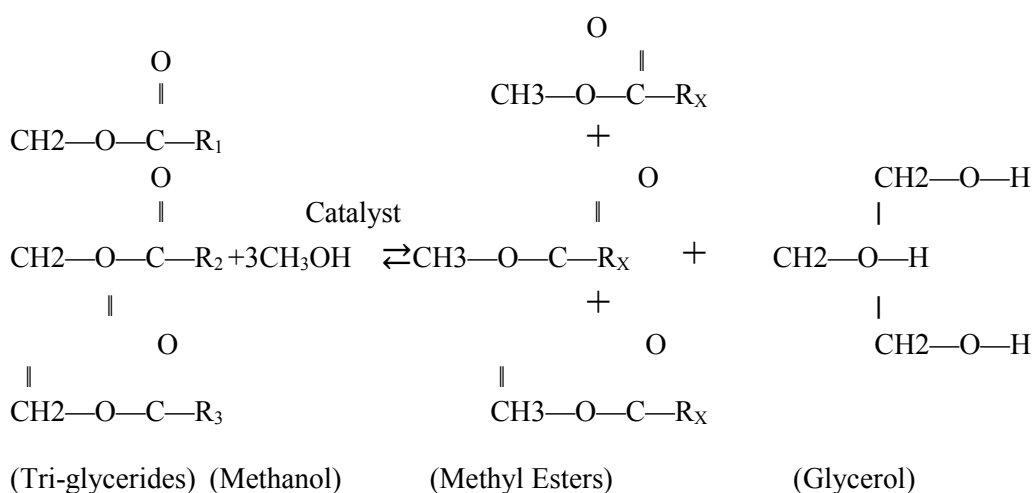
There are numerous species of plants that produce oil and that are susceptible to being unprocessed objects for obtaining biodiesel. Alternative vegetable oils are characterized, on the one hand, due to the high oil yield, as has already been stated, and, on the other hand, because it is plants that survive and develop in extreme conditions of temperature and humidity. The biodiesel from this type of food has been



called biodiesel “from second generation”, since not only do they not need strict climatic conditions, but which, in addition, can be cultivated on marginal lands. Within this enormous group of plants find, Brassica Moringaoleifera, Simmondsiachinensis, Mahuaindica, Azadirachtaindica, Pongamiapinnata, Millettiaapinnatto, Cynaracardunculus, Brassica carinata, Ricinuscomunis, of which the production of biodiesel has been satisfactorily achieved(Shereena and Thangaraj, 2009; Karmakar, Kundu and Rajor, 2018).

### 2.13.1 The Trans-esterification Reaction

The most used method to obtain biodiesel is the Trans-esterification reaction of oils and fats with low molecular weight alcohols (alcoholysis) in the presence of a catalyst appropriate. Basically the reaction consists of the displacement of the alcohol (glycerol) from the structure of the triglyceride by incorporating another short chain alcohol. This displacement involves the separation of the three fatty acid molecules that form the triglyceride, remaining as methyl esters (ME) if the alcohol used was methanol, ethyl esters (EE) if it were ethanol, and so on. Equation 2.1 represents the reaction global for the case in which the alcohol used is methanol.



$\text{R}_1, \text{R}_2, \text{R}_3$ : Aliphatic chains

**Equation 2.1 Trans-esterification reaction of a generic triglyceride with methanol**



The previous equation which represents the global Trans-esterification reaction, but in reality, This reaction occurs through the development of three reversible reactions, in series with respect to oil and in parallel with respect to alcohol (Gnanaprakasam *et al.*, 2013). Tri-glycerides are converted into di-glycerides, then mono-glycerides and finally glycerin. Equation 2.2 states that stoichiometry dictates that three moles of alcohol are required for every mole of triglyceride in order to produce three moles of esters and one mole of glycerin. In mass units, for each kilogram of triglyceride approximately another kilogram of biodiesel and 0.10 kilograms of glycerin are obtained.

Tri-glyceride + CH<sub>3</sub> OH → Di-glyceride + CH<sub>3</sub> COOR \_Step1

Di-glyceride + CH<sub>3</sub> OH → Mono-glyceride + CH<sub>3</sub> COOR \_Step2

Mono-glyceride + CH<sub>3</sub> OH → Glycerol + CH<sub>3</sub> COOR \_Step3

**Where, R1, R.2, R.3: Aliphatic Chains**

**Equation 2.2 Steps of the Trans-esterification reaction of a generic triglyceride with methanol**

In general, the oil has low solubility in alcohol, so the stage controlling the speed of the process is usually the transfer of matter. Here it is put manifest the parallel nature of the three reactions (Balat, 2008). To facilitate the transfer of matter between reagents it is necessary to increase the agitation of the sample, so, in general the reaction will take place in an agitated medium. After this first stage has been developed controlled by the transfer of matter, the serial nature of the reactions, in part, also favored by the increase in miscibility that occurs with the appearance of the first alkyl esters that act as a solvent for alcohol and glycerides. Therefore, the reaction between the vegetable oil and the reactant alcohol (step determinant) will be favored by the presence of alkyl esters, so that the Tri-glycerides will gradually react in larger amounts (Ataya, Dube and Ternan, 2006; Zaharin *et al.*, 2017). As the progress progresses reaction, increases the concentration of glycerin, this substance

being insoluble both in the esters as in tri-glycerides, which causes the formation of two phases. This phenomenon is doubly positive since it improves the displacement of the reaction towards the formation of biodiesel and facilitates the separation of the reaction products (Mustapić, Krička and Stanić, 2006).

As has been observed, the Trans-esterification reaction is also characterized by being an equilibrium reaction, so it is necessary to carry out the process under conditions that favor the production of biodiesel and avoid the displacement of the reaction towards the reagents. To this end, whenever we intend to produce biodiesel, we work with excess alcohol, which promotes the oil–alcohol reaction (Niculescu, Clenci and Iorga-Siman, 2019).

The alcohols used for the Trans-esterification reaction must be chain alcohols such as butanol, ethanol, propanol or methanol. Among all of them, ethanol and methanol are the most used, especially methanol, which has lower cost and physical-chemical properties favorable ones such as the shorter chain length and greater polarity, which favor the speed reaction with the oil. It has been shown that methanol results in a higher rate of reaction and is easy to dissolve the basic homogeneous catalysts, widely used in the Trans-esterification reaction (Gebremariam and Marchetti, 2018). For these reasons it has been decided to use this alcohol in the present doctoral thesis for the study of obtaining biodiesel. Therefore biodiesel obtained in all cases will be composed of methyl esters of fatty acids.

### **2.13.2 Catalysis of Trans-esterification Reaction**

The kinetics of triglyceride Trans-esterification is favored by raising the temperature of the reaction medium; therefore, the boiling temperature is usually used as the reaction temperature of the alcohol used at atmospheric pressure, in the case of methanol the maximum temperatures of work are usually around 60–65°C. Despite

this, the rate of the reaction remains low, for which requires the presence of a catalyst that accelerates the reaction.

Three categories of catalysts exist: enzymatic, heterogeneous, and homogeneous. Within the first and the second, both acidic and basic are differentiated, presenting different characteristics and each one being favored by different reaction conditions (Salaheldeen *et al.*, 2021).

### **2.13.3 Basic Homogeneous Catalysis**

Homogeneous catalysts are those that are soluble in the alcohols used to the Trans-esterification reaction. Specifically, basic homogeneous catalysts usually be substances with a strong basic character, the mechanism of the Trans-esterification reaction When this type of catalysts and methanol are used, it. As a step, when mixing the basic substance with methanol, the formation of the methoxide ion occurs and the protonated catalyst. The alkoxide approaches the triglyceride molecule nucleophilically, resulting in the formation of a methyl ester, diglyceride anion, and tetrahedral intermediate.

The latter deprotonates the catalyst, achieving the regeneration of the active species that will be able to react again with a second molecule of alcohol and start another catalytic cycle. The di-glycerides will be converted to mono-glycerides and these to glycerin following the same mechanism (Salaheldeen *et al.*, 2021).

Compounds with high basic character that are usually used as catalysts in the Trans-esterification reaction are hydroxides, carbonates and alkoxides of sodium and potassium. When any of these hydroxides (NaOH, KOH) or carbonates (Na<sub>2</sub>CO<sub>3</sub>, K<sub>2</sub>CO<sub>3</sub>) When mixed with alcohol, the real catalyst of the process is formed, the alkoxide group. In the industry this is the most used group of catalysts, specifically, hydroxides of Sodium and potassium are preferred due to their low price. In general,

with this type of catalysts the reaction occurs in a short time and under conditions of moderate temperature and pressure.

In addition, basic catalysts are less corrosive compounds than acids, it is necessary small amount of catalyst to achieve very high yields and excess alcohol required is lower than that necessary in other types of catalysis (Patel and Sankhavara, 2017). However, the use of this type of catalysts presents a series of drawbacks or restrictions. Separation of the catalyst from the reaction products is technically difficult, generating large quantities of alkaline wastewater that needs to be treated (Goyal *et al.*, 2021).

On the other hand, for the Trans-esterification process to be carried out properly. The raw material from which the biodiesel is going to be obtained must have a small portion of free fatty acids (FFA) and water. The availability of free fatty acids causes reaction of these with the basic catalyst giving rise to the formation of soaps that can promote the constitution of stable emulsions that prevent the separation of biodiesel and glycerin, causing loss of product and problems that affect the separation and purification of this.

Furthermore, the availability of water can lead to hydrolysis of the esters formed generating AGI and the consequent formation of soaps by reaction of saponification (Dos Reis *et al.*, 2005). The use of hydroxides as catalysts generates a small amount of water in the reaction of this with alcohol, to avoid this phenomenon you can use directly the potassium or sodium methoxides. With these catalysts the previous step described in the mechanism of equation 2.3, thus avoiding the formation of a certain amount of water. However, Greater care is necessary with these compounds since they are very hygroscopic, toxic and flammable, in addition to being more expensive (Bashir *et al.*, 2022).

#### 2.13.4 Homogeneous Acid Catalysis

The most used acid catalyst par excellence is sulfuric acid, however other acids inorganics such as hydrochloric acid, boron trifluoride and phosphoric acid; as well as acids Organic substances such as sulfonic acids have also been widely used in obtaining biodiesel(Raheem *et al.*, 2018; Sahar *et al.*, 2018). The Trans-esterification reaction promoted by acid catalysis follows a slightly different mechanism than that followed with a basic catalyst. The four stages of the aforementioned mechanism. First, the protonation of the group occurs carbonyl, which allows the nucleophilic addition of the alcohol to the carbonyl. From the tetrahedral intermediate formed, the elimination of the diglyceride occurs, forming a new ester and regenerating the catalyst(Paul, Panua and Debroy, 2017).

Acid catalysts are characterized by providing high yields in obtaining of alkyl esters but at a low reaction rate. To achieve high performance in an adequate reaction time, large quantities of catalyst are usually needed and the alcohol: oil ratio is very high. The advantage of this type of catalysts is that they can be used with raw materials with a high FFA content since they catalyze two reactions simultaneously, the Trans-esterification of tri-glycerides and the esterification of FFAs. The Esterification reaction consists of the reaction of a free fatty acid with an alcohol of short chain to give rise to the corresponding alkyl ester and water, thus avoiding formation of soaps and the loss of catalyst due to the presence of FFA (Lotero *et al.*, 2005).

#### 2.13.5 Heterogeneous Catalysis

Heterogeneous catalysts have emerged in response to the disadvantages of homogeneous. These catalysts simplify the separation of catalyst/reaction products and they can be reused. Thanks to the use of this type of catalysts, washing is eliminated of the biodiesel and glycerin purification process, thus avoiding the

generation of a contaminated aqueous effluent that would need to be treated; In exchange, it is only necessary to filter the reaction mixture to separate the catalyst (MacLeod *et al.*, 2008).

The negative points of using this type of catalysts are their high price and complicated preparation, in addition to, in many cases, the need for more extreme conditions which can range from a higher temperature or a higher excess of methanol, to times higher reaction rates or higher pressures (Gaidukevič *et al.*, 2018; Gaide *et al.*, 2021). To these aspects we must add that several of the catalysts classified as heterogeneous are to some extent soluble in the mixture of reaction, giving rise to species, such as metals, in the reaction product that are not part of the constitution of the biodiesel, the glycerin, the initial oil or the intermediate products (Arzamendi *et al.*, 2008).

#### **2.13.6 Enzymatic Catalysis**

Enzymatic catalysts such as lipases are being investigated in obtaining biodiesel, presenting high efficiency. This type of catalysts have the advantages of being able be reused, if they are capable of converting FFA into esters, as was the case with homogeneous acid catalysts, whose activity is not inhibited by the presence of water and the glycerin-rich phase is easily separated (Enweremadu and Mbarawa, 2009; Su *et al.*, 2015; Moazeni, Chen and Zhang, 2019). The drawbacks of this biodiesel production method are the need for very high reaction times, its high cost and that the purification process and Isolation of products is relatively complicated (Qing *et al.*, 2017). Some enzymes used are: Antarctic Candida, Rhizomucormiehei (Lipozyme RMIM) Candida rugosa, and Pseudomonas fluorescens (Li *et al.*, 2006; Jeong and Park, 2008; Ying *et al.*, 2008).

### **2.13.7 Alternatives to Improve the Trans-esterification Reaction**

The Trans-esterification reaction can be optimized with the choice of the alcohol to be used and the alcohol: oil ratio; with the choice of the most appropriate catalyst, temperature and pressure of the reaction and, finally, the reaction time. But in addition, some have been developed techniques that improve the process achieving a higher degree of alcohol: oil mixture, savings energy or saving of the necessary quantities of reagents and catalyst.

#### **2.13.7.1 Medium-High Pressure Processes**

Medium-high pressure processes have been considered those that take place at temperatures higher than the boiling point of methanol at atmospheric pressure (64.7 °C) and at pressures greater than atmospheric. When operating above the critical point of methanol, 240 °C and 8.09 MPa(Tomaszewski, 2018), the reaction is carried out under supercritical conditions, and when operating at temperature and pressure lower than the critical ones the reaction is being carried out under conditions subcriticisms(Alenezi and AL-ANZI33, 2013; Mathew and Anand, 2018; Niculescu, Clenci and Iorga-Siman, 2019).

Under these conditions, work is carried out at high temperatures, which favors kinetics and displaces the balance towards biodiesel production. Furthermore, when working in conditions supercritical, the problems of mass transfer between methanol and the tri-glycerides by generating a single phase, achieving high yields in short intervals of time and in the absence of catalyst. As an additional advantage, they are more tolerant processes with presence of FFA and water (Balat, 2008).

Working at supercritical conditions entails high energy consumption (temperatures close to 350 °C), which adds to the higher cost of the equipment due to having to

resist pressures of around 20 MPa and the risk of working in these conditions. For all this, it is a process hardly applicable at an industrial level(Shunaia and Jazie, 2023).

On the other hand, working in subcritical conditions means less energy consumption and less risk from working at lower temperatures and pressures; although the presence of catalyst. Another positive factor is that the concentration of catalyst that is usually required It can be up to ten times less than that used in a conventional system(Muszyński *et al.*, 2023). In the This doctoral thesis has studied the production of biodiesel under subcritical conditions using castor oil and animal fatsas raw materials for the reaction(Yin *et al.*, 2010).

#### **2.13.7.2 Application of microwave radiation**

The Trans-esterification reaction involves a necessary heating of the production medium. Reaction, an alternative way to carry out said heating is the application of microwave radiation. The main advantages of this process are its ease of operation, the energy savings that its use implies, the reduction of reaction time, which is sometimes da, and the heating rate compared to conventional systems(Rani *et al.*, 2016; Ng *et al.*, 2017).

Microwave radiation is a form of electromagnetic energy located in the range of frequencies of 0.3–300 GHz, with 2.45 GHz being the radiation used by practically all devices both domestic and applied to chemical synthesis. This frequency is found in the optimal range of relaxation times for most polar molecules organic and inorganic, resulting in a more effective heating process (Kumar *et al.*, 2020).

The thermal effect exerted by microwaves on a dielectric body originates from the interaction of the electromagnetic field of radiation with molecular dipoles, permanent or induced, present in the body that oscillate depending on the frequency of the microwave (Kumar *et al.*, 2020). Such oscillations produced against intermolecular



forces result in the heating of the material. Molecules with dipole moment align in the electric field created so that, when the electric field is suspended, the agitation thermal allows the molecule to recover the initial disorder in a time that is defined as “relaxation time”, releasing energy in the form of heat.

When the intention is to heat the interior of a container by heating conventional, such as that produced in an oil bath, the heat passes from outside the container inward so that the highest temperature would be found in the closest area to the walls (closest to the heat source) and diffuses towards the solution to be heated. On the other hand, in the heating process by microwave radiation, the radiation affects directly into the molecules inside the medium, producing internal heating which spreads from the inside out, potentially causing localized superheating, also known as “hot spots” (Error! Reference source not found.) (Kumar *et al.*, 2020; Głowniak *et al.*, 2021).

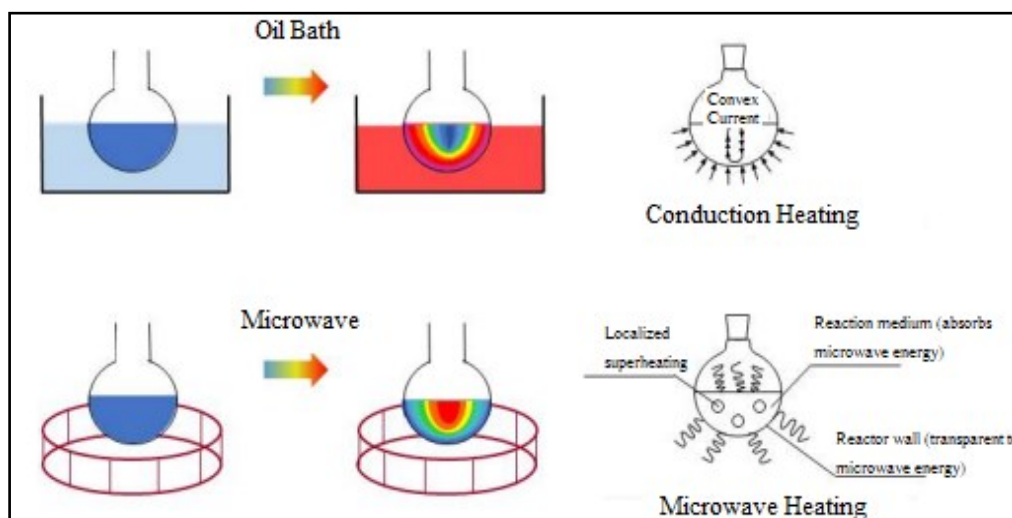


Figure 2.9 Scheme of conventional (above) and microwave (below) heating systems

In the field of chemistry, the positive effects that stand out from microwave radiation are usually the decrease in reaction times, especially those reactions that take place in a heterogeneous phase, the reduction of the thermal degradation of the reactants and/or products and improving the selectivity of chemical reactions. The solutions will experience heating by microwave radiation through two main mechanisms, the

already mentioned interaction or rotation of dipoles and ionic conduction. In the latter, the Heat is generated through friction losses that take place through the migration of dissolved ions (Melo-Junior *et al.*, 2009). Therefore, heating will be favored in compounds with high dielectric constant and ease of experiencing polarizability. In general, the Viscosity will negatively influence the heating of the solutions.

Heating by microwave radiation is presented as a heating source favorable, in contrast to traditional techniques, which can result in comparatively slow and inefficient heat transfer within samples due to the dependence of energy transfer on thermal convection currents and reaction mixture conductivity, leading to Compared to conventional heating, microwave irradiation requires less input energy to produce heat (Melo-Junior *et al.*, 2009). When this form of energy has been used to obtain biodiesel, a fuel with the same properties as the one obtained has been obtained. by conventional heating, but having reduced the reaction time and facilitating the phase separation between glycerin and biodiesel(Nayak, Bhasin and Nayak, 2019). This technology has been used successfully to obtain biodiesel from rapeseed and soybean oil (Hernando *et al.*, 2007), used cooking oil (Chen *et al.*, 2012), jatropha oil (Atabani *et al.*, 2012), palm oil(Saputro *et al.*, 2021)or Pongamiapinnata(SA and Suresh, 2014).

#### **2.13.7.3 Use of Co-Solvents**

The use of inert co-solvents in the Trans-esterification reaction improves the transfer of matter between tri-glycerides and alcohol through the formation of a single phase in which all components have been solubilized. With the improvement in the first phase of the reaction, the time required for the total conversion is reduced and a clean separation between biodiesel, glycerin, alcohol and co-solvent (Demirbas, 2008). Some examples of co-solvents are: dimethyl ether (DME), diethyl ether(DEE), tert-butyl methyl ether (TBME) or tetrahydrofuran(Guan, Sakurai and Kusakabe, 2009).

In this process it is important to eliminate any remaining co-solvent from the biodiesel that they are usually very flammable and sometimes toxic products. On the other hand, it is necessary to separate alcohol and the co-solvent, and certain difficulties may arise depending on the difference of their boiling points (Abbaszaadeh *et al.*, 2012).

#### **2.13.7.4 Application of Low Frequency Ultrasound Radiation**

The application of ultrasound radiation to a mixture of immiscible liquids causes the collapse of the bubbles that constitute the mixture, favoring the interaction between phases and altering the boundary between them, causing their emulsification (Chatel and Colmenares, 2017; Pollet and Ashokkumar, 2019; Zimmerman *et al.*, 2020). In this way you get a emulsion composed of alcohol and oil that improves the transfer of matter and the chemical reaction, reducing reaction times, necessary amount of reagents and working under more moderate pressure and temperature conditions (Chatel and Colmenares, 2017). You can find works in which ultrasound radiation is applied directly to the reaction mixture (Liu, Hu and Jin, 2016) and others in which an ultrasound bath is used in which introduces the flask where the Trans-esterification takes place (Suslick and Crum, no date).

#### **2.13.7.5 Obtaining Biodiesel “in situ”**

In this method, oilseeds are treated directly at room temperature and under pressure with a methanol-catalyst solution that directly promotes the Trans-esterification of the oil present in the seeds (Atadashi *et al.*, 2012; Srilatha *et al.*, 2012). The ground seeds are mixed with the alcohol solution and catalyst heated to reflux for several hours. At the end of the reaction, two phases are formed, and the alcohol phase can be recovered. The biodiesel is washed to remove impurities and dry over anhydrous sodium sulfate, filter and the resulting product is biodiesel (Pannacci and Tei, 2014). It

is possible to obtain a biodiesel of high purity as long as they are dried initially the seeds and their impurities are removed. This method avoids the oil extraction and refining step, which causes a substantial reduction in biodiesel production costs.

#### **2.13.7.6 Application of the design of experiments and the response surface methodology to obtaining biodiesel**

The optimization of a chemical process can be carried out in two ways. Different: traditional methodology or using an experimental design. The traditional method consists of studying the response variable by varying one factor at a time, thus revealing the influence of that factor, repeating the procedure for the rest of the factors. The problem arises when there is interaction between two or more factors, which is not reported on as one factor interacting with the other factors or how those interactions affect the response. With the method of experimental design or design of experiments, more than one factor can be varied simultaneously in each experiment, allowing information to be obtained about the interactions and reduce the number of experiments to be performed (Cash, Stanković and Štorga, 2016).

In an experimental design, the first step would be the identification of the process to be analyzed and the definition of the input variables or factors that intervene in the results in said process. Additionally, the range in which these factors will be modified must be established. TO next, the response variable is established, which will be the variable that provides useful information about the process under study and allows identifying whether the results of the process are good or bad. For example, to obtain biodiesel the input variables They could be temperature, catalyst concentration, methanol: oil molar ratio, among others and the response variable the ester content of biodiesel (Pali *et al.*, 2015; Deb *et al.*, 2017; Helmi *et al.*, 2021; Thakkar *et al.*, 2021; Balamurugan *et al.*, 2022).

In the experimental design each factor represents a spatial dimension, so that when you work with several factors, you have a multidimensional space. For sampling in this space, different methods can be used, according to the characteristics of the problems to be solved and the intrinsic advantages and disadvantages of each one. The designs that most advantages they carry when analyzing them are the complete factorial design, the central design compound, the Box Behnken and the design of mixtures, because the methodology of response surface for data analysis (Dean *et al.*, 2015; Singh Pali *et al.*, 2020), of all of them, the most used to fit second-order response surfaces, which are the most obtained in the Trans-esterification of oils and fats (Khuri and Cornell, 2018), it is the central composite design proposed by Box and Wilson (Marchetti *et al.*, 2016). These types of designs are made up of factorial treatments  $2^k$  with  $2^k$  additional combinations called axial points and  $n_c$  center points; where  $k$  is the number of input variables involved in the design. The coordinates of the axial points of the axes of the coded factor are  $(\pm\alpha, 0, 0, \dots, 0), (0, \pm\alpha, 0, \dots, 0), \dots, (0, 0, \dots, \pm\alpha)$  and the center points are of the form  $(0, 0, \dots, 0)$ . Depending on the choice of  $\alpha$  and the number of replicas of the central point, the design may have properties such as orthogonality, rotability and uniformity. Rotability consists of the fact that the variance of the estimated values is constant at points equidistant from the center of the design; For this, the value of  $\alpha$  must be  $\alpha = (2^k)^{1/4}$ . Orthogonality, in a central composite design, is achieved assigning an appropriate number of  $n_c$ , which allows the estimated coefficients in the model are not correlated with each other. And finally, uniformity indicates precision design inform that presents the same variance of the predicted response in the center of the design as in the sphere of radius 1. Figure 2.10(a) illustrates the central composite design for two factors, which would imply carrying

out nine experiments without taking into account the replications of the point central. And in Figure 2.10(b), the design for three factors would be represented in which case the number total number of experiments would be 15.

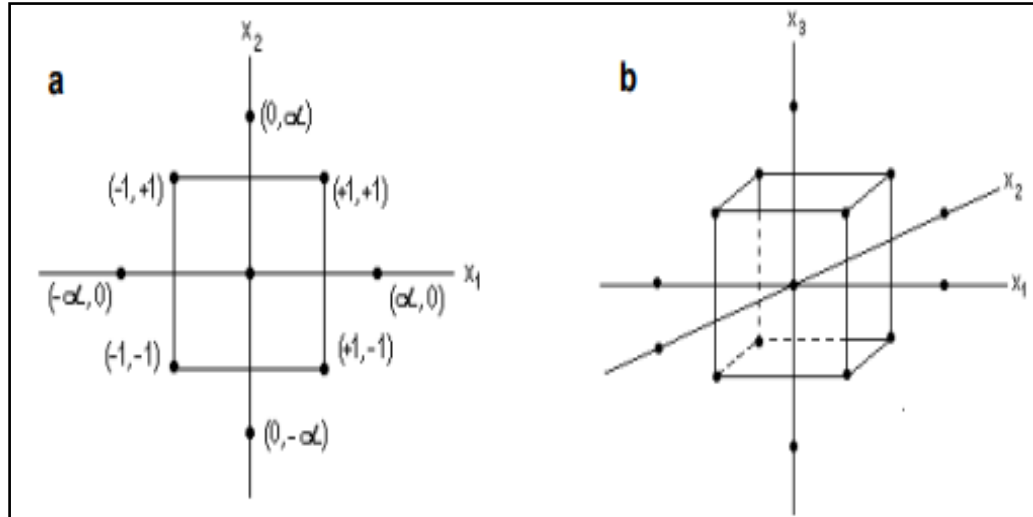


Figure 2.10 Central composite design for two factors (a) and three factors (b)

Once the experiments have been carried out and the data collected, they are analyzed using RSM, also introduced by Box and Wilson (Marchetti *et al.*, 2016) is about a collection of techniques that allow the researcher to visually inspect the response for a certain area of the levels of the factors of interest, as well as evaluate their sensitivity to the treatment factors. In general, the inspection seeks to achieve an optimal combination of levels of the variables. Polynomial models are used as practical approximations to the true or real response function; which can be the linear or first order model, the quadratic or second order or one of third order, which may include all interactions or cross products of the factors. Because it is the one that has given the best results in the field of obtaining biodiesel, the general Equation 2.3 of the quadratic or second model has been collected order:

$$y = \beta_0 + \sum_{i=1}^k \beta_i x_i + \sum_{j=2}^k \sum_{i=1}^{j-1} \beta_{ij} x_i x_j + \sum_{i=1}^k \beta_{ii} x_i^2 + \epsilon \dots \dots \dots 2.3$$

Where  $y$  represents the response variable,  $\beta_i$  each of the coefficients,  $x_i$  each of the input variables of the model and  $\epsilon$  the noise or error observed in the response.

### 2.13.8 Industrial Processes

The production of biodiesel can be carried out in a batch regime, also called “batch” type, or continuous regime. The first is the most used because the matter raw material from which biodiesel is obtained is usually not very homogeneous, this being necessary in the continuous processes. The stages of a biodiesel purification process cannot be defined exactly, because there are many equally valid alternatives; however, one of the most alternatives used is the one represented in Figure 2.11 in which after the reaction stage, they are separated crude biodiesel and glycerin phases and are purified independently [93].

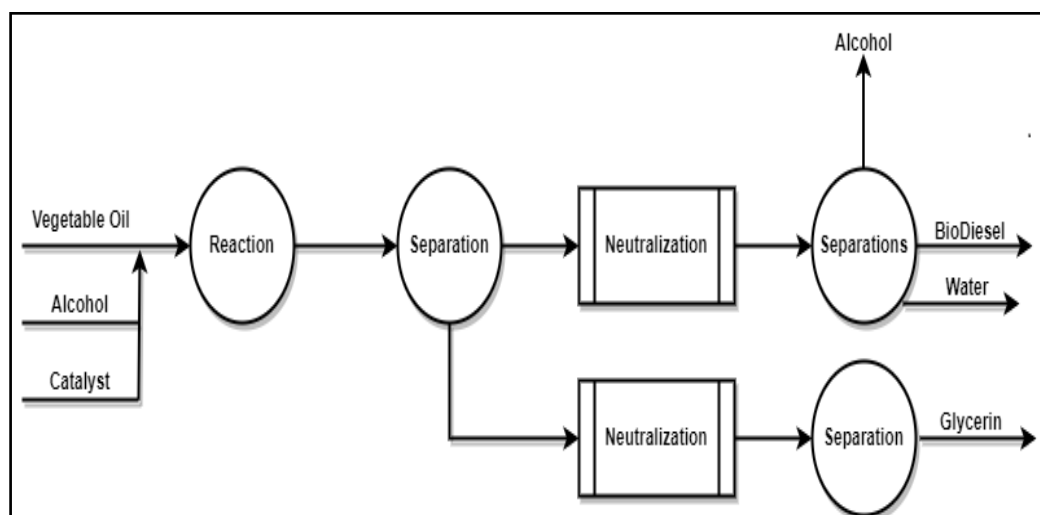


Figure 2.11 Block diagram of biodiesel production process

- **Discontinuous Processes**

In the batch process, the oil is mixed with a catalyst-alcohol solution at a temperature between 60-65 °C in the case of methanol and is kept stirred during the reaction time. There is the possibility of placing two reactors in series, carrying out the reaction in two stages, removing the glycerin generated, between the first and second stages. With This procedure achieves very high degrees of conversion, since before the Second stage, reaction products are removed and, in addition, reagents are added (catalyst– alcohol) (N. Khumdemo Ezung *et al.*, 2008b). Even though the reaction stage is a discontinuous process, various tanks are used. Storage capable of containing

the product from 3 to 4 reaction cycles to carry out the separation and purification of the products continuously.

#### **2.13.8.1 Continuous Processes**

In continuous processes, continuous stirred tank reactors (CSTRs) or plug flow reactors (PFRs). The first are the most widely implemented and are used to large reaction volumes. Several reactors are usually used in cascade, with different size and consequently different residence time, which improves overall performance of the process (Hernandez *et al.*, 2008; N. Khumdemo Ezung *et al.*, 2008b; Abdulkareem- Alsultan *et al.*, 2019). PFRs reactors are characterized because the reaction mixture advances longitudinally, the reactants are mixed in the axial direction and the flows are taken advantage of turbulent flows induced by pumps or static agitators. They have been proposed in applications industrial although they are less used (Dewi *et al.*, 2021).

#### **2.14 Hydrogen Production**

Hydrogen is widely used in industry today. It participates in industrial processes of great importance such as the synthesis of ammonia, methanol, plastics, polyester, nylon; It is part of the refining processes of fossil fuels and is used in the glass industry, the electronics field and is an important carrier of energy that is currently intended to be exploited due to the non-generation of CO<sub>2</sub> in its combustion(Riis *et al.*, 2005; Syed, 2021; Tarhan and Çil, 2021). Although hydrogen has the ability to store and release useful energy, it usually exists in molecules such as water, hydrocarbons, alcohols, or biomass rather than existing on its own in the natural world.

Initially, hydrogen production was approached from the electrolysis of water, introduced in the late 1920s(Burton *et al.*, 2021) . Other technologies used for



hydrogen production are thermal or catalytic processes such as the reforming of natural gas or other hydrocarbons, as well as the processing of renewable materials such as bio-oils and the gasification of biomass or coal. Sunlight has also been used to achieve the decomposition of water using biological or electrochemical materials in photolytic processes. Of all of them, steam methane reforming (SMR) is the currently dominant technology and, specifically, almost 95% of the hydrogen used globally comes from fossil fuels(Ewan and Allen, 2005).

In this framework, it is considered necessary to develop hydrogen production technologies that are based on renewable energy sources, that do not involve the depletion of oil and whose GHG emissions are done responsibly, with net emissions that are not too high. The use of glycerin, specifically glycerin obtained as a by-product in the production of biodiesel, would mean a renewable raw material that has an increasingly lower value in the market and that, in addition, could favor an industry such as the production of biodiesel that attempts to replace a fossil fuel with a renewable resource.

#### **2.14.1 Thermochemical Processes**

Thermochemical processes are those in which biomass is converted into energy or fuels. These processes involve irreversible chemical reactions at high temperatures and variable oxidation conditions. The gas produced, with qualities as fuel, may present a greater or lesser percentage of hydrogen and carbon monoxide, and can be used as synthesis gas for the production of other chemical compounds or as gas rich in hydrogen to obtain it (Pirzadi and Meshkani, 2022).

Depending on the reaction conditions, combustion, pyrolysis, gasification and reforming are differentiated. In the case of glycerin, the most studied thermochemical process is its reforming, intending to obtain hydrogen (Ganguli and Bhatt, 2023).

### 2.14.2 Combustion

Combustion consists of the total oxidation of the biomass by the oxygen in the air, until it becomes  $\text{CO}_2$  and  $\text{H}_2\text{O}$ . The conversion of energy produced due to burnt fuel in the form of chemical energy. This produced energy produced heat that used in the form of electricity. During this process, the chemical energy of the fuel is released in the form of heat that can be transformed into electricity. From an energy point of view, it is the process that gives the highest performance, although it involves the total destruction of organic matter and no useful commercial by-products are obtained in the case of glycerin combustion, this substance has low calorific value ( $\sim 16 \text{ MJ}\cdot\text{kg}^{-1}$ ), high density and viscosity, which makes it difficult to pump and atomize. Furthermore, it has been proven that the combustion of crude glycerin in industrial burners is difficult due to the discontinuity of the flame. Additionally, as indicated previously, the combustion of said substance produces toxic emissions of acrolein, which is not desirable.

### 2.14.3 Pyrolysis

The physical-chemical breakdown of organic matter in the absence of an oxidizing agent and with the application of heat is known as pyrolysis. This decomposition occurs through a complex series of chemical reactions, in addition to thermochemical transformation processes of biomass. In this way, gaseous, liquid or solid fuels are obtained, depending on the composition of the biomass and the operating conditions. Furthermore, pyrolysis reactions constitute the initiation and accompanying reactions of the combustion and gasification processes.

The products obtained in this way are solids (mainly charcoal), pyrolytic liquids, also called bio-oil, and gases. Due to the heterogeneity of biomass composition, products with different properties are usually obtained depending on the biomass used

(Kalghatgi, 2018; Kaskun, 2020). When the pyrolysis of glycerin is considered, these products do not usually present as much variation, due to the homogeneity of the raw material, thus the products obtained tend to be (Sansaniwal and Kaushal, 2018):

- Gaseous product: the gas obtained is mainly composed of hydrogen, monoxide, carbon dioxide, methane and ethylene.
- Liquid product: the main liquid products of glycerin pyrolysis are acetaldehyde, acetone, methanol, ethanol, water and acetic acid, and in the event that complete pyrolysis does not occur, it would be possible to find undecomposed acrolein and glycerin.
- Solid product: the solid product of pyrolysis is mainly composed of coke, almost pure carbon

The percentage of each of the aforementioned products will depend on the process conditions (Production of hydrogen and syngas via steam gasification of glycerol in a fixed-bed reactor Valliyappan *et al.*, 2008).

#### **2.14.4 Gasification**

Gasification could be defined as a gaseous state through a thermochemical process that converts organic matter through partial oxidation at high temperatures. This oxidation is produced thanks to the presence of a gasifying agent such as air, water vapor, oxygen or hydrogen. The gasification process produces a gaseous product, generally composed of hydrogen, methane, monoxide and carbon di-oxide, and with a calorific value suitable for use in gas turbines, combined cycles or alternative internal combustion engines. From an energy point of view, it is an inefficient process, since the total energy content of the products is less than that of the biomass from which it is based. The advantage of using this process is that a cleaner and more versatile gaseous fuel is obtained than the starting material (Production of hydrogen and syngas

via steam gasification of glycerol in a fixed-bed reactorValliyappan *et al.*, 2008). The main steps that make up a gasification process can be divided into three categories, the previous steps, the gasification itself and the subsequent steps(Martín and Grossmann, 2017; Othman *et al.*, 2017).

The previous steps include processing the biomass to make it suitable for gasification operations. Thus, the reduction of particle size, the drying of the biomass to an adequate humidity, its densification and the preparation of gasifying agents would be contemplated. Gasification itself encompasses the heating of the biomass and the chemical reactions necessary for its transformation. Finally, the gas washing and reforming stages are identified, as well as their use (Kumar, 2009).

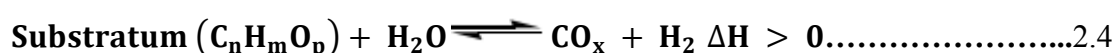
In turn, gasification itself is characterized by being composed of four stages. The first of them is drying, during which the remains of water from the biomass undergo a physical evaporation process, releasing water up to 200<sup>0</sup>C. As the temperature rises, low molecular weight compounds also volatilize. The next stage is pyrolysis, which consists of the breakdown of the large molecules that make up the biomass, giving rise to others with a shorter chain that, at the temperature of the reactor, are in the gas phase. In the third stage, the reduction of the gaseous components produced in the previous stages occurs through strong endothermic reactions, some of which can be identified as reforming reactions. And the last stage includes oxidation reactions of the heaviest fraction (carbonaceous) due to its contact with the gasifying agent.

According to the European technical specification CEN/TS 14588, biomass is defined as “all material of biological origin, excluding those that have been included in geological formations undergoing a mineralization process.” Despite the extension of the definition, biomass has traditionally been considered waste from forestry exploitation, agricultural crops or agroforestry industries. For this reason, whenever

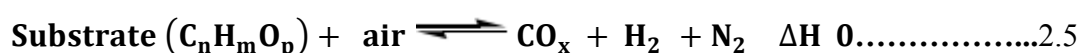
we talk about thermochemical treatment of biomass in the presence of an oxidizing agent, without taking oxidation into account, we think of gasification, as a way of transforming solid matter into gases. On the other hand, glycerin generated as a by-product of obtaining biodiesel can also be classified as biomass, but due to its chemical nature, its gasification could be simplified and categorized only as reforming, which is generally carried out with water vapor(Kofman, 2016).

#### 2.14.5 Steam Reforming

Reforming consists of the transformation of relatively light hydrocarbons, gaseous or liquid, into lighter and highly valuable gases such as hydrogen or synthesis gas, through treatment at high temperatures, in the presence of an oxidizing agent and, generally, a catalyst. There are different types of oxidizing agents, the most common in reforming is water vapor; In this case, the process takes the name steam reforming. Generally, a substrate ( $C_nH_mO_p$ ) will react with water vapor to produce a gas rich in  $H_2$ ,  $CO_2$  and  $CO$ . This process is highly endothermic and can be represented by the following reaction using Equation 2.4 (Kunkes *et al.*, 2009; Elfasakhany, 2015):



Another possibility is to use oxygen as an oxidizing agent that in quantities lower than those necessary by stoichiometry, will result in a process called partial oxidation. The Oxygen will come from the air, reaching a balance between the energy required in the process and that can be generated, since the oxidation reaction gives rise to an important generation of heat. The process could be carried out with or without a catalyst and can be represented by the following equation 2.5 (Ternan, 2006; Gielen *et al.*, 2019):



In the case of partial oxidation, due to the energy generation that occurs, it is possible to reach temperatures of up to 1000 °C, therefore it is relatively easy for steam reforming to also be carried out in the presence of water vapor. This fact is what takes advantage of the auto thermal reforming that feeds substrate, water and air in the same reactor. It is the presence of a catalyst that controls the extent of the oxidation or steam reforming reaction. The heat generated in the oxidation reactions is absorbed by the steam reforming reactions, the result being slightly exothermic equation 2.6.



Finally, it is possible to achieve the reaction of the substrate with water, which is not in a vapor state. A distinction can be made between reforming in the aqueous phase, in which the process is carried out in the liquid phase at temperatures around 270°C and pressures close to 60 bar [178]. And reforming in supercritical water, which is carried out in supercritical water conditions, 374°C, 22.1 MPa (Cortright, Davda and Dumesic, 2002).

All of the processes listed could be suitable alternatives for the use of glycerin as a source of obtaining hydrogen or synthesis gas (Cortright, Davda and Dumesic, 2002; De Souza and Silveira, 2011). Among all of them, steam reforming is the most commonly used method for the production of hydrogen in the chemical industry, as it is, of the available commercial technologies, the most efficient and profitable if applied on a large scale (Mwangi *et al.*, 2015). This technique has the benefit of not needing high pressures, which reduces risks related to it. It provides higher percentages of hydrogen in the produced gas and despite requiring high temperatures, its current development, having been carried out since the 1930s, ensures that it is an efficient and profitable process, mainly applied on a large scale (Sen, Noori and Tatari, 2017).

## 2.15 Factors that influence the steam reforming process

In the steam reforming process there are a series of factors that affect the efficiency of the process, the distribution of products and the composition of the gas produced.

These factors are as follows:

- Feed flow: overfeeding can lead to reduction in conversion performance, while the opposite results in lower gas production. The optimal flow rate maximizes energy efficiency and is directly related to the amount of catalyst used, in many cases expressing the spatial velocity of the food per gram of catalyst.
- Type and properties of the food: the most used method to obtain hydrogen is steam reforming of methane. Reaction 1.6 for this compound is reversible and the conditions must be controlled so that it moves towards the formation of hydrogen. On the other hand, for higher molecular weight hydrocarbons, said reaction is irreversible and the distribution of products will be given by the thermodynamic balance of all the reactions involved in the process, which in the case of glycerin are detailed in chapter 3 of this work.
- Temperature: this is one of the most influential factors, it affects the performance of the process, as well as the composition of the gases generated. In general, higher temperature leads to greater gas production and a higher percentage of hydrogen in the gas generated. In the case of glycerin, in the presence of various metal catalysts, good results have been achieved at temperatures of 600<sup>0</sup>C (Parlar Karakoc *et al.*, 2019; Branco *et al.*, 2020).
- Steam/carbon ratio: the steam/carbon ratio (S/C) used in reforming is important. High S/C ratios favor the inhibition of the methanation reaction, increasing hydrogen production. But a large excess of water vapor implies the need to work

with larger volumes of gas, requiring larger installations. In addition, the exit gases will be more diluted due to the excess water used.

- Catalyst or filling material: the most common is the use of a suitable catalyst that allows greater conversions of the starting material to gases, as well as directing the reaction mechanism towards obtaining one or another product. However, in cases where a catalyst is not used, the presence of a filler material can help the process proceed as desired. The particle size of this is one of the variables to control so that the transfer of matter and contact between reactants inside the reactor is favored. As for the catalyst, it is necessary to look for a suitable catalyst, since they are substances that selectively promote one reaction or another. Common catalysts in steam reforming are metals supported on metal oxides, which usually promote the formation of hydrogen over other reaction products. Chapter 3 details the role of the catalyst in the steam reforming of glycerin and details examples of catalysts, as well as the results obtained with them.

## **2.16 Literature review**

1. Maqsood et al. (Maqsood and Alsaady, 2022) depicted that, the rise in motorization and industrial activity has led to an increase in fuel demand. Biodiesel can be produced from crops that have been specially grown. However, some types of biodiesels raise ethical questions because they come from crops that are used as food. It will take research and development to create an environmentally acceptable and economically viable biodiesel production process that can compete with petroleum-based fuels while also addressing ethical concerns. By substituting a less costly oil, such WCO, for vegetable oil, the cost of producing biodiesel can be decreased. Positive outcomes have been observed in biodiesel produced from used cooking oil. Generally, to create a long-lasting



and economical biodiesel production process, the right temperature and reaction time must be combined. Using fishbone waste as a catalyst, leftover cooking oil can be metabolized as a feasible substitute. This study uses fishbone as a catalyst to simulate and optimize temperature- and time-dependent properties for the synthesis of biodiesel from used cooking oil. Response surface methodology (RSM) was employed to enhance the production of biodiesel. However, based on the findings of experiments conducted with a 6% catalyst at temperatures between 55 and 65 °C and reaction times ranging from five to 120 minutes. By simultaneously changing some process variables, modeling methods like response surface methodology are crucial to maximizing efficiency and lowering expenses associated with production. The response surface method works very well for optimizing complicated systems that are influenced by multiple variables.

2. Ghavami et al. (Ghavami *et al.*, no date) depicted that, the high combustion output, renewable nature, and environmental friendliness have made biodiesel a popular substitute for fossil fuels. This work produced biodiesel by transesterifying leftover cooking oil and sunflower oil using a K<sub>2</sub>O/RGO heterogeneous catalyst. Graphite was synthesized using a modified Hummers' process to get reduced graphene oxide (RGO), which was then coated with potassium. Many methods were used to characterize the K<sub>2</sub>O/RGO catalyst, including FTIR, SEM, XRD, ASAP, Raman spectroscopy, and TEM. The process was optimized using the response surface approach while the effects of temperature, catalyst dose, time, and methanol to oil molar ratio were investigated. The characteristics of the biodiesel were determined to be within the standard values given by ASTM D 6751 and EN 14214. The K<sub>2</sub>O/RGO catalyst

demonstrated reusability for up to four cycles. Operating parameters of 70°C temperature, 19.5 methanol to oil molar ratio, 2 weight percent catalyst dose, and 8.5 hours duration resulted in maximum biodiesel yields of 98.54% for sunflower oil and 96.89% for waste cooking oil.

3. Al-Hamamre et al. (Al-Hamamre *et al.*, 2023) depicted that, oil shale ash was converted into a solid heterogeneous catalyst by impregnating it with KNO<sub>3</sub> and then calcining it for four hours. Various preparation circumstances (calcination temperatures: 500 and 700°C, and KNO<sub>3</sub> concentrations: 0.05 and 0.1M) were investigated. Following calcinations, research was done on how reaction variables such as catalyst loading, methanol-to-oil molar ratio, and reaction time affected the conversion of waste cooking oil to biodiesel. The following techniques were used to characterize the catalyst: FT-IR, XRD, BET, TEM, and SEM. Additionally, (HNMR) was used to quantify the usual unsaturated fatty acids found in general vegetable oils, the oil-to-biodiesel conversion, and the chemical makeup of the biodiesel that was created. The catalyst that produced the highest oil-to-biodiesel conversion, almost 100% at 65°C reaction temperature, 45:1 methanol to oil molar ratio, and 2-hour reaction duration was ash impregnated with 0.1M KNO<sub>3</sub>/and calcined at 700°C (Ash 0.1/700 catalyst).
4. Aghel et al (Aghel *et al.*, 2023) depicted that, their current research attempts to use a heterogeneous catalyst derived from biological waste (animal bone) to optimize the process parameters needed to convert spent cooking oil (WCO) into methyl esters. The synthetic calcium oxide (CaO) and methyl esters derived from animal faeces were analyzed. A calcined catalyst was produced at temperatures between 90° and 95° C. Reaction effects from temperature (40–80°C), reaction

time (30–180min), and CL (0.1–0.15×10<sup>2</sup> w/w%) were investigated in a 3-level, 3-factor array using central composite design. For the investigations, ANOVA testing and R.S.M. optimization was used to determine the most significant parameter. The variables that most affected the biodiesel production were the temperature of the reaction combination (p-value of 0.0344), reaction time (p-value of 0.0339), and linear terms of CL (p-value of 0.0146). The temperature of the combining process (p-value = 0.0508) and the quadratic terms of CL (p-value = 0.0271) had the biggest effects on the oil yield. As a result, using ANOVA, R.S.M., and C.C.D. design to maximize the production of biodiesel from used cooking oil is feasible.

5. Aderibigbe et al. (Aderibigbe *et al.*, 2023) depicted that, the depletion of fossil fuels and their detrimental effects on the environment have made biofuels—alternative fuels—necessary. Because it encourages carbon neutrality, biodiesel is the form of biofuel that has garnered the most attention in the world today among the other varieties. The most popular method for producing biodiesel is still Trans-esterification and inter-esterification. This review examines the effectiveness of solid base, solid acid, and bi-functional solid acid-base catalysts in the generation of biodiesel from used cooking oil waste. The advantages of investigating biomass-derived acid-base heterogeneous bifunctional catalysts, as well as the present and potential future developments, are clarified concerning the synthesis of biodiesel from used cooking oil.
6. Hundie et al. (Hundie, Shumi and Bullo, 2022) depicted that, in this study, the Trans-esterification method was used to turn watermelon waste oil into biodiesel. The impact of Trans-esterification parameters, such as catalyst concentration (4–10%), methanol-to-oil ratio (2–10mol/mol), and reaction temperature (46–

60<sup>0</sup>C), was examined using a definitive screening strategy. The yield of biodiesel was forecast using the quadratic regression analysis. The ideal catalyst concentration, methanol-to-oil molar ratio, and reaction temperature are determined to be 5.51%, 5.77:1, and 60<sup>0</sup>C, respectively. These values produce a 96.763% yield of methyl esters, which is very close to the expected value. The outcomes showed that every variable had a noteworthy impact on the biodiesel yield. The extracted watermelon waste oil's physicochemical properties were examined, and biodiesel was generated with the best possible process settings. According to the findings, the biodiesel that was generated and the oil that was extracted satisfied the standards set by the European Committee for Standardization (EN14214) and ASTM. The predominant unsaturated fatty acids were determined to be oleic and linoleic acid, whilst the biggest proportion of saturated fatty acid was found to be palmitic acid. In summary, optimizing the Trans-esterification reaction parameters through a definite screening design is a viable strategy to increase biodiesel yield. Furthermore, this approach drastically lowers the number of trials, which is crucial when working with a restricted quantity of raw materials. Overall, this work's findings suggest that watermelon waste oils may be a viable substitute feedstock for waste materials used to make biodiesel.

7. Igbax et al.(Ityokumbul Igbax *et al.*, 2022) depicted that, the use of waste vegetable oil (WVO) to produce biodiesel is examined in this study. This study set out to investigate ways to enhance biodiesel production to attain high yields. Various oil streams were utilized as the starting material for the Trans-esterification procedures, such as virgin canola oil and waste vegetable oil (WVO). The fatty acid composition of these oils varied due to processing or

environmental factors. This study's primary goal was to evaluate how the amount of free fatty acid (FFA) affected the final yield. Furthermore, the yield was impacted by production parameters such as catalyst amount, mechanical mixing, and molar/volume ratios of alcohol to oil, reaction time, and temperature. This was achieved by automating the WVO biodiesel production process, which led to better processing and less direct human intervention. A Raspberry Pi 3 microcomputer was used in the development of a biodiesel-producing device. It was demonstrated that the specific oil type determined which of these process parameters to use. The FFA concentration of the oil was utilized to determine the volume ratios (oil to alcohol) of 4:1, 6:1, and 8:1 that were used in this study for mixes of virgin and waste vegetable oils. Apart from mechanical mixing, 500W, and 20kHz ultrasonication were employed to improve mixing by incorporating 450 kJ into the procedure. This resulted in a reduction of processing time and methoxide quantity required for base-catalyzed Trans-esterification. A temperature range of 50–65°C was maintained for the production process. This study showed that the ideal yield is influenced by temperature, the concentration of the catalyst, the oil's FFA level, and the energy added by sonication. The following conditions led to a 96% yield: a 6:1 oil-to-methanol volume ratio, a 0.6% catalyst weight concentration (NaOH) at 6.25 g, and FFA levels of roughly 5%. It was found that the suggested technique could generate biodiesel of a respectable caliber.

8. Primadi et al (Primadi *et al.*, 2021) depicted that, used cooking oil hasn't been put to any practical use up to now (Kelantan). The goal of this research is to turn this leftover cooking oil into biodiesel. Cooking oil can be transformed into methyl esters through a Trans-esterification reaction, based on the fact that it still

includes free fatty acids. This endeavor corresponds with the growing need for renewable energy sources. However, supercritical conditions are required to attain the maximal Trans-esterification reaction results without the use of a catalyst. A low-quality oil with high quantities of free fatty acids and excessive rancidity is even more wasted cooking oil. As a result, when considering the best process parameters and the required superior catalysts for the Trans-esterification process, consideration must be given.  $\text{CaO}/\text{CoFe}_2\text{O}_4$  is one catalyst that is regarded as excellent. By heating eggshell solid waste to a high temperature (calcination), it can be utilized as a naturally occurring supply of  $\text{CaO}$ . The goal of this project is to use eggshell catalysts and  $\text{CaO}/\text{CoFe}_2\text{O}_4$  to manufacture biodiesel from used cooking oil. The following key actions helped to achieve the study's objectives: (1) preparation of cooking oil waste; (2) activation of zeolite synthesis for ratification process; (3) trans-esterification reaction from cooking oil waste using  $\text{CaO}/\text{CoFe}_2\text{O}_4$  eggshell waste; (4) trans-esterification reaction optimization; and (5) characterizing the methyl esters produced and assessing their potential as biodiesel. Based on yield analysis, GC-MS, and FTIR results, methyl ester is the end product, and biodiesel is the product's potency. It is anticipated that the catalyst utilized in the Trans-esterification reaction derived from used cooking oil will yield an 80% conversion rate.

9. Andrifar et al (Andrifar *et al.*, 2022) depicted that, To fulfill the rising need for energy, the world's population is growing, and industrialization, urbanization, and economic expansion are all happening quickly, which has resulted in a constant increase in the consumption of fossil fuels. Finding suitable and sustainable fossil fuel replacements will become necessary due to the ongoing emissions caused by burning fossil fuels. Since biodiesel is non-toxic, renewable, and

ecologically benign, it is an ideal substitute fuel for diesel engines. In every nation, a significant amount of WCO is produced by the food, non-food, eatery, and household sectors. If appropriate disposal methods are not used, WCO may lead to environmental contamination. Rather than discarding it in landfills Reusing waste construction oil (WCO) can reduce environmental pollution. This work assesses the possibility of utilizing fly ash-derived zeolite as a heterogeneous alkali catalyst in a Trans-esterification reaction to generate biodiesel via WCO. A 1,000 ml boiling flask with three necks, a cooling tank, a pump, and a condenser served as the reactor in this investigation. Utilizing a magnetic stirrer and a hot plate to stir and heat during the biodiesel synthesis process. The reaction temperature is determined using the thermometer. Optimizing the generation of biodiesel using zeolite catalyst made from fly ash by adjusting the catalyst weight (1, 2, 3, and 4% weight), temperature (45<sup>0</sup>C, 55<sup>0</sup>C, and 65<sup>0</sup>C), and methanol: oil ratio (8:1, 10:1, 12:1, and 14:1). With ideal operating circumstances of a reaction period of 60 minutes, a methanol oil ratio of 8:1, an operating temperature of 55<sup>0</sup>C, and 1% by weight of catalyst, zeolite derived from fly ash yields biodiesel with a 91.67% yield. This experiment validates that fly ash waste can be used as a catalyst in the synthesis of biodiesel.

10. Lakkimsetty et al. (Lakkimsetty *et al.*, 2022) depicted that, combustible and biodegradable fuel, biodiesel is derived from vegetable or animal fat. Because it employs renewable resources that are less hazardous to the environment to create and emit fewer harmful greenhouse gases when burned as fuel, it is a desired substitute for petroleum fuel. Any car with a compression ignition engine that can run on conventional diesel fuel can run on biodiesel fuel. This technical research sought to compare the use of microwave and Trans-esterification techniques for

biodiesel production from waste cooking oil (WCO). This paper also presents the conceptual design of a production method that produces biodiesel (methyl esters) from waste cooking oil via supercritical Trans-esterification with methanol. Additionally, several studies will be conducted to investigate the feasibility of producing biodiesel from leftover cooking oil. By measuring the viscosity of the biodiesel ethyl ester at room temperature at 40°C, the Trans-esterification method yielded a value of 4.95 mm<sup>2</sup>/sec, while the microwave approach yielded a value of 6.81 mm<sup>2</sup>/sec. According to the tests, the biodiesel ethyl ester's flashpoints when measured using the microwave method, waste cooking oil, and Trans-esterification method were, respectively, 145, 340, and 150°C. Furthermore, it was discovered that the densities of the biodiesel ethyl ester made from waste cooking oil, biodiesel ethyl ester made using the microwave method, and biodiesel ethyl ester made by Trans-esterification were, respectively, 850, 974, and 897.2 kg /m<sup>3</sup>. Ultimately, 0.880, 0.888, and 0.862 were the specific gravities of the biodiesel ethyl ester produced by utilizing the microwave method, waste cooking oil, and the Trans-esterification method.

11. Alsaiani et al. (Alsaiani, Musa and Rizk, 2023) depicted that, biodiesel is thought to be more affordable, environmentally benign, and able to produce greener energy than petroleum-based fuels, it has helped to advance the bio-economy. Using recently developed heterogeneous hydroxyapatite catalysts, a novel non-edible feedstock made from date seed oil was examined for the production of environmentally friendly biodiesel. The waste camel bones were made from dried camel bone that had been calcined at various temperatures. X-ray diffraction (XRD), Brunauer-Emmett-Teller (BET), and transmission electron microscopy (TEM) were used to characterize this catalyst. The hydroxyapatite catalyst's pore



size decreased as the calcination temperature was raised, according to the results. Through the process of Trans-esterification, an optimal reaction temperature of 75°C for three hours, a four-weight percent catalyst, and an oil-to-ethanol molar ratio of 1:7 were used to generate an optimal biodiesel yield of 89 weight percent. Through the use of gas chromatography-mass spectrometry (GC–MS), the synthesis of FAME was verified. Fatty acid ethyl ester's fuel qualities met ASTM D 6751 requirements, indicating that it would be a suitable substitute fuel. Therefore, it is praiseworthy to create and implement a more environmentally friendly and sustainable energy plan employing biodiesel derived from waste and wild resources. The adoption and application of the green energy approach could have positive environmental benefits, which could improve society and the biodiesel industry's ability to grow economically on a broader scale.

12. Ramesh et al (Ramesh *et al.*, 2021) depicted that, the production of biodiesel from waste cooking oil (WCO) has the potential to increase raw material costs and solve the problem of disposing of waste oil. Ionic acid can be used as a catalyst to convert WCO into biodiesel. Trans-esterification processes are often catalyzed using alkaline-based catalysts. However, because of problems with layer isolation and saponification, direct usage of WCO is not feasible in practice due to its high free fatty acid content. To produce biodiesel, the WCO can be utilized as a raw material, which explains their different fatty acids. The physicochemical parameters of the repurposed catalyst with high yield output are connected with current standards. The first-order reaction mechanism is followed and the kinetics of this Trans-esterification reaction are assessed. This article discusses the use of WCO's biodiesel which uses ionic liquids as a catalyst.

13. Amenaghawon et al. (Amenaghawon *et al.*, 2022) depicted that, important sources of elements like calcium and potassium that can be utilized as active phases to build heterogeneous catalysts for the manufacture of biodiesel include bio-based waste products. This study evaluated the possibility of using a composite bio-based heterogeneous catalyst made of plantain peels and fused crab shells for the Trans-esterification of spent cooking oil. To evaluate their structural, compositional, morphological, and thermal properties, the catalyst and the precursor materials underwent characterization. Response surface methodology (RSM) was utilized to optimize the experimental variables and produce biodiesel using a single-step Trans-esterification process. The morphological characteristics demonstrated a surface of aggregated catalyst with pores that were well delineated. The presence of basic (potassium and calcium) and acidic (silicon and iron) oxides demonstrated the catalyst's bi-functionality. The maximum biodiesel production of 93% was achieved at a reaction temperature of 60°C, catalyst loading of 5 % (wt. %), reaction time of 149.94 min, and methanol to oil ratio of 13.03:1 thanks to the catalyst's high surface area (260.35 m<sup>2</sup>/g) and pore volume (0.65 cm<sup>3</sup>/g). It was discovered that the RSM model ( $R^2 = 0.9939$ ) was quite effective at simulating the generation of biodiesel. After six cycles, the catalyst showed significant biodiesel yields (>80%), indicating its strong stability. It was discovered that the biodiesel's characteristics were on par with industry norms. Because of its high surface area, stability, ease of synthesis, reusability, and easy access to precursor materials, the synthesized catalyst has many benefits over conventional catalysts.
14. Chen et al. (Chen, Xia and Wang, 2023) depicted that, a set of heterogeneous magnetic catalysts for biodiesel synthesis produced from waste diapers were

developed using a two-step process that involves wet-impregnation in nickel nitrate solution and subsequent calcination at 700<sup>0</sup>C. The catalyst's structure and catalytic potential were assessed using acid-base titration, BET, XRD, SEM, FTIR, and XRD methods. The investigation's findings showed that the primary constituents of WDHMCs were carbon, nickel, and sodium peroxide. The catalysts' magnetization rose and their catalytic activity fell as the ratio of nickel nitrate to used diapers increased. The resulting catalyst showed comparatively strong catalytic activity with a biodiesel yield of 96.4% and high magnetic separation property in the Trans-esterification reaction of waste cooking oil with methanol when the ratio of nickel nitrate to waste nappy was two mol/g. Furthermore, the produced heterogeneous magnetic catalyst formed from waste diapers could be readily repurposed four times without losing its high catalytic activity through straightforward magnetic separation.

15. Mothil et al. (Mothil *et al.*, 2021) depicted that, using a co-precipitation aqueous solution of  $Mg(NO_3)_2 \cdot 6H_2O$  and  $Al(NO_3)_3 \cdot 9H_2O$ , followed by a hydrothermal treatment at 110<sup>0</sup>C for 12 hours, Mg-Al hydrotalcite was created. Layered double hydroxide, also called hydrotalcite, is a compound in which trivalent cations restore the divalent cations in the brucite-like layers. Hydrotalcite is used in a variety of processes and other applications as a catalyst. Hydrotalcite finds wide-ranging uses in the medical area as an antacid, as an anion exchanger, and in a variety of wastewater treatment techniques. This new catalyst has applications in organic chemical synthesis, different oxidation reactions, Aldol condensation, Claisen-Schmidt condensation, and Knoevenagel condensation. Mg-Al hydrotalcite was used in this work to trans-esterify used cooking oil. Using methanol (20:1 to 40:1) and Mg-Al hydrotalcite, biodiesel was produced in a

single-step Trans-esterification process that involved constant stirring for 1.5 to 3.5 hours at 80 to 160<sup>0</sup>C. A filter is used to remove suspended contaminants from waste cooking oil, and the oil is then heated to 120<sup>0</sup>C to eliminate moisture. By adjusting the methanol-to-oil molar ratio, temperature, time, and heterogeneous Mg-Al hydrotalcite catalyst, the goal was to optimize the biodiesel output. By measuring and assessing the methyl ester content (FAME, %) using gas chromatography and a flame ionization detector (FID), biodiesel conversion was ascertained.

16. Niju et al.(Niju *et al.*, 2023) depicted that, potential alternative fuel that may be utilized in regular engines and has various environmental advantages is biodiesel. The high expense of the feedstock, however, makes it less viable commercially. With a focus on the utilization of modified conch shells as a solid catalyst in ultrasonic settings, this study aims to produce biodiesel using waste cooking oil (WCO) and Moringaoleifera oil (MOO) as feedstock. The appropriateness of various WCO and MOO combinations was assessed in a two-stage Trans-esterification process, and an ultrasound-assisted esterification procedure was used to lower the acid value of the WCO-MOO blend. Additionally, conch shells (CS) were used to create a calcium oxide-based catalyst that was further changed with water and methanol after being calcined for three hours at 900<sup>0</sup>C. The characterization investigations show good catalytic activity and validate the development and modification of the CS catalyst. The Box–Behnken design (BBD) based on response surface methodology (RSM) was utilized to optimize the parameters of the ultrasound-assisted Trans-esterification process. A maximum projected methyl ester conversion of 94.7% was attained by using a

catalyst loading of 5.8 weight percent, methanol to esterified oil volumetric ratio of 0.37:1, and an ultrasonication period of 57 minutes. Thus, this work contributes to the development of economical and ecologically friendly biodiesel production methods by offering insightful information about the application of modified conch shell catalysts for biodiesel production from WCO and MOO mixtures.

17. Danane et al. (Danane *et al.*, 2022) depicted that, the best alternative to diesel fuel is biodiesel made from waste cooking oil (WCO), which has nontoxic qualities, better emissions, lubricates engines, and comes from renewable resources. The primary goals of this work were to increase the experimental production of biodiesel using ethanol and to apply Response Surface Methodology (RSM) to examine the effects of three key operating factors on biodiesel yield: catalyst concentration, stirring speed, and ethanol–oil molar ratio. The separation of glycerol from biodiesel after the Trans-esterification reaction is the primary issue with using ethanol as an alcohol at the expense of methanol's toxicity. To help with this separation and enhance oil conversion, however, 1% (v/v) water and 5% (v/v) glycerol are added towards the conclusion of the procedure. Three factors are used to optimize the biodiesel that is produced: The experimental results correspond with the expected values, according to Face-Centered-Composite Design (FCCD), statistical analysis, and model construction. The model's accuracy is indicated by the model's  $R^2$  value of 0.9924, which is close to unity. A biodiesel efficiency of 89.75% was achieved by using the ideal catalyst concentration (1.62 wt %), stirring speed (200 rpm), and a molar ratio of ethanol to oil (12.9:1). Additionally, the model's experimental validation yielded a biodiesel output of almost 90%. The ethyl ester's fuel characteristics were

examined and effectively compared with baseline local diesel (NA 8110), ASTM, and EN standards.

18. Velmurugan et al. (Velmurugan, Warriar and Gurunathan, 2023) depicted that, because of their improved and controllable qualities, non-toxic nanoscale metal oxide structures are becoming more and more attractive as possible materials for energy and environmental applications. MgO nanoparticles were created using the sol-gel technique for this study. The ideal calcination temperature and duration were 600<sup>0</sup>C for two hours. The resulting 15 nm-sized mesoporous MgO nanoparticles had a band gap of about 3.3 eV. With a zeta potential of 17.3 mV, magnesium oxide nanoparticles are regarded as being in the early stages of stability. The process of producing biodiesel involved the use of cubic MgO nanoparticles. Operating variable optimization was done using a one-factor approach and response surface methodology (RSM). At ideal catalyst concentrations of 1% (w/w), methanol to oil molar ratios of 16:1, and reaction temperatures of 65<sup>0</sup>C for 42 minutes, RSM predicts 90% of biodiesel yield, which is also experimentally verified (89.5%). Using the one-factor technique, a biodiesel yield of about 92% is achieved at a higher reaction temperature of 60<sup>0</sup>C, a longer reaction time of 2 hours, a molar ratio of 12:1 methanol to oil, and 2% (w/w) of catalyst. The GC-MS spectrum indicates that during Trans-esterification, the hexadecanoic acid, stearic acid, linoleic acid, and oleic acid in the waste cooking oil change into methyl stearate, hexadecanoic acid methyl ester, 9, 12-octadecadienoic acid methyl ester, and 9-octadecenoic acid methyl ester. The Trans-esterification reaction has kinetics that are pseudo-first-order. Reusing the MgOnano-catalyst in the Trans-esterification process yields a yield of about 90% for up to four cycles.

19. Garba et al. (Garba *et al.*, 2023) depicted that, the feasibility of producing biodiesel from waste cooking oil (WCO) utilizing synthesized acid-bearing carbonaceous catalyst ( $\text{SO}_3\text{H}-\text{C}$  and  $\text{PO}_4\text{H}_2-\text{C}$ ) obtained from cassava peel was investigated. Three distinct oil-to-alcohol ratios (1:3, 1:5, and 1:7) were used in an autoclave-style reactor to test the catalyst's activity over four hours at four different temperatures (50–80°C). The efficiency of employing alcohol in the process was investigated using two different forms of alcohol: methanol ( $\text{CH}_3\text{OH}$ ) and ethanol ( $\text{C}_2\text{H}_5\text{OH}$ ). According to the study, when compared to other ratios, reactions employing a high alcohol ratio (1:7) typically produced a high yield of biodiesel. In every reaction system, the biodiesel output rose as the temperature rose as well. At 80°C and a 1:7 WCO: alcohol ratio, the carbon treated with sulphuric acid catalyst yielded the best yield, almost 90%. Additionally, it was found that methanol reactions yielded higher yields than ethanol reactions, where notable variations were seen in both temperature and ratio. X-ray powder diffraction, surface area, and pore volume measurements, and Fourier transform infrared spectroscopy were used to characterize the catalysts. The catalyst is intriguing since it is made from leftover cassava peel waste, is non-toxic, and is environmentally friendly.
20. Weldehlase et al. (Weldehlase *et al.*, 2023) depicted that, one of the alternative fuels is biodiesel, which is often made chemically with a catalyst from oil and methanol. The goal of this project is to produce as much biodiesel as possible using inexpensive, easily accessible sources of waste cooking oil (WCO) and zinc-doped calcium oxide (Zn-CaO) catalyst made of lime and manufactured using a wet impregnation method. Limestone that had been calcined was mixed with 5% zinc to create the Zn-CaO Nano catalyst. SEM, XRD, and FT-IR

spectroscopic methods were used to ascertain the shape, crystal size, and vibrational energies of the CaO and Zn-CaO nanocatalysts, respectively. The Trans-esterification reaction's primary variables were optimized using the box-Behnken design-based response surface methodology (RSM). The average crystalline size decreased from 21.14 to 12.51 nm when Zn was added to lime-based CaO, as demonstrated by the results, which also revealed an increase in surface area and structural irregularity. The maximum biodiesel conversion of 96.5% was achieved by using the following experimental parameters: temperature (57.5 °C), catalyst loading (5% wt.), methanol to oil molar ratio (14:1), and reaction period (120 min). The produced biodiesel's fuel properties met American (ASTM D6571) fuel requirements. The study makes recommendations for the possible use of WCO and catalyst based on lime as effective and affordable raw materials for large-scale biodiesel production meant for a variety of uses.

21. Bora et al. (Bora *et al.*, 2023) depicted that, biodiesel is regarded as a potential replacement for energy sources produced from non-renewable fossil fuels. However, its widespread industrial application is hampered by the high costs of feed stocks and catalysts. In this sense, using garbage as a source for catalyst production and as a feedstock for biodiesel is an uncommon endeavor. It was investigated to use leftover rice husk as a precursor to make rice husk char (RHC). To create biodiesel, highly acidic waste cooking oil (WCO) was simultaneously esterified and transesterified using sulfonated RHC as a bifunctional catalyst. The combination of sulfonation and ultrasonic irradiation has shown to be a successful method for increasing the acid density of the sulfonated catalyst. The generated catalyst has a surface area of 144 m<sup>2</sup>/g and two



different densities: 4.18 and 7.58 mol/g for the sulfonic and total acid, respectively. Using the response surface methodology, a parametric optimization was carried out for the conversion of WCO into biodiesel. The circumstances of methanol to oil ratio (13:1), reaction period (50 min), catalyst loading (3.5 wt%), and ultrasonic amplitude (56%) resulted in an ideal biodiesel yield of 96%. Up to five cycles, the developed catalyst demonstrated increased stability and produced a biodiesel yield above 80%.

22. Al-Sakkari et al. (Al-Sakkari *et al.*, 2020) depicted that, the purpose of this study is to present the techno-economic features of two clean techniques for producing biodiesel. In the first method, potassium hydroxide is used as a homogenous catalyst, and cooking oil waste as a feedstock. Virgin soybean oil and heterogeneous cement kiln dust catalysts are used in the second phase. To ascertain whether the procedure was more practical, a comparison was made between the findings of the technical and economic analyses. Theoretically, 99.99% theoretical purity of glycerol and biodiesel can be achieved by simulating both processes. Nevertheless, the homogeneous process is more advantageous economically because it has a payback period of just over a year, a return on investment of more than 74%, and a unit production cost of USD 1.067/kg biodiesel. Sensitivity analysis showed that the price of the feedstock has a significant impact on the profitability of biodiesel production and suggested switching to waste vegetable oils as a low-cost feedstock to create a workable and profitable process.
23. Selvaraj et al. (Selvaraj *et al.*, 2019) depicted that, the scarcity of petroleum resources, concerns over global warming, and the current annual increase in petroleum costs have spurred scientists to discover new, affordable energy

sources. Using edible oils, such as vegetable oils, as fuel brought human requirements for food and non-food purposes into direct competition. Moreover, the expense of planting and producing crude oils makes the use of inedible seed oils as renewable fuel sources expensive. This work has examined and characterized the physical characteristics of waste cooking oil (WCO), refined bleached deodorized (RBD) palm oil, and crude palm oil (CPO), as well as their methyl esters. Second, disparities in microwave exit powers, reaction times, and reaction temperatures were compared between the conventional and microwave irradiation methods of producing biodiesel. The ASTM method was followed in the methyl ester characterization of waste cooking oil (WCO), and the results were compared with existing information. In general, this oil's methyl ester form has a flash point that is safe to store at 131°C. The WCO methyl ester's calorific value was another outcome. At 40,870 kJ/kg, it was still less than diesel fuel but marginally more than in its raw state. WCO methyl ester had a lower cloud point and pour point (13<sup>0</sup>C) than CPO methyl ester, but a slightly higher cloud point and pour point than RBD methyl ester. At 40<sup>0</sup>C, the kinematic viscosity was 3.019 cSt, which was similar to that of regular diesel. The density of used cooking oil (0.886 kg/liter) was somewhat greater than that of regular diesel. The findings demonstrated that microwave irradiation significantly reduces the response time from 60 to 180 minutes when using conventional methods to approximately 5 to 9 minutes.

24. Ogata et al.(Ogata *et al.*, 2023) depicted that, the scarcity of petroleum resources, concerns over global warming, and the current annual increase in petroleum costs have spurred scientists to discover new, and affordable energy sources. Using edible oils, such as vegetable oils, as fuel brought human requirements for food

and non-food purposes into direct competition. Moreover, the expense of planting and producing crude oils makes the use of inedible seed oils as renewable fuel sources expensive. This work has examined and characterized the physical characteristics of waste cooking oil (WCO), refined bleached deodorized (RBD) palm oil, and crude palm oil (CPO), as well as their methyl esters. Second, a comparison between the traditional and microwave irradiation methods for producing biodiesel was conducted, with an emphasis on examining the various microwave exit powers. At 40,870 kJ/kg, it was still less than diesel fuel but marginally more than in its raw state. The WCO methyl ester's cloud point and pour point, which are 13<sup>0</sup>C and 9<sup>0</sup>C, respectively, were somewhat greater than those of the RBD methyl ester but lower than those of the CPO methyl ester. At 40<sup>0</sup>C, the kinematic viscosity was 3.019 cSt, which was similar to that of regular diesel. The density of used cooking oil (0.886 kg/liter) was somewhat greater than that of regular diesel. The findings demonstrated that microwave irradiation significantly reduces the response time from 60 to 180 minutes when using conventional methods to approximately 5 to 9 minutes. Fuel made from biodiesel (BDF) has the potential to be carbon neutral and to be a significant contributor to the fight against global warming. For many BDF manufacturers, however, its high production cost presents a challenge. The production efficiency of 35 BDF factories in Japan, which make BDF from leftover cooking oil, was assessed to develop an effective technique for BDF production and raise its cost competitiveness. Additionally, an assessment of the possible cost savings linked to increased efficiency was made. The results of the empirical analysis showed that: (1) about 92% of BDF plants produce inefficiently; (2) they show two main types of inefficiencies, namely technical and scale inefficiencies; and (3)

reducing production inefficiencies can result in an average 3.52 yen reduction in production costs per liter of BDF. Improving the quality of the used waste cooking oil and expanding the production scale is crucial for raising production efficiency. It is advised that operators of inefficient BDF facilities become familiar with the manufacturing processes used by the plants that this study found to be the most efficient. In addition, government initiatives centered on productive BDF plants are necessary to boost BDF output while utilizing constrained resources.

25. Ulfah et al.(Ulfah, Octavia and Suherman, 2019) depicted that, biodiesel made from waste cooking oil (WCO) that had been created by one-stage reactions (Trans-esterification) and two-stage reactions (esterification followed by Trans-esterification) with initial free fatty acids (FFA) of 6.67%. NaOH catalyzed the Trans-esterification reaction, while a solid catalyst made of artificially produced sulfated alumina catalyzed the esterification process. This study compares the biodiesel yield from utilizing homogeneous sulfuric acid catalysts with a heterogeneous sulfated alumina catalyst to identify the ideal conditions for biodiesel generation from WCO using sulfated alumina catalysts by esterification process. The findings demonstrated that the ideal parameters for esterification processes utilizing sulfated alumina catalyst are 1.5 wt.%/v of oil and a catalyst volume ratio of methanol to oil at a reaction period of one hour. Using a sulfuric acid and sulfated alumina catalyst, the maximal conversions of free fatty acid under ideal conditions were 90.4% and 89.95%, respectively. A two-stage Trans-esterification process yields 86.67% of biodiesel from waste cooking oil, while a one-stage approach yields 66.67%.

26. J.Sree et al. (Sree *et al.*, 2021) suggested that non-renewable diesel derived from fossil fuels may be carcinogenic and have major negative effects on both the environment and human health. To create biodiesel, a renewable diesel, by the Trans-esterification of waste cooking oil (WCO), this study looked into and identified the most appropriate heterogeneous catalyst types, including KOH/CaCO<sub>3</sub>, KOH/CaO, and KOH/K<sub>2</sub>CO<sub>3</sub>. The biodiesel was subjected to chemical and physical characterization. The KOH/CaCO<sub>3</sub> catalyst outperformed the other catalysts in terms of yield percentage and demonstrated superior fuel quality in terms of density, acid value, viscosity, and free fatty acid. This performance can be the result of its most fundamental feature compared to the others. This catalyst was chosen for the optimization study as a result. Triglyceride conversion reached its maximum at 98.12% under ideal reaction conditions of 10-weight percent catalyst loading and 1:10 oil to methanol feed mole ratio. The characterization results demonstrate that the produced fuel can be used instead of petrol diesel since the characteristics examined (i.e., density, viscosity, acid value, and free fatty acid) meet the stringent standards of the biodiesel standard.
27. Supardan et al.(Supardan, Satriana and Mahlinda, 2012) depicted that, they used a hydrodynamic cavitation apparatus to investigate the generation of biodiesel from waste cooking oil (WCO), a low-cost feedstock. The esterification and Trans-esterification processes, which use hydrodynamic cavitation to produce biodiesel from waste cooking oil (WCO), are described as two-step procedures. The first step reduces the free fatty acid (FFA) content of WCO by an acid-catalyzed esterification process. The second step is a base-catalyzed Trans-esterification process that turns WCO into biodiesel. With a methanol-to-oil

molar ratio of 5 and a temperature of 60°C, the esterification process resulted in a reduction of the initial acid value of WCO from 3.9 mg KOH/g to 1.81 mg KOH/g in 120 minutes. With a methanol-to-oil molar ratio of six, the Trans-esterification process produced the maximum output of biodiesel, 89.4%, at a reaction time of 150 minutes. Gas chromatography-mass spectrometry (GC-MS) analysis of the biodiesel produced in the experiment revealed that it mostly included five methyl esters of fatty acids. Furthermore, the characteristics of the biodiesel demonstrated that it complied with Indonesian National Standard (INS) No. 04-7182-2006 for biodiesel in every way.

28. Dharmalingam et al.(Dharmalingam *et al.*, 2023) depicted that, the goal of the current study is to maximize the biodiesel production process's characteristics using mixed waste cooking oil, which includes both palm and sunflower oil. The biocatalyst was made from vegetable wastes such as Chinese broccoli, cauliflower, and Napa cabbage. The incipient wet impregnation method was used to create the potassium hydroxide-impregnated biocatalyst. The parameters in the synthesis of biodiesel are optimized using artificial neural networks (Bayesian Regularisation, Levenberg Marquardt Neural Network, Scaled Conjugate Gradient, and RSM-based central composite design). The anticipated outcomes from the RSM and ANN models are compared to the outcomes of the experiments. According to the experiment findings, a biocatalyst impregnated with KOH generated a maximum yield of 94.7% at a reaction temperature of 60°C, a reaction time of 120 minutes, a catalyst loading of 7 weight percent, a ratio of 1:9 M, and a stirrer speed of 900 rpm. Furthermore, the BRNN neural network produced superior prediction results for biodiesel production than the other two ANN algorithms. While the efficiency of LMNN and SCGNN is

almost comparable, the BRNN model has smaller error values. The ANN and CCD models exhibit superior dependability for process optimization, as evidenced by their decreased RMSE and MAPE values (ranging from 0.001 to 0.018 and 3.22 to 4.37%, respectively) and high  $R^2$  values (between 0.97 and 0.99). To obtain the highest possible biodiesel yield, the aforementioned study suggested using a biocatalyst that has been impregnated with KOH. Furthermore, yield prediction and biodiesel process optimization are recommended using ANN and RSM approaches.

29. Widayat et al. (Widayat *et al.*, 2020) depicted that, through the esterification process, vegetable oil can be converted into biodiesel, a promising alternative fuel. Traditional homogenous acids or basic catalysts need to be separated from the product, which causes inefficient manufacturing. They also have a longer reaction time and a lower biodiesel yield. The purpose of this study was to convert used cooking oil waste into biodiesel by esterifying it using the heterogeneous catalyst potassium iodide (KI)/ $\gamma$ -aluminum oxide ( $\gamma$ -Al<sub>2</sub>O<sub>3</sub>). The impregnation method was used to manufacture the catalyst, which involved three hours of calcination at 500°C. The conditions for the esterification process were established for three hours at 65°C and a 1:14 molar ratio of oil to methanol. In addition, the yield of biodiesel produced by the heterogeneous and homogeneous catalysts was contrasted. According to the findings, the esterification process employing the catalyst KI/ $\gamma$ -Al<sub>2</sub>O<sub>3</sub> yielded a greater yield of biodiesel (88.03%) at a 2% (g catalyst/g oil) catalyst concentration than that of utilizing  $\gamma$ -aluminum oxide (58.86%) and a conventional catalyst (82.23%). The catalyst KI/ $\gamma$ -Al<sub>2</sub>O<sub>3</sub>'s reusability study revealed that, even after its initial reuse, it could still generate

biodiesel with a yield of 61·30%. The biodiesel yield following the second reuse was 52·61%, while the yield following the third reuse was 21·50%.

30. Salih et al. (Salih and Salimon, 2021) depicted that, the best temporary replacement for mineral diesel is biodiesel, which is being produced and consumed more widely due to the need for diesel fuel worldwide as well as the negative effects that direct combustion has on the environment and human health. However, the use of edible and non-edible oil feedstock in the manufacturing of biodiesel has resulted in several contentious issues, such as feedstock supply and cost, greenhouse gas emissions, land-use changes (LUC), and food competition. It is possible to efficiently address these issues with non-crop meals like waste cooking oil (WCO). In this instance, waste-based oil or fat is advised as the ideal substitute for distributing biodiesel because it disregards the expense of collection and reuse.
31. Banowati et al. (Istiningrum, Aprianto and Pamungkas, 2017) depicted that, the proposed study uses lipase that was isolated from rice bran to investigate how temperature affects the enzymatic conversion of waste cooking oil into biodiesel. The lipase enzyme was extracted using a buffer with varying pH, using simulated waste cooking oil as the input. Temperature's impact on the Trans-esterification reaction was investigated using the ideal pH buffer and titrimetric determination of the enzyme activity. The effects of temperature were evaluated between 45 and 60°C, and GC-MS was used to ascertain the methyl esters concentration of the biodiesel. The Trans-esterification reaction is greatly influenced by the reaction temperature; the best biodiesel conversion was observed at 55°C with an 81.19% methyl ester concentration. Methyl palmitate, methyl oleate, and methyl stearate make up the methyl ester makeup of the resultant biodiesel.



32. Prokaewa et al (Prokaewa *et al.*, 2022) depicted that, the generation of biodiesel from waste palm cooking oil (WPCO) was investigated. Used palm oil was transesterified with methanol using calcium oxide and a strontium ion additive (Sr-CaO) as a catalyst. Using a co-precipitation process between  $\text{SrCl}_2$  and  $\text{Ca}(\text{NO}_3)_2$ , Sr-CaO was created, and it was then calcined for five hours at  $900^\circ\text{C}$ . Thermo-gravimetric analysis (TGA), Fourier transform infrared spectrometer (FT-IR), scanning electron microscopy (SEM), and X-ray diffraction (XRD) were the methods used to characterize the catalyst. By using SEM-EDX, the shape and elemental composition of Sr and Ca in the catalyst were verified. The catalyst diameter is approximately  $12.6 \pm 5.9 \mu\text{m}$ . With a 3-hour reaction duration, 5% w/w catalyst, 9:1 methanol to oil molar ratio, and an  $80^\circ\text{C}$  reaction temperature, the maximum conversion was 99.33%. With a good yield, the catalyst can be employed through the sixth cycle. The synthetic biodiesel satisfies ASTM D445 and EN 14103 requirements for standard biodiesel. These results imply that a strontium ion-added calcium oxide (Sr-CaO) is a potent catalyst for renewable biodiesel.
33. Wicaksono et al. (Wicaksono *et al.*, 2018) depicted that, the proposed work describes the first application of non-treatment waste concrete as a heterogeneous catalyst to improve the co-solvent-free electrochemical method's ability to produce biodiesel from waste cooking oil (WCO). In-depth research was done on the characteristics of WCO and cooking oil as feedstock, waste concrete, and hydrated cement as catalysts. There was a discussion on the impact of catalyst quantity and WCO's potency as a feedstock. Additionally, we conducted a comparison of the catalytic activity of hydrated cement and waste concrete, finding that the former has higher activity. Ultimately, waste concrete actively

catalyzes the production of biodiesel using WCO as feedstock, yielding up to 92.92% of fatty acid methyl ester (FAME) under ambient conditions with 0.5 weight percent of catalyst, a methanol/oil molar ratio of 24:1, and 0.56 weight percent of NaCl (weight percentage of oil) at a constant voltage of 9.6 V for a two-hour reaction. Our findings demonstrate the great potential of these discarded, practically free materials as a catalyst for the synthesis of biodiesel.

34. Aghel et al. (Aghel *et al.*, 2022) depicted that, the proposed work intends to enhance the synthesis of biodiesel from waste cooking oil (WCO) by Trans-esterification using a graphene oxide doped magnesium oxide nano catalyst. The response surface approach is used to optimize the reaction parameter that affects the Trans-esterification reaction for the manufacture of biodiesel. The [email protected] Nano catalyst was examined using scanning electron microscopy (SEM), powder X-ray diffraction (XRD), energy-dispersive X-ray spectroscopy (EDX), and Fourier Transform Infrared Spectroscopy (FTIR). The maximum biodiesel purity for MgO and [email protected] at optimal circumstances was 93.84% and 99.23%, respectively. The catalyst dosages of 4.7% and 3.9% weight, the oil/methanol volume ratios of 2.46:1 and 2.67:1, and the reaction times of 174.2 and 176.39 seconds were the optimized parameters.
35. Nabizadeh et al. (Nabizadeh *et al.*, 2023) depicted that, the current study used a unique modeling approach to investigate the ideal conditions for producing biodiesel from waste cooking oil (WCO) from catering facilities in Iran. To maximize the calorific value of biodiesel, response surface methods based on D-optimal design were employed. After collecting WCO samples, they were centrifuged to create a bottom phase (B-WCO) and a supernatant phase (S-

WCO), which was utilized to make biodiesel. Based on the modeling results, 50°C, 45 min, 10:1 methanol to S-WCO ratio, and 0.56 wt% catalyst were shown to be the ideal conditions for the maximal calorific value (9500.74 kcal/kg). With a 95% confidence level, regression analysis of the experimental data revealed a strong link between temperature, catalyst, and the methanol-to-oil ratio. It is guaranteed that the suggested quadratic model is appropriate for the optimization of biodiesel calorific values based on the findings of the ANOVA study. The biodiesel's physical and chemical characteristics matched those of fuel specified by American, European, or German standards. Furthermore, given that B-WCO has a great deal of potential for producing solid alcohol, it can be said that WCOs are an excellent, safe, accessible, and sustainable alternative for the construction of large-scale bio-refinery facilities, which could aid in lowering concerns about the environment and the availability of energy.

**Table 2.6 Literature review of Waste cooking Oil**

Feed stock	Study	Reference	catalyst
Waste cooking oil production	Statistical review of World energy	(Suzihaque <i>et al.</i> , 2022)	
Waste cooking oil from university cafeteria	36 liter used cooking oil produced every day which can produced biodiesel having yield of 84%.	(Rahman <i>et al.</i> , 2020)	
virgin vegetable oil	Lipase, bases, and acids are typically employed as catalysts.	(Gnanaprasam <i>et al.</i> , 2013)	NaOH alkaline catalyst
Utilized cooking oil	MR 18:1, Yield of 88%	(Velmurugan and Warriar, 2022)	Bifunctional 1MgO-SnO <sub>2</sub>
vegetable oils	Oil collected from a caterer. The company's five-year strategic strategy calls for accumulating 15–20% of all ravage eatable oils produced domestically, or as much as 6000–8000 tons annually	(Topi, 2020)	NaOH alkaline catalyst
Used vegetable oil	Activated carbon filter with surface area of 1300m <sup>2</sup> /fabrication of small reactor. the cost of production \$0.52/liter	(Okoye <i>et al.</i> , 2013)	

Utilized cooking oil	The agents for promoting and executing WCO consumption and WCO-based biodiesel creation. Interpretative structural modeling (ISM)	(Kukana and Jakhar, 2021)	KOH alkaline catalyst
Rapeseed oil	yielding of 99.55%, 12:11 methanol to oil molar ratio, 70 °C reaction temperature, a catalyst quantity of 41wt% supported on oil weight, and a 6-hour retort time, catalyst quantity of 41wt% supported on oil weight	(Rezki <i>et al.</i> , 2020)	Calcining natural phosphate to a temperature of 800 <sup>0</sup> C after cesium chloride (CsCl) was impregnated on it.
Alfa WCO	Yield of 97.76 by NaOH and 94.4%, KOH catalyst	(Hamed <i>et al.</i> , 2021)	NaOH and KOH
WCO	Density of biodiesel varied from 0.80 to 0.843 g/mL; acid equivalent was 2.53 mg KOH /g	(Awad, Hreeba and Elkhidr, 2022)	NaOH alkaline catalyst
WCO	yield of WCO based biodiesel was 71.3% when H <sub>2</sub> SO <sub>4</sub> was the only catalyst used. When ZnO nanoparticles were added, the yield rose to 81.94% at a catalyst concentration of 0.5% (w/w).	(Gada, Dusi and Abrar, 2022)	ZnO and H <sub>2</sub> SO <sub>4</sub>
Used cookery oil	Modified possibility chance-constrained programming (MPCCP), Lingo 18.0 is used to solve the MPCCP model, and MATLAB is used to estimate demand using fuzzy logic.	(Munir <i>et al.</i> , 2023)	NaOH alkaline catalyst
WCO	Universiti Kebangsaan Malaysia (UKM) Bangi cafeterias to produce 1 biodiesel	(Alias, Jayakumar and Zain, 2018)	AOCS Cc 9b-55, and AOCS Cd 3-25, KOH alkaline catalyst
Used cooking oil	FTIR and X-ray diffraction (XRD) were used to characterize the biodiesel and produced catalyst	(Welela and Asere, 2022)	CaO/K <sub>2</sub> O catalyst
Used Cooking oil	maximize the biodiesel production process parameters	(Ulukardesler, 2023)	KOH and Amberlyst 15
Waste cooking oil	Biodiesel yield of 84.96%	(Ayodeji <i>et al.</i> , 2023)	CaO/ZnO
Waste Oil(Temple)	viscosity of 8.25 cSt at 40 °C, a density of 830 kg/m <sup>3</sup> , and a calorific value of 41.6 MJ/kg	(Jagadeesh, Shrigiri and Hebbal, 2022)	T25
Used Cooking oil	Response surface methodology (RSM)	(Maqsood and Alsaady, 2022)	fishbone waste as a catalyst
Used cooking oil and sunflower oil	yields of 98.54% for sunflower oil and 96.89% for waste cooking oil	(Ghavami <i>et al.</i> , no date)	K <sub>2</sub> O/RGO heterogeneous catalyst

Waste cooking oil	ANOVA testing and R.S.M. optimization. C.C.D. design to maximize the production of biodiesel	(Aghel <i>et al.</i> , 2023)	CaO
Waste cooking oil, orange peel oil	Biodiesel of WCO, it's yield and property optimization	(Mishra, Kumar and Chaudhary, 2023)	KOH
Waste orange peel oil biodiesel	Biodiesel of Orange peel oil blended with antioxidant additive	(Ganesan and Masimalai, 2019)	NaOH

The reliance of the agriculture and transportation sector on fossil-based fuels required rigorous research in the field of alternative fuels during the emerging energy crisis worldwide. However, the use of fossil fuels for fulfilling the energy demand has led to the cause of undesirable environmental effects. This involves environmental degradation and pollutant emissions such as particulate matter, smoke, nitrogen oxides (NO<sub>x</sub>), carbon monoxides (CO), carbon dioxide (CO<sub>2</sub>). This makes the replacement of conventional fuels like gasoline, diesel, and crude oil, etc with non-conventional fuels either partially or completely. The previous works of literature have revealed that the production of biofuel and its application in CI engines causes a substantial downfall of up to 40% in greenhouse gas emissions (Kim and Dale, 2005). While the suitability of alternative fuel majorly depends on its Physico-chemical properties when compared to petro-fuel whilst used in compression ignition (CI) engines (Tesfa *et al.*, 2014). However, some extensive properties such as kinematic viscosity, calorific value, cetane index, boiling point, and cold flow properties must be in the suitable range of fuel (Sakthivel *et al.*, 2018).

The application of methyl ester in the existing CI engine is not that efficient when is compared with the diesel-run engine. The use of waste cooking oil has been considered as a desirable feedstock for producing biodiesel which can be a suitable fuel for CI engines (Nayak *et al.*, 2021). However, its use in a CI engine has to lead to

an increase in harmful emissions, mainly of NO<sub>x</sub> emissions (Mishra, Chauhan and Mishra, 2020b). (Hoang and Pham, 2018) stated that Long-term use of vegetable oils as a fuel for diesel engine may result in a significant rise in toxic emissions, pollutants along with the reduced engine power, and degrades the quality of lubrication oil (LO) because of deposit development, which damaged the engine significantly. To overcome this problem, several peroxides and alcohol-based additives used as the cetane improvers are mixed with the biodiesel to improve the performance and emission parameters of the engine (Roslan, Veza and Said, 2020). A review study conducted by (Hoang, 2021), which concludes the reduction in emission characteristics of diesel engine using nanoparticles. The author also stated that NO<sub>x</sub>, CO, and HC emissions were reduced by using the CeO<sub>2</sub> nanoparticles in the CI engine.

Sometimes, vegetable oils (bio-oils) and their biodiesel has been tested as one of the main alternative fuels for its utilization in an internal combustion engine (Yilmaz, Atmanli and Vigil, 2018). However, there are certain technical limitations for using straight vegetable oil as a vehicle fuel. A study was conducted by (Hoang, Le and Pham, 2019) to investigate the spray effect of preheated and unpreheated straight jatropha oil with diesel in CI engine. It was observed that, after a long-term test of about 300 hours on a CI engine, the cone angle is reduced by 3° for straight jatropha oil, both thermal efficiency and heat release rate also getting reduced significantly. It was also observed that the straight vegetable oils are preheated before injecting into the engine or are blended with diesel (Yilmaz and Morton, 2011). These techniques may have been able to resolve the problems to some extent but did not able to eliminate them.

(Atmanli *et al.*, 2015) has done an experimental investigation by using the ternary blends of diesel-vegetable oil- alcohol in CI engine. The authors have concluded that the brake thermal efficiency (BTE), brake mean effective pressure (BMEP), & exhaust gas temperature (EGT) have decreased with the utilization of ternary blends in the CI engine. A similar investigation conducted by (Atmanlı, İleri and Yüksel, 2014), the emissions, CO and NO increased while decreasing trends in HC and CO<sub>2</sub> emissions when compared to diesel. To overcome this, (Yesilyurt *et al.*, 2020) has conducted an experimental study using vegetable oil blended with diesel-biodiesel-alcohol blends to form the quaternary blends that uplift the flow property (density and viscosity) of the overall blends. The authors have figured it out that diesel-biodiesel-vegetable oil-alcohol blends can prove to be a favorable fuel mixture to ameliorate the combustion, performance characteristics with the reduction in exhaust emissions.

(Appavu, Ramanan M and Venu, 2019) conducted an experimental investigation on CI engine fueled with a quaternary blend of diesel, biodiesel, vegetable oil, and alcohol. The authors observed that brake thermal efficiency increased for all the quaternary blends when adding up the concentration of alcohol. The study conducted by (Yilmaz, Atmanli and Vigil, 2018), using vegetable oil in a quaternary blend. The authors compared the effect of long carbon chain alcohols (propanol and pentanol) on the engine characteristics of CI engine and concluded that basic fuel properties were found to be enhanced upon adding up the alcohol. Moreover, brake-specific fuel consumption (BSFC) palliate for pentanol blends fuel with compare to propanol.

The current study aims at investigating the effect of orange peel oil (vegetable oil); which is blended with diesel-biodiesel-alcohol (ternary blend) to form quaternary blends; on the performance and emission characteristics of unmodified diesel engines.

Upon the blending of orange peel oil in the ternary blend, the blend becomes quaternary, so orange peel oil is used as fuel extender. Extraction of orange peel oil from the orange peel (agro-waste) is done by the process of cold pressing of peels. The presence of a major fraction of D-limonene (approximately 91%) components among all the volatile components in orange peel oil made it an attractive alternative fuel for utilizing it in the CI engines, either completely or in blends. From the previous literature (Jorge, Da Silva and Aranha, 2017), it can be seen that the D-Limonene has an antioxidant nature that resulted in improvement of the combustion rate of the fuel (Jha *et al.*, 2019). In the absence of unsaturated fats, the orange peel oil is considered a less-viscous low-cetane fuel because of its shorter carbon-chain length, which leads to a lower cetane index and less viscosity (Vallinayagam *et al.*, 2015).

## **2.17 Problem statement**

After analyzing the exhaustive literature review and finding the research gap, it was concluded that quaternary fuel blends is a promising technique for improving the combustion and emission characteristics of a conventional diesel engine without major modification. In this quaternary blend the waste cooking oil helps in waste management and straight vegetable oil (SVO) help to improve the physico-chemical properties of fuel blends. The quaternary blends of WCOME-SVO- n-butanol-Diesel in CI Engine have not been studied adequately. The optimization of WCOME production and their physico-chemical properties by using the Response Surface methodology (RSM). However, the oxidative stability of WCOME also analyzed. Therefore, exhaustive quaternary blends fuel in CI engine trials using WCOME-SVO- n-butanol and their blends with diesel in various proportions. The analysis that



follows could provide a clear picture of how suitable these fuel blends are for CI engines.

## **2.18 Objectives**

- Identification of utilized feedstock and alcohol for quaternary fuel blend.
- Preparation of the different quaternary fuel blends according to blending norms.
- To optimize production process parameters using response surface methodology for maximizing yield and improved physico-chemical properties.
- Determination of various physico-chemical properties of different test fuel in accordance with relevant standards.
- Performance and emission tests of diesel in a Single Cylinder/Multi-Cylinder Diesel Engine to generate baseline data for reference in all subsequent tests.
- Determine the performance, emission and combustion characteristics single stage CI engines using prepared quaternary fuels to evaluate the Ignition probability of the test fuels.
- To study the spray characteristics of different fuels using Malvern Spraytec.
- Development of the engine test rig for experimental trial.
- Experimental evaluation of combustion characteristics with different test fuels with the help of P- $\theta$  and heat release rate diagrams.
- Comparative assessment and analysis of performance, emissions & combustion characteristics of all test fuels

## **CHAPTER-3**

# **SYSTEM DEVELOPMENT AND METHODOLOGY**

---

This chapter will provide the draft layout how the research had been commenced. The working principals of the used instruments with its standards also explained in this chapter. The sequential explanation of the adopted methodology with the system development as given below

- Selection of experimental Engine Test Rig
- Selection of blending elements
- Preparation of Fuel blends
- Characterization of Fuel blends.
- Engine Test Rig &
- Analysis of test fuel based on their performance

The rigorous study shows that the self-sustainability of the alternate fuel is extremely required for the rural area. It was observed that number of researches has been done biodiesel and its blends with diesel and alcohol. In this study the blends of biodiesel of used cooking oil, n-butanol, and orange peel oil and diesel were used in different proportion to achieve the sustainable fuel for unmodified compression ignition engine. The prepared blends were used on the engine too analyzed it's perforce, emission and combustion characteristics. In this chapter the method of biodiesel production (before and after optimization), testing of physico-chemical properties with equipment/instrument used during the research are explained in this chapter.

### **3.1 Engine selection**

Traditionally, diesel is considered a primary fuel in the compression ignition (CI) engine. The Indian economy is highly reliable on diesel fuel. Diesel is also the

backbone of the transportation as well as agricultural sector. On the way to alternate fuel, biodiesel played an important role. As biodiesel has properties mostly similar to that of petro-diesel. Kirloskar make stationary direct fuel injection engine consist of single cylinder and four strokes was chosen for the current research work. It is a light duty and water cooled engine due to which it is extensively used among the farmer. Along with its favorable utilization with economic aspects. The specification of used engine is explained in Table 3.1 **Engine's Specification Selection of blending elements**

**Table 3.1 Engine's Specification Selection of blending elements**

<b>Engine's Specification</b>	
Make	Kirloskar
Model	DAF 8
Brake Power (kW)	3.5
Cylinders	1
Rated speed (rpm)	1500
Compression ratio	17.5:1
Stroke x Bore (mm)	110 x 87.5
Connecting rod length (mm)	234
Displacement	0.661

The selection of fuel is an important aspect of the research. The selection is based on two factors, first is availability and second clean and sustainable. The blends of the fuel used in the research is formed by biodiesel of used cooking oil, straight vegetable oil (orange peel oil), n-butanol and diesel. The used cooking oil is harmful for health and it's as a waste create the pollution for the earth ground. In all aspects it's totally un-useful. Its conversion into the biodiesel make it favorable as government biofuel policy. To improve its production and physico-chemical properties, RSM optimization is used. The orange peel oil is used as a straight vegetable oil. The usage

of orange peel oil helps to reduce the waste. The volatile content and less viscous are the highly appreciable factors for choosing it as a blending element. The study of all the higher alcohol it was found that n- butanol is better than other.

### **3.2 Selection of blending elements**

#### **3.2.1 Orange Peel Oil (Straight vegetable oil)**

This research aims to establish an alternative synthesis route that avoids the use of conventional solvents, replacing them with green solvents, optimizing biodiesel production, taking care of different aspects such as: the source of the oil, oil extraction to save time. , energy and resources, and generate a fuel that has lower environmental impacts than conventional diesel, therefore the orange peel oil was selected. This plant for the state of orange is an invasive species, which means that it is not native, it has a significant degree of spread in the outdoors and can be found on the sides of roads and in vacant land because it is outside of its natural distribution and is capable of surviving, reproducing, and establishing itself in natural ecosystems and environments, which in turn allow diversity native biological scenarios. Avoiding the use of oranges intended for human consumption and the use of medical areas for their production. Being a plant with high availability as a fruit which is edible and the peel of the same has approximately 10-13% oil, making it a great candidate for the generation of biodiesel.

On the other hand, one of the principles of green chemistry is the use of green solvents in a reaction or some physical process; For this reason, it is intended to use orange peel oil as solvents, they do not represent a risk to health or the environment; Furthermore, orange peel oil is a renewable resource since they can be obtained from orange peel, compared to conventional solvents such as hexane, dichloromethane, 1,2-dichloroethane, among others, known as volatile organic solvents (VOCs). , which are

obtained from oil, a non-renewable natural resource. As a result, the use of these alternative solvents during the direct trans-esterification reaction, the aim is to obtain a biodiesel-type biofuels which is expected to comply with the parameters of ASTM.

### **3.2.2 Selection of Pilot Fuel (Orange Peel Oil)**

It is the fruit that belongs to the sweet orange tree, which corresponds to the citrus genus within the Rutaceae family, reaching approximately 1,500 species around the world. This genus is the most significant of the family since it consists of approximately 20 species with fruits suitable for consumption since they have a high content of vitamin C, essential oils and flavonoids because they are species called hesperides because they contain a special characteristic in the pulp, formed by numerous vesicles that contain juice. There are around 3 varieties of orange in the world, as presented below:

**Navel:** That which contains large, but very early, parthenocarpic fruits. This includes varieties such as: Navelate, Navelina, Newhall, Washington Navel, Lane Late and Thompson, which are identified by their high energy content.

**White:** In this variety, the Valencia Late and Salustiana are identified, which are characterized by their good quality fruits containing few seeds and long-lasting conservation. They are leafy, strong and medium to large sized plants.

**Sanguine:** They are characterized by their high productivity, since fruiting influences vegetative development. In its growth it exhibits small buds and hardening of branches.

### 3.2.3 Taxonomy

The taxonomy of the orange is as follows:

**Table 3.2 Taxonomy of the orange**

<b>Scientific name</b>	<b>Citrus X Sinensis</b>
Kingdom	Plantae
Order	Sapindales
Gender	Citrus
Species	Citrus X sinensis(L.) Osb.
Class	Magnoliopsida
Division	Magnoliophyta
Family	Rutaceae
Subclass	Rosidae

### 3.2.4 Proximal characteristics of orange peel

The fat contribution of orange peel is low and similar to the peel of other species that is, between 2.9 and 0.4%. Regarding the ash value, it is similar in the husk and bagasse flours of this same product, which is directly related to its mineral content. Regarding protein intake, generally low amounts are reported (between 1 and 5%); although in some cases higher values can be reported, particularly in fresh orange peel, which could be explained by the variety or the technological process used in the fresh product. Orange peel is a waste that is little used; however, it has highly nutritional characteristics in terms of carbohydrate and fiber content of 25% and 10%, and it also has polyphenols and antioxidant properties that they are of interest to the food industry. The proximal composition of orange peel is as under:-

- ❖ Humidity %: 29.6
- ❖ Protein %: 7.78
- ❖ Fats %: 2.42
- ❖ Ashes %: 5.17

### 3.2.5 Natural extract

The compounds obtained from biologically active substances characteristic of plant tissues, by the application of solvents such as (alcohol, water, or other selective solvent) and by the application of an appropriate extraction process Figure 3.1. Depending on the part of the fruit used, the solvent and the extraction technique, a wide variety of substances can be obtained. Currently, extracts are considered of great importance to implement a balance between the environment, production and the human being, considering low or no impacts on the environment.

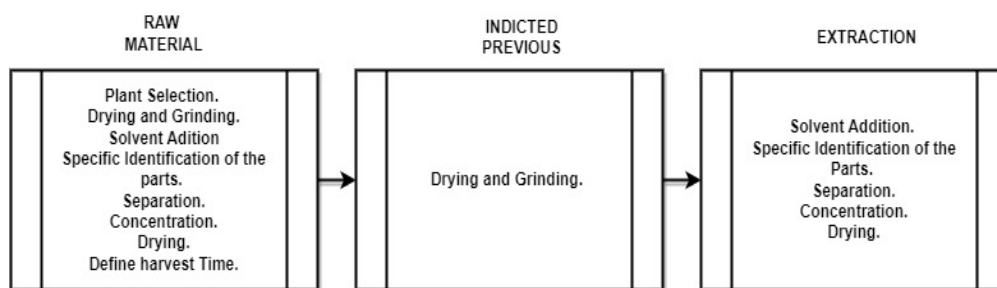


Figure 3.1 Cycle to obtain natural extract

### 3.2.6 Natural degreaser

Degreasers are those products that are normally made from acidic, neutral or alkaline substances. They can be formed by natural or artificial substances and their main characteristic is to decompose oils and fats through a chemical reaction, which, depending on the formulation, will develop in two different ways.

- Formulated in solvent base their own chemical action, which allows the dissolution of oils and fats.
- Water-based formulas molecules through the emulsion process, thus allowing a reduction in adhesion on surfaces. The development of a natural degreaser is an effective alternative for the handling and treatment of organic waste when imposing an added value on waste, however, it is not an option that eradicates the problem in its entirety. Totality since it does not help in reducing the volume of

orange peel generated. For a degreaser to be considered effective, it must maintain a slightly basic pH, to neutralize the acidic pH contained in fats.

### 3.3 Waste Cooking Oil Methyl Ester (WCOME)

#### 3.3.1 Methodology

To determine the FFA content in waste cooking oil, we use a process called titration. First, take one gram of WCO and mix it with ten milliliters of isopropyl alcohol in a container. Then, add two drops of phenolphthalein pH indicator and thoroughly mix the solution. Using N/10 NaOH titration, you can determine the FFA content by recording the amount of NaOH consumed. The titration process should continue until the solution turns pink. Ensure that the color of the obtained solution remains stable for at least ten seconds. Finally, the acid value (AV) can be calculated using Equation 3.1.

$$AV = \frac{VOL_{NaOH} \times Conc_{NaOH} (M) \times MW_{KOH}}{Sample\ weight(gr)} \dots\dots\dots 3.1$$

Where

56.1= Molecular weight of KOH is 56.1

Used volume of NaOH (in ml)

Concentration (Normality) of NaOH solution (0.1 in present research), and

Sample weight of oil in gram

#### 3.3.2 Free Fatty Acid (FFA)

Free fatty acid value is determined after the process for calculate the acid value. The empirical relation is provided in Equation 3.2.

$$FFA(\%) = V_{(T-B)} \frac{28.2N}{M} \dots\dots\dots 3.2$$

Where:

28.2= Molecular weight of oleic acid

V<sub>T</sub>= Titrant volume (in ml) b= Blank volume



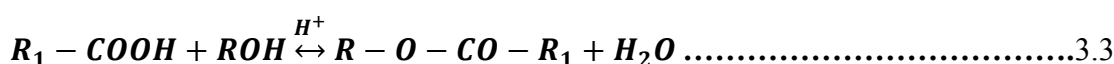
N= Normality of NaOH solution (0.1 in present research), and M= Mass of oil (in g)

OR

$$\text{FFA (\%)} = \frac{\text{Acid Number}}{1.99}$$

### 3.3.3 Esterification

The esterification procedure can lower the FFA of used cooking oil. Because there are more free short bonds in the oil when the FFA is higher than 2%, the saponification process takes precedence over the trans-esterification process. Thus, soap form as opposed to oil esters. Thus, it is necessary to lower the FFA of oil to less than 2% before pursuing the process of trans-esterification. Heating process didn't affect the reaction process, due to the available water content removed by the heating above boiling point of water 15-20 minutes. The alcohol (methanol) was used for the process of esterification by cooling down till 60°C. The boiling point of methanol is 65°C. It should be the best way that temperature couldn't cross the limit of boiling temperature. Otherwise the methanol will be evaporated and it is tough to maintain the methanol to oil ratio. The process is controlled by a magnetic stirrer with a heating plate. This apparatus helps to maintain the temperature (60°C) and the agitation speed (250 rpm) to complete the reaction. Separately prepared a solution of PTSA and methanol in the ratio of 0.5w/w and 10%v/v. This solution fed into the heated mixture in a regular interval of time in a small quantity. Calculate the FFA of small sample of oil and keep in mind that the value of FFA would not be lower than 2%.The performed reaction during this process is provided in equation 3.3.



Where:

R<sub>1</sub>COOH-Carboxylic Acid

ROH-Alcohol

R-O-CO-R<sub>1</sub>-Ester

H<sub>2</sub>O: Water

### 3.3.4 Trans-esterification

The biodiesel produced during the process. The chemical reaction took place. The produced oil reacted with alcohol. Here the alcohol worked as catalyst of the reaction. The fatty acid transformed into the fatty acid methyl ester (FAME). The FAME is known as Biodiesel. The reaction process is world-wide accepted for the biodiesel production.

On the basis of used catalyst the biodiesel production process is classified into two categories:

a) Alkaline catalyst b) Acidic catalyst

It is explained in many researches that production of yield is found more through acidic catalyst trans-esterification as compared to alkaline trans-esterification. Due to the higher reaction time by acidic trans-esterification, it is costlier than other types of processes. In the present research work the base type biodiesel production was opted. To produce biodiesel, oil with an FFA content of less than 2% must first be heated above 100°C to eliminate any excess methanol and water from the oil, leaving only pure oil. After that, the oil is cooled to between 50 and 60°C, which is the same temperature at which the reaction occurs. In the meantime, methanol and KOH were combined to create a solution in a different beaker. The catalyst concentration is maintained between 0.5% and 1.5%, and the ratio of methanol to oil (Molar Ratio) is taken within the range of 3:1 to 9:1. The prepared solution was mixed with oil at a regular interval of time. Due to the higher reaction time of base catalyst process, with the help of a continuous agitator it was completed. A constant-speed magnetic stirrer heating pad was used to perform the reaction. 30 minutes to 120 minutes required to

complete the reaction. The timing varied according to the quantity of oil. So be cautious during the reaction of trans-esterification. After the completion of reaction the solution left for approximately 20-24 hr. in a gravity separator. There were two layers were observed in the separating funnel. The dark colour bottom layer of glycerol and the upper layer which was mixture of biodiesel. Take out the glycerol from the funnel in a beaker. The left mixture of biodiesel was mixed with warm water taking in the 40% v/v. This process to remove the extra glycerol and methanol in the biodiesel. This solution of water and biodiesel was appropriately mixed and remained left for gravity separation again for 5 minutes. There were produced two layers; the bottom layer contained a mixture of water, methanol and glycerol with light white. The upper layer contains biodiesel and ethanol.

Continue doing this until the separating funnel's bottom layer is made entirely of pure water. After removing all of the glycerol from the biodiesel, heat it for at least 30 minutes at 120<sup>0</sup>C to make sure that all of the extra menthol and water that formed during the reaction evaporate and that only pure biodiesel remains inside the container.

### **3.4 Production and Physico-Chemical Properties optimization**

In the current study, we used alcohol-oil MR, CC, RT, R Temp, and agitation speed as input variables, while yield, CV, FP, KV, and PP are the necessary responses. We determined the limit of input variables using the results of the pilot run test and literature review. We validated the center value using the available data. The trans-esterification process could not be completed in both the upper and lower range of the input parameters, or the biodiesel produced did not meet ASTM standards. We discovered that the RSM technique is one of the appropriate experiment designs after carrying out a thorough experimental analysis. This strategy aids in the modelling of

the interaction between the variables and responses by combining statistical and mathematical techniques [231]. The table of coded stags was created using Minitab software version 19 and RSM statistical analysis of the experimental data. To determine the output parameter's ideal value, the CCRD was used. The generated response factor's complete quadratic equation was created. Equation 3.4 expresses a quadratic equation in its general form:

$$= \beta_0 + \sum_{i=1}^5 \beta_i x_i + \sum_{i=1}^5 \beta_{ii} x_i^2 + \sum_{ij=1}^5 \beta_{ij} x_i x_j \dots\dots\dots 3.4$$

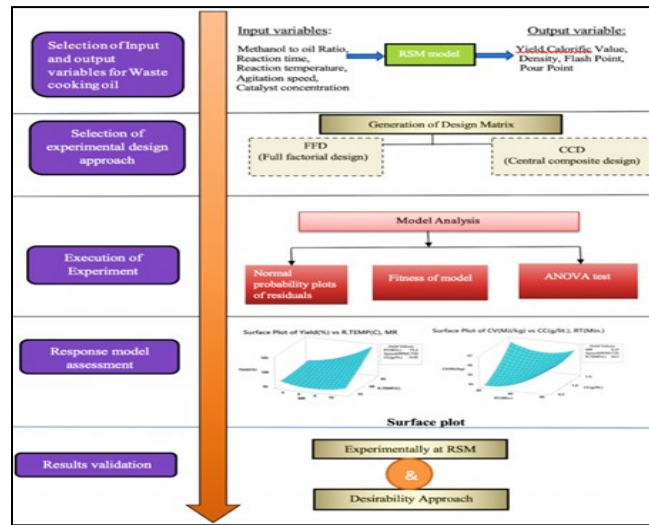


**Figure 3.2 Optimization methodology**

Where Y is the predicted output parameter (yield, CV, KV, FP and PP),  $x_i$ , and  $x_j$  are the un-coded parameter and  $\beta_0$ ,  $\beta_i$ ,  $\beta_{ii}$  and  $\beta_{ij}$  are the coefficient of the model. According to the design standard of the RSM optimization, total thirty-three runs were performed in randomized order. The experimental points in both coded and uncoded values are presented in Table 3.3. The whole work optimization methodology is depicted in Figure-3.2.

One of the key elements of RSM, central composite design (CCRD), was used to evaluate the RSM analysis for the optimization process. The axial and factorial points in the design of the experimental runs are involved in the five-level CCRD experimental model. As observed in Table 3.3, these variables ranged at five different levels (-2, -1, 0, +1, +2).

**Table 3.3 Coded stages for waste cooking oil production and characterization**

Input parameters	Symbol	Coded Levels				
		-2	-1	0	1	2
<b>MR (Methanol/oil)</b>	NA	3:01	5:01	7:01	9:01	11:01
<b>Reaction Time</b>	Minutes	40	50	60	70	80
<b>Agitation Speed</b>	RPM	400	500	600	700	800
<b>Catalyst Concentration</b>	g/lit	0.5	0.75	1	1.25	1.5
<b>Reaction Temperature</b>	<sup>0</sup> C	54	57	60	63	66

In this RSM study, a total layout of 33 experimental data matrices was analyzed. The experiments were conducted at random to prevent methodological error. The engine feedback at all input conditions according to the experimental layout is listed in Table 3.4.

**Table 3.4 Experimental data as per L33 RSM array**

Exp. Run	MR	RT (min)	Speed (RPM)	CC (g/lit)	R.TEMP (°C)	Yield (%)	CV (MJ/kg)	KV (mm <sup>2</sup> /sec)	FP (°C)	CP (°C)
1	9	70	700	0.75	57	97.36	44.78	5.94	149	1.6
2	7	60	600	1	60	96.34	43.26	6.11	154	1.7
3	7	60	600	1	60	96.36	43.32	6.13	154	1.8
4	9	50	500	0.75	57	94.28	41.98	5.91	154	1.5
5	5	50	700	1.25	63	96.36	44.89	5.78	159	1.1
6	7	60	600	1	60	96.34	43.16	6.12	154	1.8
7	5	70	500	0.75	57	93.48	42.67	6.37	161	2.1
8	5	50	500	0.75	63	92.62	41.86	5.63	174	1.5
9	9	70	700	1.25	63	99.28	46.76	5.42	146	1.4
10	5	50	500	1.25	57	98.64	41.94	5.78	148	1.6
11	5	70	700	1.25	57	97.38	44.56	5.79	151	1.3
12	7	60	600	1	60	96.36	43.29	6.13	154	1.8
13	5	50	700	0.75	57	95.18	42.58	6.29	163	1.9
14	9	50	700	1.25	57	97.95	44.87	6.08	148	1.8
15	9	50	700	0.75	63	98.27	44.85	6.09	167	1.7
16	9	70	500	1.25	57	97.93	44.51	5.98	131	1.3
17	5	70	500	1.25	63	95.75	42.98	5.76	164	1.2
18	9	50	500	1.25	63	97.86	43.86	5.62	145	1.6
19	7	60	600	1	60	96.36	43.24	6.12	154	1.7
20	9	70	500	0.75	63	97.17	44.78	6.12	167	1.5
21	7	60	600	1	60	96.35	43.24	6.11	154	1.8
22	5	70	700	0.75	63	97.76	44.76	5.73	178	1.4
23	7	60	600	0.5	60	95.91	42.65	6.39	163	1.9

24	7	80	600	1	60	97.75	44.72	6.16	156	1
25	7	60	600	1	54	96.17	43.12	6.31	151	1.9
26	7	60	400	1	60	95.83	42.34	6.21	158	2
27	7	60	600	1	66	96.97	43.87	5.89	159	1.8
28	3	60	600	1	60	96.76	42.26	6.38	168	2.1
29	7	60	600	1	60	96.34	43.26	6.10	154	1.6
30	7	60	800	1	60	95.26	44.27	6.03	156	1.4
31	11	60	600	1	60	98.67	45.21	5.62	141	1.1
32	7	40	600	1	60	95.36	42.58	6.22	155	2.1
33	7	60	600	1.5	60	97.49	43.87	5.86	145	1.2

### 3.5 Selection of Alcohol

In the present research the direct injection single cylinder four stroke engine was used. The biodiesel of used cooking oil were used as a blending element. The aim of this study to reduce the waste and sustainability of alternative fuel in context of the India. The viscosity is major concern while using the biodiesel. For this the alcohol has the good characteristic when it blend with diesel. All the types of alcohols procured from the authorized vendor of CASRAE, Delhi Technological University, and Delhi. All the properties measured found under acceptance criteria. The comparative study shown in Table 3.5

**Table 3.5 Physio-chemical properties of higher alcohol**

Properties	Unit	Diesel	Methanol	Ethanol	n-Butanol	n-Pentanol
Kinematic viscosity @40°C	mm <sup>2</sup> /s	3.1	0.58-0.6	1.1-1.13	3.6	2.89
Density @15°C	kg/m <sup>3</sup>	833	791.3	789.4	810	814.8
Flash point	°C	67	11-12	17	37	49
Pour point	°C	-1.8	-95.8	-73.4	-45	-26.4
Calorific value	MJ/kg	45.82	19.58	26.83	33.20	34.65
Sulphur content (S 15 grade)	ppm	47.8	-	-	-	-
Cetane number	-	59	2-5	8-11	13.21	18.2-20
Latent heat of vaporization	(kJ/kg)	251	1162.64	918.42	585	308.05
Boiling Point	°C	180-360	64.7-65	78-78.3	118	137.9

### 3.5.1 Preparation of Quaternary Blends

To analyze the output of the CI engine's data, the physiological properties played an important role. So it is compulsory that all the properties should be measured with an appropriate process to learn how they affect in engine performance. It is to be explained in this chapter that the adopted method for the measuring the physico-chemical properties of the test fuel blends with ASTM standards.

The ASTM D445 standard is used to measure the kinematic viscosity of all test fuels using a capillary column viscometer, while the ASTM D4052 standard is used to measure density. A digital density meter was used to measure the density of each fuel that was put through testing. Additionally, the oxygen bomb calorimeter, which uses ASTM D240, measures the calorific value of all tested fuels.

Together with all the previously mentioned attributes, the flash point of every fuel tested is also examined at CASRAE, DTU, Delhi. Using an automatic flash point tester, the flash point was determined in accordance with ASTM D93 standard. In accordance with ASTM D4737, the cetane index was also determined using four different techniques. In addition, all tested fuels' fatty acid profiles are measured using the standard ASTM D6584. The fatty acid profile is measured using gas chromatography (GC) equipment. This test was carried out in a different lab. Table 3.7 lists the manufacturers and operating ranges of the instruments used to measure these properties.

Every blend was made in accordance with the National Biofuel Policy [234], which permits BD to blend up to 5% of waste cooking oil with diesel. The quaternary blends utilized here were prepared by adjusting the n-butanol proportion from 2% to 14% (v/v) and the SVO proportion from 3% to 21% (v/v). WCOBD was maintained at a constant concentration of 5% (v/v). Splash blending was the technique used to prepare

the test fuel blends. After the prepared blends were stored for 120 hours, phase separation was not observed in the mixtures. The quaternary blends' nomenclature is derived from the  $O_XB_Y$  presentation, where X and Y represent the blends' %v/v in Table 3.6.

**Table 3.6 Nomenclature of fuel blends**

<b>Nomenclature</b>	<b>Diesel</b>	<b>WCOBD</b>	<b>Orange Peel Oil</b>	<b>n-butanol</b>
<b>D100</b>	100	0	0	0
<b>O3B2</b>	90	5	3	2
<b>O9B6</b>	80	5	9	6
<b>O15B10</b>	70	5	15	10
<b>O21B14</b>	60	5	21	14

**Table 3.7 Equipments used for properties test**

<b>Standard Method</b>	<b>Equipment</b>	<b>Accuracy</b>	<b>Property</b>
ASTM D445	Viscobath, Petrotest	$\pm 0.01 \text{ mm}^2/\text{s}$	Kinematic viscosity @ $40^\circ\text{C}$ ( $\text{mm}^2/\text{s}$ )
ASTM D4052	Anton Parr DMA 4500	$\pm 0.1 \text{ kg/m}^3$	Density @ $15^\circ\text{C}$ ( $\text{kg/m}^3$ )
ASTM D93	Pensky-Martens (AD0093–600)	$\pm 0.1 \text{ }^\circ\text{C}$	Flash point ( $^\circ\text{C}$ )
ASTM D240	Parr 6100 Oxygen Bomb Calorimeter	$\pm 0.001 \text{ MJ/kg}$	Calorific value ( $\text{MJ/kg}$ )
ASTM D7039	XOS SindieSulphur analyzer		Sulphur content (ppm)
ASTM D4737		$\pm 0.1$	Cetane number
ASTM D 6584	Gas Chromatography		Fatty Acid profile

To meets the domestic demand for vegetable oil India import 15.1 million tons i.e. 70% of annual demand [235]. WCO was collected from a nearby restaurant that was utilized as a refined oil of soya bean which is a form of vegetable oil serving more than 100 clients each day with 2 to 3 incessant oil changes for every week. Every used utensil was first cleaned with liquid detergent, then rinsed with distilled water and 20% (v/v) nitric acid. To remove the suspended food particle from oil, the filtration was done for physical cleaning. Then after it was heated up to  $120^\circ\text{C}$  for 2 hr. to eliminate the water content from the oil.



**Table 3.8 ASTM D6751 and EN 14214 standards for BD fuels and ASTM D 975 for petroleum diesel fuel**

Properties	Unit	Diesel ASTM D975			BD-ASTM 6751[65]		BD - EN 14214[65]	
		Test Method	Limit	Diesel	Test Method	Limit	Test Method	Limit
Kinematic viscosity @ 40°C	mm <sup>2</sup> /s	ASTM D445	2.0-4.5	2.91	ASTM D445	1.9-6.0	EN ISO 3104	3.5-5.0
Density @ 15°C	kg/m <sup>3</sup>	ASTM D1298	850	839.0	ASTM D 1298	880.0	EN ISO 3675/12185	860-900
Flash point	°C	ASTM D975	60 - 80	71.5	ASTM D 93	130 min	EN ISO 3679	>101
Pour point	°C	ASTM D975	-15 to 5	1.0	ASTM D97	-15 to -16		-
Cloud point	°C	ASTM D975	-35 to 15	2.0	ASTM D2500 -	-3 to -12		-
Calorific value	MJ/kg		42-46	45.825		-		35
Sulphur content (S 15 grade)	ppm		-	3.93 [236]		15 max		-
Cetane number	-	ASTM D4737	40-55	49.7	ASTM D613	47 min	EN ISO 3679	51 min

The density (at 15°C) and KV (at 40°C) of the WCO were measured to be 911 kg/m<sup>3</sup> and 38.43 cSt respectively. The WCO was filtrated through a 20 m channel and moisture was evaporated by warming the oil in an open beaker at 70°C–100°C for 1 hour. The reagents used to produce WCOME were Methanol (99.8%), Para toluene Sulfonic acid (PTSA), Phenolphthalein indicator, 0.1N (NaOH), filter paper of 125mm size, and KOH (85%purity) pallets.

### 3.6 Sample preparation from WCO

The WCO sample used here for the investigation, the FFA was measured to be 2.5 %. To reduce the FFA value, one-step esterification was carried out. Methanol (20% w/w) and p-Toluene sulfonic acid (0.5% w/w) were added to 1-liter oil at 60°C. The blend was left for 2 hours on a magnetic stirrer stirring at 450 rpm. The FFA value for WCO after the esterification was measured to 1.3.

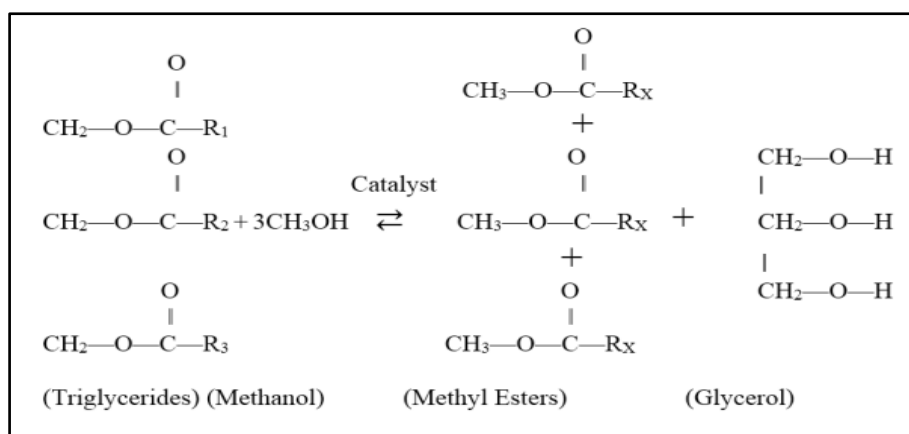


Figure 3.3 Process of trans-esterification

As shown in Figure 3.3, WCOME is the result of the trans-esterification process, which involves the reaction of present tri-glycerides with methanol in the presence of KOH as a base catalyst. Following a number of steps, the esterification process' oil was mixed with 20% v/v methanol and KOH pellets, which served as the base catalyst (0.5% w/w). Every step-by-step procedure utilized to produce WCOME is shown in

Figure 3.4.

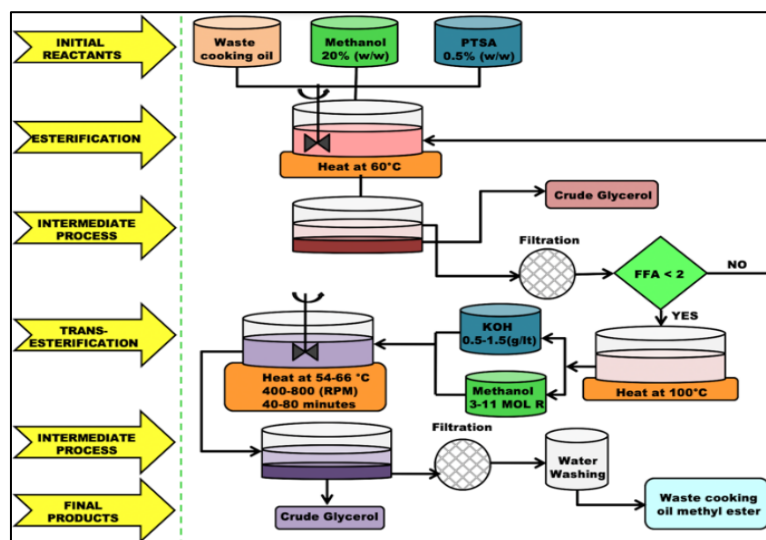
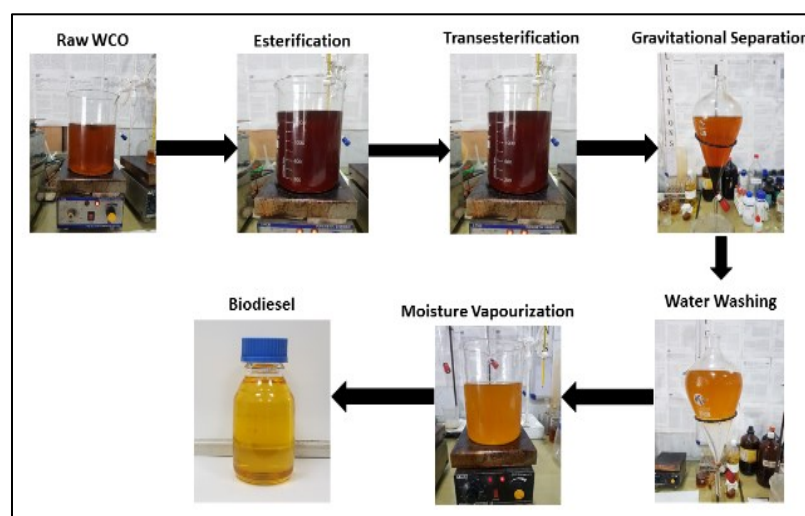


Figure 3.4 Flow diagram of Waste cooking oil biodiesel production

After being stirred at 450 rpm for 90 minutes, the mixture was left alone for an additional 12 hours. After filtering the crude glycerol, the leftover oil was water washed to produce clear WCO biodiesel. The WCO biodiesel is then heated to

eliminate the moisture, as shown in the biodiesel production process shown in Figure 3.5



**Figure 3.5 Waste cooking oil biodiesel production**

### 3.6.1 Kinematic Viscosity (KV)

As the fluid gets viscous its flowability is reduced. The viscosity of BD is higher as compared to diesel. Also, the kinematic viscosity of BD keeps on increases with the storage time. This increased value of viscosity created an obstacle to the fuel flow which causes difficulties in the combustion of fuel.



**Plate No. 3.1 Viscobath Apparatus**

The kinematic viscosity is a temperature-based phenomenon. The temperature and kinematic viscosity have an inverse relationship. It was explained [236] in the two-term model generation that temperature had affected the value of kinematic viscosity

and other physiochemical characteristics. The viscosity measuring apparatus is shown in Plate No. 3.1. It is reported [237] that vegetable oil is 9-16 times more viscous and BD is around 1.5 times more viscous than diesel. The kinematic viscosity of neat WCO was measured to be quite high. It was drastically reduced after the conversion into methyl ester, due to reduction in unwanted fatty acids. It can be calculated in Equation 3.5 as:

$$\text{Kinematic viscosity}(\mu) = k * t \dots\dots\dots 3.5$$

Where:

$\mu$ = Kinematic viscosity (centistokes)

k= Viscometer constant (centistokes/s)

t= oil flow time (s)

### 3.6.2 Calorific Value (CV)

The amount of chemical energy produced by complete combustion per unit of mass is called heating value[61]. The value affects the thermal efficiency as well as combustion characteristics. Although, parameters of heating value provides the energy content but moisture content is also an important aspect. As the moisture content of the fuel increases, the higher heating value increases as well. Using a Parr 6100 oxygen bomb calorimeter, the current study, shown in Plate No. 3.2, was used which works in accordance with the ASTM D-240 standard. The crucible is filled with a predetermined amount of fuel and set between the electrodes. A nichrome wire is inserted into the electrode's ends and dipped in fuel to complete the circuit. After that, the electrodes are inserted into the bomb and fully tightened, allowing oxygen to enter. The bomb is then put inside the water-filled bucket, and the entire apparatus is kept inside the calorimeter, which determines the calorific value.



**Plate No. 3.2 Isothermal Bomb Calorimeter**

### 3.6.3 Density

Mass per unit of volume of a solid or liquid substance or degree of compactness is known as density. In a CI engine, fuel with higher density exerted more resistance to flow. The density of BD is higher as compared to diesel which may cause serious engine problems. The combustion process in the engine get affected by higher density of BD which effect the process of atomization thus resulting in lower engine performance[238]. Anton Parr, Model DMA 4500 used to measure the density of fuel (Plate No. 3.3). the equipment measured the density according to ASTM D-4502 standard.



**Plate No. 3.3 Anton Parr, DMA 4500 (Desitymeter)**

It calculate the specific gravity of the tested fuel at 15<sup>0</sup>C. Before starting of the process first the toluene is used to clean the fuel line of testing the density. The 10 ml of toluene injected in the injecting port. After cleaning of the fuel line 10 ml of test sample of fuel blend was injected through the same port. The same process repeat thrice then take the average all the three values found satisfactory and was taken as final value.

### **3.6.4 Flash point (FP)**

Under specific test conditions, “the flash point is the lowest temperature at which fuel produces enough vapors to ignite and result in the formation of flames”[53].For the purpose of storage and transportation of fuel, the flashpoint plays an very important role[239]. The BD generally has a higher flash point as compared to diesel. That’s why the storage and transportation of it becomes more convenient and less risky[240]. Pansky Martens Automatic Flash Point Apparatus made by Dott Gianni Scavini and Co. as shown in Plate No.3.4.



**Plate No.3.4 Pensky Martens Automatic Flash Point apparatus**

The testing procedure follows ASTM D-93 standards. A small amount of the test sample is placed in a test cup and heated at a consistent rate while being stirred continuously. At regular intervals, a small flame is directed towards the cup while it is

being stirred. The measured value of temperature at which the vapors formed above the sample ignite momentarily when the test flame is brought close to the sample contained cup is the flash point.

### **3.6.5 Distillation**

The tested sample is made up of various parts, each of which has a unique boiling point. Therefore, knowledge of the distillation temperature aids in comprehension of the fuel's vaporization properties within the combustion chamber. Additionally, the temperature at which distillation occurs is used to calculate the fuel's cetane index, which aids in understanding how the fuel burns. The distillation procedure followed ASTM D86 standards. [241].

The 100 ml sample is placed in a specially made distillation flask that has sensors and thermocouples to continuously monitor the temperature, pressure, and volume of the sample inside the flask in order to determine the distillation temperature of the tested fuels. Next, place the flask on the heater and adjust the heating rate so that only four to five milliliters of oil evaporate per minute [242]. The condenser helps to cool the sample oil vapors, keeping them at a temperature of 10°C. The unit is showing in Plate No.3.5.



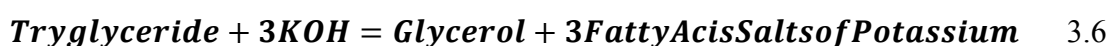
**Plate No.3.5 Distillation Unit**



A digital volume sensor is used to measure the condensate's volume after it has been collected in a vessel. With varying condensate volumes, the distillation temperature is recorded. In order to calculate the cetane index, the temperature is recorded at 10%, 50%, and 90% condensate volumes.

### 3.6.6 Saponification value

The fuel's saponification value, also known as its saponification number, is the weight of triglyceride found in the tested fuel. Titration is a common technique for determining the tested fuel's saponification value. Using this method, 10 milliliters of KOH are reacted with one gr. of oil. Either room temperature or a vapor environment is used for the reaction. In the vapor environment, the rate of reaction is faster. The solution is then exposed to HCl treatment in order to quantify the quantity of KOH used during neutralization. Prior to titration, the solution also contains two drops of the indicator. The amount of KOH in the solution is determined by measuring the amount of HCl used during the titration process. This amount is then subtracted from the 10 ml to calculate the saponification value of the fuel. The reaction takes place during this process is given below in equation 3.6:



$$\text{SV} = 560(\% \text{FC}) / \text{M}$$

SV- Saponification Value

M- Molecular mass of each fatty acid component

FC- % of each fatty acid component

### 3.6.7 Cetane Index

The formulas provided in ASTM D-4737 are used to calculate the cetane index, which depends on the test fuel's density and boiling point temperature. When there is a lack



of test engine or a small sample size, it is helpful. It is computed utilizing Equation 3.7.

$$CI = 45.2 + 0.0892 * T_{10N} + (0.131 - 0.901 * B) * T_{50N} + (0.0523 - 0.42 * B) * T_{90N} + 0.00049 * ((T_{10N})^2 - (T_{90N})^2) + 107 * B + 60 * B^2 \dots\dots\dots 3.7$$

Where

$$T_{10N} = T_{10} - 215 \dots\dots\dots 3.8$$

$$T_{50N} = T_{50} - 260 \dots\dots\dots 3.9$$

$$T_{90N} = T_{90} - 310 \dots\dots\dots 3.10$$

“T<sub>10</sub> is 10% (V/V) distillation recovery temperature in °C

T<sub>50</sub> is 50% (V/V) distillation recovery temperature in °C

T<sub>90</sub> is 90% (V/V) distillation recovery temperature in °C”

$$B = [\exp (-0.0035 * D_N)] - 1 \dots\dots\dots 3.11$$

$$D_N = D - 850 \dots\dots\dots 3.12$$

### 3.6.8 Cloud Point and pour point

It is essential to investigate the performance of the fuel at low temperature. For this, it is required to evaluate the cloud point[243]. The minimum temperature which results in the formation of cloud or wax in crystal form in the fuel is known as the cloud point. It helps to identify the flow properties of fuel[244]. The fuel filter was blocked as the solidification started. It led to degrading the performance of the engine. . It tells about the pumping ability of the fuel.

“Pour point of the fuel is the minimum temperature till which the flow ability is maintained. Pour point is a breakeven point”[245]. Besides this point, the fuel turns into a gel like system which easily clog the fuel lines and filters. The lesser is the concentration of diesel in the BD-diesel blend, the higher is the value of the cloud and pour points of the blend.

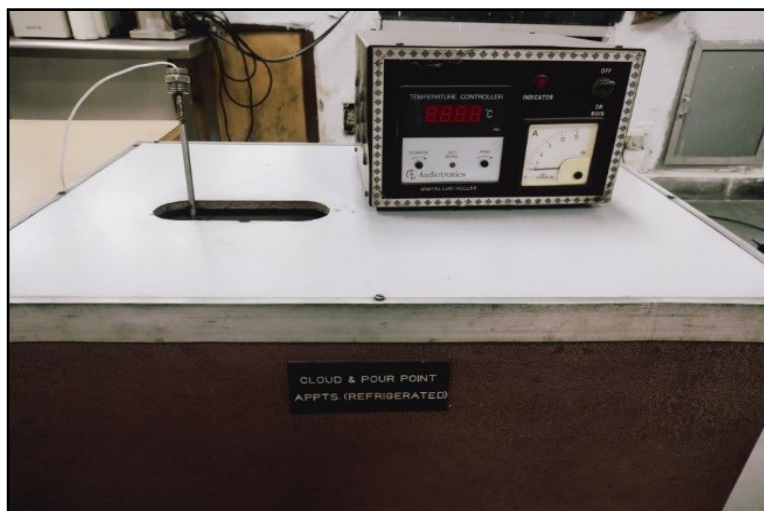


**Plate No. 3.6 Cloud Point and Pour Point Apparatus**

A Koehler-made instrument, shown on Plate No. 3.6 is used to measure the cloud point. The ASTM D-2500 test procedures are used to calculate Cloud Point. The sample is periodically examined and cooled at a predetermined rate in order to determine the cloud point. Cloud point is the temperature at which haziness or cloudiness appears at the bottom of the jar. The pour point is then provided by the temperature record and the jel-like formation. Sulphur Analyzer

After the implementation of BS VI norms by Government of India, it is mandatory all the new make automobile vehicle after April 1, 2020 that only use the fuel grade contained the sulphur content allowed not more than 10 ppm. Whereas compare to the BS-IV norms till 50 ppm was permitted. Due to the usage of such type of fuel grade the NOX was reduced by approximately by 70% while 25% by Petro fuel. The used

test fuel blends measured the available sulphur content by Sulphuranalyzer , Make by XOS, model Sindie 7039 as shown in Plate.

Test fuel sample contained in Accu cell sample. Accucell placed in the machine gently after opening the top cover. Be aware the top cover should be closed before starting the experiment. A digital screen directed for the next followed steps. The measuring of the sulphur content only start after achieving the temperature of 460C and pressure of 1 torr. Once the process will start, the progress will display on the screen. Once the process complete the sulphur content display on the screen.



**Plate No. 3.7Sulphur Analyzer Apparatus**

### **3.6.9 Iodine Value**

To determine the iodine value, 0.13 to 0.15 g of sample was weighed, which was diluted in 20 mL of chloroform, homogenized and 15 mL of reagent was used, covered with aluminum foil to prevent contact with light and let it rest for one hour inside the extraction hood. After time, 20mL of a solution of potassium iodide in 50 mL of distilled water was added to each sample. Finally, the sample was titrated with sodium thiosulfate until the yellow color of this changed to a lighter color, then a pinch of starch was added which caused a dark blue color in the sample and the titration continued until this color becomes transparent. The calculation of the iodine value was carried out using Equation 3.13:

$$\text{Iodine value} = \frac{(V_1 - V_2) * N * 12.69}{P_m} \dots\dots\dots 3.13$$

Where:

V<sub>1</sub>: Volume of the titration in mL of the blank.

V<sub>2</sub>: Titration volume in mL of the sample.

N: Normality of the titrant solution.

P<sub>m</sub>: Sample weight.

### **3.6.10 Fatty Acid Composition**

Depending on their distinct physical and chemical properties and how they interact with the stationary phase, a specific column filling, different chemical components of a sample can pass through a gas stream (carrier gas, mobile phase), a flow-through narrow tube used in gas chromatographs. As the chemicals exit the end of the column, they are electronically identified and detected. Each component leaves the column at a distinct time (the retention time) as a result of the stationary phase in the column's function of separating the various components. The carrier gas flow rate, column length, and temperature are additional variables that can be used to change the retention order or duration.

The mobile phase in gas-liquid chromatography is an inert carrier gas, such as nitrogen or hydrogen. This elutes through the column carrying the components of the analytic mixture-a substance whose chemical constituents are being identified and measured. There is typically an immobilized stationary phase in the column. Gas chromatography (GC) equipment was used in the present study as shown in Plate No. 3.8.



**Plate No. 3.8 Gas Chromatograph (GC Machine)**

### **3.6.11 Test for calculating the average particle size of the test fuel spray**

To start the experiment procedure, after the injection of fuel in the cylinder, the spray particle size played an important role. This spray phenomena known as atomization. The size of spray particle affected by the three parameters; first is injection pressure, viscosity and the density of the tested fuel. During injection of fuel the spray particle when the injection pressure is high with lower viscosity of the fuel. These fine spray particle helps to reduce the ignition delay due to large surface area of particle. Although the penetration strength of such spray particle is less due to its less momentum and low velocity of relative to available air caused to reduce utilization of the air. It is found that increase heat release with more pressure rise during diffusion combustion stage for such spray particle. Other side larger droplet size with lower injection pressure, lowers the pressure rise during the second stage of combustion and smoother engine operation. Finally conclude that it is mandatory the optimum particle size is required for the efficient functioning of the engine. Laser diffraction system is used to evaluate the particle size of the fuel spray Plate. In the present work research, the Malvern Spraytech setup is used to calculate the Sauter Mean Diameter (SMD) of the tested fuel spray. Its specifications are given in Appendix – II



**Plate No. 3.9 Set-up of Malvern Spraytec**



**Plate No. 3.10 Three holes injector**



**Plate No. 3.11 Test fuel storage tank**





**Plate No. 3.12 Fuel Pump and motor assembly**

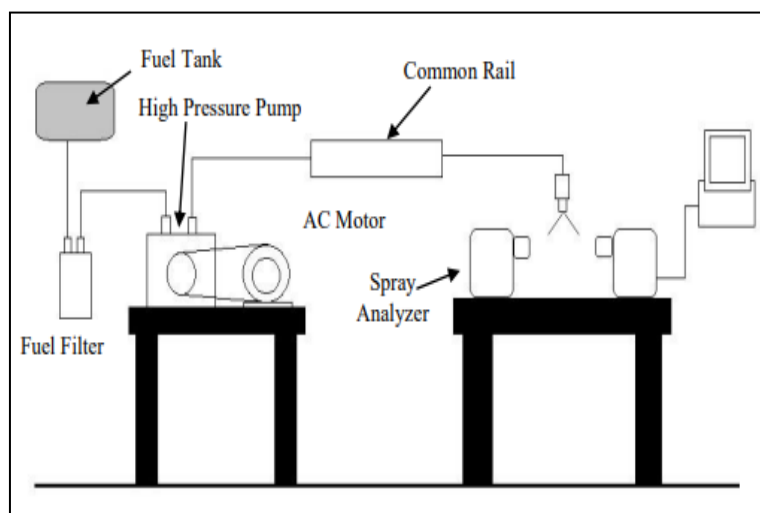


**Figure 3.6 Schematic of Spraytec machine**

The working principle of Spraytec is based on the Doppler Effect, wherein the fuel spray particle passed through the laser beam, the scattering of the beam used to predict the spray particle size. There are two end of the system one is analyzer from where the laser beam is projected and second end is receiver where the projected laser beam is received as shown in Figure 3.6. The experimental setup is shown in Plate No. 3.9. It is ideally assumed that the spray particle in spherical size and depends on the scattering pattern its size and concentration is determined. An injection system (Plate No. 3.10) was used for spray the fuel in between the projected laser beam. The system consist of fuel tank (Plate No. 3.11) in which the test fuel was stored. For supplying the test fuel from storage tank to common rail, a high pressure pump was

installed. This high pressure pump is operated by electric motor through a V-belt. Pump and motor assembly shown in Plate No. 3.12. The fuel injector attached with common rail by a high pressure fuel line. The injector Plate No. 3.10 consists of three holes, two of which were closed so that fuel would spray through only one hole which was kept open. As per the rated value of injector pressure during experiment was kept fixed at 200 bar. The particle size determination was repeated for five times for each type of test fuel blends. The data was collected for 200ms although a single injection lasted about 12ms. In order to facilitate a clear comparison of the droplet distribution in the middle of the injection, the data reported in his work is displayed at a rate of 6 ms. The test was carried out in a low-light room under atmospheric conditions in order to lessen the impact of sunlight. To study the initial primary fuel atomization it is required.

### **3.7 Engine test rig**

We analyzed the Kirloskar diesel engine Plate No. 3.13. This single-cylinder, four-stroke engine is popular in India. To reduce vibration effects, we installed it on a concrete foundation. We added a second fuel tank for other tested fuels, but one tank is reserved for petroleum diesel. Before using a different test fuel, the tank is cleaned with methanol.

The governor is responsible for regulating the fuel supply to the engine, ensuring that it runs at a constant speed regardless of the load. Fuel injectors and pumps are used to control the fuel injection pressure. The fuel pump is governed by a shaft connected to the prime mover shaft. Cams and followers are used to mechanically manage the intake and exhaust valves of the fuel pump. The same shaft is also used to connect the cams for controlling the intake and exhaust valves.



This shaft moves at half the prime mover shaft's speed. On the exhaust manifold, a k-type thermocouple was installed to monitor the temperature of the exhaust gas. The air box, which is attached to the intake manifold, provided air to the current research engine. The installation of the air box serves two purposes: first, it measures the air mass flow rate; second, it provides the engine with cool air. In order to regulate the intake air's temperature, a heater was also added to the air box.

A k-type thermocouple at the intake manifold measures the intake air temperature, while a U-tube manometer at the air box measures the air flow rate. A magnetic pickup speed sensor is mounted on the prime mover shaft of the engine to monitor its speed. For analyzing the inside cylinder pressure of the engine, a single Kebelepierzo pressure sensor with a 1°CA maximum resolution is mounted above the engine, taking into account the combustion characteristics of all test fuels and loads.

The pressure measuring unit has a pressure transducer and a data amplifier, which are connected to a computer running engine soft software. An eddy current dynamometer was attached to the engine's prime mover shaft to observe its performance under different loading scenarios. The dynamometer includes a stator equipped with electromagnets and a rotor disc. The magnetic flux in the electromagnets creates eddy current in the stator during rotor rotation, which loads the prime mover.

Heat is continuously removed from the dynamometer by adding cold water. This process is initiated by the constant resistance to motion. The main thing to worry about is the pollution that a diesel engine emits. For this reason, the current study also included an analysis of the exhaust gas. In this study, the main pollutants, such as CO, HC, NOX, and smoke opacity, were measured.

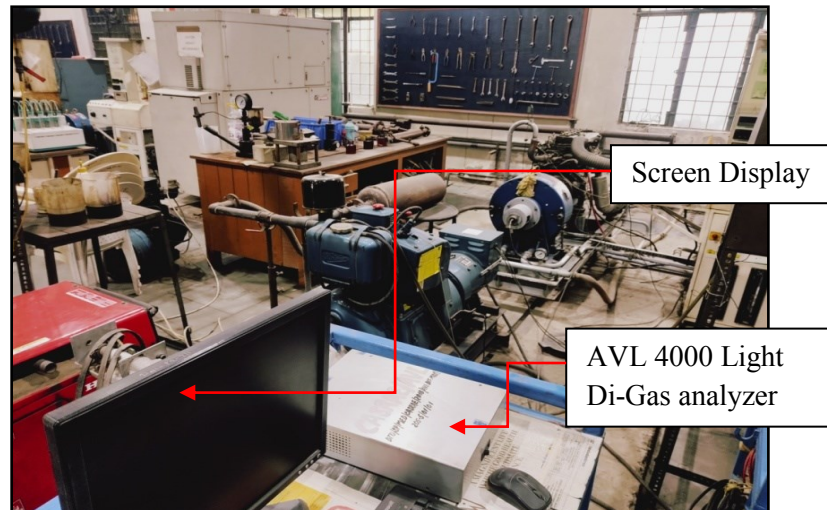


**Plate No. 3.13 AVL 4000 Light Di-Gas analyzer**

Using an AVL 4000 Light Di-Gas analyzer, the research engine's exhaust emissions were measured (Plate No. 3.14). Conversely, the AVL 437 smoke meter Plate No. 3.15 was used to measure the research engine's smoke opacity, another significant emission parameter.



**Plate No. 3.14 AVL 437 smoke meter**

This chapter details the measurement process. The control panel next to the engine includes load varying switch, fuel burette, fuel switching valve, and a charge amplifier connected to a PC. The speed indicator is also put on the control panel and all this data through the data acquisition system is sent to a personal computer.

It's worth mentioning that the test rig used for this study was comprised of several key components. These included a lightweight, water-cooled CI engine, fuel filters, a fuel supply and measuring unit, a fuel switching system, temperature and speed sensors,

exhaust gas emissions and smoke analysis units, an air filter, a control panel, a loading and measuring unit, a digital data acquisition system, and a personal computer equipped with both data analysis and engine software.



**Plate No. 3.15 Test CI Engine**

The test rig used in the present research is shown in Plate No. 3.15&Figure 3.7represents the schematic diagram of the setup used in current research. Eddy's current dynamometer is shown in Plate No. 3.16.

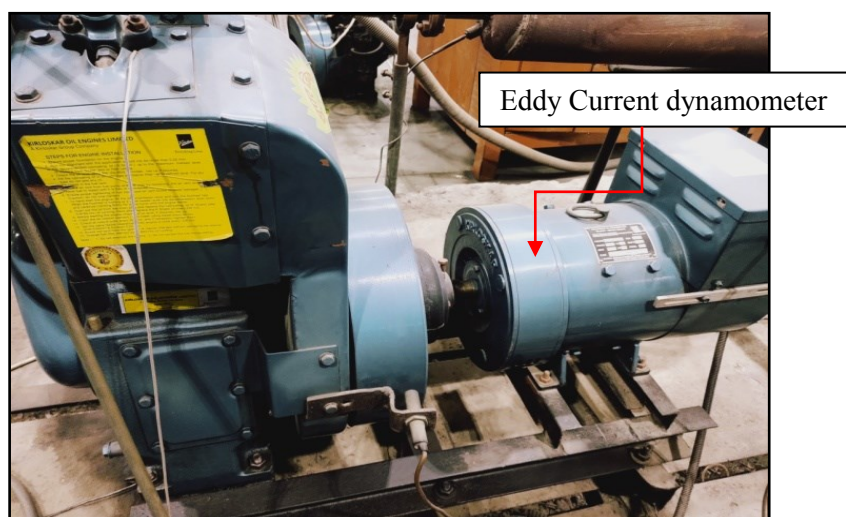


**Plate No. 3.16 Eddy current dynamometer**

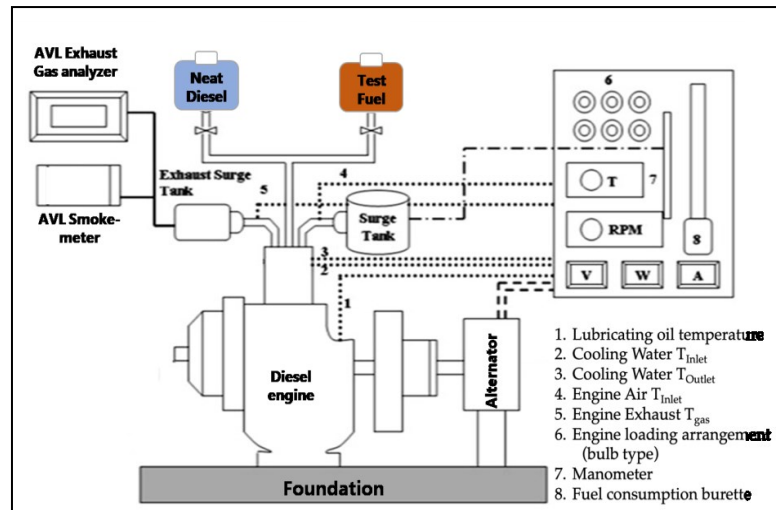


Figure 3.7 Test Engine schematic diagram

Table 3.9 represents the specifications of the dynamometer utilized during the current research. The test rig is shown in Plate No. 3.15 and the schematic diagram in Figure 3.7.

### 3.8 Selection of engine test Parameters

All engine testing is performed as per IS 10000 (Part viii) standard. During the experimental run of the engine there are two types of parameters were needed to be taken as:

#### The various observed parameters:

- Engine Load
- Engine speed
- Air flow rate
- Fuel consumption rate
- Temperature
- In-cylinder pressure
- Exhaust emission
- Smoke opacity

#### Calculated parameters:

- Brake thermal efficiency
- Brake specific energy consumption
- Pressure rise rate
- Heat release rate

**Table 3.9 Technical description of the engine and alternator**

<b>Specification of Diesel Engine</b>			
Make	Kirloskar	Cooling Type	Air cooled (Radial cooled)
Model	DAF 8	Fuel injection timing	23 degree BTDC
Brake Power (kW)	3.5	No. of injector holes	3
Cylinders	1	Nozzle diameter (mm)	9
Rated speed (rpm)	1500	DI Type	Mechanical pump
Injection Pressure (bar)	200	Compression ratio	17.5:1
Stroke x Bore (mm)	110 x 87.5	Lubricating system	Forced feed
Connecting rod length (mm)	234	Cubic capacity	0.78 L
Displacement	0.661	Starting	Hand Start with cranking handle
<b>Dynamometer Specification</b>			
Manufacturer	Kirloskar Electric	Rated voltage (V)	230
Rated output (KVA)	5 @1500 rpm		
Dynamometer type	1 phase, 50 Hz, AC	Rated current (A)	32.6

### 3.9 Measured Parameters

All the required measured parameters listed above. With the help of the instrument they were being measured.

#### 3.9.1 Measurement of engine speed

The end of the toothed dynamometer shaft had a magnetic pickup-style rpm sensor attached. A coil, yoke, and permanent magnet make up this kind of sensor. The location of this sensor was near a toothed gear Plate No. 3.17. An AC voltage pulse was generated in the coil as each tooth passed by the sensor. There was a pulse from each tooth. There were more pulses generated as the gear rotated more quickly. The data acquisition system received these impulse signals digitally.

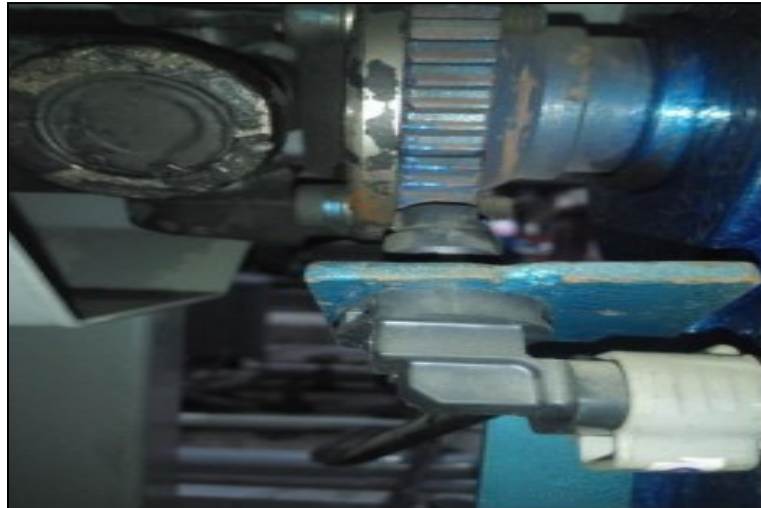


**Plate No. 3.17 Engine speed sensor**

The engine rpm was computed by the data acquisition system's engine control module and subsequently displayed in the control panel. The formula for evaluating the engine speed is provided in equation 3.14

$$\text{Engine Speed(RPM)} = \frac{\text{Number of pulses per minute}}{\text{Number of teeth on the shaft}} \dots\dots\dots 3.14$$

### **3.9.2 Engine load**

This study used four fuel blends to test the combustion, performance, and exhaust emissions of an engine with a rated power of 3.5 kW. The engine was tested at 1500 rpm with seven different loads ranging from 0.05 to 0.35MPa at an injection pressure of 200 bar using an eddy current dynamometer.

### **3.9.3 Measurement of flow rate of fuel**

To calculate the working performance of the engine which was being used in the research, it was necessary to have data on fuel flow rate and loading. For this purpose, a burette was mounted at the control panel to monitor the fuel flow rate. The fuel supply to the engine is designed to allow it to receive fuel continuously from various fuel tanks and burettes. The fuel tank supplies fuel to the burette. To measure the fuel flow rate, the supply test fuel to the research engine is cut off from the fuel tank, and a fixed volume of fuel is supplied and measured using a stopwatch.

To test a fuel at a specific load, the following procedure is repeated five times. The time taken to use up a fixed volume of fuel is recorded each time, and the average of these readings is taken as the final result. Using the fuel density, the mass flow rate of fuel can be calculated by multiplying the fixed volume consumed and dividing by the average time of the five readings. This can be expressed mathematically as shown in equation 3.15.

$$\text{Rate of fuel consumption} = \frac{\text{Fixed volume of fuel} \times \text{Density of fuel}}{\text{Average time to consumed fixed volume of fuel}} \dots\dots\dots 3.15$$

In the current study, the fuel volume was set at 20 milliliters. To compare the various tested fuels, the energy flow rate was calculated. Comparing fuels in terms of mass flow rate is challenging due to their unique calorific value. The energy flow rate is determined by multiplying the mass flow rate of fuel with its calorific value. Measuring fuel flow is possible with an electronic device called the differential pressure (DP) oil flow transmitter, which works on the differential pressure diaphragm principle. To validate data obtained from the transmitter, a burette and stopwatch installed on the control panel can measure flow rate. For accuracy, the two readings were compared. Equation 3.16 provides the analytical formula used to calculate the rate of energy consumption.

$$\text{Rate of Energy flow} = \text{Fuel mass flowrate} \times \text{calorific Value} \dots\dots\dots 3.16$$

### 3.9.4 Measurement of airflow rate

To measure the airflow, a U-tube manometer is mounted at the air box through an opening that connects to the intake manifold. The airflow rate is calculated using the equation provided. The data acquisition system receives information from the airflow transmitter to calculate the airflow. An air box with an orifice in the control panel is used to analytically calculate the flow rate, which helps validate the air quantity



measured by the sensor. The airflow transmitter is installed inside of control panel. It can be calculated according to equation 3.17.

$$\text{Air flow rate}(\dot{m}_a) = C_d \times A \times \sqrt{(2gh_w \rho_w / \rho_a)} \dots \dots \dots 3.17$$

Where:

$C_d$  = Co-efficient of discharge of venturi (0.9 in the present case)

$A$  = Orifice area

$g$  = Acceleration due to gravity

$h_w$  = Height of water column

$\rho_w / \rho_a$  = Density of water/air

### 3.9.5 Inside cylinder pressure

To analyze the combustion properties of test fuels in the research engine, it is crucial to examine the internal cylinder pressure. This involves measuring the change in internal pressure in relation to each crank angle rotation. In the research engine, a piezoelectric transducer was placed over the engine head to measure the internal cylinder pressure. The signal from the piezo sensor is amplified by a charge amplifier and sent to the data acquisition channel, where it is transformed into digital data by the software. Additionally, the engine speed and internal pressure are synchronized by the software, and the speedometer data is transferred to the data channel. During the testing, the KiBox database software was used to measure and record the internal cylinder pressure in relation to the crank rotation angle. To ensure accuracy, the inside cylinder pressure was analyzed at each angle of the crank rotation for a total of 150 cycles. This helped to minimize the possibility of errors.

### 3.9.6 Measurement of exhaust temperature

The exhaust temperature is crucial for analyzing engine combustion, performance, and emissions. High gas temperatures cause sudden combustion and increased NOX



emissions. Plate No. 3.18 has a K-type thermocouple at the exhaust pipe's end for accurate temperature measurement.

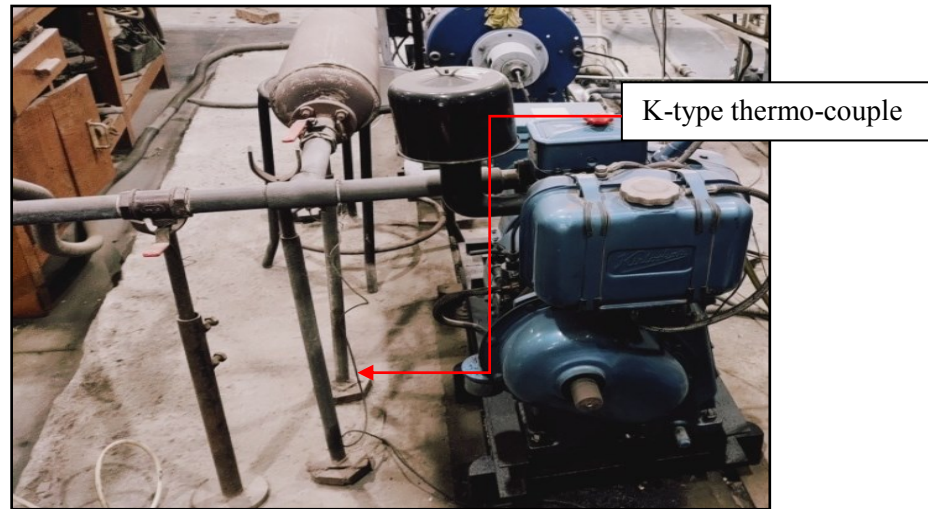


**Plate No. 3.18 Temperature measuring thermo couple**

The thermocouple is regularly calibrated and incredibly accurate. The enginesoft database software and the temperature indicator mounted on the control panel both display the thermocouple-measured temperature.

### **3.9.7 Measurement of exhaust emissions**

To measure the smoke opacity of the research engine, we chose the AVL-437 smoke meter. And, to measure exhaust gases like NOX, HC, and CO, we chose the AVL-4000 di-gas analyzer. The AVL-4000 di-gas analyzer has multiple sensors for every significant exhaust emission. All these sensors are exposed to exhaust emissions, and it takes time for them to process, analyze, and display the data on a digital meter. On the other hand, the AVL-437 smoke meter uses a technique called light projection. It projects a light beam over the exhaust gas once it enters the smoke meter.

When exhaust gas is released, it contains pollutants that scatter and absorb light. The remaining light that does pass through is used to create a photoelectric current at the absorber location, opposite the beam source. This current measurement helps determine the smoke opacity of the exhaust.

Every instrument requires a warm-up period, which is why both instruments are warmed up before use. One by one, the instruments' probes are inserted into the exhaust manifold, and given enough time to stabilize before taking a reading. To reduce errors, three readings are taken for each loading condition of the tested fuel. The AVL4000 and AVL-437 are shown in Plate No. 3.3 and Plate No. 3.14 respectively, while the specifications of AVL-4000 and AVL437 is an exhibit in Table 3.10 respectively.

**Table 3.10 Emission Test rig specification**

S.N	Instrument Name	Measurement Range	Resolution	Measurement Technique	% Uncertainty
<b>AVL DI Gas Analyzer</b>					
1	carbon Monoxides	0-10% volume	0.01% volume	Non dispersive infra-red sensor	0.20%
2	Hydrocarbon	0-20,000 ppm Volume	1 ppm	Flame Ionization detector (FID)	0.20%
3	Oxides of Nitrogen	0-5,000 ppm volume	1 ppm	Chemiluminescence principle, electro chemical sensor	0.20%
<b>AVL Smoke meter</b>					
1	Smoke Opacity	0-100%	± 1 % volume	Hatridge principle	0.10%

### 3.10 Engine calculated parameters

To analyze an engine's performance, certain parameters are essential to measure. However, some of these parameters cannot be measured directly through instruments and devices. In such cases, other significant parameters can be calculated using the data obtained from the measured parameters. These parameters are known as calculated parameters, and their computation involves the use of equations, relationships, and principles of thermodynamics. Both computer-based and manual computations are used to calculate these parameters. This section focuses on the principles, equations, and relationships that are used in these calculations. The engine's calculated parameters discussed in this section are shown in Figure 3.8:

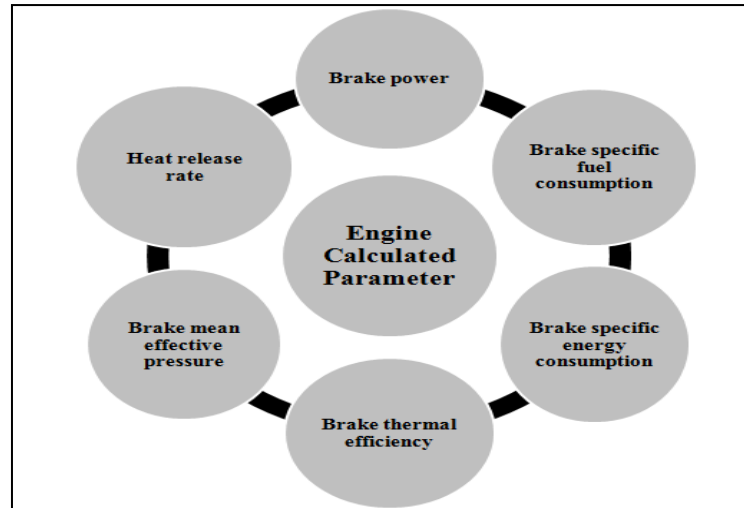


Figure 3.8 Engine calculated parameter

### 3.10.1 Brake power

Brake power can be defined as the available power on prime mover shaft is called brake power. In general the term brake power refers to engine load. The dynamometer is helps to find this. In the current research work an eddy current dynamometer was used. In this dynamometer the load was applied in the form of electric current i.e. voltage and current through load controller. The formula used for this is giving below in equation 3.18:

$$\text{BP(kW)} = \frac{2\pi NT}{60 \times 1000} \dots\dots\dots 3.18$$

$$T = W \times 9.81 \times R$$

Where,

T = Torque

W = Load (kg)

R = Arm length of dynamometer (meter)

### 3.10.2 Brake mean effective pressure

It is tough to compare the engine on same plate form as rated power is different for different engine however the brake mean effective pressure is same for all. So it plays an important role to compare the engines. Due to which the calculation and

comparison made easy of such due to this calculation. In this section the calculation of brake mean effective pressure illustrate as follow in equation 3.19.

$$\text{BMEP} = \frac{2 \times 60 \times \text{BP(kW)}}{L \times A \times N \times 101.325} \text{ bar} \dots\dots\dots 3.19$$

Where:

L- Stroke length (meter)

X-sectional area of piston ( $\frac{\pi * D^2}{4}$ )

“N/60-Rotational speed of the engine in revolution per second

101.325 kPa is the atmospheric pressure

2 is used for the four stroke engine

BP- Brake power of the engine”

### 3.10.3 Brake specific fuel consumption

Brake specific fuel consumption (BSFC) defined as the rated fuel consumption per unit of brake power. In this section, BSFC can also explained as the fuel required for per kW of brake power. It represents the performance of the engine. In vice versa the less fuel consumption show the better performance of the engine. The empirical formula used for the calculation of BSFC is giving below in equation 3.20.

$$\text{BSFC} = \frac{\text{mass flow rate of fuel} \times 3600}{\text{BP(kW)}} \left( \frac{\text{g}}{\text{kWhr}} \right) \dots\dots\dots 3.20$$

### 3.10.4 Brake specific energy consumption

The different fuel blends carried the different calorific value due to which they delivered the different energy. So that to meet all the tested fuel blends on the same platform for the purpose of comparison the brake specific energy consumption (BSEC) is being measured, however the BSFC didn't provide the symmetrical analysis. Therefore the multiplication of BSFC with the calorific value provide the BSEC. The formula used for the calculation of BSEC as given in equation 3.21.:

$$\text{BSEC} = \frac{\text{mass flow rate of fuel} \times \text{CV} \times 3600}{\text{BP(kW)}} \left( \frac{\text{MJ}}{\text{kWhr}} \right) \dots\dots\dots 3.21$$

Where:

CV- calorific value of used tested fuel in MJ

Also, BSEC = BSFC × CV

### 3.10.5 Brake thermal efficiency

Brake thermal efficiency (BTE) represent the effectiveness of test fuel with reliability of the engine. The BTE is calculated by division of BP of the engine with the energy consumption for produce that BP. Conclusion that it is the reciprocal of BSEC. The relation used for the calculating it, is giving below in equation 3.22.

$$\text{BTE} = \frac{\text{BP(kW)}}{\text{m} \times \text{CV}} \dots\dots\dots 3.22$$

### 3.10.6 Heat release rate and ignition delay

The evaluation of heat release per unit of crank angle rotation is provide the heat release rate (HRR). HRR has a great significance in a CI engine during the combustion. It also referred as heat engine. It provides the efficiency, power output as well as emission. For the prediction of the rate of heat release so many mathematical models proposed by the researchers. In the present work the method proposed by the Heywood[246] was being used. The Heywood model is based on first law of thermodynamics and it is a single model zone. This model doesn't distinguished between the created zones (burned and unburned zone). In the context of multi zones models are found in different researches, but developer had to observe all zones for evaluating the heat transfer. Due to the uncertainties of evolved zones during the combustion the model didn't show large benefits. The HRR is given by following equation 3.23:

$$\frac{dQ}{d\theta} = \frac{\gamma}{\gamma-1} * P * \frac{dV}{d\theta} + \frac{1}{\gamma-1} * V * \frac{dP}{d\theta} - \frac{dQ_w}{d\theta} \dots\dots\dots 3.23$$

Where

$dQ/d\theta$ - rate of heat release during inside the engine cylinder ( $J/^\circ CA$ );

$dQ_w/d\theta$  - heat transfer rate through wall of the cylinder ( $J/^\circ CA$ )

$\gamma$ - Specific heat ratio

P - Cylinder pressure (bar)

V- Gas volume ( $m^3$ )

$\theta$  – Crank angle ( $^\circ$ )

This study also calculated the ignition delay, which was defined as the crank angle interval between the fuel injection and the beginning of the rapid increase in heat release. The time interval between the beginning and the end of the heat release is known as the combustion duration.

### **3.11 Engine trial procedure**

Before starting the experiment firstly engine started at no load condition. After attaining the steady state condition, then supply of tested fuel was started. At this condition engine was operated for the thirty minutes so that engine can stabilizing with tested fuel. All the measuring data at each load was noted down when the engine reached at stable condition. The data acquisition from the instruments were properly calibrated periodically. The injector pressure was kept as per the rated data.

The load is gradually increase from no load to full load condition. At each load the all the measuring data (air flow rate, fuel rate, emissions of NO<sub>x</sub>, HC, CO and smoke opacity) were recording precisely. The pressure crank angle history of 50 cycles was also noted down by data acquisition system on the computer system.

### 3.12 Accuracy and uncertainty of measuring instrument

All the used instruments in the experimental procedures are calibrated. The range of all the measuring instruments with accuracies is provided in the Table 3.11 and Table 3.1. As per the received data, the instruments show higher accuracy.

During the experimental run on the engine the data collected by the acquisition system found differ from the true value still when it is kept in mind its ideal procedures. This different in measured quantity or error classified as systematic or random errors. The first type of errors (systematic) could be predicted while other ones (random error) couldn't. Its availability can be observed when the same quantity is measured under same experiment environment.

**Table 3.11 Accuracy and uncertainty of measuring instrument**

Measurement	Measuring Principle	Range	Accuracy
Engine load	Strain gauge type load cell	0-25 kg	± 0.1kg
Engine speed	Magnetic pick-up type	0-2000 rpm	±20 rpm
Time	Stop-watch	-	±0.5%
Exhaust temperature	K-type thermocouple	0-1000°C	±1°C
Crank angle encoder	Optical	0-720°CA	±0.2°CA
Pressure	Piezoelectric	0-200 bar	±1 bar

To estimate the uncertainty, Gaussian distribution method is helpful. The Gaussian distribution method is more effective the confidence level of  $\pm 2\sigma$  (95.45% of the measured data lie within this limit). This can be estimated using the equation 3.24.

$$\text{Uncertainty of parameter}(\Delta X) = \frac{2\sigma}{\bar{X}} \times 100 \dots\dots\dots 3.24$$

The purpose of the experiments was to find the standard deviation ( $\sigma$ ) and mean ( $\bar{X}$ ) of any parameter that was measured. The method presented by Kline and McClintock is used to compute the uncertainty based on the measured parameters[247].

Let R be the computed quantity from 'n' independent measured parameters.

$X_1, X_2, X_3, \dots, X_n$

Thus  $R = R(X_1, X_2, X_3, \dots, X_n)$

Assumed the limits of uncertainty for this measured parameter be

$X_1 \pm \Delta X_1, X_2 \pm \Delta X_2, X_3 \pm \Delta X_3, \dots, X_n \pm \Delta X_n$

$R \pm \Delta R$  be the limit of uncertainty for evaluated parameter.

Equation 3.25 provides the magnitude of error. The root-sum-squared method is used to evaluate the actual or realistic error limit for any measured quantity based on multiple measured quantities.

$$\Delta R = \text{QRT} \left( \left( \frac{\partial R}{\partial X_1} * \Delta X_1 \right)^2 + \left( \frac{\partial R}{\partial X_2} * \Delta X_2 \right)^2 + \left( \frac{\partial R}{\partial X_3} * \Delta X_3 \right)^2 + \dots + \left( \frac{\partial R}{\partial X_n} * \Delta X_n \right)^2 \right) \dots 3.25$$

Using 3.25 the uncertainty for the given operating condition can be evaluated and sample calculation is explained in Appendix-I.



## CHAPTER-4

### RESULTS AND DISCUSSION

---

#### 4.1 Introduction

WCO was collected from a nearby restaurant that was utilized as a refined oil of soya bean which is a form of vegetable oil serving more than 100 clients each day with 2 to 3 incessant oil changes for every week. All the utilized utensils initially, properly washed with detergent, rinsed with concentration of 20% (v/v) nitric acid and lastly rinsed with distilled water. To remove the suspended food particle from oil, the filtration was done for physical cleaning. Then after it was heated up to 120°C for 2 hr. to eliminate the water content from the oil.

The density (at 15°C) and KV (at 40°C) of the WCO were measured to be 911 kg/m<sup>3</sup> and 38.43 cSt respectively. The WCO was filtrated through a 20 m channel and moisture was evaporated by warming the oil in an open beaker at 70°C–100°C for 1 hour. The reagents used to produce WCOME were Methanol (99.8%), Para toluene Sulfonic acid (PTSA), Phenolphthalein indicator, 0.1N (NaOH), filter paper of 125mm size, and KOH (85%purity) pallets .

The WCO sample used here for the investigation, the FFA was measured to be 2.5 %. To reduce the FFA value, one-step esterification was carried out. Methanol (20% w/w) and p-Toluene sulfonic acid (0.5% w/w) were added to 1-liter oil at 60°C. The blend was left for 2 hours on a magnetic stirrer stirring at 450 rpm. Following esterification, the FFA value for WCO was determined to be 1.3.

WCOME is the result of the trans-esterification process, which involved the reaction of present tri-glycerides with methanol in the presence of a base catalyst, KOH. Following various steps, the oil from the esterification process was combined with methanol (20% v/v) and KOH pellets as the base catalyst (0.5% w/w).

After 90 minutes of agitation, the mixture rested for 12 hours. The oil was then washed with water to produce WCO biodiesel, which was heated to remove moisture.

## 4.2 Characterization methods

To determine the proportion of FFA (Free Fatty Acid) in waste cooking oil, titration is used. Take one gram of the oil and add ten milliliters of isopropyl alcohol into a container. Thoroughly mix them and add two drops of phenolphthalein pH indicator. Use N/10 NaOH titration to determine the FFA content, and record the amount of NaOH used until the solution turns pink. The solution should remain pink for at least ten seconds to ensure accuracy. Acid value (AV) expressed as in Equation 4.1

$$AV = \frac{Vol_{NaOH} \times Conc_{NaOH} (M) \times MW_{KOH}}{Sample\ weight(gr)} \dots\dots\dots 4.1$$

Gas Chromatography (GC) with inbuilt flame ionization detector was used for analyzing the fatty acid composition bio-diesel. To perform this analysis, 0.2µg of WCOME was injected into the GC chamber equipped with a split/ split-less injection port with split ratio 50:1. Initially the temperature held at 120<sup>0</sup>C for 2 min and then ramped to final temperature of 240<sup>0</sup>C at a rate of 4<sup>0</sup>C/minute. The obtained GC graph shown in Figure 4.1

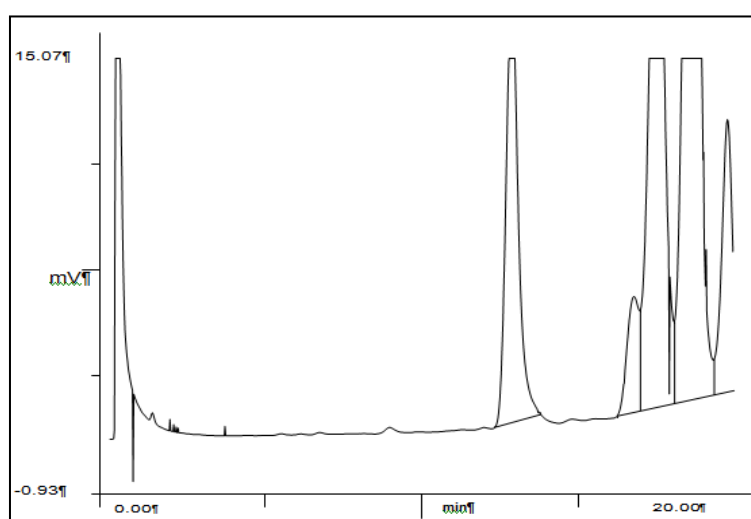


Figure 4.1 Gas chromatography of waste cooking oil biodiesel

Simultaneously held for 7 min at this temperature. The nitrogen gas was used as a carrier gas at a flow rate of 8ml/min. Five peaks of Palmitic acid (C16:0), Stearic acid (C18:0), Oleic acid (C18:1), Linoleic acid (C18:2) and linolenic acid (C18:3) with GC area yield of 13.0264%, 3.3501%, 24.1820, 51.7410% and 7.7003% respectively as shown in Table 4.1 were observed during GC operation.

**Table 4.1 Fatty acid composition of waste cooking oil biodiesel**

Sl. No.	Fatty acid	Carbon Structure	Waste cooking oil biodiesel (wt %)	Peak width
1	Palmitic acid methyl ester	C16:0	13.0264	0.396
2	Stearic acid methyl ester	C18:0	3.3501	0.442
3	Oleic acid methyl ester	C18:1	24.1820	0.505
4	Linoleic acid methyl ester	C18:2	51.7410	0.412
5	linolenic acid methyl ester	C18:3	7.7003	0.369

**Table 4.2 Physico-chemical properties of Waste cooking oil biodiesel**

Properties	ASTM Method	Unit	Diesel	WCOBD	Test Equipment Used	Accuracy
Kinematic viscosity @40°C	D445	cSt	3.1	6.11	Visco bath, Petrotest	±0.01 cSt
Flash point	D975	°C	67	154	Pensky-Martens (AD0093–600)	±0.1 °C
Pour point	D975	°C	-1.8	-11	-	-
Calorific value	D6751	MJ/kg	45.82	43.26	Parr 6100 Oxygen Bomb Calorimeter	±0.001 MJ/kg

### 4.3 Results and discussion

#### 4.3.1 Regression analysis (ANOVA)

Analysis of variance (ANOVA) helps forecast the simulation of data obtained from the design matrix [248]. ANOVA result explains in Table 4.3, Table 4.4, and Table 4.5. The most considerable factor in ANOVA result as p-value. The significance is to examine the necessity of the factor. The critical value is 0.05, greater the value replicate not an important parameter. A value less than 0.05 had a great impact on the developed model. It is clearly shown in ANOVA results of yield, FP, KV, FP and PP,

p-value of all the process parameters (MR, CC, RT, R.TEM, and agitation speed) below 0.05.

**Table 4.3 ANOVA results for Yield and Calorific value**

Source	Yield					Calorific value				
	DF	Adj SS	Adj MS	F-Value	P-Value	DF	Adj SS	Adj MS	F-Value	P-Value
Model	21	60.764	2.89352	4.72	0.005	21	41.082	1.95629	18.28	0
Blocks	1	0.002	0.00196	0	0.056	1	0.5168	0.51675	4.83	0.05
Linear	5	14.4231	2.88462	4.7	0.015	5	0.9356	0.18712	1.75	0.020
MR	1	3.3994	3.39939	5.54	0.038	1	0.2356	0.23556	2.2	0.011
RT	1	1.1634	1.16344	1.9	0.196	1	0.0379	0.03793	0.35	0.012
Speed	1	0.0732	0.07317	0.12	0.036	1	0.181	0.18099	1.69	0.027
CC	1	8.8871	8.88708	14.49	0.003	1	0.0949	0.09493	0.89	0.066
R.TEMP	1	0.4666	0.46658	0.76	0.002	1	0.3948	0.39483	3.69	0.014
Square	5	5.348	1.06961	1.74	0.025	5	2.2369	0.44738	4.18	0.021
MR*MR	1	3.5949	3.5949	5.86	0.014	1	1.0364	1.03641	9.69	0.01
RT*RT	1	0.0911	0.09106	0.15	0.007	1	0.8122	0.8122	7.59	0.019
Speed*Speed	1	1.1802	1.18017	1.92	0.043	1	0.1824	0.18238	1.7	0.058
CC*CC	1	0.251	0.25104	0.41	0.034	1	0.1334	0.13338	1.25	0.028
R.TEMP*R.TEMP	1	0.1039	0.10392	0.17	0.042	1	0.4736	0.47361	4.43	0.031
2-Way Interaction	10	20.4165	2.04165	3.33	0.030	10	1.8151	0.18151	1.7	0.019
MR*RT	1	0.2048	0.20476	0.33	0.011	1	0.1541	0.15406	1.44	0.025
MR*Speed	1	0.0203	0.02031	0.03	0.018	1	0.0915	0.09151	0.86	0.037
MR*CC	1	0.6202	0.62016	1.01	0.036	1	0.077	0.07701	0.72	0.041
MR*R.TEMP	1	3.2852	3.28516	5.36	0.011	1	0.1173	0.11731	1.1	0.031
RT*Speed	1	0.5968	0.59676	0.97	0.113	1	0.1661	0.16606	1.55	0.023
RT*CC	1	2.1683	2.16826	3.54	0.017	1	0.3813	0.38131	3.56	0.026
RT*R.TEMP	1	1.4102	1.41016	2.3	0.018	1	0.1106	0.11056	1.03	0.033
Speed*CC	1	6.5408	6.54081	10.67	0.008	1	0.2783	0.27826	2.6	0.013
Speed*R.TEMP	1	1.3983	1.39831	2.28	0.015	1	0.273	0.27301	2.55	0.013
CC*R.TEMP	1	4.1718	4.17181	6.8	0.024	1	0.1661	0.16606	1.55	0.023
Error	11	6.745	0.61318	*	*	11	1.177	0.107	*	*
Lack-of-Fit	6	6.7445	1.12409	11628.53	0	6	1.1621	0.19368	65.07	0
Pure Error	5	0.0005	0.0001	*	*	5	0.0149	0.00298	*	*
Total	32	67.5091	*	*	*	32	42.259	*	*	*

**Table 4.4 ANOVA result for Kinematic viscosity and Flash Point**

Source	Kinematic viscosity					Flash Point				
	DF	Adj SS	Adj MS	F-Value	P-Value	DF	Adj SS	Adj MS	F-Value	P-Value
Model	21	1.69611	0.080767	3.72	0.014	21	2692.86	128.232	8.98	0
Blocks	1	0.16801	0.168014	7.75	0.018	1	4.38	4.379	0.31	0.041
Linear	5	0.16627	0.033255	1.53	0.025	5	57.9	11.579	0.81	0.015
MR	1	0.00138	0.001384	0.06	0.010	1	6.56	6.556	0.46	0.012
RT	1	0.07376	0.073762	3.4	0.022	1	30.69	30.692	2.15	0.011
Speed	1	0.08379	0.083792	3.86	0.015	1	3.23	3.227	0.23	0.024
CC	1	0.0093	0.009295	0.43	0.152	1	12.09	12.093	0.85	0.037
R.TEMP	1	0.03957	0.039575	1.83	0.021	1	1.83	1.828	0.13	0.027
Square	5	0.23391	0.046782	2.16	0.013	5	39.98	7.997	0.56	0.029
MR*MR	1	0.13398	0.133976	6.18	0.031	1	2.95	2.951	0.21	0.025
RT*RT	1	0.011	0.011003	0.51	0.041	1	9.56	9.563	0.67	0.05
Speed*Speed	1	0.04044	0.040442	1.87	0.019	1	26.56	26.563	1.86	0.041
CC*CC	1	0.03773	0.037726	1.74	0.021	1	1.06	1.062	0.07	0.041
R.TEMP*R.TEMP	1	0.05225	0.052253	2.41	0.014	1	5.78	5.785	0.41	0.045
2-Way Interaction	10	0.50176	0.050176	2.31	0.042	10	221.62	22.162	1.55	0.024

**Table 4.5 ANOVA results for Pour Point**

Model	DF	Adj SS	Adj MS	F-Value	P-Value
Blocks	21	4.89663	0.23317	4.03	0.01
Linear	1	0.89833	0.89833	15.52	0.002
MR	5	0.97262	0.19452	3.36	0.044
RT	1	0.01346	0.01346	0.23	0.039
Speed	1	0.05574	0.05574	0.96	0.034
CC	1	0.02148	0.02148	0.37	0.05

R.TEMP	1	0.07541	0.07541	1.3	0.027
Square	1	0.89267	0.89267	15.42	0.002
MR*MR	5	1.72996	0.34599	5.98	0.007
RT*RT	1	0.48621	0.48621	8.4	0.014
Speed*Speed	1	0.17844	0.17844	3.08	0.010
CC*CC	1	0.08121	0.08121	1.4	0.026
R.TEMP*R.TEMP	1	0.17844	0.17844	3.08	0.010
2-Way Interaction	1	1.08344	1.08344	18.72	0.001
MR*RT	10	0.67625	0.06762	1.17	0.039
MR*Speed	1	0.00562	0.00562	0.1	0.027
MR*CC	1	0.03062	0.03062	0.53	0.048
MR*R.TEMP	1	0.00062	0.00062	0.01	0.041
RT*Speed	1	0.05062	0.05062	0.87	0.037
RT*CC	1	0.27562	0.27562	4.76	0.031
RT*R.TEMP	1	0.14063	0.14063	2.43	0.014
Speed*CC	1	0.01563	0.01563	0.27	0.014
Speed*R.TEMP	1	0.10562	0.10562	1.82	0.020
CC*R.TEMP	1	0.00062	0.00062	0.01	0.019
Error	1	0.05063	0.05063	0.87	0.037
Lack-of-Fit	11	0.6367	0.05788	*	*
Pure Error	6	0.62337	0.1039	38.96	0
Total	5	0.01333	0.00267	*	*
Model	32	5.53333	*	*	*

Table 4.6 displays the yield, CV, KV, FP, and PP model summary. The adjusted  $R^2$  obtained from Table 4.6 was found to be reasonably close to the predicted  $R^2$ , indicating good significance and a sufficient correlation between the input and output values. Consequently, it verified that the model could be approved. The  $R^2$  value near 1 indicates both the excellent output variation between the response and the targets and the excellent consistency of the fit[249].

The model's fitness increases with a higher  $R^2$  value. Adj.  $R^2$  (Adjusted  $R^2$ ): the percentage variation regarding the response. The number of predictors and observations in the model determines how the value is modified. Selecting the appropriate model based on the quantity of predictors is beneficial.  $R^2$  Pred. (estimated  $R^2$ ): When observation is removed, it establishes the precision of the model's estimations.

**Table 4.6 Model summary**

Responses	S	$R^2$	Adj $R^2$	Pred $R^2$
Yield	0.783061	98.01%	96.93%	95.21
CV	0.327106	97.21%	94.90%	93.13%
KV	0.147251	96.67%	95.13%	94.37%

<b>FP</b>	3.77813	95.49%	93.97%	91.53%
<b>PP</b>	0.240587	93.49%	92.53%	91.65%

The generated model pass through the computational approach by using the coefficient  $R^2$ . The  $R^2$  value observed for the yield, CV, KV, FP, and PP is as 98.01%, 97.21%, 96.21%, 96.67%, 95.49%, and 93.49% respectively. All the values of  $R^2$  reflect that the suggested model gave a reliable result.

#### 4.3.2 RSM Optimization

Figure 4.2 shows RSM optimizer used to find the best possible input parameters setting for best possible WCOME production. The multi-objective optimization was carried with different weightage of input factors. In this work, the objective is to improve the biodiesel production yield, CV, and FP of biodiesel, remaining other properties (PP and KV) should be minimum to attend the best quality of WCOME production.

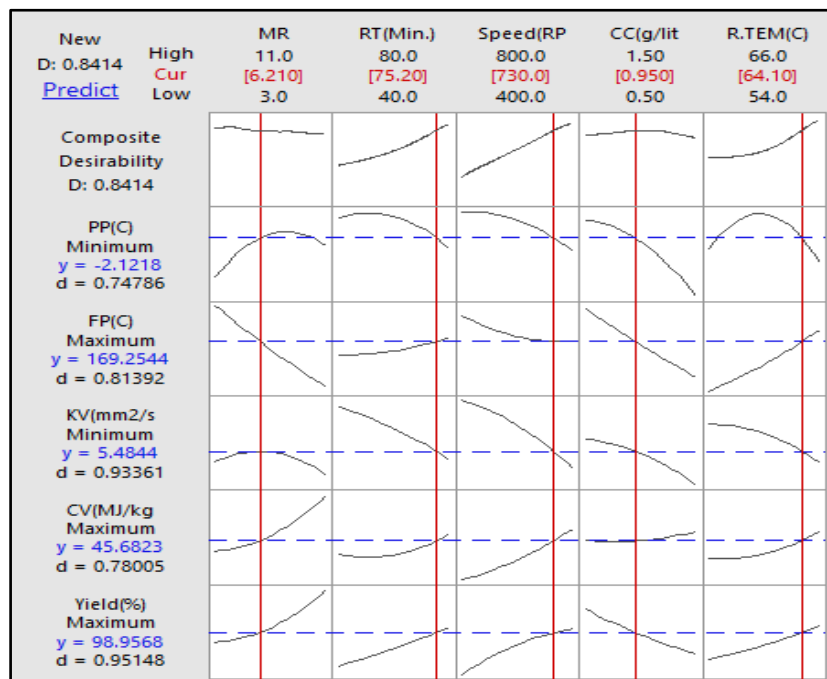


Figure 4.2. Optimization plot: Effect of process parameters on responses

Optimum RSM suggested input parameters MR, CC, R Temp, Agitation speed and RT were found 6.2 (Methanol/oil), 0.95 g/lit, 64.1<sup>0</sup>C, 730 rpm , and 75.2 minutes respectively. At the above said input setting, optimum responses were found 98.95 %

WCO biodiesel production yield, -2.12<sup>0</sup>C (PP), 169.25<sup>0</sup>C (FP), 45.68 MJ/kg (CV), and 5.48 cSt (KV).

Now, we can conclude that above said process parameter setting good for WCOME production process to get a good production yield with quality. Further impact of process parameters on different responses discussed in the upcoming section. Here we can see that at a time can observe only two process variables in one-time frame but we have five process parameters. So, the rest of the three process parameters will be hold at the optimum value suggested by RSM optimizer Figure 4.2.

By using Table 4.7 we can obtain regression equation of all response value at any range of process parameters. Regression Equation can be generated by submission of factors multiply by coefficient given under the response column of response.

**Table 4.7 Output responses equations**

Factors	Yield	CV	KV	FP	PP
Constant	149.7	87.7	-18.8	235	-81.1
MR	-5.23	-1.376	-0.0106	7.3	--0.329
RT	-0.627	0.113	0.1579	-3.22	0.137
Speed	-0.0157	-0.0247	0.01683	0.104	0.0085
CC	67.9	7.02	2.20	79.2	6.25
R.TEMP	-1.75	-1.612	0.510	-3.47	2.424
MR*MR	0.0862	0.0463	-0.01665	0.078	-0.0317
RT*RT	0.00055	0.001639	-0.000191	0.00563	-0.000768
Speed*Speed	-0.000020	0.000008	-0.000004	0.00094	-0.000005
CC*CC	1.46	1.063	-0.565	3.0	-1.229
R.TEMP*R.TEMP	0.0065	0.01391	-0.00462	0.0486	-0.02104
MR* RT	0.00566	0.00491	-0.00128	-0.0969	0.00094
MR*Speed	0.000178	0.000378	-0.000047	0.00281	0.000219
MR*CC	-0.394	0.139	-0.0063	-1.62	0.012
MR*R.TEMP	0.0755	0.0143	0.00698	-0.094	0.0094
RT*Speed	0.000193	-0.000102	0.000166	-0.000938	0.000131
RT*CC	-10.1472	-0.0618	-0.0138	-0.125	-0.0375
RT*R.TEMP	0.00990	-0.00277	-0.00023	0.0646	0.00104
Speed*CC	-0.02558	0.00528	-0.00022	0.0375	0.00325
Speed*R.TEMP	0.000985	0.000435	-0.000035	-0.00354	0.000021
CC*R.TEMP	-0.681	-0.136	-0.0092	-1.92	-0.0750

### 4.3.3 Control of process variable on biodiesel yield

“Stoichiometric trans-esterification, the reaction between three moles of methanol and one mole of tri-glycerides produced three moles of FAME and one mole of glycerol as a by-product”[250]. Alcohol (methanol) to oil ratio, RT, agitation speed, CC and R Temp are the several factors that affect its yield although it's Physico-chemical properties. In the present investigation, the process parameters vary in a defined range such as MR from 3:1 to 11:1, RT 40-80minute, agitation speed 400-800 rpm, CC 0.5-1.5 gram/lit, R Temp 54-66<sup>0</sup>C Because KOH is less corrosive than alcohol, it was used as a catalyst, and methanol was chosen because it was less expensive. Four circumstances were taken into consideration during the statistical analysis. For each analysis, three process parameters were kept constant while the other two were varied. The surface plots obtained in this analysis shown in Figure 4.3 and ANOVA result provided in Table 4.3

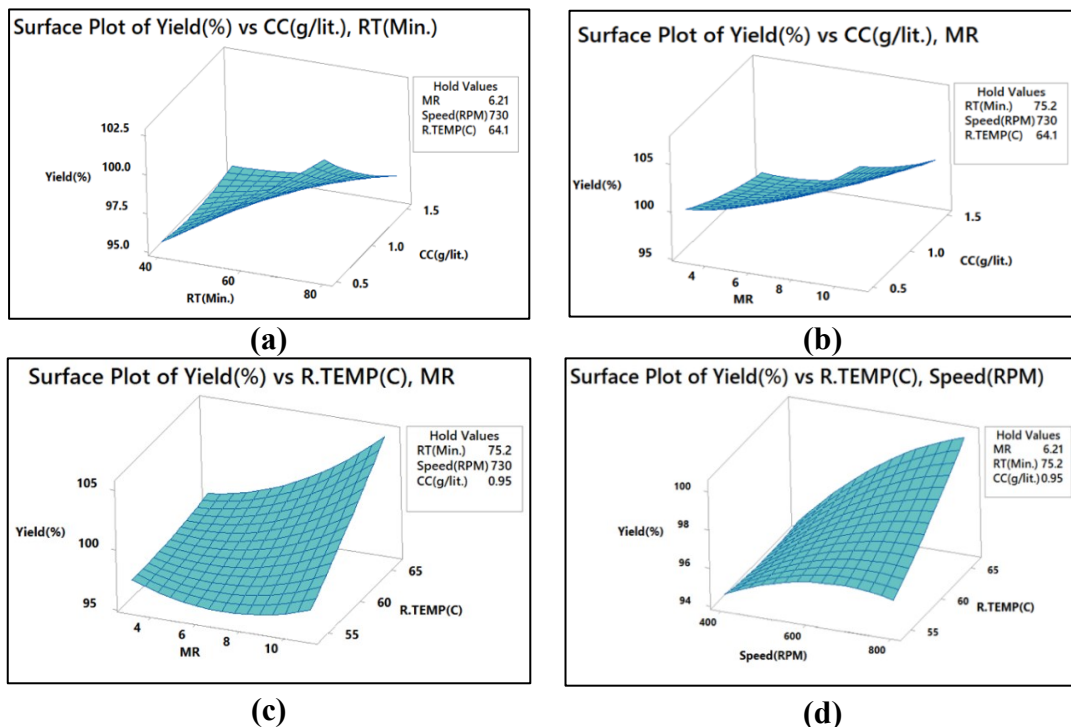


Figure 4.3 Control of process variable on yield

The yield of the biodiesel was found to increase on enhance the value of MR as well as CC. 98% maximum yield obtained at MR of 6.2. Higher the MR involved in



reversible reaction however its lower value is insufficient to complete the reaction. The nature of MR is depicted in Figure 4.3 (b) and (c). The catalyst amount also affects it as its lower value cause incomplete reaction whereas emulsion and saponification may cause due to its higher value. The trend of CC is justified in Figure 4.3 (a) and (b).

The effect of R Temp found in Figure 4.3 (c) and (d) for the trans-esterification reaction. Increased R Temp results in improve biodiesel yield. But after the certain limit, it found decrease. This act was found due to the boiling temperature of methanol as it is  $64.5^{\circ}\text{C}$  and methanol got evaporate. So maximum yield achieved just before saturation temperature.

The rate of reaction is also affected by the agitation speed. Higher the speed the reaction rate will be higher. The inverse relationship between agitation speed and FFA conversion suggests that turbulence enhanced the frequency of molecular interactions between the reactants.[251]. The speed of reaction and FFA conversion also increase with high agitation because it reduces the resistance experienced during mass transfer. When agitation reaches 680 rpm, FFA conversion is seen to marginally decline, most likely due to inadequate reaction time between the reactants.[252]. The affected trend of yield with the effect of agitation speed is showing in Figure 4.3 (d). Increased RT improved biodiesel productivity. More the RT helped to complete the trans-esterification reaction. Figure 4.3 (a) depicted that increased amount CC required more time to complete the reaction. Higher CC with shorter RT reduced the yield. The full quadratic equation must be obtained by providing the value of uncoded parameters and coefficients of the model from Table 4.7 in Equation 4.3. The general equation of yield % expressed in equation 4.2.

### **Regression Equation**

$$\text{Yield (\%)} = 82.30 + 0.349 \text{ MR} + 0.0405 \text{ RT (Min.)} + 0.00445 \text{ Speed(RPM)} \\ + 3.032 \text{ CC(g/lit.)} + 0.0621 \text{ R.TEM(C)}, \dots \dots \dots 4.2$$

### Regression Equation in Uncoded Units

$$\text{Yield(\%)} = 149.7 - 5.23 \text{ MR} - 0.627 \text{ RT(Min.)} - 0.0157 \text{ Speed(RPM)} \\ + 67.9 \text{ CC(g/lit.)} - 1.75 \text{ R.TEM(C)} + 0.0862 \text{ MR*MR} + 0.00055 \text{ RT(Min.)*RT(Min.)} - \\ 0.000020 \text{ Speed(RPM)*Speed(RPM)} + 1.46 \text{ CC(g/lit.)*CC(g/lit.)} + 0.0065 \text{ R.TEM(C)} \\ * \text{R.TEM(C)} + 0.00566 \text{ MR*RT(Min.)} - 0.000178 \text{ MR*Speed(RPM)} - \\ 0.394 \text{ MR*CC(g/lit.)} + 0.0755 \text{ MR*R.TEM(C)} + 0.000193 \text{ RT(Min.)*Speed(RPM)} - \\ 0.1472 \text{ RT(Min.)*CC(g/lit.)} + 0.00990 \text{ RT(Min.)*R.TEM(C)} - \\ 0.02558 \text{ Speed(RPM)*CC(g/lit.)} + 0.000985 \text{ Speed(RPM)*R.TEM(C)} - \\ 0.681 \text{ CC(g/lit.)*R.TEM(C)} \dots \dots \dots 4.3$$

#### 4.3.4 Control of process variable on kinematic viscosity

As the fluid gets viscous its flowability is reduced. This increased value of KV created an obstacle to the fuel flow which causes difficulties in the combustion of fuel that led to carbon deposition on injectors and valve. Illustrate the effect of process parameters on KV. It is a temperature-based phenomenon. There is an inverse relationship between the KV and temperature. At the temperature of 40<sup>0</sup>C the tri-glycerides diverted to fatty acid methyl ester. It was explained [236] in the two-term model generation that temperature had affected the value of KV and other physiochemical characteristics. Figure 4.4 (c) and (d) explain that increasing trend of temperature favors the improve KV of fuel. The reason behind this may the production of methyl ester, due to a reduction in unwanted fatty acids [253]. As depicted in Figure 4.4 (c) that increasing the MR and R Temp leads to a decrease in the KV however higher the methanol to lipid ratio and RT poor the KV. FFA found increased as disappointing of fatty ester when increase in RT as the backward reaction initiates that results in decreasing the KV as shown in Figure 4.4 (a). Unfortunately,

an excess of KOH was added, resulting in an obvious large amount of soap. Enhanced saponification brought on by an excess of CC rather than the tri-glycerides' transesterification has been proposed as the cause of this observation.[254], trends of CC shown in Figure 4.4 (a) and (b). The regression equation for biodiesel KV with different process parameters can be obtained by the value from Table 4.7 and put in Equation 4.5. The general regression equation of kinematic viscosity represent in Equation 4.4.

$$\text{KV}(\text{mm}^2/\text{sec}) = 9.219 - 0.0310 \text{ MR} - 0.00079 \text{ RT}(\text{Min.}) - 0.000171 \text{ Speed}(\text{RPM}) - 0.488 \text{ CC}(\text{g/lit.}) - 0.0393 \text{ R.TEM}(\text{C}) \dots\dots\dots 4.4$$

#### **Regression Equation in Uncoded Units**

$$\begin{aligned} \text{KV}(\text{mm}^2/\text{sec}) = & -18.0 - 0.106 \text{ MR} + 0.1579 \text{ RT}(\text{Min.}) + 0.01683 \text{ Speed}(\text{RPM}) \\ & + 2.20 \text{ CC}(\text{g/lit.}) + 0.510 \text{ R.TEM}(\text{C}) - 0.01665 \text{ MR} * \text{MR} - \\ & 0.000191 \text{ RT}(\text{Min.}) * \text{RT}(\text{Min.}) - 0.000004 \text{ Speed}(\text{RPM}) * \text{Speed}(\text{RPM}) - \\ & 0.565 \text{ CC}(\text{g/lit.}) * \text{CC}(\text{g/lit.}) - 0.00462 \text{ R.TEM}(\text{C}) * \text{R.TEM}(\text{C}) - 0.00128 \text{ MR} * \text{RT}(\text{Min.}) \\ & - 0.000047 \text{ MR} * \text{Speed}(\text{RPM}) - 0.0063 \text{ MR} * \text{CC}(\text{g/lit.}) + 0.00698 \text{ MR} * \text{R.TEM}(\text{C}) - \\ & 0.000166 \text{ RT}(\text{Min.}) * \text{Speed}(\text{RPM}) - 0.0138 \text{ RT}(\text{Min.}) * \text{CC}(\text{g/lit.}) - \\ & 0.00023 \text{ RT}(\text{Min.}) * \text{R.TEM}(\text{C}) - 0.00022 \text{ Speed}(\text{RPM}) * \text{CC}(\text{g/lit.}) - \\ & 0.000035 \text{ Speed}(\text{RPM}) * \text{R.TEM}(\text{C}) - 0.0092 \text{ CC}(\text{g/lit.}) * \text{R.TEM}(\text{C}) \dots\dots\dots 4.5 \end{aligned}$$

#### **4.3.5 Control of process variable on calorific value**

FP can be defined for fuel as the amount of chemical energy produced during the complete combustion per unit of mass. During the performance and combustion analysis, the CV mentioned its important role. The available moisture content in the fuel the CV reduced by 10-20%.[255]. It is to be desired that to obtain better performance and combustion analysis a fuel has higher FP. During the investigation hold the MR at 6.21, agitation speed at 730 RPM, R Temp at 64.1<sup>0</sup>C, and RT for 75.2

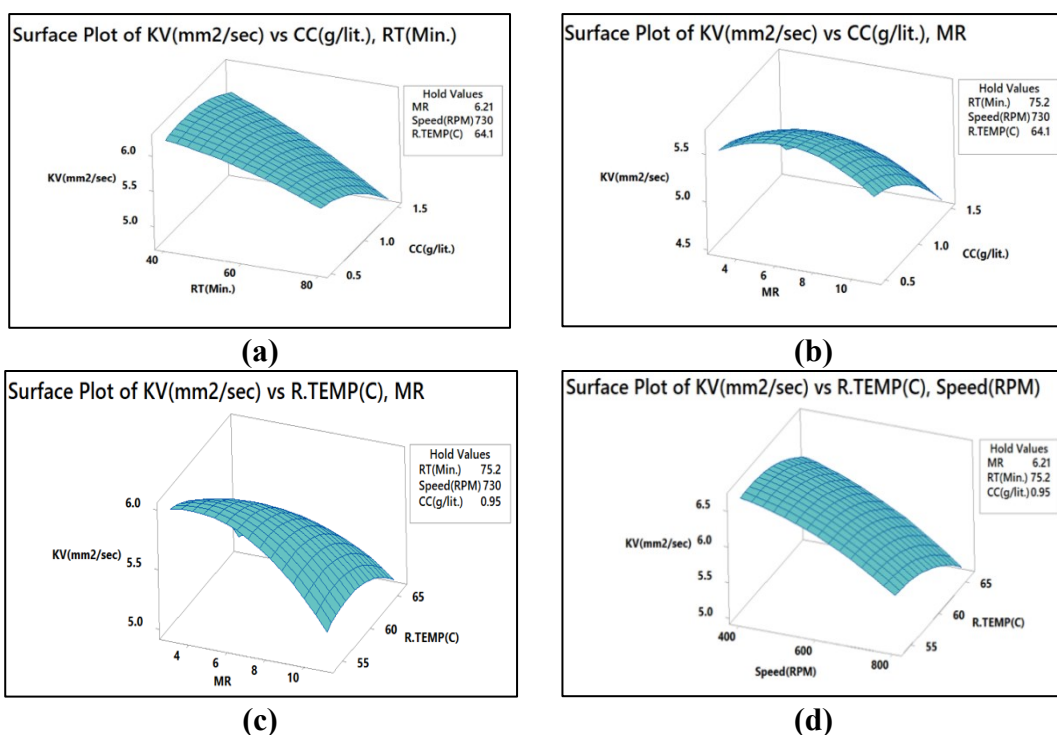


**Figure 4.4 Control of process variable on kinematic viscosity**

minute, and CC at 0.95. Keeping the three process parameters to be constant and vary the rest parameters. Figure 4.5 (a) depicted for variation in CC and RT. It was observed that a nonlinear trend followed for the CV. Mono-glyceride has a higher CV as compared to branched-chain [256]. The decreasing trend of CV was observed as increase in the CC due to the formation of aromatic compounds. At optimal MR provide a better CV. However higher its value reduces it due to the presence of alcohol as shown in Figure 4.5 (b) and (d). Although the scarcity of alcohol (methanol) at the boiling point the fatty acid component convert into higher acid which tends to decrease the CV.

However, there is no trace of reduction in CV as shown in Figure 4.5 (c) and (d) due to the coded stage s of R Temp is near by its boiling point. The reaction duration also has a significant impact on CV of waste cooking oil bio diesel. The graph CV vs. RT gave a nonlinear trend Figure 4.5 (a) depicted that CV improve as increase in RT. At 68 minute it was observed decrease due to reverse conversion favor to dominate the

production of fatty acid. Enhance the agitation speed improve the CV with a lower rate Figure 4.5 (c).

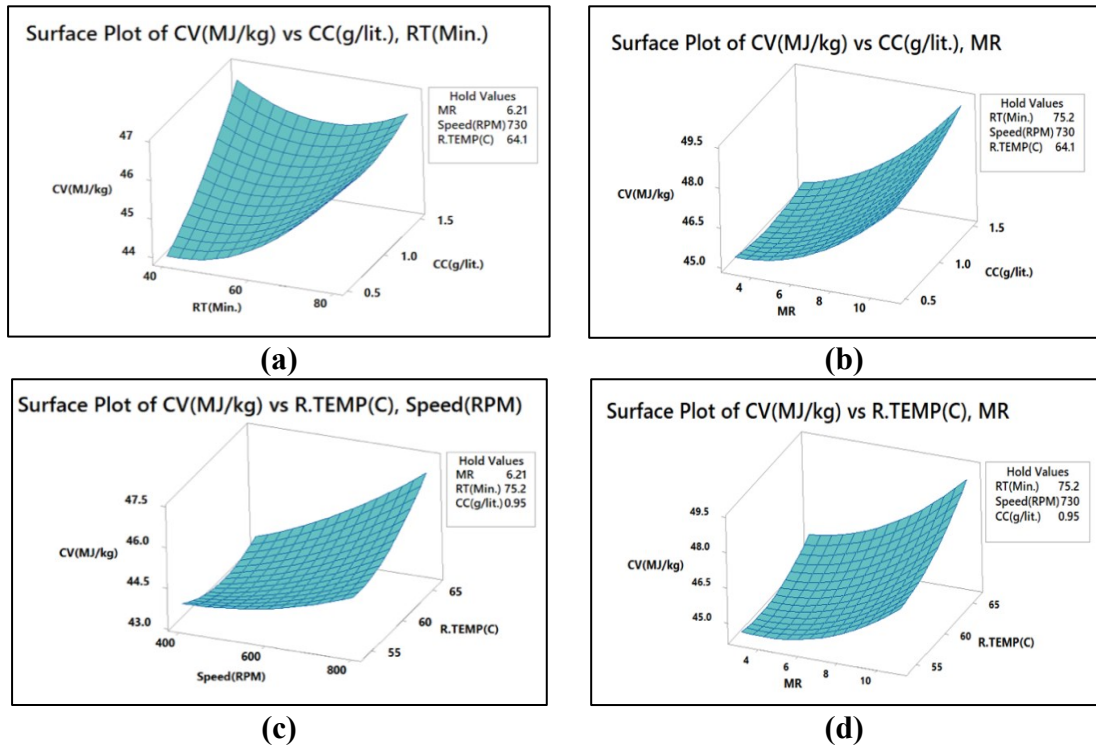


**Figure 4.5 Control of process variable on calorific value**

As it helps to homogeneous mixing of elements of trans-esterification. It was also depicted from the Figure 4.5 (c) that lower the value of agitation speed from optimal value leads to lowered the value of CV. The regression equation can be obtained by Table 4.7 after putting the value in Equation 4.7. The general regression equation of calorific value is provided in Equation 4.6.

$$\begin{aligned} \text{CV(MJ/kg)} = & 25.28 + 0.3344 \text{ MR} + 0.05521 \text{ RT(Min.)} + 0.007221 \text{ Speed(RPM)} \\ & + 1.425 \text{ CC(g/lit.)} + 0.1160 \text{ R.TEM(C)} \dots\dots\dots 4.6 \end{aligned}$$

#### **Regression Equation in Uncoded Units**

$$\begin{aligned} \text{CV(MJ/kg)} = & 87.7 - 1.376 \text{ MR} + 0.113 \text{ RT(Min.)} - 0.0247 \text{ Speed(RPM)} \\ & + 7.02 \text{ CC(g/lit.)} - 1.612 \text{ R.TEM(C)} + 0.0463 \text{ MR*MR} \\ & + 0.001639 \text{ RT(Min.)*RT(Min.)} + 0.000008 \text{ Speed(RPM)*Speed(RPM)} \\ & + 1.063 \text{ CC(g/lit.)*CC(g/lit.)} + 0.01391 \text{ R.TEM(C)*R.TEM(C)} \end{aligned}$$

$$\begin{aligned}
&+ 0.00491 \text{ MR} \cdot \text{RT}(\text{Min.}) - 0.000378 \text{ MR} \cdot \text{Speed}(\text{RPM}) + 0.139 \text{ MR} \cdot \text{CC}(\text{g/lit.}) \\
&+ 0.0143 \text{ MR} \cdot \text{R.TEM}(\text{C}) - 0.000102 \text{ RT}(\text{Min.}) \cdot \text{Speed}(\text{RPM}) - \\
&0.0618 \text{ RT}(\text{Min.}) \cdot \text{CC}(\text{g/lit.}) - 0.00277 \text{ RT}(\text{Min.}) \cdot \text{R.TEM}(\text{C}) \\
&+ 0.00528 \text{ Speed}(\text{RPM}) \cdot \text{CC}(\text{g/lit.}) + 0.000435 \text{ Speed}(\text{RPM}) \cdot \text{R.TEM}(\text{C}) - \\
&0.136 \text{ CC}(\text{g/lit.}) \cdot \text{R.TEM}(\text{C}) \dots\dots\dots 4.7
\end{aligned}$$

#### 4.3.6 Control of process variable on Flash point

“The minimum temperature which is sufficient to produce the vapor pressure of hydrocarbon has sufficient vapors to cause ignition which leads to flame generation under the specified conditions”[53], known as FP. For transportation and storage of fuel, FP is a key parameter. It was claimed in many types of research that FP of methyl ester is higher as compared to diesel so that it’s easy to transport and store. As Figure 4.6 (b) and (c) depicted that the as on increase the MR, the decreasing trend observed in FP. This negative was observed due to the availability of alcohol (methanol) which has low boiling point. During the present study increased duration of reaction not so much effective to provide the variation in FP. Increased value of CC withholding the value of MR results in decreasing trend of FP Figure 4.6 (a) and (b). A sharp negative trend was observed in surface plot Figure 4.6 (b) for FP on a variation of MR and CC. RT also affects the FP of WCOME. It was already explained in fatty acid composition major portion of WCOME consists of unsaturated fatty acid. The melting point is much lower as compared to saturated fatty acid [257].

So that it requires more temperature to produce sufficient vapors to ignite which leads to flaming. For the higher MR required to more R Temp so reaction must be completed. Simultaneously the alcohol (methanol) vaporized. Overall the FP will increase as on increasing the MR and R Temp. This trend is shown in Figure 4.6 (c) Agitation speed is helpful to promote homogeneity of reaction so that available

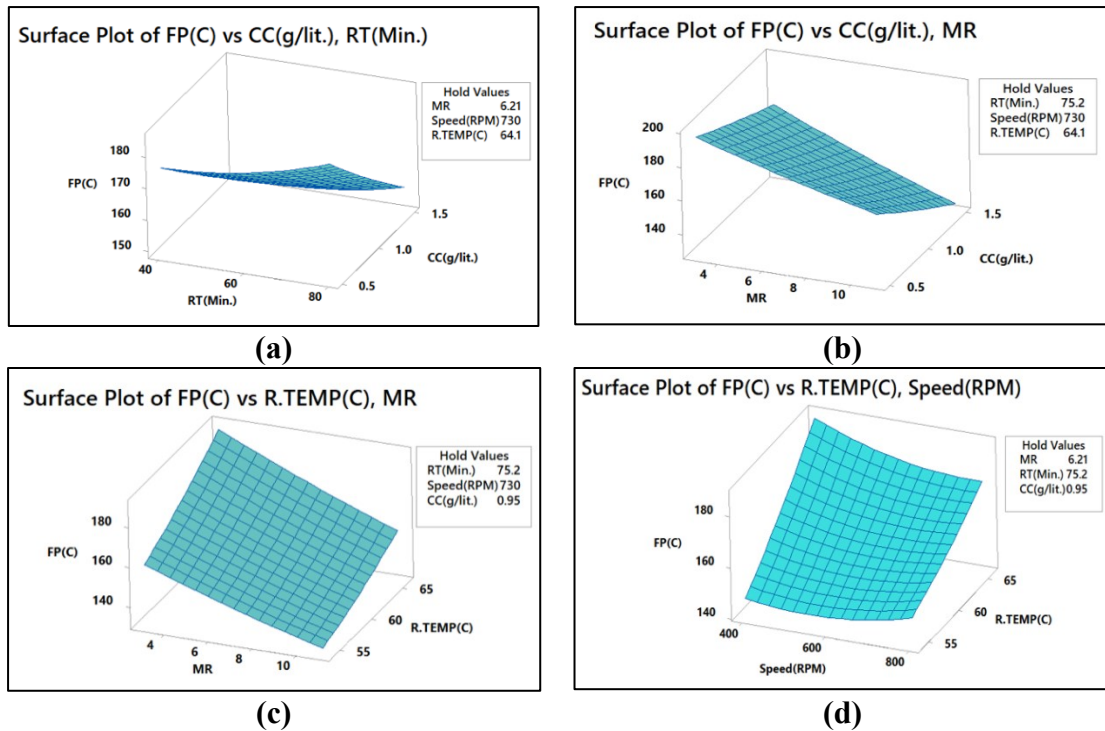


**Figure 4.6 Control of process variable on flash point**

constituents in the reaction are mixed properly. On the variation of speed from the optimal value slightly change observed in the value of FP. Figure 4.6(d) depicted higher FP at lower speed and higher R Temp. However simultaneously holding three process parameters such as MR, RT and CC at 6.21, 75.2 minute and 0.95 respectively. The value of coefficient from Table 4.7 provide the quadratic equation, after putting in Equation 4.9. The regression equation of flash point is provided in Equation 4.8.

$$FP(C) = 109.4 - 3.021 MR - 0.0375 RT(\text{Min.}) + 0.00542 \text{ Speed(RPM)} - 26.17 CC(\text{g/lit.}) + 1.542 R.TEM(C) \dots \dots \dots 4.8$$

Regression Equation in Uncoded Units

$$FP(C) = 235 + 7.3 MR - 3.22 RT(\text{Min.}) + 0.104 \text{ Speed(RPM)} + 79.2 CC(\text{g/lit.}) - 3.47 R.TEM(C) + 0.078 MR * MR + 0.00563 RT(\text{Min.}) * RT(\text{Min.}) + 0.000094 \text{ Speed(RPM)} * \text{Speed(RPM)} + 3.0 CC(\text{g/lit.}) * CC(\text{g/lit.}) + 0.0486 R.TEM(C) * R.TEM(C) - 0.0969 MR * RT(\text{Min.}) + 0.00281 MR * \text{Speed(RPM)} - 1.62 MR * CC(\text{g/lit.}) - 0.094 MR * R.TEM(C) -$$

$$0.000938 \text{ RT}(\text{Min.}) * \text{Speed}(\text{RPM}) - 0.125 \text{ RT}(\text{Min.}) * \text{CC}(\text{g/lit.}) \\ + 0.0646 \text{ RT}(\text{Min.}) * \text{R.TEM}(\text{C}) + 0.0375 \text{ Speed}(\text{RPM}) * \text{CC}(\text{g/lit.}) - \\ 0.00354 \text{ Speed}(\text{RPM}) * \text{R.TEM}(\text{C}) - 1.92 \text{ CC}(\text{g/lit.}) * \text{R.TEM}(\text{C}) \dots \dots \dots 4.9$$

#### 4.3.7 Control of process variable on pour point

The minimum temperature to which the flowability of the fluid is maintained is known as pour point. At the sub cooled operating temperature, fuel may be solidified and affect the fuel line [245]. Resulted from that clog the fuel line and filters. The PP is strongly affected by fatty acid composition. The unsaturated fatty acid composition leads to reflects better PP properties. Whereas saturated fatty acid had a poor PP. The PP characteristic improves with unsaturated fatty acid content [241]. In this section, the effect of process parameters on PP will be shown. The holding value will be the same as previously defined. The effect of process parameters shown in Figure 4.7. The surface plot Figure 4.7 (a) shown the effect of CC and MR on PP. It was found that PP significantly increased up to 7.4. This improvement was found due to the chemical kinetics of the trans-esterification reaction. RT is an influential parameter of biodiesel production.

The PP does not so much by RT. RT at 63 minutes depicted the good result of PP Figure 4.7 (b). The lower and higher value of RT affects the rate of reaction, resulting in the formation of fatty acid composition. As previously discussed, that fatty acid composition hampers the PP of fuel. The surface plot for various process parameters depicted that the MR and CC played an important role to decide the PP. The fully quadratic regression equation obtains from the value from Table 4.7 and put in Equation 4.11. The general regression equation of pour point provided in Equation 4.10



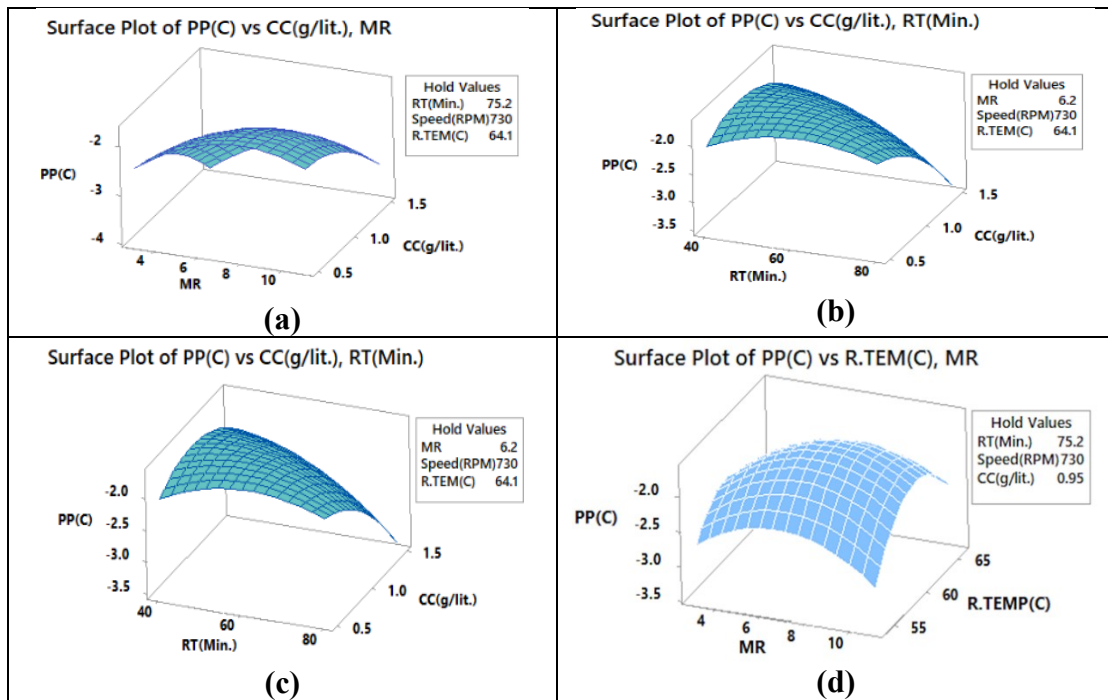


Figure 4.7 Effect of process variable on pour point

$$PP(C) = 1.29 - 0.0104 MR - 0.00208 RT(\text{Min.}) + 0.000458 \text{ Speed}(\text{RPM}) - 0.917 CC(\text{g/lit.}) - 0.0347 R.TEM(C) \dots \dots \dots 4.10$$

#### Regression Equation in Uncoded Units

$$PP(C) = -81.1 - 0.329 MR + 0.137 RT(\text{Min.}) + 0.0085 \text{ Speed}(\text{RPM}) + 6.25 CC(\text{g/lit.}) + 2.424 R.TEM(C) - 0.0317 MR*MR - 0.000768 RT(\text{Min.})*RT(\text{Min.}) - 0.000005 \text{ Speed}(\text{RPM})*\text{Speed}(\text{RPM}) - 1.229 CC(\text{g/lit.})*CC(\text{g/lit.}) - 0.02104 R.TEM(C)*R.TEM(C) + 0.00094 MR*RT(\text{Min.}) + 0.000219 MR*\text{Speed}(\text{RPM}) + 0.012 MR*CC(\text{g/lit.}) + 0.0094 MR*R.TEM(C) - 0.000131 RT(\text{Min.})*\text{Speed}(\text{RPM}) - 0.0375 RT(\text{Min.})*CC(\text{g/lit.}) + 0.00104 RT(\text{Min.})*R.TEM(C) + 0.00325 \text{ Speed}(\text{RPM})*CC(\text{g/lit.}) + 0.000021 \text{ Speed}(\text{RPM})*R.TEM(C) - 0.0750 CC(\text{g/lit.})*R.TEM(C) \dots \dots \dots 4.11$$

#### 4.4 Validation of experimental results

In order to confirm the optimized output response, the experiment was carried out using the current lab configuration of input variables produced by the RSM optimizer, specifically at a 6.21 MR ratio, RPM 730, 0.95 g/lit CC with reaction temperature

64.1<sup>0</sup>C for 75.2 minutes reaction time. The output results of pour point, flash point, kinematic viscosity, Calorific value, and production yield are Error was calculated when the prediction value from the RSM model was compared as shown in Table 4.8.

**Table 4.8 Verification of output responses**

<b>Experimental setting at 6.21 MR, RPM 730, 0.95 g/lit CC, R Temp 64.1<sup>0</sup>C and 75.2 RT</b>			
<b>Response</b>	<b>RSM predicted value</b>	<b>Experimental value</b>	<b>Error (%)</b>
Production yield	98.95 %	97.5 %	1.46
Calorific value	45.68 MJ/kg	44.2 MJ/kg	3.23
Pour point	-2.122 <sup>0</sup> C	-2. <sup>0</sup> C	5.74
Kinematic viscosity	5.48 cSt	5.8 cSt	5.8
Flash point	169.254 <sup>0</sup> C	160.5 <sup>0</sup> C	5.17

Between the expected value and the experimental value of the output response, there appears to be some marginal error. For biodiesel production yield, CV, KV, FP and PP the error percentage is 1.46%, 3.23%, 5.74%, 5.8%, and 5.17% respectively which are within an acceptable limit.

#### 4.5 Preparation of Quaternary Blends

All the blends were prepared as per National Biofuel Policy [234] in which up to 5% of waste cooking oil BD is allowed to blend with diesel. The preparation of quaternary blends used here was done by varying the proportion of SVO from 3% to 21% (v/v) and n-butanol from 2% to 14% (v/v). The concentration of WCOBD was kept constant at 5% (v/v). All prepared blends are showing in the Plate No. 4.1. The method employed for the test fuel blends preparation was splash blending. The prepared blends were kept for 120 h and there was no phase separation found in blends. The nomenclature of the quaternary blends is based on O<sub>x</sub>B<sub>y</sub> presentation, where X and Y are the %v/v in the blends in Table 4.9.

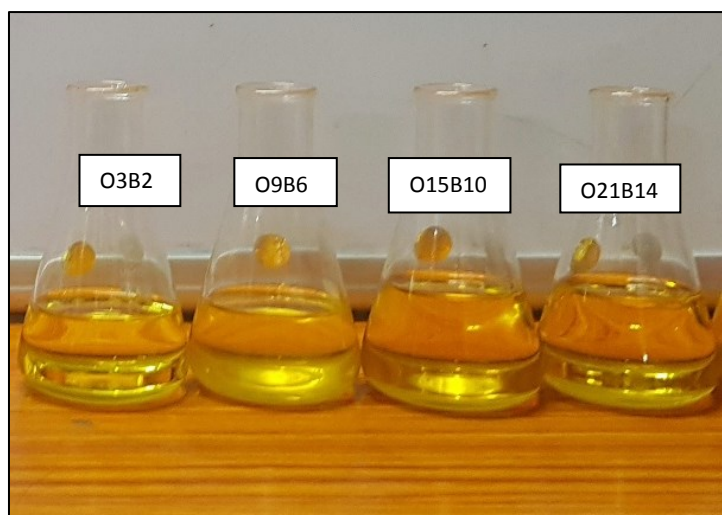


**Plate No. 4.1 Prepared test fuel blends**

During the preparation of test fuel blends the required used cooking oil was procured from local restaurant. The cost was ₹30/liter. For the experiment purpose the quantity bought was 5 liter. The orange peel oil was procured from market and it cost of ₹ 400 per liter. The n-butanol was procured from chemical supplier at the price of ₹50 per liter and diesel at the market price of ₹ 86.67 per liter. For the preparation of test fuel blends the cost of O3B2, O9B6, O15B10, and O21B14 was ₹92, ₹110, ₹126, and ₹143 per liter.

**Table 4.9 Nomenclature of fuel blends**

<b>Nomenclature</b>	<b>Diesel</b>	<b>WCOBD</b>	<b>Orange Peel Oil</b>	<b>n-butanol</b>
D100	100	0	0	0
O3B2	90	5	3	2
O9B6	80	5	9	6
O15B10	70	5	15	10
O21B14	60	5	21	14

## **4.6 Physico-Chemical Properties of Fuel Blends**

### **4.6.1 Kinematic viscosity**

The kinematic viscosity of neat WCO was quite high. It was drastically reduced after conversion in methyl ester. The kinematic viscosity of the WCO sample was found a little higher. It was 38.43 cSt Some of the research shown that limonene helped to

reduce viscosity [242]. The trend in Figure 4.8 was observed that after increasing the fraction of orange peel oil the viscosity got reduced. The blend O21B154 had lower viscosity of 2.20 cSt Figure 4.8. The value fulfilled the ASTM D 6751. The value FOUND under the recommended value i.e. 1.9-6.0 cSt.

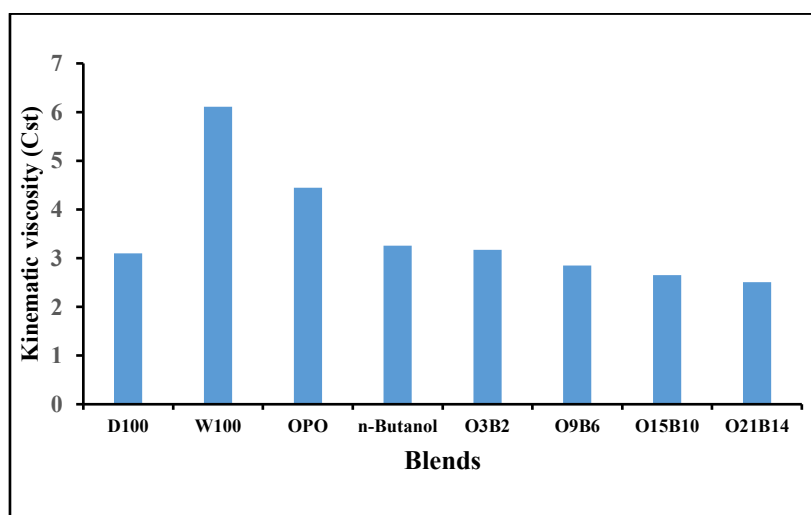


Figure 4.8 Kinematic Viscosity

#### 4.6.2 Density

As per ASTM equipment followed ASTM D4052 with an accuracy of  $\pm 0.1 \text{ kg/m}^3$ . The recommended values  $839 \text{ kg/m}^3$  and  $880 \text{ kg/m}^3$  as per ASTM D1298 for diesel and biodiesel respectively. Although  $860\text{-}900 \text{ kg/m}^3$  as per EN ISO 3675.

As the density of WCOME (W100) was found higher. To improve the density characteristic Henceforth to overcome this problem mixed the n-butanol. The density of n-butanol ( $810 \text{ kg/m}^3$ ) is much lower as compared to WCOME ( $897 \text{ kg/m}^3$ ) and orange peel oil ( $851 \text{ kg/m}^3$ ). As the fraction of orange peel increased the density found increased. As shown in Figure 4.9 As the marginal increasing trend was achieved during the study. The density followed the standard of ASTM D 1298.

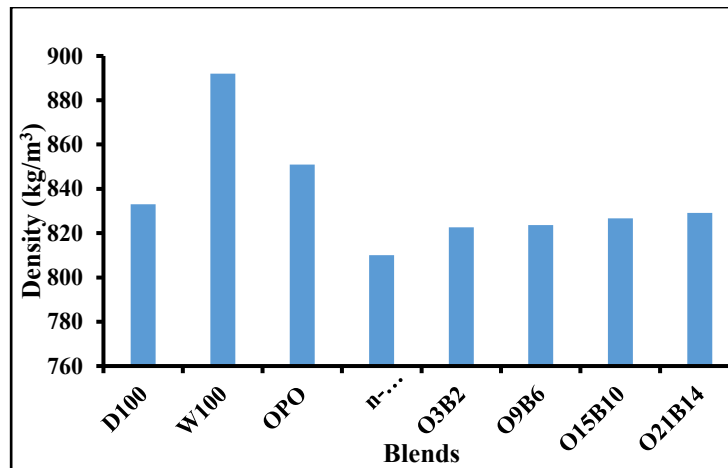


Figure 4.9 Density of Fuel Blends

#### 4.6.3 Calorific Value (Heating Value)

The chemical energy released during combustion per unit of mass is called heating value[61]. The value affects the thermal efficiency as well as combustion characteristics. The trend was found with a marginal difference in the blends as shown in Figure 4.10. It was found in the investigation that the volume fraction of n-butanol increases the simultaneously increase heating value. Although the decreasing trend got achieve after 10% of n-butanol. This happened due to the low calorific value of n-butanol. Figure 4.10 showed the highest recommended calorific value observed in O15B10.

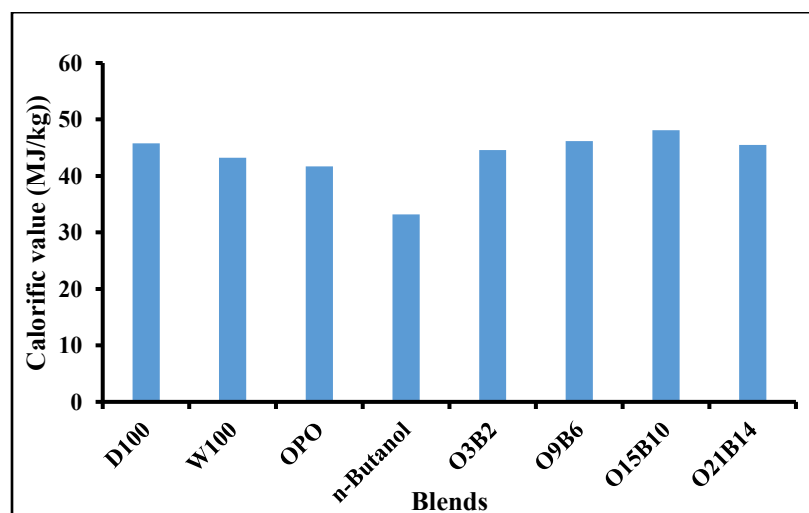


Figure 4.10 Calorific Value of Fuel Blends

#### 4.6.4 Flash Point

At the time of heating of fuel in environmental conditions (atmospheric pressure and temperature), they attained the lowest temperature at which it provided a sufficient amount of fuel vapors to generate inflammable mixture at the surface of the fuel[53], [258] achieved temperature is the flashpoint. For storage and transportation of fuel, the flashpoint has an important role [239]. The biodiesel has a higher flash point ( $>130^{\circ}\text{C}$ ) s compared to diesel ( $52^{\circ}\text{C}$ ). That's why the storage and transportation of it more convenient and less risky[240], [259]. Some of the researches revealed that the flashpoint reduced as increased storage hour [258]. During the investigation, it was found all the blend followed the standard of ASTM D93. The flash point exhibit by blend O15B10 i.e.  $81.6^{\circ}\text{C}$  as shown in Figure 4.11.

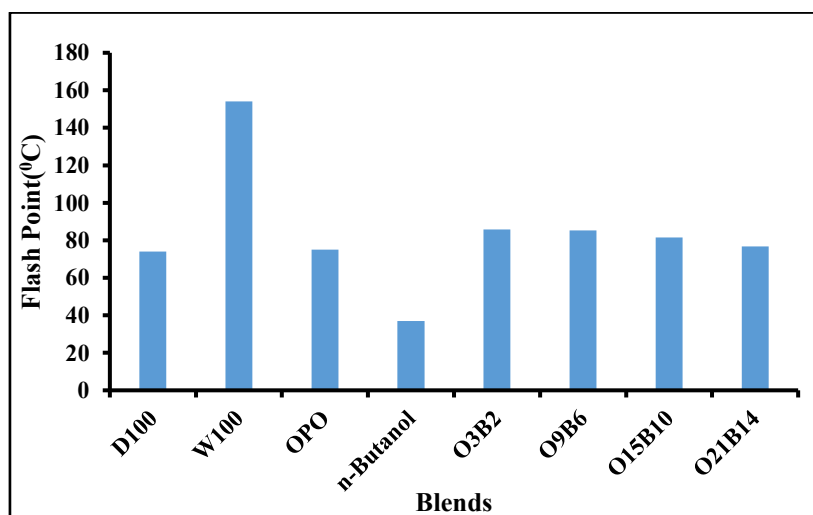


Figure 4.11 Flash Point of Fuel Blends

#### 4.6.5 Cloud point and pour point

It is essentials to investigate the performance of the fuel at low temperature, required to evaluate the cloud point and pour point[243]. The lowest temperature at which the formation of cloud or wax in crystal form in the fuel that limited temperature is known as the cloud point. This helped to identify the flow properties of fuel [244]. The fuel filter was blocked as the solidification started. It led to degrading the performance of the engine. Pour point is a breakeven point[245]. Meanwhile, the fuel

can flow till that temperature and ceased the flow of fuel when decreased this temperature. As literature expressed that  $-0.80^{\circ}\text{C}$  and  $-8.50^{\circ}\text{C}$  is the recommended value of cloud and pour point of diesel respectively [260]. According to ASTM D975 pour point and cloud point of diesel the recommended ranges are  $-15$  to  $5$  and  $-35$  to  $15$  respectively. Although  $-15$  to  $-16$  as per ASTM D 97 and  $-3$  to  $-12$  as per ASTM D2500 recommended for pour point and cloud point of biodiesel [261]. The fraction part of orange peel oil played an important role. Whenever it increased, it affected the pour and cloud point. The results revealed that  $-14.6^{\circ}\text{C}$ ,  $-8.5^{\circ}\text{C}$  pour and cloud point of O15B10 shown in Figure 4.12. In the winter season it created low measures as compared to other blends.

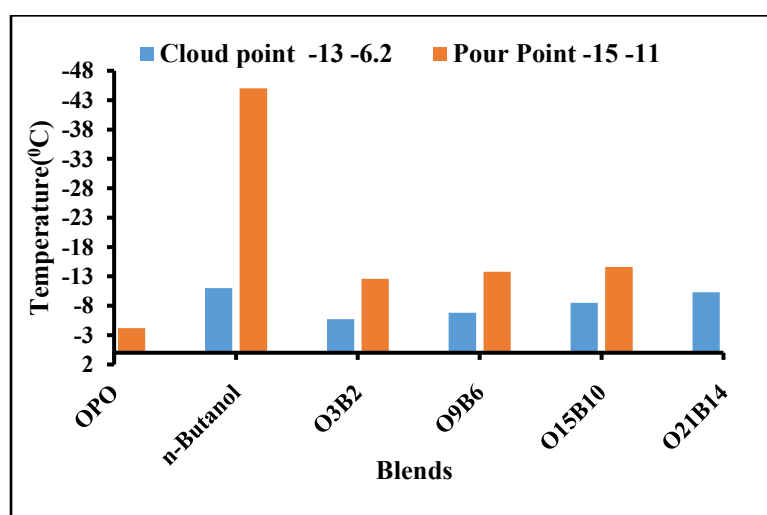


Figure 4.12 Cloud Point and Pour Point of Fuel Blends

#### 4.6.6 Cetane number

The ignition quality could be assured by the cetane number. The value reflects how much time is taken by the fuel for combustion. As soon as the fuel ignited inside the cylinder the operation would be smooth. The fuel having higher the cetane number, the emission and performance will be improved[262]. Although the lower cetane number fuel produced more unburnt hydrocarbon (UHC) also the CO. the biodiesel having a higher cetane number as compared to diesel that's why it is permissible fuel for CI engine[263]. The recommended range of 40-55 for diesel as per ASTM D4737.

However minimum 47 and minimum 51 for biodiesel as per ASTM D613 and EN ISO 3679 respectively. It was found in so much literature that the cetane number FAME is much higher as compared to diesel. The cetane number of n-butanol as compared to WCOME and orange peel oil found lower. It was observing trend during the experimental investigation that as cetane number decreased when a fraction of butanol increased. The blend D90W5O2B3.had the highest cetane number of 51.3 as shown in Figure 4.13.

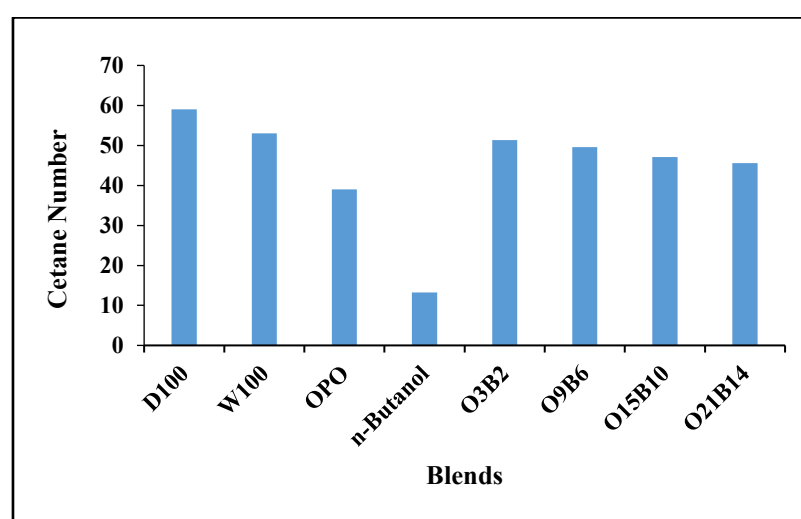


Figure 4.13 Cetane Number of Fuel Blends

#### 4.6.7 Sulphur content

The value of sulphur content is an important study. It provides the lubricity of the fuel. As the BS-VI norms stated that the permissible concentration of sulphur content in the diesel not more than 5 ppm. While in BS-IV norms it was 50 ppm[264]. Lubricity inside the engine will reduce as increase in the Sulphur content. The reduction in lubricity reduces the operational life of an engine. It will lead to more wear and tear. This investigation was conducted on the XOS Sindie Sulphur analyzer as per ASTM D 7039. The maximum permissible value is 5 ppm for diesel and 15 ppm for biodiesel. The decreasing trend Figure 4.14 found during the study. Sulphur content in the biodiesel is less. Although, the n-butanol has no mark of presence of Sulphur content. Moreover, the Sulphur content did not so much affected by mixing



of SVO of orange peel. All the tested blends of orange peel oil had the permissible Sulphur content (7.85 ppm-5.61 ppm).

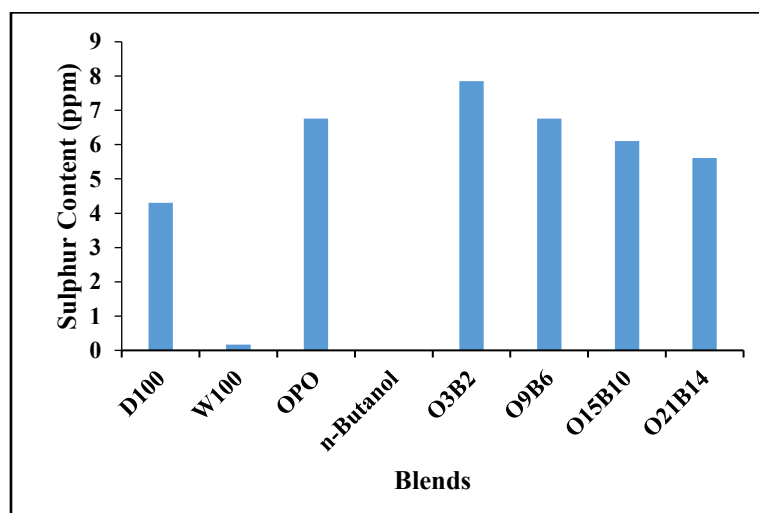


Figure 4.14 Sulphur Content of Fuel Blends

#### 4.6.8 Micro carbon residue

“Micro carbon residue test uses to calculate the amount of carbonaceous residue formed after complete evaporation and pyrolysis of diesel under specified conditions”. To some extent, it also provides a sign of coke formation[265], [266]. This experiment was conducted on MCRT 160 Alcor-micro carbon residue tester. The recommended value of 0.2% (mass) as per ASTM D 4530 for diesel and 0.05% for biodiesel according to ASTM D 130. EN ISO 10370 is recommended for a maximum of 0.3% [265]. The trend Figure 4.15 was observed during the experiment that beyond the 12% of orange peel oil the coke formation tendency increased.

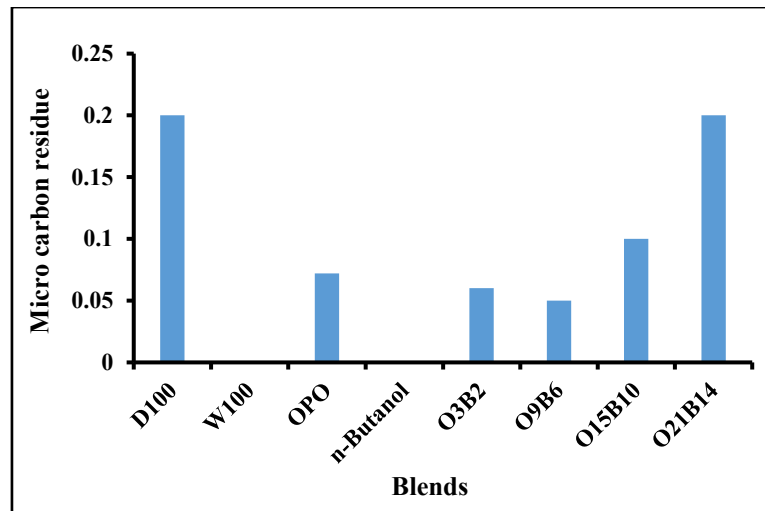


Figure 4.15 Micro-Carbon Residue of Fuel Blends

#### 4.7 Sauter mean diameter

Every time fuel is injected, a variety of sized particles are released into the spray. Consequently, the Sauter mean diameter (SMD), which is the average particle size, is determined statistically. The fuel's characteristics determine the particle size, including such as viscosity, density, and surface tension. The SMD of neatdiesel and it's blends is shown in Figure 4.16. The SMD of waste cooking oil biodiesel is more than neat diesel due to the higher viscosity.

Fuel that has been sprayed breaks up into fine particles because of instabilities in the fuel. On the other hand, there is less collision force between the closely packed molecules of high-viscosity fuel. As a result, the fuel molecules can't move in proximity to one another inside of the spray; as a result, the fuel jet is stable and unable to split, which causes the particle size to increase. Because of their higher viscosity than diesel, biodiesel made from different edible oils also has a higher SMD than diesel.

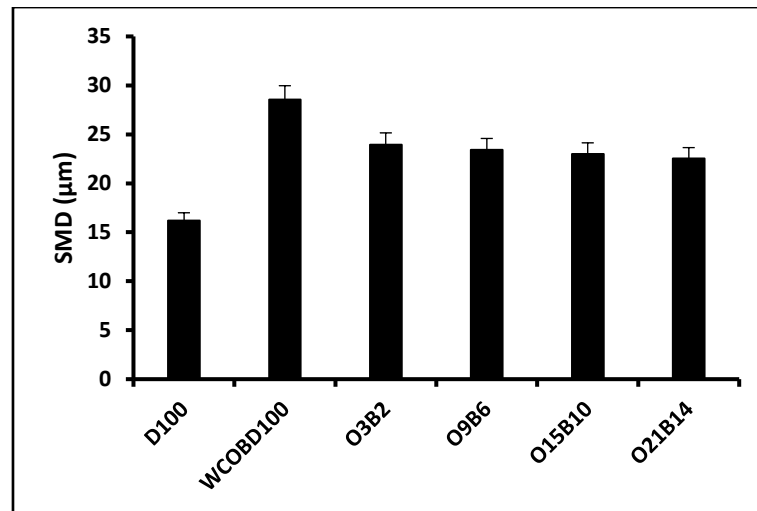


Figure 4.16 Sauter mean diameter for test fuel blends

In Figure 4.17 shown that the Sauter surface area. It is the particle's surface area divided by its volume. Higher surface area particles will be surrounded by more oxygen, which will shorten the ignition delay and improve combustion. It was observed during the experimental trial the graph reveals that the higher surface area of the fuel blend which has the lowest Sauter mean diameter. The higher surface among the blends represented by O21B14 i.e.  $0.296 \text{ mm}^2/\text{cc}$ .

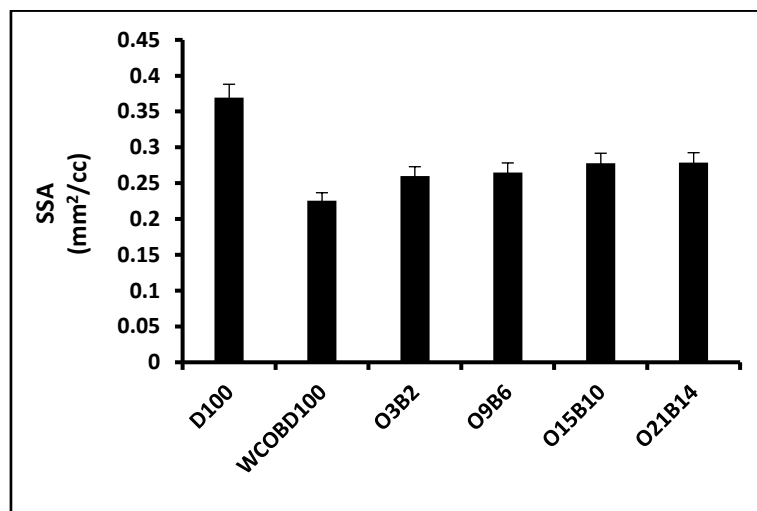


Figure 4.17 Sauter surface area for the test fuel blends

#### 4.8 Experimental setup

The experimental analysis was performed on “an air-cooled, single-cylinder, four-stroke, naturally aspirated, DI diesel engine”. The engine specifications are listed in

Table 4.10, and the experimental test engine setup schematic diagram is displayed in Figure 3.7.

In this study, the experiments were conducted with 200 bar injection pressure using four different test fuel blends at 1500 rpm engine speed and seven varying loads (0.05, 0.1, 0.15, 0.20, 0.25, 0.3, and 0.35MPa). The test fuels blends were prepared using the splash blending method. The concentration of WCOME is kept constant at 5% (v/v) while that of n-butanol (2-14% v/v) and orange peel oil (3-21% v/v) is varied in the diesel. The various physico-chemical properties of the prepared fuel-blends are given in Table 4.12 and are in accordance with ASTM standards. Emission characteristics are measured using an AVL Di-gas analyzer and AVL smoke meter. The list of instruments employed and their range, accuracy & uncertainties are provided in Table 3.11.

**Table 4.10 Technical specification of the engine and alternator**

<b>Diesel Engine specification</b>			
Make	Kirloskar	Cooling Type	Air cooled (Radial cooled)
Model	DAF 8	Fuel injection timing	23 degree BTDC
Brake Power (kW)	3.5	No. of injector holes	3
Cylinders	1	Nozzle diameter (mm)	9
Rated speed (rpm)	1500	DI Type	Mechanical pump
Compression ratio	17.5:1	Injection pressure	200 bar
Stroke x Bore (mm)	110 x 87.5	Lubricating system	Forced feed
Connecting rod length (mm)	234	Cubic capacity	0.78 L
Displacement	0.661	Starting	Hand Start with cranking handle
<b>Dynamometer specification</b>			
Manufacturer	Kirloskar Electric Co. Ltd. India	Rated voltage	230V
Dynamometer type	Single phase, 50 Hz, AC alternator	Rated current	32.6 A
Rated output	5 KVA @1500 rpm		

**Table 4.11 Equipment used for properties evaluation**

Property	Equipment & Standard Method	Accuracy
Kinematic viscosity @ 40°C (mm <sup>2</sup> /s)	Visco bath, Petrotest ASTM D445	±0.01 mm <sup>2</sup> /s
Density @ 15°C (kg/m <sup>3</sup> )	Anton Parr DMA 4500 ASTM D4052	±0.1 kg/m <sup>3</sup>
Flash point (°C)	Pensky-Martens (AD0093–600) ASTM D93	±0.1 °C
Cloud Point (°C)	-	-
Pour Point (°C)	-	-
Calorific value (MJ/kg)	Parr 6100 Oxygen Bomb Calorimeter ASTM D240	±0.001 MJ/kg
Sulphur content (ppm)	XOS Sindie Sulphur analyzer ASTM D7039	0.5 (repeatability)
Cetane number	ASTM D4737	±0.1

**Table 4.12 Physical and chemical properties of fuel blends**

Property	Unit	n-Butanol	OPO	Diesel	WCOME	O3B2	O9B6	O15B10	O21B14
Kinematic viscosity @40°C	mm <sup>2</sup> /s	3.6	1.71	3.1	6.21	3.17	2.65	2.39	2.20
Density @15 °C	kg/m <sup>3</sup>	810	851	833	892	822.6	823.6	826.7	829.1
Flash point	°C	37	75	74	154	85.8	85.2	81.6	76.7
Pour point	°C	-45	-	-15 to 5	-11	-12.6	13.8	14.6	-15.6
Cloud point	°C	-115.5	-	-13 to 15	-6.2	-5.7	-6.8	-8.5	-10.3
Calorific value	MJ/kg	33.20	41.72	45.8	43.2	44.6	46.2	48.1	45.5
Sulphur content	ppm	-	6.76	4.3	0.17	7.85	6.76	6.11	5.61
Cetane number	-	13.21	39	59	53	51.3	49.6	47.1	45.6
Micro carbon residue (100% Sample)	%m/m		0.072	0.2 max	0.33	0.06	0.05	0.10	0.20

## 4.9 Performance characteristic

### 4.9.1 Brake Thermal Efficiency (BTE)

The BTE vs. BMEP graph for different fuels blends is shown in Figure 4.18(a). The trends in the figure show that, with the increase in BMEP, the BTE first increases up to a maximum limit and then decreases. Also, with the increase in the concentration of

orange peel oil in the fuel blends, an increasing trend of BTE is observed at a particular BMEP. This is due to the increase in the concentration of orange peel oil in the fuel blends which exhibits better combustion characteristics because of its lower viscous property and lower boiling point. However, the calorific value of orange peel oil is slightly lower but according to [267] when a low viscous and low boiling point fuel is mixed with diesel, it enhances the air-fuel blends mixing process and thus enhances the evaporation process that favors the better combustion inside the cylinder. At higher loads, the BTE obtained are 21.99, 22.09%, 22.31%, and 22.49%, for O3B2, O9B6, O15B10, and O21B14 respectively as compared to neat diesel.

#### **4.9.2 Exhaust Gas Temperature (EGT)**

The quality of fuel and the combustion process inside the cylinder have a notable effect on the temperature of exhaust gas (EGT). The fuel-air ratio, cetane index, lower heating value (LHV), and calorific value are crucial factors affecting EGT. It should be mentioned that when the load increases and more fuel is injected to meet the energy requirements, the EGT increases proportionality. Figure 4.19 shows how exhaust gas temperature varies with load for the fuels tested. Compared to diesel, all blends caused an increase in exhaust gas temperature during engine operation.

The EGT with O21B14 was higher than the EGT with other blends as increase the proportion of orange peel oil. The EGT at full load with diesel, D100, O3B2, O9B6, O15B10 and O21B14 was 410, 475, 482, 638, and 654<sup>0</sup>C, respectively. As the blends contain more biodiesel, the Exhaust Gas Temperature (EGT) enhance due to the higher greater released during the diffusion combustion phase. However, in the blends containing biodiesel, the heat release in the second stage of combustion begins later than in the blends that have undergone hydro treatment.

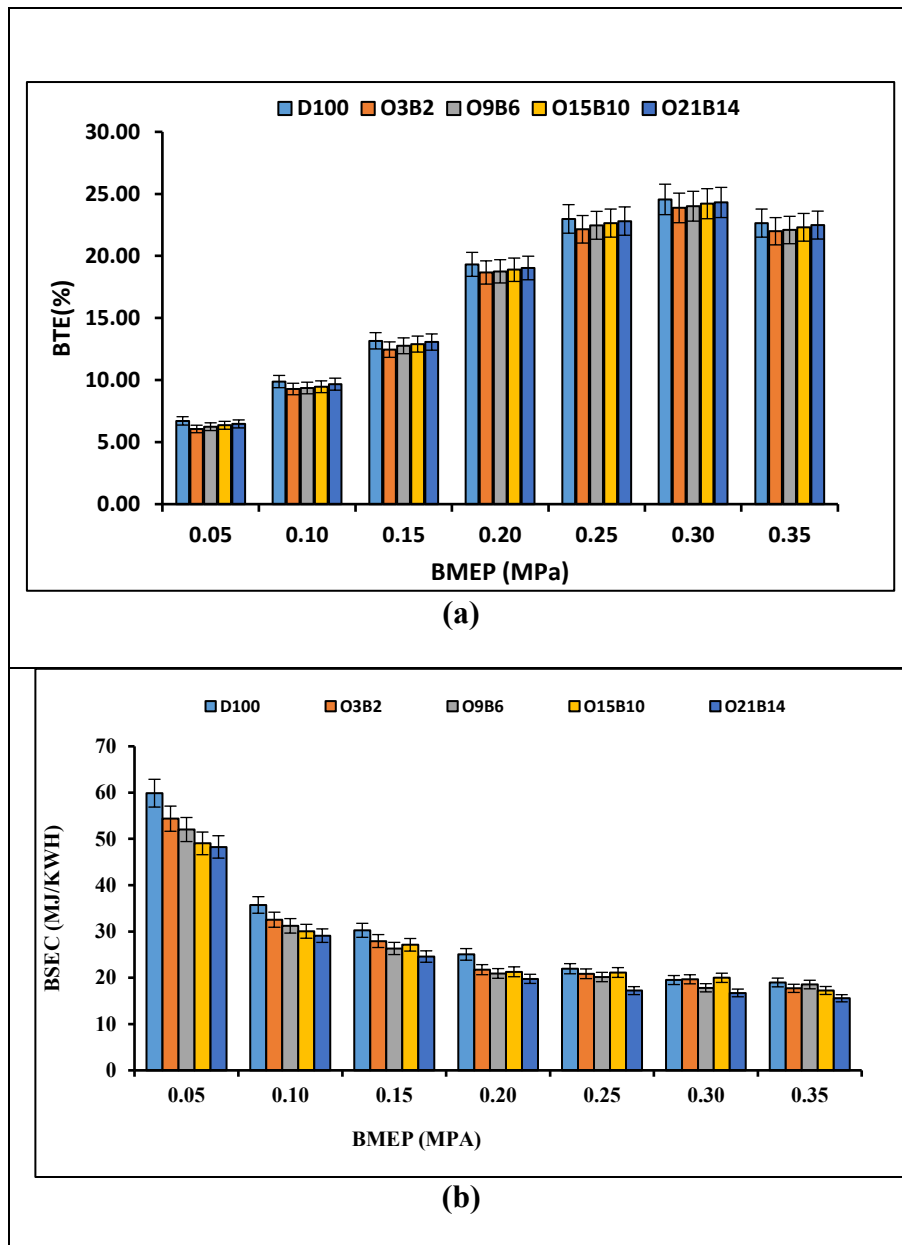
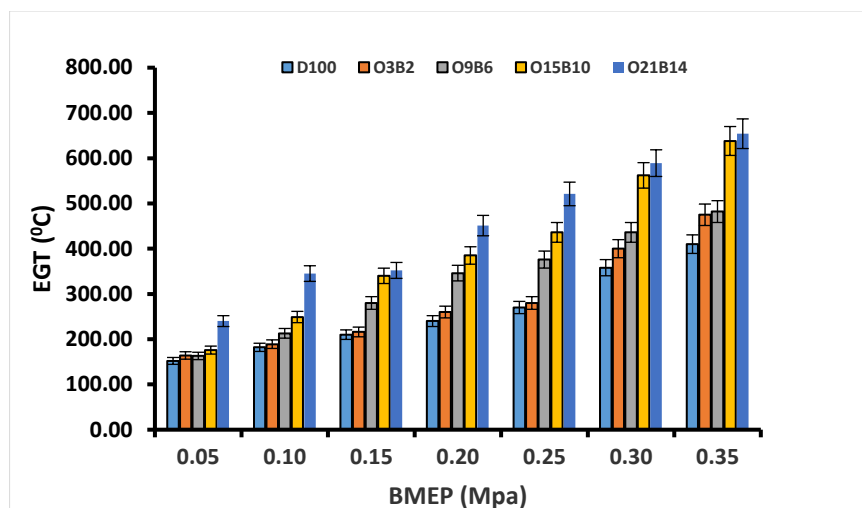


Figure 4.18 Effect of orange peel oil addition on (a) BTE and (b) BSEC on different engine loads at 1500 rpm.

This delay in heat release results in the heat being released later in the expansion stroke, which produces waste heat and less useful work for the engine.

#### 4.9.3 Brake Specific Energy Consumption (BSEC)

The BSEC vs. BMEP graph for different fuels blends is shown in Figure 4.18(b). The trend in the figure shows that with the increase in BMEP, the BSEC decreases. Also, with the increase in the concentration of orange peel oil in the fuel blends, a decreasing trend of BSEC is observed at a particular BMEP.



**Figure 4.19 Variation of EGT with BMEP**

This is due to the addition of low viscous orange peel oil in the fuel blends which significantly reduced the BSEC. At higher loads, the BSEC obtained are 7.75%, 17.2%, 21.08%, and 23.77% for O3B2, O9B6, O15B10, and O21B14 respectively as compared to neat diesel. For fuels with nearly equal calorific values, the fuel with a higher viscosity property has a higher BSEC, according to the literature review. For fuels with nearly equal calorific values, the fuel with a higher viscosity property has a higher BSEC, according to the literature review[268].

#### **4.10 Emission characteristic**

##### **4.10.1 Hydrocarbon emission**

Poor air entrainment, multiple rich zone regions forming, and incorrect mixing of fuel blend particles with air are the causes of the HC creation during engine combustion.[269]. This can be formed inside the engine cylinder wherever the air-fuel mixture is beyond the ignition limit. The HC vs. BMEP graph for different fuels blends is shown in Figure 4.20(b).

The data depicted in the image indicates that the emissions of hydrocarbons (HC) rise in direct proportion to the increase in brake mean effective pressure (BMEP). Additionally, a decreasing trend in HC emissions is evident at a specific BMEP level as the concentration of orange peel oil in the fuel blends increases. The figure further



illustrates that, compared to pure diesel fuel at maximum load, the HC emissions have been reduced by 9.72% for O3B2, 19.44% for O9B6, 34.72% for O15B10, and 40.27% for O21B15. The article [270] highlights how the fuel's surface tension and viscosity can affect the fuel's atomization and mixing.

As the viscosity and boiling point of the orange peel oil is relatively lower, its increasing concentration in the fuel blends enhances the overall atomization that leads to finer droplet size and faster evaporation inside the cylinder, thus causes the complete combustion process.

#### **4.10.2 Oxides of nitrogen emission (NO<sub>x</sub>)**

Thermal NO<sub>x</sub>, fuel NO<sub>x</sub>, and quick NO<sub>x</sub> are the three main forms of NO<sub>x</sub> formation. Out of the three, thermal NO<sub>x</sub> plays a crucial role in enhancing engine efficiency.[271].The NO<sub>x</sub> vs. BMEP graph for different fuels blends is shown in Figure 4.20(b). The trend in the Figure 4.20(b) shows that with the increase in BMEP, the NO<sub>x</sub> emissions increase. Also, with the increase in the concentration of orange peel oil in the fuel blends, an increasing trend of NO<sub>x</sub> is observed at a particular BMEP. As seen from the figure, the NO<sub>x</sub> emission has been reduced by 2.93% for O3B2, 2.49% for O9B6, 0.93% for O15B10, and 0.46% for O21B15 respectively as compared to neat diesel at full load. This is due to the addition of orange peel oil that lowers the overall cetane index of the fuel blends. As the cetane index is the significant parameter for defining the self-ignition property of the fuel, the reduction in the cetane index increases the period of ignition delay under all loading conditions. This longer ignition delay period causes the accumulation of a larger amount of air-fuel mixture that results in a higher in-flame temperature during the premixed combustion stage.[272], [273]shows that the addition of lower cetane index fuel could cause fuel deposition during a longer ignition delay period that leads to an increase in the combustion temperature and heat release rate.

#### 4.10.3 Carbon mono oxide (CO) Emissions

When there is insufficient oxygen or an incorrect air-fuel ratio entrained during the oxidation chemical processes, partial or incomplete combustion in a diesel engine is measured by the production of carbon monoxide (CO). The creation of CO emissions is primarily impacted by various factors such as the air-fuel equivalency ratio, fuel quality, and timing of injection, fuel injection parameters, and combustion chamber

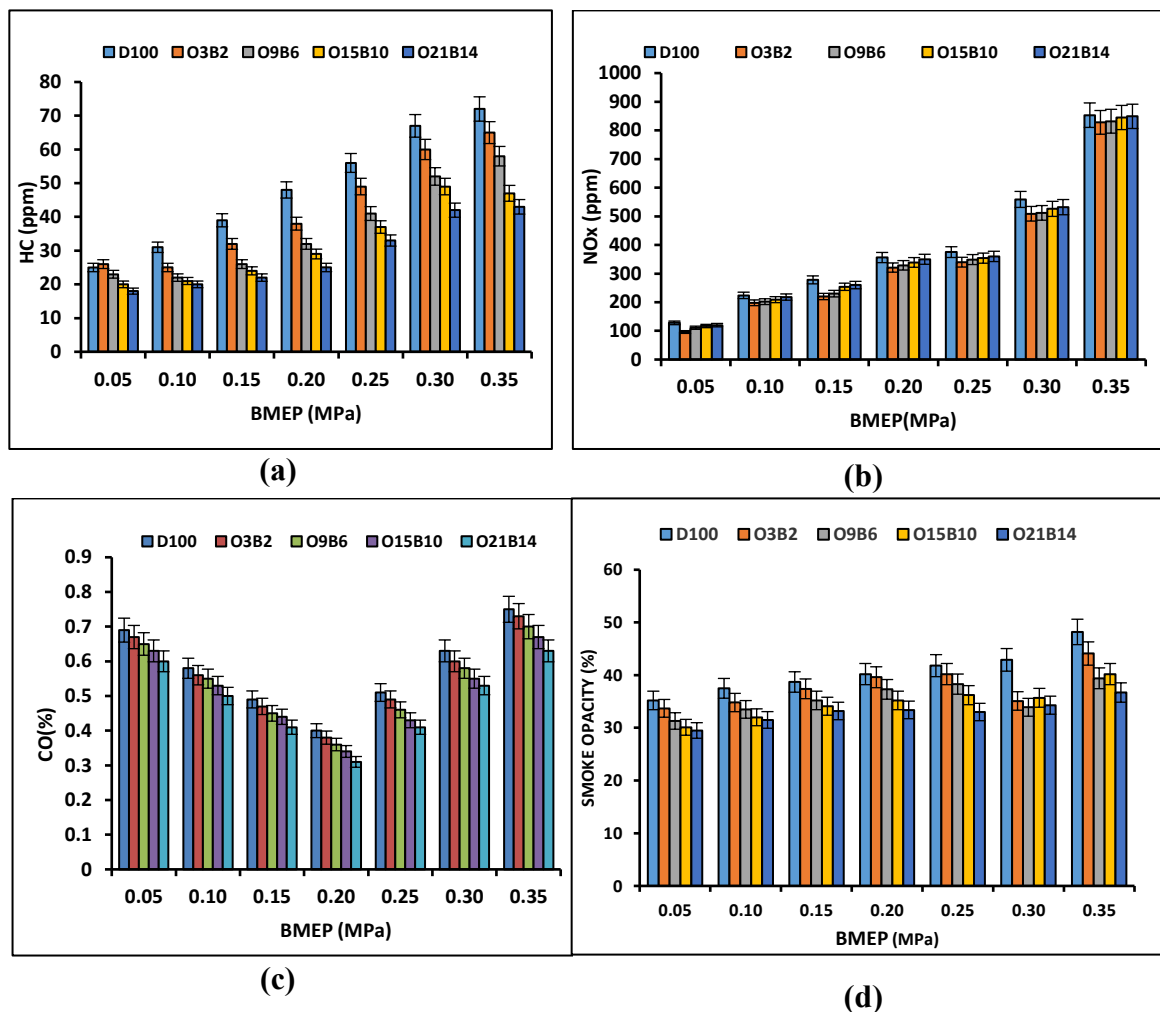


Figure 4.20 Variation of emission parameter with BMEP

design, among many others[274], [275]. The CO vs. BMEP graph for different fuel blends is shown in Figure 4.20 (c). The trend in the figure shows that with the increase in BMEP, the CO emissions firstly decrease and then increases. Also, with the increase in the concentration of orange peel oil in the fuel blends, a decreasing trend of CO is observed at a particular BMEP. As seen from the figure, the CO

emission has reduced by 2.66% for O3B2, 6.66% for O9B6, 10.66% for O15B10, and 16.00% for O21B15 respectively as compared to neat diesel at full load. The decreasing trend for CO emissions for different fuel blends is due to the presence of orange peel oil which is an antioxidant additive[276].

#### **4.10.4 Emissions of smoke opacity**

The smoke formation, in general, can be correlated with the formation of CO and HC emissions for all biofuels. The smoke vs. BMEP graph for different fuels blends is shown in Figure 4.20 (d). The trend in the figure shows that with the increase in BMEP, there is a slight increase in smoke emissions. Also, with the increase in the concentration of orange peel oil in the fuel blends, the decreasing trend of smoke is observed at a particular BMEP. As seen from the figure, the smoke emission has reduced by 9.72% for O3B2, 19.44% for O9B6, 34.72% for O15B10, and 40.27% for O21B15 respectively as compared to neat diesel at full load. The decreasing trend is due to the presence of orange peel oil in the fuel blends which is an antioxidant additive that improves the combustion process[276]. Also, as the viscosity and boiling point of the orange peel oil is relatively lower, its increasing concentration in the fuel blends enhances the atomization that leads to finer droplet size and faster evaporation inside the cylinder, thus causes the complete combustion process. This, overall, resulted in the lower smoke formation.

#### **4.11 Combustion Characteristics**

The conventional diesel engine is a type of heat engine that converts one form of energy into another. Hydrocarbons, which are found in fuel, are an excellent source of chemical energy. This energy is then transformed into heat energy by the combustion chamber. During the process of combustion, the fuel reacts with atmospheric oxygen resulting in the production of nitrogen CO<sub>2</sub>, H<sub>2</sub>O, in theory. However, the actual combustion process is more complex than the simple chemical reaction. The fuel's

properties during combustion determine the amount of heat energy that is released. Mass fuel burn and a piezo pressure sensor installed in the engine cylinder head can be used to analyze the temperature and pressure increases caused by the heat energy produced during combustion.

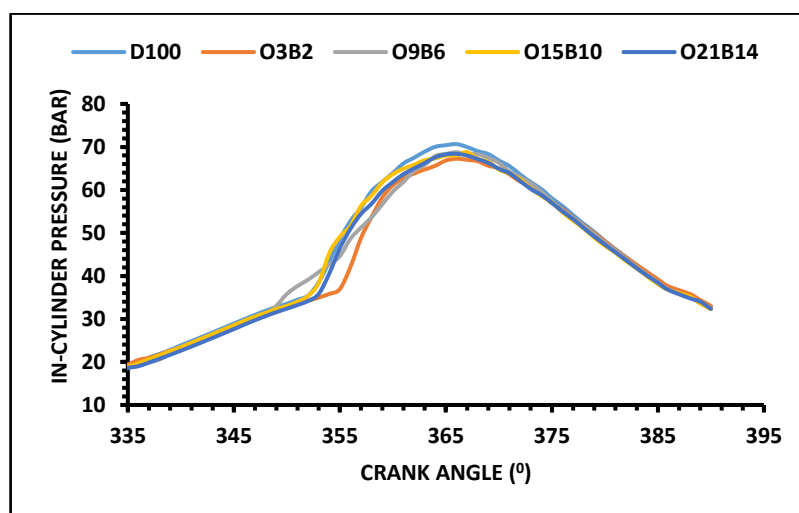


Figure 4.21 Variation of P- $\Theta$

Chapter 3 outlines a procedure that measures the change in inside cylinder pressure as the engine's crank angle rotates. This procedure helps determine the engine's combustion characteristics based solely on the inside cylinder pressure. The data collected from this procedure can then be used to analyze other parameters, such as heat release rate, rate of pressure rise, cumulative heat release, and mass fraction burned. The pressure inside the cylinder is largely determined by the engine's hardware design and the combustion properties of the fuel, which are influenced by factors such as calorific value, viscosity, cetane index, flash point temperature, etc. This section provides a detailed explanation of every aspect of the engine and fuel's combustion process.

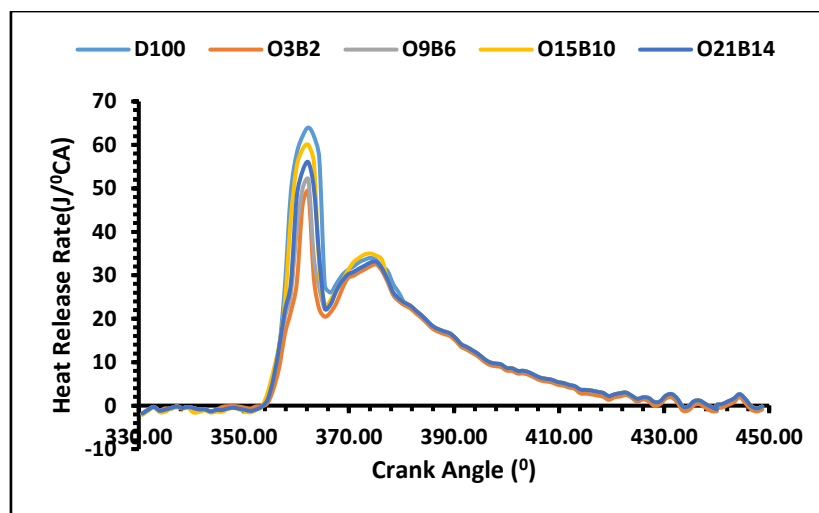


Figure 4.22 Heat release rate (HRR) with crank angle

#### 4.11.1 Inside Cylinder Pressure

When an engine is in operation, the internal cylinder pressure changes continuously. There are two primary reasons behind this change in pressure: the movement of the piston and the burning of fuel during the power stroke. While the change in internal cylinder pressure caused by fuel combustion is more intricate and results in a much shorter pressure rise, the change in internal cylinder pressure caused by piston movement can be calculated using a simple thermodynamic process. To analyze the impact of fuel combustion on internal cylinder pressure, a single piezoelectric instrument was installed in the cylinder head and synchronized with a PC through a data acquisition device. Thermodynamic properties can be observed to analyze fuel combustion. To analyze the combustion properties, these attributes were measured in this case.

Figure 4.21 displays the variation in the fuel blend's cylinder pressure in relation to crank angle at maximum engine load. The diesel fuel engine's peak in-cylinder pressure was found to be higher than that of diesel. The blends' increased viscosity causes a longer ignition delay overall even though it also slows down mixing, increases penetration, decreases the cone angle, and hinders the quality of atomization. The peak pressure was noticed for D100 was 70.22 bar among all test

fuels owing to higher CV. The other fuels O3B2, O9B6, O15B10 and O21B14 were 66.35, 67.56, 67.78 and 68.48 bar respectively.

The proportion of n-butanol in the mixture of diesel, orange peel oil, and WCO biodiesel reduces the blend's cetane index, calorific value, and viscosity as well as the peak inside cylinder pressure because it has a significantly lower cetane index and CV than any of the parent fuels. But because blend O21B14 had a higher ID and less viscosity than blends O15B10, O9B6, and O3B2, it burned with greater effectiveness. Sahoo and Das [286], Rakopoulos et al. [287], and Nour et al. [259] observed similar trends.

#### **4.11.2 Heat release rate (HRR)**

The combustion chamber's internal fuel burning physiognomies are displayed by the HRR per degree crank angle (CA) under the given conditions. The majority of the heat is discovered to be released approximately  $10^\circ$  of crank displacement following the commencement of combustion. This section presents the results for full load, but the HRR of different test fuels in a stationary engine running at constant speed is analyzed for all loading conditions. Additionally, as more fuel is added to meet the energy requirement that is discussed in this section, HRR increases with an increase in load and is found to be extreme at full load conditions.

As was previously mentioned, the engine's speed was kept constant at 1500 rpm under all loading circumstances, making it simple to analyze the HRR for different fuels at maximum load. The HRR is calculated using data obtained from internal cylinder pressure measurements. Chapter 3 already provides an explanation of the procedures and formulas used to compute HRR.

The study concludes that a higher peak pressure leads to a developed HRR for that fuel. Higher absolute pressure attained as a result of the fuel burning quickly and in large quantities. Therefore, a higher heat release rate at that time is caused by the

sudden combustion of a larger volume of fuel at a shorter crank angle rotation. Figure 4.22 shows the heat release rate for each tested fuel at maximum capacity. Calculating the HRR for each crank angle rotation

Due to the extra fuel evaporating during the delay period and heat transfer cooling the engine cylinder wall when combustion is initiated, there was a negative heat release at the beginning of the graph. However, as time passed, the heat release eventually became a positive value. All blends have a slightly lower maximum heat release than diesel due to their lower CN. This causes a delay period that is mainly felt in the later stages of incineration. [267] Due to a greater CV, mineral diesel fuel had the highest HRR of all test fuels, measuring  $62.22 \text{ J/}^\circ\text{CA}$ . The peak heat release rate of O3B2, O9B6, O15B10 and O21B14 was  $51.14 \text{ J/}^\circ\text{CA}$ ,  $55.95 \text{ J/}^\circ\text{CA}$ ,  $56.38 \text{ J/}^\circ\text{CA}$ ,  $60.12 \text{ J/}^\circ\text{CA}$  respectively. It is perceived, blending of orange peel oil and n-butanol increases HRR of blends however, the presence of orange peel oil impacts more on the heat release rate. Fuel blends with a proportion of orange peel oil added have better combustion characteristics, burning a lot of fuel in less time. Although n-butanol has a similar effect to orange peel oil, it has a much lower density and calorific value. Greater kinematic viscosity and density lead to slower combustion, atomization rate reduction, and heat release rate decrease. These results are comparable to those of Nantha gopal et al. [268].

## CHAPTER 5

# CONCLUSIONS AND FUTURE SCOPE

---

### 5.1. Conclusions:

The aim of the study was to minimize the usage of fossil fuel (diesel) in an unmodified CI engine. The aim was achieved by blending of orange peel oil, used cooking oil biodiesel and n-butanol. The utilization of above mentioned elements served the following purposes and result:

1. The environmental/ground pollution can be reduced by preparing the biodiesel of used cooking oil.
2. Derived the clean and sustainable solution and minimized the usage of diesel.
3. To achieve the optimized production and properties of waste cooking oil, Response surface methodology tool was used. During the process optimization the RSM contained 5 process parameters.
4. Production yield was found 98.95% by weight keeping the process parameter molar ratio, catalyst concentration; reaction temperature and reaction time were 6.2 methanol to oil, 0.95 g/lit, 64.1<sup>0</sup>C, and 75.2 min respectively at 730 RPM agitation speed.
5. Optimized results for biodiesel quality parameters calorific value and Kinematic viscosity were found 45.68 MJ/kg and 5.48 cSt at the above said input parameters.
6. Biodiesel another working properties (Pour point and flash point) were also found -2.12 <sup>0</sup>C and 169.25 <sup>0</sup>C at RSM optimized process parameters for biodiesel production.



7. The RSM model optimizer noticed an error percentage ranging from 1 to 7% when compared to the projected value, indicating the correctness of the model. The outcomes show that every fuel property was much enhanced and met ASTM requirements.
8. Every response regression model that was generated was deemed statistically significant at 95% confidence level.
9. In comparison to baseline diesel, the BTE for O3B2, O9B6, O15B10, and O21B14 are 21.99, 22.09%, 22.31%, and 22.49%, respectively.
10. All of the quaternary blends have BSEC values that are lower than those of pure diesel, and these values drop as the blends' content of orange peel oil rises. This is as a result of the fuel mixes' incorporation of less viscous fuel, which lowers the BSEC.
11. It becomes apparent that the NO<sub>x</sub> emissions of all quaternary blends are lower than those of pure diesel and that they reach as the blends' concentration of orange peel oil increases. This is due to the fact that adding orange peel oil lowers the fuel blends' overall cetane index, which expands the ignition delay period.
12. HC, CO, and smoke opacity of all the quaternary blends is observed lower than pure diesel and decreases with an increase in orange peel oil concentration in the blends.
13. The test fuel blends O3B2, O9B6, O15B10 and O21B14 were showing the in-cylinder pressure of 66.35, 67.56, 67.78 and 68.48 bar respectively.
14. The peak heat release rate of O3B2, O9B6, O15B10 and O21B14 was 51.14J/<sup>0</sup>CA, 55.95J/<sup>0</sup>CA, 56.38 J/<sup>0</sup>CA, 60.12J/<sup>0</sup>CA respectively.

## 5.2. Future scope

1. In summary, the utilization of orange peel oil in blends comprising diesel, biodiesel, alcohols, and vegetable oil can serve as a substitute for diesel fuel while enhancing engine performance, emission and combustion characteristics.
2. The Spraytec apparatus was used to do the spray analysis. Researchers in the future can also use the computational fluid dynamics technique to predict the fuel sample's spray and compare the results with those from experiments.
3. Software such as ANSYS offers multi-dimensional models for studying combustion characteristics, which can be verified by experimental outcomes.
4. To investigate the fuels' environmental sustainability, life cycle analysis can be done.

The primary goal of this research is to determine which vegetable oil—orange peel oil—is best suited for use in quaternary mixes. Before adding orange peel oil as an ingredient to blends, more research is needed in the areas of manufacturing and stability.

## REFERENCES

---

- [1] K. W. Alt, A. Al-Ahmad, and J. P. Woelber, "Nutrition and Health in Human Evolution–Past to Present," *Nutrients*, vol. 14, no. 17, p. 3594, 2022.
- [2] S. R. James *et al.*, "Hominid use of fire in the Lower and Middle Pleistocene: A review of the evidence [and comments and replies]," *Curr. Anthropol.*, vol. 30, no. 1, pp. 1–26, 1989.
- [3] R. Lewin, *Human evolution: an illustrated introduction*. John Wiley & Sons, 2004.
- [4] J. Wenzel and P. Yaeger, *Fueling Culture: 101 Words for Energy and Environment*. Fordham Univ Press, 2017.
- [5] T. Brosch, D. Sander, and M. K. Patel, *Understanding the Human Factor of the Energy Transition: Mechanisms Underlying Energy-Relevant Decisions and Behaviors*. Frontiers Media SA, 2016.
- [6] P. N. Stearns, *The industrial revolution in world history*. Routledge, 2020.
- [7] J. M. Marchetti *et al.*, "Density, flash point and heating value variations of corn oil biodiesel-diesel fuel blends," *Fuel*, vol. 36, no. 9, p. 120218, 2016, doi: 10.1016/j.enconman.2016.02.034.
- [8] P. Johnstone and C. McLeish, "World wars and the age of oil: Exploring directionality in deep energy transitions," *Energy Res. Soc. Sci.*, vol. 69, p. 101732, 2020.
- [9] T. H. Mehedi, E. Gemechu, and A. Kumar, "Life cycle greenhouse gas emissions and energy footprints of utility-scale solar energy systems," *Appl. Energy*, vol. 314, p. 118918, 2022.

- [10] P. Nowak, K. Kucharska, and M. Kamiński, “Ecological and health effects of lubricant oils emitted into the environment,” *Int. J. Environ. Res. Public Health*, vol. 16, no. 16, p. 3002, 2019.
- [11] D. Gielen, F. Boshell, D. Saygin, M. D. Bazilian, N. Wagner, and R. Gorini, “The role of renewable energy in the global energy transformation,” *Energy Strateg. Rev.*, vol. 24, pp. 38–50, 2019.
- [12] L. S. Zangerolame Taroco and A. C. Sabbá Colares, “The un framework convention on climate change and the Paris agreement: Challenges of the conference of the parties,” *Prolegómenos*, vol. 22, no. 43, pp. 125–135, 2019.
- [13] “IPCC — Intergovernmental Panel on Climate Change.” <https://www.ipcc.ch>.
- [14] V. P. Oktyabrskiy, “A new opinion of the greenhouse effect,” *St. Petersburg. Polytech. Univ. J. Phys. Math.*, vol. 2, no. 2, pp. 124–126, 2016.
- [15] “IPCC — Intergovernmental Panel on Climate Change.” .
- [16] S. O. Gardarsdottir, “LowEmission Annual report 2022,” 2023.
- [17] V. Ortega, “Which countries are the world’s biggest carbon polluters? Climate Trade.” 2021.
- [18] S. Manikandan, R. Subbaiya, M. Biruntha, R. Y. Krishnan, G. Muthusamy, and N. Karmegam, “Recent development patterns, utilization and prospective of biofuel production: Emerging nanotechnological intervention for environmental sustainability—A review,” *Fuel*, vol. 314, p. 122757, 2022.
- [19] B. Bharathiraja, J. Jayamuthunagai, and R. P. Kumar, *BIOFUELS: A Promising Alternate for Next Generation Fuels*. MJP Publisher, 2019.
- [20] I. Ballesteros, M. Ballesteros, P. Manzanares, M. J. Negro, J. M. Oliva, and F.

- Sáez, “Dilute sulfuric acid pretreatment of cardoon for ethanol production,” *Biochem. Eng. J.*, vol. 42, no. 1, pp. 84–91, 2008.
- [21] A. Demirbas, A. Bafail, W. Ahmad, and M. Sheikh, “Biodiesel production from non-edible plant oils,” *Energy Explor. Exploit.*, vol. 34, no. 2, pp. 290–318, 2016.
- [22] S. Pinzi, I. L. Garcia, F. J. Lopez-Gimenez, M. D. Luque de Castro, G. Dorado, and M. P. Dorado, “The ideal vegetable oil-based biodiesel composition: a review of social, economical and technical implications,” *Energy & Fuels*, vol. 23, no. 5, pp. 2325–2341, 2009.
- [23] I. M. Atadashi, M. K. Aroua, and A. A. Aziz, “High quality biodiesel and its diesel engine application: a review,” *Renew. Sustain. energy Rev.*, vol. 14, no. 7, pp. 1999–2008, 2010.
- [24] A. Skaib and R. Zedan, “Bioenergy: Socio-Economic and Environmental Implications and Future of Biofuels,” *African J. Adv. Pure Appl. Sci.*, pp. 19–35, 2023.
- [25] A. K. Agarwal, “Biofuels (alcohols and biodiesel) applications as fuels for internal combustion engines,” *Prog. energy Combust. Sci.*, vol. 33, no. 3, pp. 233–271, 2007.
- [26] D. Singh, D. Sharma, S. L. Soni, S. Sharma, and D. Kumari, “Chemical compositions, properties, and standards for different generation biodiesels: A review,” *Fuel*, vol. 253, pp. 60–71, 2019.
- [27] M. Ahmad, M. A. Khan, M. Zafar, and S. Sultana, *Practical handbook on biodiesel production and properties*. CRC press, 2012.
- [28] P. Benjumea, J. Agudelo, and A. Agudelo, “Effect of altitude and palm oil

biodiesel fuelling on the performance and combustion characteristics of a HSDI diesel engine,” *Fuel*, vol. 88, no. 4, pp. 725–731, 2009.

- [29] D. Drabik and T. Venus, “EU biofuel policies for road and rail transportation sector,” *EU bioeconomy Econ. policies Vol. II*, pp. 257–276, 2019.
- [30] F. Fernández-Tirado, C. Parra-López, and M. Romero-Gámez, “A multi-criteria sustainability assessment for biodiesel alternatives in Spain: Life cycle assessment normalization and weighting,” *Renew. Energy*, vol. 164, pp. 1195–1203, 2021.
- [31] S.-Y. No, *Application of liquid biofuels to internal combustion engines*. Springer Nature, 2020.
- [32] D. Casanave, J. L. Duplan, and E. Freund, “Diesel fuels from biomass,” *Pure Appl. Chem.*, vol. 79, no. 11, pp. 2071–2081, 2007, doi: 10.1351/pac200779112071.
- [33] P. S. Agrawal, P. N. Belkhode, and S. L. Rokhum, *Sustainability in Biofuel Production Technology*. John Wiley & Sons, 2022.
- [34] N. M. Carlson, “OIL MARKETS IN 2020 1 An Analysis of the Global Oil Market in 2020,” 2023.
- [35] L. F. R. Pinto, *A closer look at biodiesel production*. Nova Science Publishers, 2019.
- [36] F. H. Sobrino, C. R. Monroy, and J. L. H. Pérez, “Biofuels and fossil fuels: Life Cycle Analysis (LCA) optimisation through productive resources maximisation,” *Renew. Sustain. Energy Rev.*, vol. 15, no. 6, pp. 2621–2628, 2011.

- [37] S. P. Singh and D. Singh, "Biodiesel production through the use of different sources and characterization of oils and their esters as the substitute of diesel: a review," *Renew. Sustain. energy Rev.*, vol. 14, no. 1, pp. 200–216, 2010.
- [38] A. Demirbas, "Biofuels sources, biofuel policy, biofuel economy and global biofuel projections," *Energy Convers. Manag.*, vol. 49, no. 8, pp. 2106–2116, 2008, doi: 10.1016/j.enconman.2008.02.020.
- [39] D. Kumar, G. Kumar, and C. P. Singh, "Fast, easy ethanolysis of coconut oil for biodiesel production assisted by ultrasonication," *Ultrason. Sonochem.*, vol. 17, no. 3, pp. 555–559, 2010.
- [40] M. Melikoglu, V. Singh, S. Y. Leu, C. Webb, and C. S. K. Lin, "Biochemical production of bioalcohols," *Handb. Biofuels Prod. Process. Technol. Second Ed.*, pp. 237–258, 2016, doi: 10.1016/B978-0-08-100455-5.00009-6.
- [41] S. Majer, F. Mueller-Langer, V. Zeller, and M. Kaltschmitt, "Implications of biodiesel production and utilisation on global climate—a literature review," *Eur. J. lipid Sci. Technol.*, vol. 111, no. 8, pp. 747–762, 2009.
- [42] R. Luque and J. Clark, *Handbook of biofuels production: Processes and technologies*. Elsevier, 2010.
- [43] S. Eiadtrong, K. Maliwan, G. Prateepchaikul, T. Kattiyawan, P. Thephsorn, and T. Leevijit, "Preparation, important fuel properties, and comparative use of un-preheated palm fatty acid distillate-diesel blends in a single cylinder diesel engine," *Renew. Energy*, pp. 1089–1098, 2019, doi: 10.1016/j.renene.2018.09.043.
- [44] J. A. DeMello, C. A. Carmichael, E. E. Peacock, R. K. Nelson, J. S. Arey, and C. M. Reddy, "Biodegradation and environmental behavior of biodiesel

- mixtures in the sea: an initial study,” *Mar. Pollut. Bull.*, vol. 54, no. 7, pp. 894–904, 2007.
- [45] J. C. Pasqualino, D. Montane, and J. Salvado, “Synergic effects of biodiesel in the biodegradability of fossil-derived fuels,” *Biomass and bioenergy*, vol. 30, no. 10, pp. 874–879, 2006.
- [46] K. M. Shereena and T. Thangaraj, “Biodiesel: an alternative fuel produced from vegetable oils by transesterification,” *Electron. J. Biol.*, vol. 5, no. 3, pp. 67–74, 2009.
- [47] O. M. Ali, R. Mamat, N. Abdullah, and A. A. Abdullah, “Importance of palm biodiesel as a transportation fuel in Malaysia,” 2008.
- [48] S. Mishra, A. Chauhan, and K. B. Mishra, “Role of binary and ternary blends of WCO biodiesel on emission reduction in diesel engine,” *Fuel*, vol. 262, no. October, p. 116604, 2020, doi: 10.1016/j.fuel.2019.116604.
- [49] M. T. Pham, N. V. L. Le, H. C. Le, T. H. Truong, and D. N. Cao, “A comprehensive review on the use of biodiesel for diesel engines,” *Int. J. Renew. Energy Dev.*
- [50] M. M. Musthafa, T. A. Kumar, T. Mohanraj, and R. Chandramouli, “A comparative study on performance, combustion and emission characteristics of diesel engine fuelled by biodiesel blends with and without an additive,” *Fuel*, vol. 225, no. February 2017, pp. 343–348, 2018, doi: 10.1016/j.fuel.2018.03.147.
- [51] Z. Ullah, M. A. Bustam, and Z. Man, “Characterization of Waste Palm Cooking Oil for Biodiesel Production,” *Int. J. Chem. Eng. Appl.*, vol. 5, no. 2, pp. 134–137, 2014, doi: 10.7763/ijcea.2014.v5.366.



- [52] G. Knothe and L. F. Razon, “Biodiesel fuels,” *Prog. Energy Combust. Sci.*, vol. 58, pp. 36–59, 2017, doi: 10.1016/j.pecs.2016.08.001.
- [53] F. Pradelle, S. Leal Braga, A. R. Fonseca de Aguiar Martins, F. Turkovics, and R. Nohra Chaar Pradelle, “Experimental assessment of some key physicochemical properties of diesel-biodiesel-ethanol (DBE) blends for use in compression ignition engines,” *Fuel*, vol. 248, no. March, pp. 241–253, 2019, doi: 10.1016/j.fuel.2019.03.087.
- [54] N. A. Amran, U. Bello, and M. S. H. Ruslan, “The role of antioxidants in improving biodiesel’s oxidative stability, poor cold flow properties, and the effects of the duo on engine performance: A review,” *Heliyon*, 2022.
- [55] A. Brown *et al.*, “Advanced biofuels—potential for cost reduction,” *IEA Bioenergy*, vol. 88, pp. 1–3, 2020.
- [56] T. Mizik and G. Gyarmati, “Economic and sustainability of biodiesel production—a systematic literature review,” *Clean Technol.*, vol. 3, no. 1, pp. 19–36, 2021.
- [57] R. K. Mathur *et al.*, “Oilseeds and Oil Palm,” in *Trajectory of 75 years of Indian Agriculture after Independence*, Springer, 2023, pp. 231–264.
- [58] B. A. Alhammad, A. Jamal, C. Carlucci, M. F. Saeed, M. F. Seleiman, and M. F. Pompelli, “Non-Conventional Oilseeds: Unlocking the Global Potential for Sustainable Biofuel Production,” *Catalysts*, vol. 13, no. 9, p. 1263, 2023.
- [59] F. Jamil, “A Review on Biodiesel Production, Analysis, and Emission Characteristics from Non-Edible Feedstocks,” *ChemistrySelect*, vol. 8, no. 31, p. e202300800, 2023.
- [60] N. Khumdemo Ezung *et al.*, “Special Issue on ‘Biodiesel Production Processes

- and Technology,”” *Bioresour. Technol.*, vol. 11, no. 1, p. 384, 2008, [Online].  
Available: [https://kvk.icar.gov.in/API/Content/PPupload/k0660\\_32.pdf](https://kvk.icar.gov.in/API/Content/PPupload/k0660_32.pdf).
- [61] A. E. Atabani, A. S. Silitonga, I. A. Badruddin, T. M. I. Mahlia, H. H. Masjuki, and S. Mekhilef, “A comprehensive review on biodiesel as an alternative energy resource and its characteristics,” *Renew. Sustain. Energy Rev.*, vol. 16, no. 4, pp. 2070–2093, 2012, doi: 10.1016/j.rser.2012.01.003.
- [62] N. Khumdemo Ezung *et al.*, “Special Issue on ‘Biodiesel Production Processes and Technology,’”” *Bioresour. Technol.*, vol. 11, no. 1, p. 384, 2008.
- [63] D. McDowell, C. T. Elliott, and A. Koidis, “Characterization and comparison of UK, Irish, and French cold pressed rapeseed oils with refined rapeseed oils and extra virgin olive oils,” *Eur. J. Lipid Sci. Technol.*, vol. 119, no. 8, p. 1600327, 2017.
- [64] M. Das, M. Sarkar, A. Datta, and A. K. Santra, “Study on viscosity and surface tension properties of biodiesel-diesel blends and their effects on spray parameters for CI engines,” *Fuel*, vol. 220, no. November 2017, pp. 769–779, 2018, doi: 10.1016/j.fuel.2018.02.021.
- [65] S. M. Supriya, V. V Kulkarni, C. N. Ranganatha, and P. G. Suresha, “Quantitative analysis of oil yield and its Components in newly developed hybrids of sunflower (*Helianthus annuus* L.),” *Int. J. Curr. Microbiol. Appl. Sci.*, vol. 6, no. 8, pp. 3088–3098, 2017.
- [66] R. Sakthivel, K. Ramesh, R. Purnachandran, and P. Mohamed Shameer, “A review on the properties, performance and emission aspects of the third generation biodiesels,” *Renew. Sustain. Energy Rev.*, vol. 82, no. November, pp. 2970–2992, 2018, doi: 10.1016/j.rser.2017.10.037.

- [67] C. Dueso *et al.*, “Performance and emissions of a diesel engine using sunflower biodiesel with a renewable antioxidant additive from bio-oil,” *Fuel*, vol. 234, no. May 2017, pp. 276–285, 2018, doi: 10.1016/j.fuel.2018.07.013.
- [68] R. Gautam and N. Kumar, “Comparative study of performance and emission characteristics of Jatropha alkyl ester/butanol/diesel blends in a small capacity CI engine,” *Biofuels*, vol. 6, no. 3–4, pp. 179–190, 2015, doi: 10.1080/17597269.2015.1068081.
- [69] V. Amol and K. R. Bhati, “Nutritive Benefits of Soybean (Glycine max),” *Indian J. Nutr. Diet.*, pp. 522–533, 2021.
- [70] H. Yerrennagoudaru, K. Manjunatha, K. R. Vijaya Kumar, and M. Dodda Basavanagouda, ““investigation and assessment of performance and emissions of an IC engine fuelled with diesel and different bio-fuels blended with Ethanol,”” *Mater. Today Proc.*, vol. 5, no. 2, pp. 6238–6246, 2018, doi: 10.1016/j.matpr.2017.12.233.
- [71] C. Engineering, “Binary blends of petrodiesel with biodiesels derived from soyabean and groundnut oils Auwal Aliyu , Oche Adoyi and Abdulhamid Hamza \* Pelagia Research Library Abdulhamid Hamza et al Pelagia Research Library,” vol. 3, no. 1, pp. 611–614, 2012.
- [72] A. Hira and D. Das, “Performance and emission evaluation of diesel engine fuelled with biodiesel produced from high free fatty acid crude soyabean oil,” *Biofuels*, vol. 7, no. 4, pp. 413–421, 2016, doi: 10.1080/17597269.2016.1147920.
- [73] B. P. Mshelmbula, S. Hashimu, T. P. Terna, and S. T. Akinyosowe, “Comparative growth and yield responses of improved and local varieties of

- soybean (*Glycine max* (L.) Merrill) in Lafia, Nasarawa State,” *Ilorin J. Sci.*, vol. 10, no. 1, pp. 19–27, 2023.
- [74] S. Sumangala and U. N. Kulkarni, “Acceptable qualities of black soybean genotypes (*Glycine max*),” *Pharm Innov*, vol. 8, pp. 1125–1128, 2019.
- [75] N. Guzeler and C. Yildirim, “The utilization and processing of soybean and soybean products,” *J. Agric. Fac. Uludag Univ*, vol. 30, pp. 546–553, 2016.
- [76] W. H. Foo, W. Y. Chia, D. Y. Y. Tang, S. S. N. Koay, S. S. Lim, and K. W. Chew, “The conundrum of waste cooking oil: Transforming hazard into energy,” *J. Hazard. Mater.*, vol. 417, p. 126129, 2021.
- [77] M. Hajjari, M. Tabatabaei, M. Aghbashlo, and H. Ghanavati, “A review on the prospects of sustainable biodiesel production: A global scenario with an emphasis on waste-oil biodiesel utilization,” *Renew. Sustain. Energy Rev.*, vol. 72, no. October 2015, pp. 445–464, 2017, doi: 10.1016/j.rser.2017.01.034.
- [78] K. Ferdous, A. Deb, J. Ferdous, R. Uddin, M. R. Khan, and M. A. Islam, “Preparation of Biodiesel from Higher FFA Containing Castor Oil,” *Int. J. Sci. Eng. Res.*, vol. 4, no. 12, 2013, [Online]. Available: <http://www.ijser.org>.
- [79] L. B. Moyo, S. E. Iyuke, R. F. Muvhiiwa, G. S. Simate, and N. Hlabangana, “Application of response surface methodology for optimization of biodiesel production parameters from waste cooking oil using a membrane reactor,” *South African J. Chem. Eng.*, vol. 35, no. July 2019, pp. 1–7, 2021, doi: 10.1016/j.sajce.2020.10.002.
- [80] H. Palüzar, “Production of High Quality Biodiesel from Sunflower Acid Oil Obtained by Acidulation of Soapstock from Refining Process: Immobilized Pancreatic Lipase for Biodiesel Production,” 2023.

- [81] S. Tamalampudi and H. Fukuda, "Biodiesel," 2011.
- [82] B. Abdi, "India's bio-diesel blending for road transport to remain muted in 2019: US Dept of Agriculture," *Economic times*, 2019.
- [83] A. Rahman, I. W. K. Suryawan, A. Sarwono, N. L. Zahra, and Z. M. Faruqi, "Estimation of biodiesel production from used cooking oil of university cafeteria to support sustainable electricity in Universitas Pertamina," in *IOP Conference Series: Earth and Environmental Science*, 2020, vol. 591, no. 1, p. 12013.
- [84] M. A. F. Vela, J. C. Acevedo-Páez, N. Urbina-Suárez, Y. A. R. Basto, and Á. D. González-Delgado, "Enzymatic transesterification of waste frying oil from local restaurants in east colombia using a combined lipase system," *Appl. Sci.*, vol. 10, no. 10, 2020, doi: 10.3390/app10103566.
- [85] T. Tsoutsos *et al.*, "Quality Characteristics of Biodiesel Produced from Used Cooking Oil in Southern Europe," *ChemEngineering*, vol. 3, no. 1, p. 19, 2019, doi: 10.3390/chemengineering3010019.
- [86] M. Banja, R. Sikkema, M. Jégard, V. Motola, and J.-F. Dallemand, "Biomass for energy in the EU—The support framework," *Energy Policy*, vol. 131, pp. 215–228, 2019.
- [87] N. Kumar and Sidharth, "Some Studies on use of ternary blends of diesel, biodiesel and n-octanol," *Energy Sources, Part A Recover. Util. Environ. Eff.*, vol. 40, no. 14, pp. 1721–1728, 2018, doi: 10.1080/15567036.2018.1486902.
- [88] S. Mishra, A. Chauhan, and K. B. Mishra, "Role of binary and ternary blends of WCO biodiesel on emission reduction in diesel engine," *Fuel*, vol. 262, p. 116604, 2020, doi: <https://doi.org/10.1016/j.fuel.2019.116604>.

- [89] P. Yadav, K. Alivelu, G. D. S. Kumar, and M. Sujatah, . “Survey of per capita consumption of vegetable oil in India. *Current Science.*,” 2022.
- [90] E. Conservation, B. Code, and <http://mospi.nic.in>, “ENERGY STATISTICS 2019 (Twenty Sixth Issue) CENTRAL STATISTICS OFFICE MINISTRY OF STATISTICS AND PROGRAMME IMPLEMENTATION GOVERNMENT OF INDIA NEW DELHI [http://mospi.nic.in/sites/default/files/publication\\_reports/Energy Statistics 2019-final.pdf](http://mospi.nic.in/sites/default/files/publication_reports/Energy%20Statistics%202019-final.pdf),” 2007.
- [91] B. K. Gusamo and M. Jimbudo, “Tree-borne Oilseed Crops: *Jatropha curcas*, *Ricinus communis*, *Anacardium occidentale* and Some Native Trees for Oil Production for Bio-energy Source in Papua New Guinea,” *J. Agric. Environ. Sci.*, vol. 4, no. 2, pp. 113–123, 2015.
- [92] R. Karmakar, K. Kundu, and A. Rajor, “Fuel properties and emission characteristics of biodiesel produced from unused algae grown in India,” *Pet. Sci.*, vol. 15, no. 2, pp. 385–395, 2018, doi: 10.1007/s12182-017-0209-7.
- [93] A. Gnanaprakasam, V. M. Sivakumar, A. Surendhar, M. Thirumarimurugan, and T. Kannadasan, “Recent strategy of biodiesel production from waste cooking oil and process influencing parameters: a review,” *J. Energy*, vol. 2013, 2013.
- [94] M. Balat, “Biodiesel fuel production from vegetable oils via supercritical ethanol transesterification,” *Energy Sources, Part A Recover. Util. Environ. Eff.*, vol. 30, no. 5, pp. 429–440, 2008.
- [95] F. Ataya, M. A. Dube, and M. Ternan, “Single-phase and two-phase base-catalyzed transesterification of canola oil to fatty acid methyl esters at ambient

- conditions,” *Ind. Eng. Chem. Res.*, vol. 45, no. 15, pp. 5411–5417, 2006.
- [96] M. S. M. Zaharin, N. R. Abdullah, G. Najafi, H. Sharudin, and T. Yusaf, “Effects of physicochemical properties of biodiesel fuel blends with alcohol on diesel engine performance and exhaust emissions: A review,” *Renew. Sustain. Energy Rev.*, vol. 79, no. May, pp. 475–493, 2017, doi: 10.1016/j.rser.2017.05.035.
- [97] Z. Mustapić, T. Krička, and Z. Stanić, “Biodiesel as alternative engine fuel,” *J. Energy-Energija*, vol. 55, no. 6, pp. 634–657, 2006.
- [98] R. Niculescu, A. Clenci, and V. Iorga-Siman, “Review on the use of diesel-biodiesel-alcohol blends in compression ignition engines,” *Energies*, vol. 12, no. 7, pp. 1–41, 2019, doi: 10.3390/en12071194.
- [99] S. N. Gebremariam and J. M. Marchetti, “Economics of biodiesel production: Review,” *Energy Convers. Manag.*, vol. 168, no. May, pp. 74–84, 2018, doi: 10.1016/j.enconman.2018.05.002.
- [100] M. Salaheldeen, A. A. Mariod, M. K. Aroua, S. M. A. Rahman, M. E. M. Soudagar, and I. M. R. Fattah, “Current state and perspectives on transesterification of tri-glycerides for biodiesel production,” *Catalysts*, vol. 11, no. 9, p. 1121, 2021.
- [101] R. L. Patel and C. D. Sankhavara, “Biodiesel production from Karanja oil and its use in diesel engine: A review,” *Renew. Sustain. Energy Rev.*, vol. 71, no. December 2016, pp. 464–474, 2017, doi: 10.1016/j.rser.2016.12.075.
- [102] A. Goyal, B. Tanwar, M. K. Sihag, V. Kumar, V. Sharma, and S. Soni, “Rapeseed/canola (*Brassica napus*) seed,” *Oilseeds Heal. Attrib. Food Appl.*, pp. 47–71, 2021.

- [103] S. C. M. Dos Reis, E. R. Lachter, R. S. V Nascimento, J. A. Rodrigues, and M. G. Reid, "Transesterification of Brazilian vegetable oils with methanol over ion-exchange resins," *J. Am. Oil Chem. Soc.*, vol. 82, pp. 661–665, 2005.
- [104] M. A. Bashir, S. Wu, J. Zhu, A. Krosuri, M. U. Khan, and R. J. N. Aka, "Recent development of advanced processing technologies for biodiesel production: A critical review," *Fuel Process. Technol.*, vol. 227, p. 107120, 2022.
- [105] Sahar *et al.*, "Biodiesel production from waste cooking oil: An efficient technique to convert waste into biodiesel," *Sustain. Cities Soc.*, vol. 41, no. May, pp. 220–226, 2018, doi: 10.1016/j.scs.2018.05.037.
- [106] A. Raheem, P. Prinsen, A. K. Vuppalladiyam, M. Zhao, and R. Luque, "A review on sustainable microalgae based biofuel and bioenergy production: Recent developments," *J. Clean. Prod.*, vol. 181, pp. 42–59, 2018.
- [107] A. Paul, R. Panua, and D. Debroy, "An experimental study of combustion, performance, exergy and emission characteristics of a CI engine fueled by Diesel-ethanol-biodiesel blends," *Energy*, vol. 141, pp. 839–852, 2017, doi: 10.1016/j.energy.2017.09.137.
- [108] E. Lotero, Y. Liu, D. E. Lopez, K. Suwannakarn, D. A. Bruce, and J. G. Goodwin, "Synthesis of biodiesel via acid catalysis," *Ind. Eng. Chem. Res.*, vol. 44, no. 14, pp. 5353–5363, 2005.
- [109] C. S. MacLeod, A. P. Harvey, A. F. Lee, and K. Wilson, "Evaluation of the activity and stability of alkali-doped metal oxide catalysts for application to an intensified method of biodiesel production," *Chem. Eng. J.*, vol. 135, no. 1–2, pp. 63–70, 2008.



- [110] J. Gaidukevič *et al.*, “Modified graphene-based materials as effective catalysts for transesterification of rapeseed oil to biodiesel fuel,” *Chinese J. Catal.*, vol. 39, no. 10, pp. 1633–1645, 2018.
- [111] I. Gaide, V. Makareviciene, E. Sendzikiene, and K. Kazancev, “Natural rocks–heterogeneous catalysts for oil transesterification in biodiesel synthesis,” *Catalysts*, vol. 11, no. 3, p. 384, 2021.
- [112] G. Arzamendi, E. Arguinarena, I. Campo, S. Zabala, and L. M. Gandía, “Alkaline and alkaline-earth metals compounds as catalysts for the methanolysis of sunflower oil,” *Catal. Today*, vol. 133, pp. 305–313, 2008.
- [113] C. C. Enweremadu and M. M. Mbarawa, “Technical aspects of production and analysis of biodiesel from used cooking oil-A review,” *Renew. Sustain. Energy Rev.*, vol. 13, no. 9, pp. 2205–2224, 2009, doi: 10.1016/j.rser.2009.06.007.
- [114] F. Moazeni, Y. C. Chen, and G. Zhang, “Enzymatic transesterification for biodiesel production from used cooking oil, a review,” *J. Clean. Prod.*, vol. 216, pp. 117–128, 2019, doi: 10.1016/j.jclepro.2019.01.181.
- [115] F. Su, G.-L. Li, Y.-L. Fan, and Y.-J. Yan, “Enhancing biodiesel production via a synergic effect between immobilized *Rhizopus oryzae* lipase and Novozym 435,” *Fuel Process. Technol.*, vol. 137, pp. 298–304, 2015.
- [116] S. H. U. Qing, T. Guo-qiang, L. I. U. Feng-sheng, Z. O. U. Wen-qiang, and H. E. Jiang-fan, “Preparation and application of a novel Brönsted-Lewis acid catalyst LaPW 12 O 40/SiO 2 for the synthesis of biodiesel via esterification reaction,” *燃料化学学报 (中英文)*, vol. 45, no. 8, pp. 939–949, 2017.
- [117] L. Li, W. Du, D. Liu, L. Wang, and Z. Li, “Lipase-catalyzed transesterification

- of rapeseed oils for biodiesel production with a novel organic solvent as the reaction medium,” *J. Mol. Catal. B Enzym.*, vol. 43, no. 1–4, pp. 58–62, 2006.
- [118] G.-T. Jeong and D.-H. Park, “Lipase-catalyzed transesterification of rapeseed oil for biodiesel production with tert-butanol,” in *Biotechnology for Fuels and Chemicals: Proceedings of the Twenty-Ninth Symposium on Biotechnology for Fuels and Chemicals Held April 29–May 2, 2007, in Denver, Colorado, 2008*, pp. 649–657.
- [119] Y. Ying, P. Shao, S. Jiang, and P. Sun, “Artificial neural network analysis of immobilized lipase catalyzed synthesis of biodiesel from rapeseed soapstock,” in *International Conference on Computer and Computing Technologies in Agriculture*, 2008, pp. 1239–1249.
- [120] R. Tomaszewski, “A comparative study of citations to chemical encyclopedias in scholarly articles: Kirk-Othmer Encyclopedia of Chemical Technology and Ullmann’s Encyclopedia of Industrial Chemistry,” *Scientometrics*, vol. 117, no. 1, pp. 175–189, 2018.
- [121] R. Alenezi and B. AL-ANZI33, “Kinetic mechanism of transesterification of vegetable oil with supercritical methanol for Biodiesel production,” *J. Eng. Res.*, vol. 1, pp. 81–96, 2013.
- [122] A. Mathew and K. Anand, “Comparison of engine characteristics with biodiesels produced from fresh and waste cooking oils,” *Biofuels*, vol. 0, no. 0, pp. 1–9, 2018, doi: 10.1080/17597269.2018.1519761.
- [123] A. A. Shunaia and A. A. Jazie, “Applications of Super Critical Technology in Biodiesel Production,” in *IOP Conference Series: Earth and Environmental Science*, 2023, vol. 1232, no. 1, p. 12011.

- [124] M. Muszyński, J. Nowicki, M. Zygałło, and G. Dudek, “Comparision of Catalyst Effectiveness in Different Chemical Depolymerization Methods of Poly (ethylene terephthalate),” *Molecules*, vol. 28, no. 17, p. 6385, 2023.
- [125] J.-Z. Yin, Z. Ma, D.-P. Hu, Z.-L. Xiu, and T.-H. Wang, “Biodiesel production from subcritical methanol transesterification of soybean oil with sodium silicate,” *Energy & fuels*, vol. 24, no. 5, pp. 3179–3182, 2010.
- [126] K. N. P. Rani, T. S. V. R. Neeharika, T. P. Kumar, B. Satyavathi, and C. Sailu, “Kinetics of non-catalytic esterification of free fatty acids present in Jatropha oil,” *J. Oleo Sci.*, vol. 65, no. 5, pp. 441–445, 2016.
- [127] J. H. Ng, S. K. Leong, S. S. Lam, F. N. Ani, and C. T. Chong, “Microwave-assisted and carbonaceous catalytic pyrolysis of crude glycerol from biodiesel waste for energy production,” *Energy Convers. Manag.*, vol. 143, pp. 399–409, 2017, doi: 10.1016/j.enconman.2017.04.024.
- [128] A. Kumar, Y. Kuang, Z. Liang, and X. Sun, “Microwave chemistry, recent advancements, and eco-friendly microwave-assisted synthesis of nanoarchitectures and their applications: A review,” *Mater. Today Nano*, vol. 11, p. 100076, 2020.
- [129] S. Głowniak, B. Szczęśniak, J. Choma, and M. Jaroniec, “Advances in microwave synthesis of nanoporous materials,” *Adv. Mater.*, vol. 33, no. 48, p. 2103477, 2021.
- [130] C. A. R. Melo-Junior *et al.*, “Use of microwave irradiation in the noncatalytic esterification of C18 fatty acids,” *Energy & Fuels*, vol. 23, no. 1, pp. 580–585, 2009.
- [131] S. N. Nayak, C. P. Bhasin, and M. G. Nayak, “A review on microwave-assisted

- transesterification processes using various catalytic and non-catalytic systems,” *Renew. Energy*, vol. 143, pp. 1366–1387, 2019.
- [132] J. Hernando, P. Leton, M. P. Matia, J. L. Novella, and J. Alvarez-Builla, “Biodiesel and FAME synthesis assisted by microwaves: homogeneous batch and flow processes,” *Fuel*, vol. 86, no. 10–11, pp. 1641–1644, 2007.
- [133] K.-S. Chen, Y.-C. Lin, K.-H. Hsu, and H.-K. Wang, “Improving biodiesel yields from waste cooking oil by using sodium methoxide and a microwave heating system,” *Energy*, vol. 38, no. 1, pp. 151–156, 2012.
- [134] W. Saputro *et al.*, “Availability of Palm Oil Biodiesel in Indonesia and Its Effect on Diesel Engine: A Review,” *BIOMEJ*, vol. 1, no. 2, pp. 33–43, 2021.
- [135] R. P. SA and K. V Suresh, “Pongamia Pinnata (karanja) Biodiesel as an Alternative fuel for Diesel Engine: A Review,” 2014.
- [136] G. Guan, N. Sakurai, and K. Kusakabe, “Synthesis of biodiesel from sunflower oil at room temperature in the presence of various cosolvents,” *Chem. Eng. J.*, vol. 146, no. 2, pp. 302–306, 2009.
- [137] A. Abbaszaadeh, B. Ghobadian, M. R. Omidkhah, and G. Najafi, “Current biodiesel production technologies: A comparative review,” *Energy Convers. Manag.*, vol. 63, pp. 138–148, 2012.
- [138] G. Chatel and J. C. Colmenares, “Sonochemistry: from basic principles to innovative applications,” *Top. Curr. Chem.*, vol. 375, pp. 1–4, 2017.
- [139] J. B. Zimmerman, P. T. Anastas, H. C. Erythropel, and W. Leitner, “Designing for a green chemistry future,” *Science (80-. )*, vol. 367, no. 6476, pp. 397–400, 2020.

- [140] B. G. Pollet and M. Ashokkumar, *Introduction to ultrasound, sonochemistry and sonoelectrochemistry*. Springer Nature, 2019.
- [141] H. Liu, B. Hu, and C. Jin, “Effects of different alcohols additives on solubility of hydrous ethanol/diesel fuel blends,” *Fuel*, vol. 184, pp. 440–448, 2016, doi: 10.1016/j.fuel.2016.07.037.
- [142] K. S. Suslick and L. A. Crum, “THE HANDBOOK OF ACOUSTICS Chapter 26: Sonochemistry and Sonoluminescence.”
- [143] K. Srilatha, B. L. A. Prabhavathi Devi, N. Lingaiah, R. B. N. Prasad, and P. S. Sai Prasad, “Biodiesel production from used cooking oil by two-step heterogeneous catalyzed process,” *Bioresour. Technol.*, vol. 119, pp. 306–311, 2012, doi: 10.1016/j.biortech.2012.04.098.
- [144] I. M. Atadashi, M. K. Aroua, A. R. A. Aziz, and N. M. N. Sulaiman, “Production of biodiesel using high free fatty acid feedstocks,” *Renew. Sustain. energy Rev.*, vol. 16, no. 5, pp. 3275–3285, 2012.
- [145] E. Pannacci and F. Tei, “Effects of mechanical and chemical methods on weed control, weed seed rain and crop yield in maize, sunflower and soyabean,” *Crop Prot.*, vol. 64, pp. 51–59, 2014.
- [146] P. Cash, T. Stanković, and M. Štorga, “An introduction to experimental design research,” *Exp. Des. Res. Approaches, Perspect. Appl.*, pp. 3–12, 2016.
- [147] S. Balamurugan, D. Seenivasan, R. Rai, and A. Agrawal, “Optimization of biodiesel production process for mixed nonedible oil (processed dairy waste, mahua oil, and castor oil) using response surface methodology,” *Proc. Inst. Mech. Eng. Part E J. Process Mech. Eng.*, p. 09544089221147392, 2022.
- [148] A. Deb, J. Ferdous, K. Ferdous, M. R. Uddin, M. R. Khan, and M. W. Rahman,

- “Prospect of castor oil biodiesel in Bangladesh: Process development and optimization study,” *Int. J. Green Energy*, vol. 14, no. 12, pp. 1063–1072, 2017.
- [149] M. Helmi, K. Tahvildari, A. Hemmati, P. Aberoomand azar, and A. Safekordi, “Phosphomolybdic acid/graphene oxide as novel green catalyst using for biodiesel production from waste cooking oil via electrolysis method: Optimization using with response surface methodology (RSM),” *Fuel*, vol. 287, no. March, p. 119528, 2021, doi: 10.1016/j.fuel.2020.119528.
- [150] K. Thakkar, S. S. Kachhwaha, P. Kodgire, and S. Srinivasan, “Combustion investigation of ternary blend mixture of biodiesel/n-butanol/diesel: CI engine performance and emission control,” *Renew. Sustain. Energy Rev.*, vol. 137, no. February, p. 110468, 2021, doi: 10.1016/j.rser.2020.110468.
- [151] H. S. Pali, N. Kumar, Y. Alhassan, and A. Deep, “Process Optimization of Biodiesel Production from Sal Seed Oil using Response Surface Methodology [RSM] and Diesel,” *SAE Tech. Pap.*, vol. 2015-April, no. April, 2015, doi: 10.4271/2015-01-1297.
- [152] A. M. Dean, M. Morris, J. Stufken, and D. Bingham, *Handbook of design and analysis of experiments*, vol. 7. CRC Press Boca Raton, FL, USA:, 2015.
- [153] H. Singh Pali, A. Sharma, Y. Singh, and N. Kumar, “Sal biodiesel production using Indian abundant forest feedstock,” *Fuel*, vol. 273, no. April, p. 117781, 2020, doi: 10.1016/j.fuel.2020.117781.
- [154] A. I. Khuri and J. A. Cornell, *Response surfaces: designs and analyses*. Routledge, 2018.
- [155] G. Abdulkareem-Alsultan, N. Asikin-Mijan, H. V Lee, U. Rashid, A. Islam,

- and Y. H. Taufiq-Yap, “A review on thermal conversion of plant oil (edible and inedible) into green fuel using carbon-based nanocatalyst,” *Catalysts*, vol. 9, no. 4, p. 350, 2019.
- [156] R. Hernandez *et al.*, “Mississippi State Biodiesel Production Project,” Mississippi State Univ., Starkville, MS (United States), 2008.
- [157] R. G. Dewi *et al.*, “Production of Biodegradable Sulfonated Methyl Ester by a Falling Film Reactor for ASP Flooding in EOR,” *J. Eng. Technol. Sci.*, vol. 53, no. 1, 2021.
- [158] C. Tarhan and M. A. Çil, “A study on hydrogen, the clean energy of the future: Hydrogen storage methods,” *J. Energy Storage*, vol. 40, p. 102676, 2021.
- [159] M. B. Syed, “Technologies for renewable hydrogen production,” in *Bioenergy Resources and Technologies*, Elsevier, 2021, pp. 157–198.
- [160] T. Riis, G. Sandrock, Ø. Ulleberg, and P. J. S. Vie, “Hydrogen storage—gaps and priorities,” *HIA HCG storage Pap.*, vol. 11, pp. 1–11p, 2005.
- [161] N. A. Burton, R. V Padilla, A. Rose, and H. Habibullah, “Increasing the efficiency of hydrogen production from solar powered water electrolysis,” *Renew. Sustain. Energy Rev.*, vol. 135, p. 110255, 2021.
- [162] B. C. R. Ewan and R. W. K. Allen, “A figure of merit assessment of the routes to hydrogen,” *Int. J. Hydrogen Energy*, vol. 30, no. 8, pp. 809–819, 2005.
- [163] Z. Pirzadi and F. Meshkani, “From glycerol production to its value-added uses: A critical review,” *Fuel*, vol. 329, p. 125044, 2022.
- [164] A. Ganguli and V. Bhatt, “Hydrogen production using advanced reactors by steam methane reforming: a review,” *Front. Therm. Eng.*, vol. 3, p. 1143987,

2023.

- [165] G. Kalghatgi, “Is it really the end of internal combustion engines and petroleum in transport?,” *Appl. Energy*, vol. 225, no. April, pp. 965–974, 2018, doi: 10.1016/j.apenergy.2018.05.076.
- [166] S. Kaskun, “An overview of hydrogen-rich gas production from biomass by using thermal technologies,” in *IOP Conference Series: Earth and Environmental Science*, 2020, vol. 614, no. 1, p. 12010.
- [167] S. K. Sansaniwal and R. Kaushal, “Biomass Pyrolysis for Sustainable Development of Bio-Products,” pp. 656–663, 2018.
- [168] T. Production of hydrogen and syngas via steam gasification of glycerol in a fixed-bed reactorValliyappan, D. Ferdous, N. N. Bakhshi, and A. K. Dalai, “Pyrolysis of glycerol for the production of hydrogen or syn gas. Bioresource technology,” *Top. Catal.*, vol. 49, pp. 59–67, 2008.
- [169] M. Martín and I. E. Grossmann, “Towards zero CO<sub>2</sub> emissions in the production of methanol from switchgrass. CO<sub>2</sub> to methanol,” *Comput. Chem. Eng.*, vol. 105, pp. 308–316, 2017, doi: 10.1016/j.compchemeng.2016.11.030.
- [170] M. F. Othman, A. Adam, G. Najafi, and R. Mamat, “Green fuel as alternative fuel for diesel engine: A review,” *Renew. Sustain. Energy Rev.*, vol. 80, no. August 2016, pp. 694–709, 2017, doi: 10.1016/j.rser.2017.05.140.
- [171] A. Kumar, *Biomass thermochemical gasification: Experimental studies and modeling*. The University of Nebraska-Lincoln, 2009.
- [172] P. D. Kofman, “Review of worldwide standards for solid biofuels,” *COFORD, Process.*, vol. 39, pp. 1–12, 2016.



- [173] A. Elfasakhany, “Investigations on the effects of ethanol–methanol–gasoline blends in a spark-ignition engine: Performance and emissions analysis,” *Eng. Sci. Technol. an Int. J.*, vol. 18, no. 4, pp. 713–719, 2015, doi: 10.1016/j.jestch.2015.05.003.
- [174] E. L. Kunkes, R. R. Soares, D. A. Simonetti, and J. A. Dumesic, “An integrated catalytic approach for the production of hydrogen by glycerol reforming coupled with water-gas shift,” *Appl. Catal. B Environ.*, vol. 90, no. 3–4, pp. 693–698, 2009.
- [175] M. Ternan, “The potential of direct hydrocarbon fuel cells for improving energy efficiency,” in *2006 IEEE EIC Climate Change Conference*, 2006, pp. 1–4.
- [176] R. D. Cortright, R. R. Davda, and J. A. Dumesic, “Hydrogen from catalytic reforming of biomass-derived hydrocarbons in liquid water,” *Nature*, vol. 418, no. 6901, pp. 964–967, 2002.
- [177] A. C. C. De Souza and J. L. Silveira, “Hydrogen production utilizing glycerol from renewable feedstocks - The case of Brazil,” *Renew. Sustain. Energy Rev.*, vol. 15, no. 4, pp. 1835–1850, 2011, doi: 10.1016/j.rser.2010.12.001.
- [178] J. K. Mwangi, W. J. Lee, Y. C. Chang, C. Y. Chen, and L. C. Wang, “An overview: Energy saving and pollution reduction by using green fuel blends in diesel engines,” *Appl. Energy*, vol. 159, pp. 214–236, 2015, doi: 10.1016/j.apenergy.2015.08.084.
- [179] B. Sen, M. Noori, and O. Tatari, “Will Corporate Average Fuel Economy (CAFE) Standard help? Modeling CAFE’s impact on market share of electric vehicles,” *Energy Policy*, vol. 109, pp. 279–287, 2017.

- [180] O. Parlar Karakoc, M. E. Kibar, A. N. Akin, and M. Yildiz, “Nickel-based catalysts for hydrogen production by steam reforming of glycerol,” *Int. J. Environ. Sci. Technol.*, vol. 16, pp. 5117–5124, 2019.
- [181] N. F. M. Branco, A. I. M. C. Lobo Ferreira, J. C. Ribeiro, L. M. N. B. F. Santos, and J. A. P. Coutinho, “Understanding the thermal behaviour of blends of biodiesel and diesel: Phase behaviour of binary mixtures of alkanes and FAMES,” *Fuel*, vol. 262, no. January 2019, p. 116488, 2020, doi: 10.1016/j.fuel.2019.116488.
- [182] K. Maqsood and M. Alsaady, “Optimization using response surface methodology for producing biodiesel from waste cooking oil using fishbone catalyst,” *Materwiss. Werksttech.*, vol. 53, no. 10, pp. 1242–1248, 2022.
- [183] S. Ghavami, F. Akhlaghian, S. Mohammadiazar, and F. Rahmani, “Biodiesel production from sunflower and waste cooking oils using K<sub>2</sub>O/RGO catalyst,” *Environ. Prog. Sustain. Energy*, p. e14235.
- [184] Z. Al-Hamamre, A. Sandouqa, B. Al-Saida, R. A. Shawabkeh, and M. Alnaief, “Biodiesel production from waste cooking oil using heterogeneous KNO<sub>3</sub>/Oil shale ash catalyst,” *Renew. Energy*, vol. 211, pp. 470–483, 2023.
- [185] B. Aghel, M. Mohadesi, M. H. Razmehgir, and A. Gouran, “Biodiesel production from waste cooking oil in a micro-sized reactor in the presence of cow bone-based KOH catalyst,” *Biomass Convers. Biorefinery*, vol. 13, no. 15, pp. 13921–13935, 2023.
- [186] F. A. Aderibigbe *et al.*, “Waste Cooking Oil Conversion to Biodiesel Using Solid Bifunctional Catalysts,” *ChemBioEng Rev.*, vol. 10, no. 3, pp. 293–310, 2023.

- [187] K. B. Hundie, L. D. Shumi, and T. A. Bullo, “Investigation of biodiesel production parameters by transesterification of watermelon waste oil using definitive screening design and produced biodiesel characterization,” *South African J. Chem. Eng.*, vol. 41, pp. 140–149, 2022.
- [188] S. Ityokumbul Igbax, D. Swartling, A. ElSawy, and S. Idem, “Improving the Yield of Biodiesel Production Using Waste Vegetable Oil Considering the Free Fatty Acid Content,” in *ASME International Mechanical Engineering Congress and Exposition*, 2022, vol. 86687, p. V006T08A028.
- [189] T. R. Primadi, F. Fajaroh, A. Santoso, and O. D. Fernanda, “Biodiesel production from cooking oil waste (jelantah) using egg shells waste catalyst  $\text{CaO/CoFe}_2\text{O}_4$ ,” in *AIP Conference Proceedings*, 2021, vol. 2384, no. 1.
- [190] M. Andrifar, F. Goembira, M. Ulfah, R. Putri, R. Yuliarningsih, and R. Aziz, “Optimization of sustainable biodiesel production from waste cooking oil using heterogeneous alkali catalyst,” *J. Rekayasa Proses*, 2022.
- [191] N. R. Lakkimsetty, M. Lakavat, S. Walke, S. Gandhi, G. Kavitha, and F. Shaik, “Comprehensive process design of biodiesel from waste cooking oil (WCO) using magnetic nano-catalyst,” in *AIP Conference Proceedings*, 2022, vol. 2463, no. 1.
- [192] R. A. Alsaiani, E. M. Musa, and M. A. Rizk, “Biodiesel production from date seed oil using hydroxyapatite-derived catalyst from waste camel bone,” *Heliyon*, vol. 9, no. 5, 2023.
- [193] M. Ramesh, S. Praveen, N. Kuppuswamy, A. Khan, and A. M. Asiri, “Biodiesel production from waste cooking oil using ionic liquids as catalyst,” in *Advanced Technology for the Conversion of Waste into Fuels and*

*Chemicals*, Elsevier, 2021, pp. 215–230.

- [194] A. N. Amenaghawon, K. Obahiagbon, V. Isesele, and F. Usman, “Optimized biodiesel production from waste cooking oil using a functionalized bio-based heterogeneous catalyst,” *Clean. Eng. Technol.*, vol. 8, p. 100501, 2022.
- [195] H. Chen, W. Xia, and S. Wang, “Biodiesel production from waste cooking oil using a waste diaper derived heterogeneous magnetic catalyst,” *Brazilian J. Chem. Eng.*, vol. 40, no. 2, pp. 511–520, 2023.
- [196] S. Mothil, V. C. Devi, R. S. Raam, P. Asmitha, A. Gokul, and B. Balakumar, “Biodiesel production from waste cooking oil through transesterification using novel double layered hydroxide catalyst,” in *AIP Conference Proceedings*, 2021, vol. 2387, no. 1.
- [197] S. Niju, K. Aishwarya, M. Balajii, and P. Asaithambi, “Statistical optimization of ultrasound-assisted biodiesel production from Moringa oleifera oil–waste cooking oil mixture using modified conch shell catalyst,” *Environ. Prog. Sustain. Energy*, p. e14243, 2023.
- [198] F. Danane *et al.*, “Experimental optimization of Waste Cooking Oil ethanolysis for biodiesel production using Response Surface Methodology (RSM),” *Sci. Technol. Energy Transit.*, vol. 77, p. 14, 2022.
- [199] A. Velmurugan, A. R. Warriar, and B. Gurunathan, “Biodiesel production by transesterification of low-cost feedstock (waste cooking oil) using mesoporous cubic-MgO nanocatalyst: Optimization using response surface methodology,” *Energy Environ.*, p. 0958305X231199242, 2023.
- [200] M. D. Garba, A. M. Sunusi, S. A. Hassan, and S. D. Jackson, “Biodiesel Production from Waste Cooking Oil, Using an Acid Modified Carbon Catalyst

Derived from Cassava Peels,” *Catal. Ind.*, vol. 15, no. 1, pp. 99–107, 2023.

- [201] M. G. Weldeslase, N. E. Benti, M. A. Desta, and Y. S. Mekonnen, “Maximizing biodiesel production from waste cooking oil with lime-based zinc-doped CaO using response surface methodology,” *Sci. Rep.*, vol. 13, no. 1, p. 4430, 2023.
- [202] A. P. Bora, L. D. Konda, P. Paluri, and K. S. Durbha, “Valorization of hazardous waste cooking oil for the production of eco-friendly biodiesel using a low-cost bifunctional catalyst,” *Environ. Sci. Pollut. Res.*, vol. 30, no. 19, pp. 55596–55614, 2023.
- [203] E. G. Al-Sakkari *et al.*, “Comparative technoeconomic analysis of using waste and virgin cooking oils for biodiesel production,” *Front. Energy Res.*, vol. 8, p. 583357, 2020.
- [204] R. Selvaraj, I. G. Moorthy, R. V. Kumar, and V. Sivasubramanian, “Microwave mediated production of FAME from waste cooking oil: Modelling and optimization of process parameters by RSM and ANN approach,” *Fuel*, vol. 237, no. August 2018, pp. 40–49, 2019, doi: 10.1016/j.fuel.2018.09.147.
- [205] M. Ogata, T. Nakaishi, H. Takayabu, S. Eguchi, and S. Kagawa, “Production efficiency and cost reduction potential of biodiesel fuel plants using waste cooking oil in Japan,” *J. Environ. Manage.*, vol. 331, p. 117284, 2023.
- [206] M. Ulfah, S. Octavia, and H. Suherman, “Biodiesel production through waste cooking oil (WCO) esterification using sulfated alumina as catalyst,” in *IOP Conference Series: Materials Science and Engineering*, 2019, vol. 543, no. 1, p. 12007.
- [207] J. V. Sree, B. A. Chowdary, K. S. Kumar, M. P. Anbazhagan, and S.

- Subramanian, “Optimization of the biodiesel production from waste cooking oil using homogeneous catalyst and heterogeneous catalysts,” *Mater. Today Proc.*, vol. 46, pp. 4900–4908, 2021.
- [208] M. D. Supardan, S. Satriana, and M. Mahlinda, “Biodiesel production from waste cooking oil using hydrodynamic cavitation,” *Makara J. Technol.*, vol. 16, no. 2, p. 10, 2012.
- [209] B. Dharmalingam *et al.*, “Comparison of neural network and response surface methodology techniques on optimization of biodiesel production from mixed waste cooking oil using heterogeneous biocatalyst,” *Fuel*, vol. 340, p. 127503, 2023.
- [210] W. Widayat *et al.*, “Production of biodiesel from waste cooking oil using heterogeneous catalysts KI/ $\gamma$ -Al<sub>2</sub>O<sub>3</sub>,” *J. Environ. Eng. Sci.*, vol. 15, no. 3, pp. 107–112, 2020.
- [211] N. Salih and J. Salimon, “A review on eco-friendly green biolubricants from renewable and sustainable plant oil sources,” *Biointerface Res. Appl. Chem.*, vol. 11, no. 5, pp. 13303–13327, 2021.
- [212] R. B. Istiningrum, T. Aprianto, and F. L. U. Pamungkas, “Effect of reaction temperature on biodiesel production from waste cooking oil using lipase as biocatalyst,” in *AIP Conference Proceedings*, 2017, vol. 1911, no. 1.
- [213] A. Prokaewa, S. M. Smith, A. Luengnaruemitchai, and M. Kandiah, “Biodiesel production from waste cooking oil using a new heterogeneous catalyst SrO doped CaO nanoparticles,” *J. Met. Mater. Miner.*, vol. 32, no. 1, pp. 79–85, 2022.
- [214] W. P. Wicaksono, A. L. Marcharis, Y. P. Sari, P. W. Citradewi, and G. Kadja,

- “High-yield co-solvent free electrochemical production of biodiesel from waste cooking oil using waste concrete as heterogeneous catalyst,” in *AIP Conference Proceedings*, 2018, vol. 2026, no. 1.
- [215] B. Aghel, A. Gouran, E. Parandi, B. H. Jumei, and H. R. Nodeh, “Production of biodiesel from high acidity waste cooking oil using nano GO@ MgO catalyst in a microreactor,” *Renew. Energy*, vol. 200, pp. 294–302, 2022.
- [216] R. Nabizadeh *et al.*, “Biodiesel production from supernatant waste cooking oil by a simple one-step technique: calorific value optimization using response surface methodology (RSM) based on D-optimal design,” *J. Mater. Cycles Waste Manag.*, pp. 1–17, 2023.
- [217] M. U. H. Suzihaque, H. Alwi, U. K. Ibrahim, S. Abdullah, and N. Haron, “Biodiesel production from waste cooking oil: A brief review,” *Mater. Today Proc.*, vol. 63, pp. S490–S495, 2022.
- [218] A. Velmurugan and A. R. Warriar, “Production of biodiesel from waste cooking oil using mesoporous MgO-SnO<sub>2</sub> nanocomposite,” *J. Eng. Appl. Sci.*, vol. 69, no. 1, pp. 1–22, 2022.
- [219] D. Topi, “Transforming waste vegetable oils to biodiesel, establishing of a waste oil management system in Albania,” *SN Appl. Sci.*, vol. 2, pp. 1–7, 2020.
- [220] E. K. Okoye, C. P. C. Edeh, C. O. Ezumazu, and E. C. Ejiogu, “Biodiesel production from used cooking oil using controlled reactor plant,” in *2013 Africon*, 2013, pp. 1–4.
- [221] R. Kukana and O. P. Jakhar, “An appraisal on enablers for enhancement of waste cooking oil-based biodiesel production facilities using the interpretative structural modeling approach,” *Biotechnol. Biofuels*, vol. 14, no. 1, p. 213,

2021.

- [222] B. Rezki, Y. Essamlali, M. Aadil, N. Semlal, and M. Zahouily, "Biodiesel production from rapeseed oil and low free fatty acid waste cooking oil using a cesium modified natural phosphate catalyst," *RSC Adv.*, vol. 10, no. 67, pp. 41065–41077, 2020.
- [223] H. H. Hamed, A. E. Mohammed, O. A. Habeeb, O. M. Ali, O. S. Aljaf, and M. A. Abdulqader, "Biodiesel Production From Waste Cooking Oil using Homogeneous Catalyst," *Egypt. J. Chem.*, vol. 64, no. 6, pp. 2827–2832, 2021.
- [224] M. H. Awad, K. A. Hreeba, and H. E. Elkhidr, "Production of Biodiesel From Waste Cooking Oil," *Sciences (New. York).*, vol. 7, no. 13, 2022.
- [225] P. Gada, S. K. Dusi, and I. Abrar, "Enhanced Biodiesel Production from Waste Cooking Oil Using ZnO Nanocatalyst," in *International Conference on Nanotechnology: Opportunities and Challenges*, 2022, pp. 47–54.
- [226] M. A. Munir *et al.*, "Development of a supply chain model for the production of biodiesel from waste cooking oil for sustainable development," *Front. Energy Res.*, vol. 11, p. 1222787, 2023.
- [227] N. I. Alias, J. K. Jayakumar, and S. M. Zain, "Characterization of waste cooking oil for biodiesel production," *J. Kejuruter.*, vol. 1, no. 2, pp. 79–83, 2018.
- [228] M. Welela and T. G. Asere, "Biodiesel production from waste frying oil using catalysts derived from waste materials," *J. Turkish Chem. Soc. Sect. A Chem.*, vol. 9, no. 3, pp. 939–952, 2022.
- [229] A. H. Ulukardesler, "Biodiesel production from waste cooking oil using different types of catalysts," *Processes*, vol. 11, no. 7, p. 2035, 2023.



- [230] A. Ayodeji, C. Gozirim, A. Cedar, M. Oke, and B. Philip, “Production of waste vegetable oil biodiesel using calcined periwinkle shells as catalyst,” *Chem. Pap.*, vol. 77, no. 11, pp. 6647–6654, 2023.
- [231] A. Jagadeesh, B. M. Shrigiri, and O. D. Hebbal, “Production of Biodiesel Using Temple Waste Oil,” in *Recent Advances in Hybrid and Electric Automotive Technologies: Select Proceedings of HEAT 2021*, Springer, 2022, pp. 81–90.
- [232] D. Mishra, N. Kumar, and R. Chaudhary, “Effect of orange peel oil on the performance and emission characteristics of diesel engine fueled with quaternary blends,” *Energy Sources, Part A Recover. Util. Environ. Eff.*, vol. 45, no. 1, pp. 650–660, 2023, doi: 10.1080/15567036.2023.2171510.
- [233] N. Ganesan and S. Masimalai, “Experimental investigation on a performance and emission characteristics of single cylinder diesel engine powered by waste orange peel oil biodiesel blended with antioxidant additive,” *Energy Sources, Part A Recover. Util. Environ. Eff.*, vol. 0, no. 0, pp. 1–12, 2019, doi: 10.1080/15567036.2019.1604856.
- [234] NationalPolicyonBiofules, “National Policy on Biofules-2018,” vol. 2018, no. D, pp. 1–23, 2018, [Online]. Available: <http://petroleum.nic.in/national-policy-biofuel-2018-0>.
- [235] S. Ghosal, “Edible oil consumption may rise 15% in June-July Read more at: [https://economictimes.indiatimes.com/markets/commodities/edible-oil-consumption-may-rise-15-per-cent-in-june-july/articleshow/64552354.cms?utm\\_source=contentofinterest&utm\\_medium=ext&utm\\_campaign=](https://economictimes.indiatimes.com/markets/commodities/edible-oil-consumption-may-rise-15-per-cent-in-june-july/articleshow/64552354.cms?utm_source=contentofinterest&utm_medium=ext&utm_campaign=)”

<https://economictimes.indiatimes.com/markets/commodities/edible-oil-consumption-may-rise-15-per-cent-in-june-july/articleshow/64552354.cms?from=mdr>.

- [236] M. Gülüm and A. Bilgin, “Measurements and empirical correlations in predicting biodiesel-diesel blends’ viscosity and density,” *Fuel*, vol. 199, no. x, pp. 567–577, 2017, doi: 10.1016/j.fuel.2017.03.001.
- [237] B. Sajjadi, A. A. A. Raman, and H. Arandiyan, “A comprehensive review on properties of edible and non-edible vegetable oil-based biodiesel: composition, specifications and prediction models,” *Renew. Sustain. Energy Rev.*, vol. 63, pp. 62–92, 2016.
- [238] A. T. Hoang, “Prediction of the density and viscosity of biodiesel and the influence of biodiesel properties on a diesel engine fuel supply system,” *J. Mar. Eng. Technol.*, pp. 1–13, 2018.
- [239] P. Kumar and N. Kumar, “Experimental investigation of Jatropha oil methyl ester (JOME) as pilot fuel with CNG in a dual fuel engine,” *Biofuels*, vol. 7, no. 5, pp. 511–520, 2016, doi: 10.1080/17597269.2016.1163215.
- [240] H. S. Pali, N. Kumar, and K. Singh, “Optimisation of Process Parameters of EDM on Al6082/SiC Metal Matrix Composite,” *SAE Tech. Pap.*, vol. 2016-April, no. April, 2016, doi: 10.4271/2016-01-0533.
- [241] G. Martínez, N. Sánchez, J. M. Encinar, and J. F. González, “Fuel properties of biodiesel from vegetable oils and oil mixtures. Influence of methyl esters distribution,” *Biomass and Bioenergy*, vol. 63, pp. 22–32, 2014, doi: 10.1016/j.biombioe.2014.01.034.
- [242] T. A. L. Do, J. Vieira, J. M. Hargreaves, B. Wolf, and J. R. Mitchell, “Impact

- of limonene on the physical properties of reduced fat chocolate,” *JAACS, J. Am. Oil Chem. Soc.*, vol. 85, no. 10, pp. 911–920, 2008, doi: 10.1007/s11746-008-1281-3.
- [243] R. Abd Rabu, I. Janajreh, and D. Honnery, “Transesterification of waste cooking oil: Process optimization and conversion rate evaluation,” *Energy Convers. Manag.*, vol. 65, pp. 764–769, 2013, doi: 10.1016/j.enconman.2012.02.031.
- [244] Y. Xue *et al.*, “Ternary blends of biodiesel with petro-diesel and diesel from direct coal liquefaction for improving the cold flow properties of waste cooking oil biodiesel,” *Fuel*, vol. 177, pp. 46–52, 2016, doi: 10.1016/j.fuel.2016.02.087.
- [245] P. Kumar, M. P. Sharma, and G. Dwivedi, “Impact of ternary blends of biodiesel on diesel engine performance,” *Egypt. J. Pet.*, vol. 25, no. 2, pp. 255–261, 2016, doi: 10.1016/j.ejpe.2015.06.010.
- [246] K. M. Chun and J. B. Heywood, “Estimating heat-release and mass-of-mixture burned from spark-ignition engine pressure data,” *Combust. Sci. Technol.*, vol. 54, no. 1–6, pp. 133–143, 1987.
- [247] R. J. Moffat, “Uncertainty analysis,” in *Thermal Measurements in Electronics Cooling*, CRC Press, 2020, pp. 45–80.
- [248] H. Singh Pali, A. Sharma, N. Kumar, and Y. Singh, “Biodiesel yield and properties optimization from Kusum oil by RSM,” *Fuel*, vol. 291, no. January, p. 120218, 2021, doi: 10.1016/j.fuel.2021.120218.
- [249] C. E. Onu, J. T. Nwabanne, P. E. Ohale, and C. O. Asadu, “Comparative analysis of RSM, ANN and ANFIS and the mechanistic modeling in eriochrome black-T dye adsorption using modified clay,” *South African J.*

*Chem. Eng.*, vol. 36, pp. 24–42, 2021, doi: 10.1016/j.sajce.2020.12.003.

- [250] S. Zhao *et al.*, “Experimental investigation on biodiesel production through transesterification promoted by the La-dolomite catalyst,” *Fuel*, vol. 257, p. 116092, 2019.
- [251] S. Dharma *et al.*, “Optimization of biodiesel production process for mixed *Jatropha curcas*-*Ceiba pentandra* biodiesel using response surface methodology,” *Energy Convers. Manag.*, vol. 115, pp. 178–190, 2016, doi: 10.1016/j.enconman.2016.02.034.
- [252] B. Karmakar, S. H. Dhawane, and G. Halder, “Optimization of biodiesel production from castor oil by Taguchi design,” *J. Environ. Chem. Eng.*, vol. 6, no. 2, pp. 2684–2695, 2018, doi: 10.1016/j.jece.2018.04.019.
- [253] L. F. Chuah, S. Yusup, A. R. Abd Aziz, A. Bokhari, J. J. Klemeš, and M. Z. Abdullah, “Intensification of biodiesel synthesis from waste cooking oil (palm olein) in a hydrodynamic cavitation reactor: effect of operating parameters on methyl ester conversion,” *Chem. Eng. Process. Process Intensif.*, vol. 95, pp. 235–240, 2015.
- [254] D. Y. C. Leung and Y. Guo, “Transesterification of neat and used frying oil: Optimization for biodiesel production,” *Fuel Process. Technol.*, vol. 87, no. 10, pp. 883–890, 2006, doi: 10.1016/j.fuproc.2006.06.003.
- [255] B. Ashok, K. Nanthagopal, D. Arumuga Perumal, J. M. Babu, A. Tiwari, and A. Sharma, “An investigation on CRDi engine characteristic using renewable orange-peel oil,” *Energy Convers. Manag.*, vol. 180, no. October 2018, pp. 1026–1038, 2019, doi: 10.1016/j.enconman.2018.11.047.
- [256] Z. Ni *et al.*, “Reaction kinetics analysis of branched-chain alkyl esters of

- palmitic acid and cold flow properties,” *Renew. Energy*, vol. 147, pp. 719–729, 2020.
- [257] L. F. Chuah, J. J. Klemeš, S. Yusup, A. Bokhari, and M. M. Akbar, “Influence of fatty acids in waste cooking oil for cleaner biodiesel,” *Clean Technol. Environ. Policy*, vol. 19, no. 3, pp. 859–868, 2017, doi: 10.1007/s10098-016-1274-0.
- [258] A. Khalid *et al.*, “Effects of storage duration on biodiesel properties derived from waste cooking oil,” *Appl. Mech. Mater.*, vol. 554, pp. 494–499, 2014, doi: 10.4028/www.scientific.net/AMM.554.494.
- [259] R. Gautam and N. Kumar, “Effect of ethanol addition on the properties of Jatropha ethyl ester,” *Energy Sources, Part A Recover. Util. Environ. Eff.*, vol. 38, no. 23, pp. 3464–3469, 2016, doi: 10.1080/15567036.2016.1145766.
- [260] N. Kumar and M. Tomar, “Influence of nanoadditives on ignition characteristics of Kusum (*Schleichera oleosa*) biodiesel,” *Int. J. Energy Res.*, vol. 43, no. 8, pp. 3223–3236, 2019, doi: 10.1002/er.4446.
- [261] M. R. Uddin, K. Ferdous, M. R. Uddin, M. R. Khan, and M. A. Islam, “Synthesis of biodiesel from waste cooking oil,” *Chem. Eng. Sci.*, vol. 1, no. 2, pp. 22–26, 2013.
- [262] V. Sharma and G. Duraisamy, “Production and characterization of bio-mix fuel produced from a ternary and quaternary mixture of raw oil feedstock,” *J. Clean. Prod.*, vol. 221, pp. 271–285, 2019, doi: 10.1016/j.jclepro.2019.02.214.
- [263] P. S. Mehta and T. Jeyaseelan, “Controlling nitric oxide in CI engine-bio-mix approach,” SAE Technical Paper, 2014.
- [264] International Council on Clean Transportation, “Technical Background on

- India BS VI Fuel Specifications,” no. 119, pp. 9–12, 2016, doi: 10.4271/2012-01-1274.4.
- [265] S. Fernando, P. Karra, R. Hernandez, and S. K. Jha, “Effect of incompletely converted soybean oil on biodiesel quality,” *Energy*, vol. 32, no. 5, pp. 844–851, 2007, doi: 10.1016/j.energy.2006.06.019.
- [266] M. Mani, G. Nagarajan, and S. Sampath, “Characterisation and effect of using waste plastic oil and diesel fuel blends in compression ignition engine,” *Energy*, vol. 36, no. 1, pp. 212–219, 2011, doi: 10.1016/j.energy.2010.10.049.
- [267] R. Vallinayagam, S. Vedharaj, W. M. Yang, P. S. Lee, K. J. E. Chua, and S. K. Chou, “Combustion performance and emission characteristics study of pine oil in a diesel engine,” *Energy*, vol. 57, pp. 344–351, 2013, doi: <https://doi.org/10.1016/j.energy.2013.05.061>.
- [268] K. Anandavelu, N. Alagumurthi, and C. G. Saravannan, “Experimental Investigation of Using Eucalyptus Oil and Diesel Fuel Blends in Kirloskar TV1 Direct Injection Diesel Engine,” *J. Sustain. Energy Environ.*, vol. 2, no. March, pp. 93–97, 2011.
- [269] P. A. Lakshminarayanan, N. Nayak, S. V. Dingare, and A. D. Dani, “Predicting hydrocarbon emissions from direct injection diesel engines,” *J. Eng. Gas Turbines Power*, vol. 124, no. 3, pp. 708–716, 2002, doi: 10.1115/1.1456091.
- [270] S. H. Park, H. K. Suh, and C. S. Lee, “Nozzle flow and atomization characteristics of ethanol blended biodiesel fuel,” *Renew. Energy*, vol. 35, no. 1, pp. 144–150, 2010, doi: <https://doi.org/10.1016/j.renene.2009.06.012>.
- [271] A. Omari, S. Pischinger, O. P. Bhardwaj, B. Holderbaum, J. Nuottimäki, and M. Honkanen, “Improving Engine Efficiency and Emission Reduction

Potential of HVO by Fuel-Specific Engine Calibration in Modern Passenger Car Diesel Applications,” *SAE Int. J. Fuels Lubr.*, vol. 10, no. 3, pp. 756–767, 2017, doi: 10.4271/2017-01-2295.

- [272] W. J. Lee *et al.*, “Assessment of energy performance and air pollutant emissions in a diesel engine generator fueled with water-containing ethanol-biodiesel-diesel blend of fuels,” *Energy*, vol. 36, no. 9, pp. 5591–5599, 2011, doi: 10.1016/j.energy.2011.07.012.
- [273] Q. Zhang, M. Yao, Z. Zheng, H. Liu, and J. Xu, “Experimental study of n-butanol addition on performance and emissions with diesel low temperature combustion,” *Energy*, vol. 47, no. 1, pp. 515–521, 2012, doi: <https://doi.org/10.1016/j.energy.2012.09.020>.
- [274] M. Annamalai *et al.*, “An assessment on performance, combustion and emission behavior of a diesel engine powered by ceria nanoparticle blended emulsified biofuel,” *Energy Convers. Manag.*, vol. 123, pp. 372–380, 2016, doi: 10.1016/j.enconman.2016.06.062.
- [275] K. Nantha Gopal and R. Thundil Karupparaj, “Effect of pongamia biodiesel on emission and combustion characteristics of di compression ignition engine,” *Ain Shams Eng. J.*, vol. 6, no. 1, pp. 297–305, 2015, doi: 10.1016/j.asej.2014.10.001.
- [276] N. Jorge, A. C. Da Silva, and C. P. M. Aranha, “Antioxidant activity of oils extracted from orange (*Citrus sinensis*) seeds,” *Int. News Fats, Oils Relat. Mater.*, vol. 28, no. 6, pp. 23–26, 2017.

## Sample calculation for finding the uncertainty

At 100% load condition

Speed  $N = 1500\text{rpm}$

Load  $W = 12.5\text{kg}$

Fuel Volume  $f = 10\text{cc}$

Brake Power  $BP = 3.5\text{kW}$

### 3. Brake Power

$$BP = \frac{2 * \pi * N(\text{rpm}) * \text{Load}(\text{kg}) * 9.81 * \text{Dynamometer arm length (m)}}{60 * 1000}$$

$$BP = \frac{2 * \pi * 1500 * 12.5 * 9.81 * 0.185}{60 * 1000} = 3.5\text{kW}$$

$$BP = f(W)$$

$$\frac{\partial BP}{\partial W} = \frac{2 * \pi * 1500 * 9.81 * 0.185}{60 * 1000} = 0.285$$

$$\Delta BP = \left[ \left( \frac{\partial BP}{\partial W} * \Delta W \right)^2 \right]$$

$$\Delta BP = [\sqrt{(0.285 * 0.2)^2}]$$

$$\Delta BP = 0.057\text{kW}$$

Therefore, the uncertainty in brake power is  $\pm 0.057\text{kW}$  and the uncertainty limits in the calculation of BP are  $3.5 \pm 0.057\text{kW}$ .

### 4. Total fuel consumption

$$\text{TFC} = \frac{10 * 3600 * 0.835}{t * 100}$$

$$\text{TFC} = \frac{10 * 3600 * 0.835}{29.5 * 100} = 1.02\text{kg/h}$$



$$TFC = f(t)$$

$$\frac{\partial TFC}{\partial t} = - \frac{10 * 3600 * 0.835}{t^2 * 100}$$

$$\frac{\partial TFC}{\partial t} = - \frac{10 * 3600 * 0.835}{29.5^2 * 100} = -0.0345$$

$$\Delta TFC = [ \left( \frac{\partial TFC}{\partial T} * \Delta T \right)^2 ]$$

$$\Delta TFC = [\sqrt{(-0.0345 * 0.18)^2}]$$

$$\Delta TFC = 0.00621 \text{ kg/h}$$

The uncertainty in TFC is  $\pm 0.00621 \text{ kg/h}$  and the limits of uncertainty are  $0.93 \pm 0.00517 \text{ kg/h}$ .

##### 5. Brake thermal efficiency

$$\eta = \frac{BP * 3600 * 100}{\text{mass flow rate} * \text{Calorific value}}$$

$$\eta = \frac{3.5 * 3600 * 100}{1.02 * 42570} = 29.01\%$$

$$\eta = f(BP, MFR)$$

$$\frac{\partial \eta}{\partial BP} = \frac{3600 * 100}{MFR * 42570}$$

$$\frac{\partial \eta}{\partial BP} = \frac{3600 * 100}{1.02 * 42570} = 8.29$$

$$\frac{\partial \eta}{\partial MFR} = - \frac{BP * 3600 * 100}{MFR^2 * 42570}$$

$$\frac{\partial \eta}{\partial MFR} = - \frac{3.5 * 3600 * 100}{1.02^2 * 42570} = -28.45$$

$$\Delta \eta = [\sqrt{\left( \frac{\partial \eta}{\partial BP} * \Delta BP \right)^2 + \left( \frac{\partial \eta}{\partial MFR} * \Delta MFR \right)^2}]$$

$$\partial BP$$

$$\partial MFR$$

$$\Delta\eta = [\sqrt{(8.29 * 0.057)^2 + (-28.45 * 0.00621)^2}]$$

$$\Delta\eta = 0.5044\%$$

The uncertainty in brake thermal efficiency is  $\pm 0.5044\%$  and the limits of uncertainty are  $29.01 \pm 0.5044\%$ .

#### 6. Brake specific energy consumption

$$BSEC = \frac{\text{mass flow rate} * \text{Calorific value}}{BP * 1000}$$

$$BSEC = \frac{1.02 * 42570}{3.5 * 1000} = 12.406 \text{ MJ/kWh}$$

$$BSEC = f(MFR, BP)$$

$$\frac{\partial BSEC}{\partial MFR} = \frac{42570}{BP * 1000}$$

$$\frac{\partial BSEC}{\partial MFR} = \frac{42570}{3.5 * 1000} = 12.16$$

$$\frac{\partial BSEC}{\partial BP} = - \frac{MFR * 42570}{BP^2 * 1000}$$

$$\frac{\partial BSEC}{\partial BP} = - \frac{1.02 * 42570}{3.5^2 * 1000} = 3.544$$

$$\Delta BSEC = [\sqrt{(\frac{\partial BSEC}{\partial BP} * \Delta BP)^2 + (\frac{\partial BSEC}{\partial MFR} * \Delta MFR)^2}]$$

$$\Delta BSEC = [\sqrt{(3.544 * 0.057)^2 + (12.16 * 0.00621)^2}]$$

$$\Delta BSEC = 0.2156 \text{ MJ/kWh}$$

The uncertainty in brake specific energy consumption is  $\pm 0.2156 \text{ MJ/kWh}$  and the limits of uncertainty are  $12.406 \pm 0.2156 \text{ MJ/kWh}$ .

#### 7. Temperature measurement

Uncertainty in temperature is:  $\pm 1 \%$  ( $T > 150 \text{ }^\circ\text{C}$ )  
 $\pm 2 \%$  ( $150 \text{ }^\circ\text{C} < T < 250 \text{ }^\circ\text{C}$ )  
 $\pm 3 \%$  ( $T < 150 \text{ }^\circ\text{C}$ )

#### 8. Percentage of uncertainty for NO, HC, CO, smoke and pressure is given below.

NO	:1.2
HC	: 0.1
CO	: 0.76
Smoke	: 2.1
Pressure	: 1.3

## Specification of Malvern Spraytec

Measurment Principle	Laser diffraction
Size range	0.1 – 2000 $\mu$ m
Optical Models	Mie theory and Fraunhofer Approximation including Patented Multiple Scattering correction
Lens ranges	750 mm lens: 2.0–2000 $\mu$ m ( $D_{v50}$ : 5–1600 $\mu$ m)
Working range	100mm at 0.5 $\mu$ m, >1m at 10 $\mu$ m
Concentration range	Minimum acceptable transmission: 5% (dependent on particle size range)
Detection system	35 element log-spaced silicon diode detector array
Light source	632.8 nm, 5mW helium–neon laser
Maximum acquisition rate	Continuous mode: 1 Hz Rapid mode: 2.5 kHz as standard, 10 kHz with additional software feature key
Accuracy	Better than $\pm 1\%$ on the $D_{v50}$
Precisions/repeatability	Better than $\pm 1\%$ COV on the $D_{v50}$

## LIST OF PUBLICATIONS

---

1. **DUSHYANT MISHRA**, NAVEEN KUMAR, RAJIV CHAUDHARY, Effect of orange peel oil on the performance and emission characteristics of diesel engine fueled with quaternary blends, Energy Sources, Part A: Recovery, Utilization, and Environmental Effects..DOI:10.1080/15567036.2023.2171510 (Publisher: Taylor and Francis).Available Online
2. NAVEEN KUMAR, RAJIV CHAUDHARY **DUSHYANT MISHRA**, Biodiesel production from cooking oil: Yield and characteristic optimization, International journal of Oil, gas and Coal Technology (Publisher: Inderscience Limited) DOI: 10.1504/IJOGCT.2023.10057091. Available Online
3. **DUSHYANT MISHRA**, NAVEEN KUMAR, RAJIV CHAUDHARY, comprehensive review on performance combustion and emission characteristics of diesel/biodiesel/alcohol and their blends, 8th International Symposium on Fusion of Science & Technology (ISFT-2020) DOI 10.1088/1757-899X/804/1/012030 (IOP publishing)
4. **DUSHYANT MISHRA**, NAVEEN KUMAR, RAJIV CHAUDHARY, Influence of Orange Peel Oil and n- Butanol on Characteristic of diesel engine, paper presented in International conference on Sustainable Material Manufacturing and Energy technologies (SMMET-2022)
5. **DUSHYANT MISHRA**, NAVEEN KUMAR, RAJIV CHAUDHARY, A Step Towards The Biofuel: A Hope for IC Engine, 10<sup>th</sup> International Symposium on Fusion of Science & Technology (ISFT-2024)

**ENGINEERING PROFESSIONAL & ACADEMICIAN**

Ph.D. from Delhi Technological University (formerly Delhi College of Engineering) in the department of Mechanical Engineering

---

**PROFESSIONAL EXPERIENCE (15 years)**

Venkateshwara group of Institutions, Meerut	Aug-2022- Till Now
Delhi College of Engineering (Research Associates)	Dec 2018 – Aug-2022
KCC Institute of Management & Technology	Aug 2014 – Dec-2018
ITS Engineering College	Aug 2011 – Aug 2014
GGIT, GREATER NOIDA	Sept 2009 – Sept 2011
Accurate Institute of Management & Technology, Greater Noida	Nov 2008 – Sept 2009
NIET GREATER NOIDA	Aug 2006 – Aug 2008

---

**EDUCATIONAL CREDENTIALS**

M. Tech. (Energy and Environment Management) 2011	IIT, Delhi;
B. Tech. in Mechanical Engineering 2006	NIET, Greater Noida

---

**PAPERS AND PATENTS**

- A comprehensive review on performance combustion and emission characteristics of diesel/biodiesel/alcohol and their blends <https://doi.org/10.1088/1757-899X/804/1/012030>
  - Book chapter published in springer on Methanol based economy: A way forward to Hydrogen. [https://doi.org/10.1007/978-981-15-5667-8\\_23](https://doi.org/10.1007/978-981-15-5667-8_23)
  - Patent no: 202011030786, Date: 20-07-2020 Title: “CNG NATURAL GAS KIT DESIGN FOR TWO WHEELERS” Applicant and Inventor Name: Dushyant Mishra
  - Patent no: 202021033148, Date: 28-08-2020 Title: “N-SIDE-STAND: NOVEL SIDE-STAND FOR TWO WHEELERS” Applicant and Inventor Name: Dushyant Mishra
  - Active solar distillation technology: A wide overview <https://doi.org/10.1016/j.desal.2020.114652> published in Q1 journal
  - Effect of orange peel oil on the performance and emission characteristics of diesel engine fueled with quaternary blends DOI: <https://doi.org/10.1080/15567036.2023.2171510> published in Q2 journal
  - Biodiesel production from cooking oil: Yield and characteristic optimization. The paper has been accepted in SCI journal
-